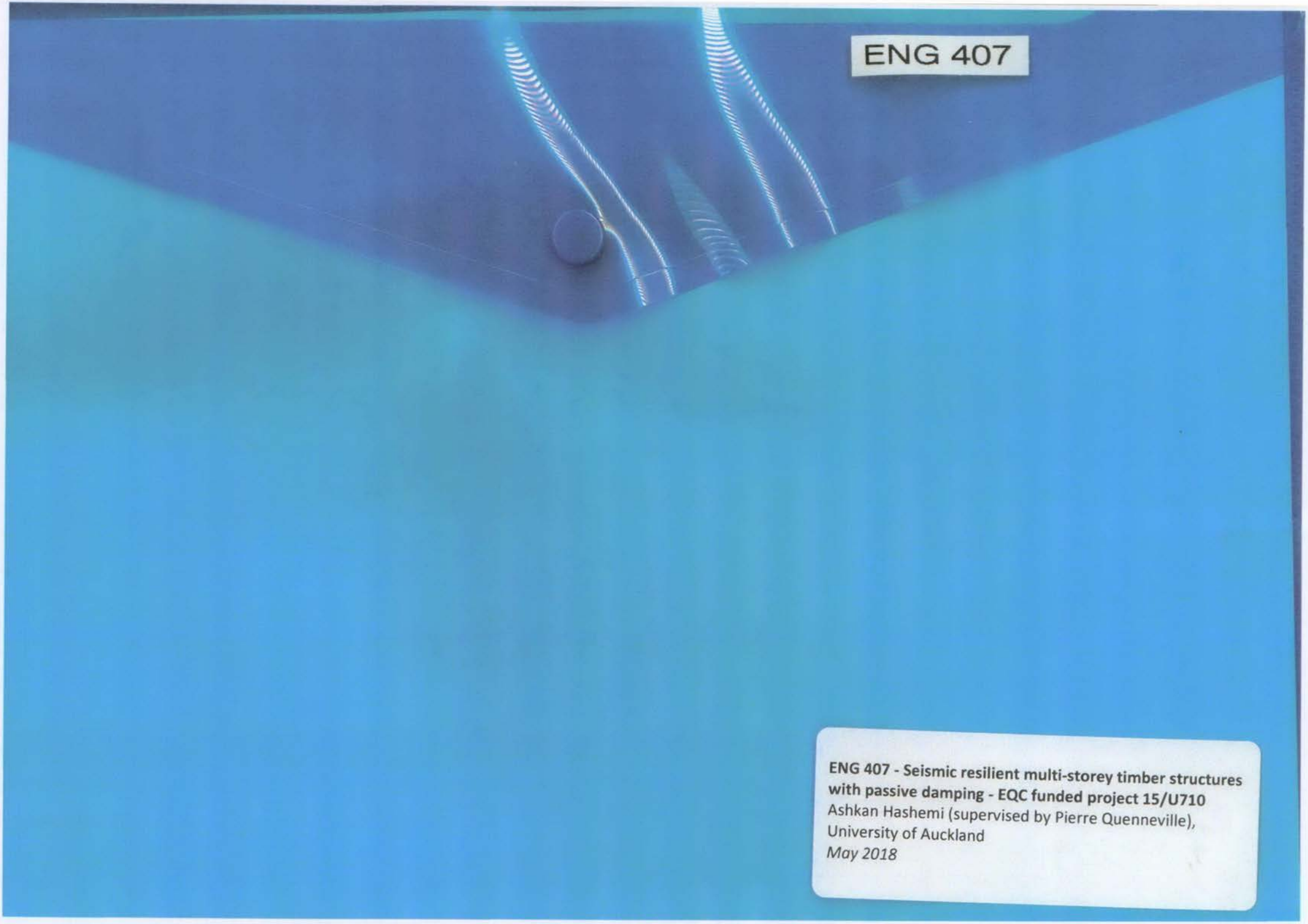

ENG 407 - Seismic resilient multi-storey timber structures with passive damping - EQC funded project 15/U710

Ashkan Hashemi (supervised by Pierre Quenneville),
University of Auckland

May 2018

ENG 407

15/0710

Seismic resilient multi-story timber structures with passive damping

PhD student: Ashkan Hashemi

Supervisor: Professor Pierre Quenneville

1. Introduction

It is a well-known fact that in a seismic resistant timber structure, the timber elements have to behave elastically during an earthquake and all of the energy dissipation has to occur in the connections. In traditional timber structures in which the connections include conventional metal fasteners such as nails, screws, rivets or bolts, the required ductility and energy dissipation are provided by the connections. However, since the energy dissipation in timber connections always involve plastic deformation of the fasteners, irrecoverable damage to the connections is highly probable. Thus, the structure requires serious repair and may need to be dismantled. Moreover, the stiffness and strength of the structure may significantly decrease making it highly vulnerable even to a minor aftershock. As a result, a mixing of the timber members and novel energy dissipation devices is required for the structure to be able to tolerate a severe seismic event and the associated aftershocks.

Conventional slip friction connections with flat plates sliding on each other have always been recognized to have one of the most efficient passive damping mechanisms. The provided hysteresis which is close to an elastic-perfectly-plastic one combined with the cost effectiveness of these devices has made them very favourable. Nevertheless, the lack of self-centring behaviour is a major disadvantage which may result in considerable residual displacements after an earthquake.

The aim of this project is to develop damage avoidance concepts for lateral load resisting systems in multi-story timber and hybrid structures that offer compatibility of deformations for all the elastic timber systems in the structure and that can dissipate the energy through friction. The performance of the conventional slip friction connections in seismic resistant structures is investigated and the consequent damage caused by the lack of self-centring behaviour is studied. To provide the self-centring behaviour, alternative novel solutions are proposed. The performance of the structures containing the proposed solutions is examined by joint component testing, large scale experimental tests and numerical analyses. Analytical design procedures are proposed and validated by the experimental data. This report contains the summary of conducted research and the developed solutions. Each of the following sections is a chapter in the thesis and also published as a journal paper. A list of publications including all of the journal papers and conference papers is presented at the end.

2. A numerical study of coupled timber walls with slip friction damping devices

In this section, the application of slip friction connections in timber coupled walls is investigated by developing and analysing detailed numerical models. The proposed structural concept includes rocking Cross Laminated Timber (CLT) or Laminated Veneer Lumber (LVL) walls with slip friction hold-downs at the base and friction ductile links between the adjacent walls.

The components of the system transfer the lateral forces to the foundation while providing the required ductility at a given drift. The walls are typically CLT or LVL which the type is generally determined based on the required capacity. A numerical model for the proposed system is developed and was subjected to displacement-control quasi static and non-linear dynamic time-history simulations. Furthermore, the numerical results were compared with the results from a similar model with the slip friction connections replaced with traditional nail plates. This comparison showed that the proposed concept has a superior seismic behaviour relative to traditional systems yet showed residual displacement after the seismic events. The outcomes are published as a journal paper in Construction and Building Materials. The reader is referred to the following link for more information.

https://doi.org/10.1016/j.conbuildmat.2016.05.160

3. Seismic performance of hybrid self-centring steel-timber rocking core walls with slip friction connections

In this section, an innovative damage avoidance steel-timber rocking core as the main lateral force resisting system is developed to efficiently lessen the post-earthquake damage. This system includes rocking timber walls, steel corner columns and supplementary slip friction dampers to dissipate the seismic energy. Moreover, high strength post-tensioned steel strands were used through the steel beams to self-centre the structure after the earthquake. The efficiency of this system is inspected by displacement-control quasi-static and non-linear dynamic time-history analyses. Furthermore, a design procedure based on the Displacement Based Design (DBD) approach is introduced to design the system in accordance with the induced seismic loads. Finally, a numerical model for the proposed timber rocking core system is developed and subjected to dynamic time-history simulations. The results showed that the system has a fully self-centring behaviour with a significant decrease in peak roof accelerations when compared with traditional systems. The outcomes are published as a journal paper in the Journal of Constructional Steel Research. The reader is referred to the following link for more information.

https://doi.org/10.1016/j.jcsr.2016.07.022

4. Seismic resistant rocking coupled walls with innovative Resilient Slip Friction (RSF) joints

In this section, a damage avoidance timber coupled rocking wall system with innovative Resilient Slip Friction (RSF) joints as the ductile links between the adjacent walls or columns is developed. In this system, boundary steel columns at the ends of the coupled walls are considered instead of the hold-down connectors. Owing to the unique characteristics offered by the RSF joints, this innovative lateral load resisting system is able to provide self-centring behaviour in addition to significant rate of seismic energy dissipation. A simple procedure for designing the joint is presented and the results of RSF joint component tests are discussed. Furthermore, a numerical model is developed to demonstrate the seismic performance of the proposed system. The numerical technique used for modelling of the RSF joints is verified by the experimentally obtained data. To investigate the efficiency of the system, the model is subjected to displacement-control quasi-static cyclic simulations and non-linear dynamic time-history records. The results showed a fully self-centring behaviour given no residual displacement was recorded. Moreover, the maximum recorded displacements were within the indicated thresholds by the New Zealand standard for the Ultimate Limit State (ULS) seismic events and Maximum Credible Earthquake (MCE). The outcomes are published as a journal paper in the Journal of Constructional Steel Research. The reader is referred to the following link for more information.

https://doi.org/10.1016/j.jcsr.2016.11.016 ✓

5. Experimental testing of rocking Cross Laminated Timber (CLT) walls with Resilient Slip Friction (RSF) joints

This section presents the large scale experimental testing of the concept of rocking CLT walls with RSFJ hold-downs as the lateral load resisting system. The hysteretic behaviour of this innovative system is verified and the feasibility and effectiveness of the adopted solution for connecting the RSF joints to the CLT wall was confirmed. Furthermore, an analytical design procedure for predicting the hysteretic behaviour of the wall was developed and verified by comparing the experimental results with the analytically obtained hysteretic loops. Also, a numerical tool for modelling the structures containing the proposed concept is introduced. Overall, the test results showed an excellent seismic performance which suggests the potential for application in seismic resilient structures when a damage avoidance design philosophy is adopted. The outcomes are published as a journal paper in the Journal of Structural Engineering (ASCE). The reader is referred to the following link for more information.

https://doi.org/10.1061/(ASCE)ST.1943-541X.0001931 ✓

6. Seismic resilient lateral load resisting system for timber structures

In this section, a seismic resilient solution for timber and hybrid timber-steel structures is developed and investigated on the system level. The proposed system includes rocking wall panels with RSF joints (as the hold-down connectors) and load-bearing components on the two sides of the wall panels. This system offers adequate ductility for the building while energy dissipations and self-centring are provided by the RSF joints. A preliminary design procedure for the proposed system based on the Displacement Based Design (DBD) approach is also introduced. To further investigate the seismic performance of this system, a numerical model for a five-story prototype building was developed and subjected to non-linear dynamic time-history records. The results were compared with those obtained from similar models in which the RSF joints were replaced with conventional connectors such as symmetric friction dampers and nailed connections. Additionally, the models were subjected to sequences of earthquakes to investigated the resiliency of the concept in a series of seismic event. The results showed excellent seismic behaviour in terms of self-centring behaviour, response accelerations and peak roof drifts. The outcomes are published as a journal paper in Construction and Building Materials. The reader is referred to the following link for more information.

https://doi.org/10.1016/j.conbuildmat.2017.05.112

7. List of publications:

PhD thesis:

A. Hashemi, "Seismic Resilient Multi-story Timber Structures with Passive Damping," A thesis submitted for fulfilment of the requirements of the degree of Doctor of Philosophy, University of Auckland, Auckland, New Zealand.

Journal papers:

A. Hashemi, P. Zarnani, and P. Quenneville, "Damage Avoidance Self-Centering Steel Moment Resisting Frames (MRFs) Using Innovative Resilient Slip Friction Joints (RSFJs)," Key Engineering Materials, vol. 763, pp. 726–734, 2018.

A. Hashemi, P. Zarnani, R. Masoudnia, P. Quenneville, "Seismic resilient lateral load resisting system for timber structures," Construction and Building Materials, vol. 149, pp. 432–443, 2017.

A. Hashemi, P. Zarnani, R. Masoudnia, P. Quenneville, "Experimental testing of rocking Cross Laminated Timber (CLT) walls with Resilient Slip Friction (RSF) joints," Journal of Structural Engineering (USA), vol. 144, Issue 1, pp. 04017180-1 to 16, 2017.

A. Hashemi, P. Quenneville, "Earthquake resilient timber structures using Cross Laminated Timber (CLT) walls coupled with Resilient Slip Friction Joints (RSFJs)," New Zealand Timber Design Journal, vol. 25, Issue 3, pp. 12-19, 2017.

A. Hashemi, P. Zarnani, R. Masoudnia, P. Quenneville, "Seismic resistant rocking coupled walls with innovative Resilient Slip Friction (RSF) joints," Journal of Constructional Steel Research, vol. 129, pp. 215–226, 2017.

A. Hashemi, P.Zarnani, R. Masoudnia, P. Quenneville, "Novel self-centring friction damping system for seismic resistant cross laminated structures," New Zealand Timber Design Journal, vol. 24, pp. 10-17, 2016.

A. Hashemi, R. Masoudnia, P. Quenneville, "Seismic performance of hybrid self-centering steel-timber rocking core walls with slip friction connections," Journal of Constructional Steel Research, vol. 126, pp. 201-213, 2016.

A. Hashemi, R. Masoudnia, P. Quenneville, "A numerical study of coupled timber walls with slip friction damping devices," Construction and Building Materials, vol. 121, pp. 373–385, 2016.

Conference papers:

A. Hashemi, S.M.M Yousef-Beik, B. Zaboli, F.M. Darani, G.C. Clifton, P. Zarnani, P. Quenneville, "Seismic Performance of Resilient Slip Friction Joint (RSFJ) Brace with Collapse Prevention Mechanism", Proceedings of New Zealand Society for Earthquake Engineering Conference (NZSEE), Auckland, New Zealand, 2018.

A. Hashemi, P. Zarnani, P. Quenneville, "Earthquake Resilient Cross Laminated Timber (CLT) lateral load resisting system with innovative Resilient Slip Friction Joints (RSFJs)", Proceedings of , Structural Engineering Society of New Zealand Conference (SESOC), Wellington, New Zealand, 2017.

A. Hashemi, P. Zarnani, P. Quenneville, "Seismic resilient structures with Cross Laminated Timber (CLT) walls coupled with innovative Resilient Slip Friction (RSF) joints", Proceedings of New Zealand Society for Earthquake Engineering Conference (NZSEE), Wellington, New Zealand, 2017.

A. Hashemi, P. Zarnani, R. Masoudnia, and P. Quenneville, "Seismic Resistant Cross Laminated Timber (CLT) Structures with Innovative Resilient Slip Friction (RSF) Joints," in World Conference of Earthquake Engineering (16WCEE), Santiago, Chile, 2017.

A. Hashemi, P. Zarnani, A. Valadbeigi, R. Masoudnia, P. Quenneville, "Seismic Resistant Timber Walls with New Resilient Slip Friction Damping Devices," International Network of Timber Engineering Research Conference, Graz, Austria, 2016.

A. Hashemi, W. Y. Loo, R. Masoudnia, P. Zarnani, P. Quenneville, "Ductile Cross Laminated Timber (CLT) Platform Structures with Passive Damping," in World Conference of Timber Engineering WCTE2016, Vienna, Austria, 2016.

A. Hashemi, P. Zarnani, A. Valadbeigi, R. Masoudnia, P. Quenneville, "Seismic resistant cross laminated timber structures using an innovative resilient friction damping system", Proceedings of New Zealand Society for Earthquake Engineering Conference (NZSEE), Christchurch, New Zealand, 2016.

Journal of Constructional Steel Research 129 (2017) 215–226

Contents lists available at ScienceDirect

Journal of Constructional Steel Research

Seismic resistant rocking coupled walls with innovative Resilient Slip Friction (RSF) joints

Ashkan Hashemi [a,*], Pouyan Zarnani [b], Reza Masoudnia [a], Pierre Quenneville [a]

[a] Department of Civil and Environmental Engineering, Faculty of Engineering, The University of Auckland, Private bag 92019, Auckland 1142, New Zealand
[b] Department of Built Environment Engineering, School of Engineering, Computer and Mathematical Sciences, Auckland University of Technology, Private bag 92006, Auckland 1142, New Zealand

ARTICLE INFO

Article history:
Received 26 September 2016
Received in revised form 9 November 2016
Accepted 15 November 2016
Available online xxxx

Keywords:
Coupled rocking walls
Low damage
RSF joints
Self-centring
Damage avoidance
Resilience

ABSTRACT

Multi-story hybrid timber-steel structures are becoming progressively desirable owing to their aesthetic and environmental benefits and also to the relatively higher strength to weight ratio of timber. Moreover, there is an increasing public pressure to have low damage structural systems to minimize the destruction after severe earthquakes. A recent trend in the timber building industry is the use of cross laminated timber (CLT) wall systems. CLT is a relatively novel engineered wood based product well suited for multi-story structures. Latest research findings have shown that CLT buildings constructed with traditional steel connectors can experience high damage mainly because of stiffness degradation in the fasteners.

It has been proven that friction joints can provide a perfectly elastoplastic behaviour and a stable hysteretic response. Up until now, the main disadvantage of the friction joints has been the undesirable residual displacements after an earthquake. This study presents a hybrid damage avoidant steel-timber wall system using the innovative Resilient Slip Friction (RSF) joint. The proposed system includes coupled timber walls and boundary steel column as the main lateral load resisting members. RSF joints are used as ductile links between the adjacent walls or between the walls and the steel boundary columns. The efficiency of the system has been investigated by experimental joint component tests on the RSF joint followed by reversed cyclic numeral analyses and dynamic non-linear time-history simulations on the wall system. The results confirmed that the proposed system has the potential to be recognised as an efficient lateral load resisting system.

1. Introduction

Multi-story hybrid buildings built with structural timber members are becoming progressively desirable for engineers and building owners because of the aesthetic and environmental benefits of the wood and engineered wood products and further for the relatively higher strength to weight ratio of timber. Furthermore, there is an increasing public pressure to have low damage structural systems in order to minimize the earthquake destruction after moderate to severe seismic events. This is important as the building could be quickly reoccupied with minimal business interruption and repair costs.

Cross laminated timber (CLT) is a new generation of engineered wood product which was firstly developed in Europe in the 1990s and then expanded globally as a reliable construction material [1]. It is a strong, sustainable and dimensionally stable product which offers different structural characteristics similar to that of a pre-cast concrete panel, yet it has relatively higher strength to weight ratio. Additionally, CLT structures possess flexible planning and high level of prefabrication which considerably accelerate the construction process and reduce the overall cost. Hence, CLT has been notably gaining popularity among building owners and designers and as a consequence, numerous CLT buildings have been built in different countries over the last decade.

During the PRESSS (PREcast Seismic Structural Systems) program in the early 1990's, a new design approach for structural walls was introduced which was based on the application of simple joints between the prefabricated panels in order to localize the inelastic deformations in those joints [2]. In addition, unbounded post-tensioned steel members were employed to provide the self-centring behaviour. The dissipation capacity of such system is highly related to the type of the dissipaters implemented between the walls (also known as the sacrificial fuses). For timber structures, Palermo et al. adopted a similar approach and conducted preliminary experimental tests on laminated veneer lumber (LVL) walls with different types of fuses [3,4]. The results confirmed that the enhanced performance of the system was attributed to the ductile joints between the members. Smith et al. further extended the concept into coupled wall systems [5]. They proved that the design flexibility of the hybrid coupled wall systems combined with the offered speed of construction creates a significant potential for such system in multi-story buildings. Iqbal et al. studied the application of U-shaped Flexural Plates (UFPs) as supplementary damping devices in post-tensioned LVL timber coupled rocking walls [6]. The test results exhibited

* Corresponding author.
E-mail address: ahas439@aucklanduni.ac.nz (A. Hashemi).

http://dx.doi.org/10.1016/j.jcsr.2016.11.016
0143-974X/

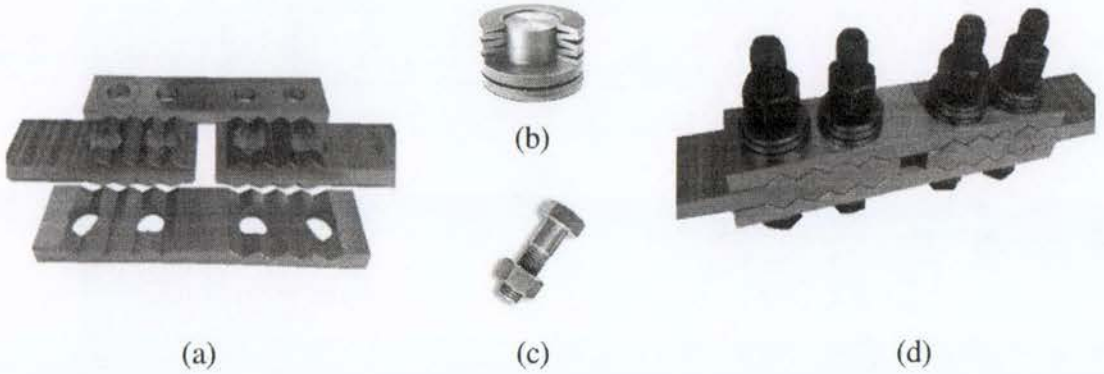

Fig. 1. RSF joint: a) Cap plates and slotted centre plates b) Belleville springs c) High strength bolts d) Assembly of the joint.

an efficient energy dissipation mechanism over the deformation of the UFPs during the earthquakes. Sarti et al. experimentally investigated the seismic performance of the hybrid rocking walls with end columns [7]. Their experimental results confirmed a notable improvement in the seismic performance of the introduced system in terms of energy dissipation and stability of the hysteretic behaviour. Iqbal et al. tested coupled post-tensioned rocking LVL walls with sacrificial nailed plywood sheets as hysteretic dissipative elements [8]. The experimental results affirmed the seismic performance of the system. Nevertheless, relatively lower hysteretic stability was observed compared to the similar systems with UFPs.

Friction based passive damping devices were originally introduced for steel structures. Popov et al. proposed symmetric slotted bolted connections which dissipate energy through friction during equilateral tension and compression cycles [9]. Popov's comprehensive experiments exhibited stable rectangle-shaped hysteretic loops. Clifton et al. proposed the asymmetric sliding hinge joint for steel moment resisting frames which had non-rectangular yet stable force-deformation behaviour [10]. Khoo et al. developed design models for the asymmetric slotted bolted connections based upon numerous experiments and rigorous analyses [11].

For the first time in timber structures, Filiatrault used friction dampers at the four corners of a traditional timber sheathed shear wall [12]. The results demonstrated a significant improvement in hysteretic behaviour of the walls while large amount of seismic energy was absorbed through friction. Loo et al. investigated the application of slip friction connections as the replacement of traditional hold-downs in LVL rocking walls [13,14]. The experimental results showed an excellent seismic performance in terms of hysteretic behaviour and the minimized residual deflections. Additionally, and most importantly, the timber wall remained in the elastic region after several non-linear dynamic numerical analyses. Furthermore, no substantial damage was observed in the timber members during the quasi-static experimental tests. Hashemi et al. introduced the application of slip friction connections in CLT coupled walls as the hold-down connections and also as ductile links between the wall panels [15,16]. The numerical results confirmed the efficiency of the introduced system in terms of seismic energy absorption and durability of the hysteretic behaviour. The proposed concept was further developed to hybrid rocking core walls in which the post-tensioned joints are used as supplementary devices in the beam-column connections to provide a self-centring system [17].

This study seeks to develop a damage avoidant CLT coupled rocking wall system which includes innovative Resilient Slip Friction (RSF) introduced by Zarnani and Quenneville [18] as the ductile links between the adjacent walls or columns. Owing to the characteristics offered by the RSF joints, this innovative lateral load resisting system is able to provide self-centring behaviour in addition to significant rate of seismic energy dissipation. A simple procedure for designing the joint is described and the results of RSF joint component tests are presented. Furthermore, a numerical model is developed to demonstrate the seismic performance of the proposed system. To investigate the efficiency of the system, the model is subjected to displacement-control quasi-static cyclic simulations and also non-linear dynamic time-history analyses.

2. Resilient Slip Friction (RSF) joint

The concept of slip friction connections using flat steel plates sliding over each other has already been recognised as an effective energy dissipating structural solution and the energy absorption mechanism of the friction joints has been known as one of the most efficient ones

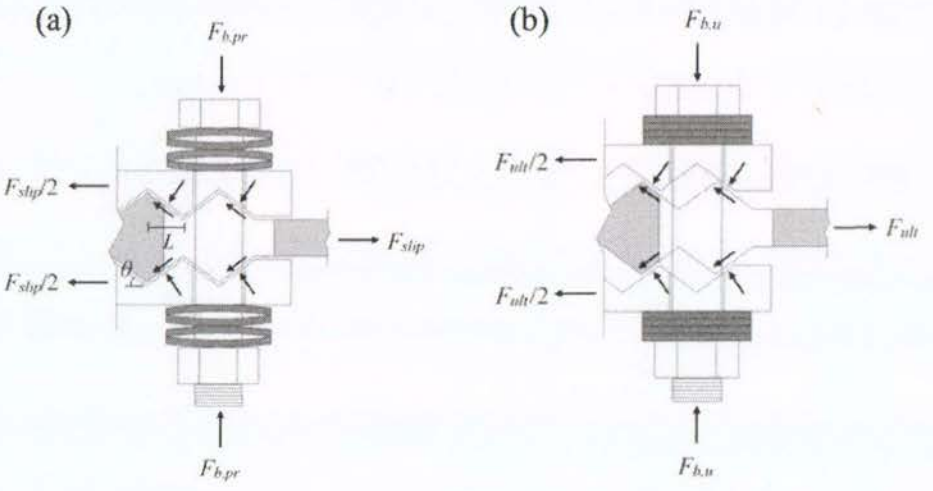

Fig. 2. Free body diagrams for a symmetric RSF joint: a) On the brink of slippage b) At ultimate deflection

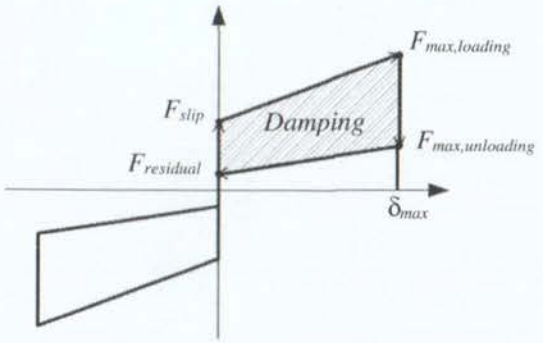

Fig. 3. Schematic load-deformation loop for the RSF joint.

among the passive devices [10,17,19]. Nevertheless, the lack of self-centring behaviour in these joints requires the use of an additional system to bring back the structure to its initial position after a seismic event, which is always costly. One of the common techniques for providing self-centring is the use of post-tensioned tendons which has two major drawbacks. Firstly, approximately 30% (or even more in some cases) of tendon force losses can take place during the service life of the structure which considerably reduces the efficiency of the system [20]. To decrease the total force loss, re-stressing of the tendons is required which is only possible with a special type of accessible anchorage. Secondly, the losses highly depend on the humidity of the environment. Although controlling the humidity reduces the losses, however, it is not possible to control it in all situations.

In recognition of the mentioned difficulties with the conventional sliding friction devices, a novel friction joint is presented in which the components are formed and arranged in a way that the self-centring behaviour is achieved as well as damping, all in one compact device. Fig. 1 shows the components and the assembly of the Resilient Slip Friction (RSF) joint [18]. The specific shape of the grooves combined with the use of Belleville springs (conical disc springs) and high strength bolts provide the desirable self-centring behaviour. The angle of the grooves is designed in such a way that at the time of unloading, the reversing force induced by the elastically compacted Belleville springs is larger than the resisting friction force between the plate surfaces. As a consequence, the elastic force of the springs re-centres the slotted plates to their initial position. Note that Fig. 1 exhibits a symmetric double acting RSF joint in which two centre slotted plate are used to maximize the deflection.

A design procedure has been developed for the prediction of the performance of the RSF joint based on the free body diagrams shown in Fig. 2. The slip force (F_{slip}) for a symmetric configuration can be determined by Eq. (1). As reported in [21], in addition to the presented symmetric RSF joint, there are other possible configurations such as asymmetric and combined symmetric-asymmetric with different assemblies and design provisions applicable for specific situations.

$$F_{slip} = 2n_b F_{b,pr}\left(\frac{\sin\theta + \mu_s \cos\theta}{\cos\theta - \mu_s \sin\theta}\right) \tag{1}$$

where $F_{b,pr}$ is the clamping force in the bolt due to pre-stressing of the Belleville springs, n_b is the number of the bolts on each splice (e.g. in Fig. 1(d), n_b equals 2), θ is the angle of the grooves and μ_s is the static coefficient of friction. Fig. 3 shows the schematic hysteretic loop for a RSF joint. The residual force in the joint at the end of the unloading can be determined by Eq. (2) where μ_k is the kinetic coefficient of friction.

$$F_{residual} = 2n_b F_{b,pr}\left(\frac{\sin\theta - \mu_k \cos\theta}{\cos\theta + \mu_k \sin\theta}\right) \tag{2}$$

The ultimate force upon loading ($F_{ult,loading}$) and unloading ($F_{ult,unloading}$) can be calculated by respectively replacing μ_s, μ_k and $F_{b,pr}$ with μ_k, μ_s and $F_{b,u}$ in Eq. (1) and Eq. (2). The ultimate force in the bolt

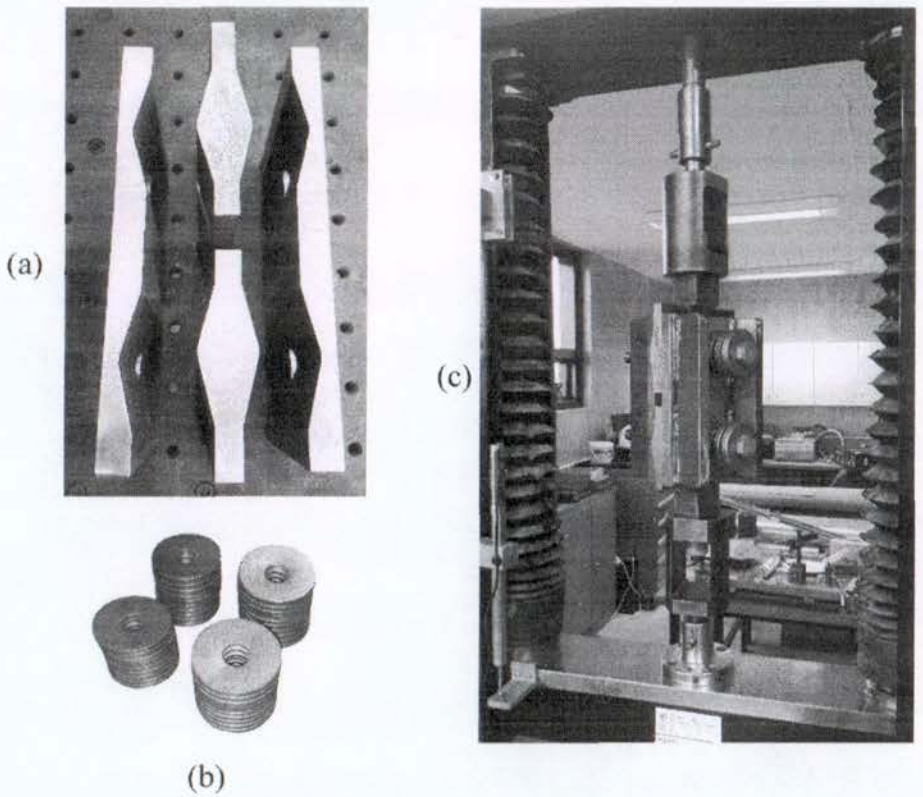

Fig. 4. RSF joint component test: a) Cap plates (before attaching the stiffeners) and centre slotted plates b) Belleville springs c) Assembly and test setup.

Table 1
Characteristics of the tested RSF joint.

Parameter	Value
Angle of the grooves	15
Slotted whole length (each direction) (mm)	35
n_b	1
μ_s	0.19
Belleville spring thickness (mm)	6.5
Belleville spring overall height (mm)	80
Belleville spring internal height (mm)	1.5
Belleville spring outside diameter (mm)	70
Belleville spring inside diameter (mm)	21
Belleville spring capacity (kN)	110
Number of the springs per bolt	18

($F_{b,u}$) can be determined by Eq. (3) in which k_s and Δ_s are correspondingly the total stiffness of the springs and their maximum deflection after pre-stressing when they are fully compressed (the springs become flat).

$$F_{b,u} = F_{b,pr} + k_s\Delta_s \tag{3}$$

The maximum deflection in a RSF joint is given by Eq. (4) where n_j is the number of joints acting in a series (e.g. n_j equals 1 for a single acting joint and equals 2 for a double acting one).

$$\delta_{max} = n_j \frac{\Delta_s}{\tan\theta} \tag{4}$$

It should be noted that for achieving a self-centring behaviour in the joint, it is necessary to satisfy $\tan\theta > \mu_s$ and $L > \frac{\Delta_u}{\sin\theta}$ where L is the horizontal distance between the top and bottom of a groove.

3. RSF joint component test

In order to experimentally investigate the hysteretic behaviour of the RSF joint, a series of joint component tests were conducted. Fig. 4 displays the components and the assembly of the manufactured specimen which was a symmetric double acting RSF joint comprised of two centre slotted plates and two cap plates. All plates were manufactured using mild steel grade 350. The angle of the grooves was 15 degrees in order to increase the deformation capacity of the joint. Moreover, Two 20 * 50 * 220 mm mild steel stiffeners were later welded to the grooved part of the cap plates (see Fig. 4(a)) to restrain them against out of plane bending.

The testing has been conducted using a 100 kN Instron Universal Test Machine with a load cell mounted on the crosshead above the RSF joint prototype to monitor the overall applied force. In order to measure the overall displacement within the joint, a Linear Variable Differential Transducer (LVDT) device was employed. It should be noted that the measured deflection is the relative displacement between the two slotted centre plates which the loading heads are attached to them.

The Belleville springs that have been used in the test have a maximum capacity of 110 kN and a maximum deflection of 1.5 mm at the flat state which equals to spring's internal height. Two high resistant 8.8 bolts with nine springs in series per side were used [13]. Table 1 presents the design parameters and the capacity of the manufactured RSF joint based on the design procedure described in the previous section. Moreover, Fig. 5 schematically shows the deformation of the employed Belleville springs and definition of the parameters presented in Table 1.

The displacement schedule displayed in Fig. 6(a) with an average loading rate of 0.5 mm/s was applied to the specimen with different pre-stressing forces and different deflections. This schedule which is based on the previous experiments carried out on the similar slip friction connections includes three reverse cycles at 20%, 40%, 67% and 100% of the maximum targeted displacement [19]. Fig. 6 shows the obtained experimental data where in each figure the overall displacement measured by the LVDT is plotted against the applied force recorded by the machine's built-in load cell. For the first three tests (Fig. 6(b)–(d)), a maximum deflection of 30 mm was adopted. For the last test the target displacement was increased to 40 mm (Fig. 6(e)) to assess the performance of the joint in different situations. Note that for the last test, the displacement schedule is adjusted for the altered maximum deflection.

The slip force (F_{slip}) was 15 kN, 24 kN, 31 kN for the first three tests and 10 kN for the fourth test. In order to achieve these forces, the Belleville spring were compacted using the turn-of-nut method, in which the number of rotations of the nut required to achieve a targeted deflection was determined by dividing this deflection to the pitch of the threaded bolts.

It should be pointed out that for all of the tests (except for the last one), the specimen was only subjected to tension as would be the case if the device were implemented as a hold-down connection for a shear wall. However, the specimen was manufactured in a way that it is able to accommodate up to 15 mm of deformation in compression as well. Accordingly, to evaluate the response of the joint in compression, the final test was carried out in both directions where the maximum displacement in tension and compression was 40 mm and 15 mm, respectively. Nevertheless, previous experimental tests by the authors proved that the RSF joint is capable of providing symmetrical hysteretic response in both directions (tension and compression) if it is designed for such a purpose [22]. Note that a specific lubricant is used between the cap plates and centre plates to increase the durability of the sliding surfaces by controlling the possible galling and rusting. In this way, a coefficient of friction of 0.19 was found for the tested device.

From Fig. 6(b)–(e), it can be seen that the load-deformation behaviour of the RSF joint represents "flag-shaped" hysteretic curves which imparts the self-centring behaviour as well as a significant rate of energy dissipation. It is apparent that the bounded area between the hysteretic loops, which represents the dissipated energy, is increasing at a constant rate. In other words, as the deflection within the joints

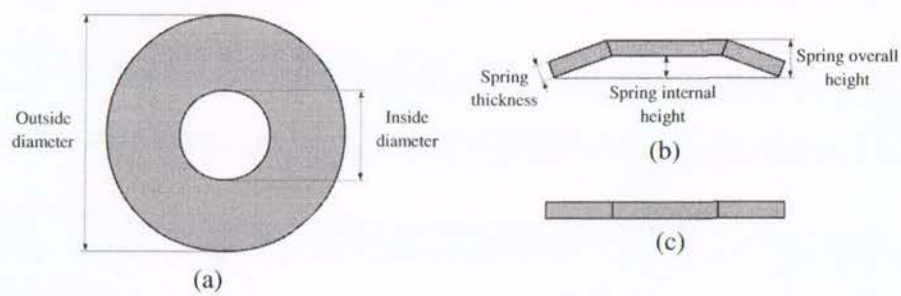

Fig. 5. Tested Belleville spring: a) Top view b) Section view before deflection c) Section view at the ultimate deflection (flat state).

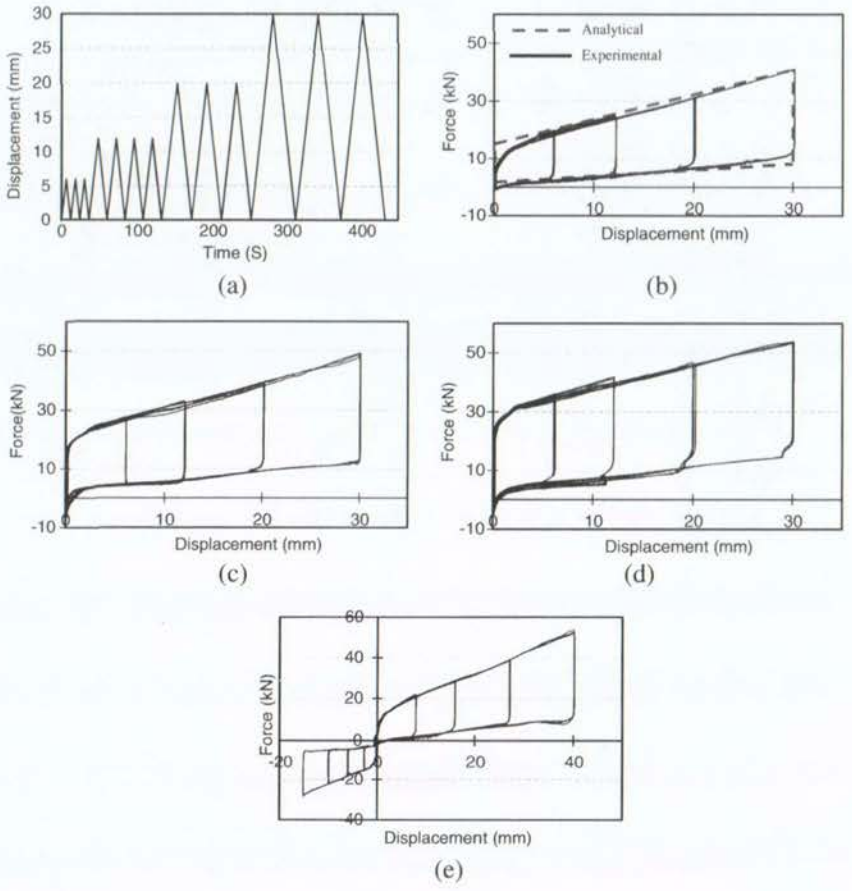

Fig. 6. RSF joint component test results: a) The applied displacement schedule b) Hysteretic behaviour for $F_{slip} = 15$ kN and comparison to the analytical prediction c) Hysteretic behaviour for $F_{slip} = 24$ kN d) Hysteretic behaviour for $F_{slip} = 31$ kN e) Hysteretic behaviour for $F_{slip} = 10$ kN in tension and compression.

increases, the absorbed energy through friction increases as well which vividly demonstrates a damage avoidant behaviour. This is because the joint maintains its stiffness and strength through numerous cycles of loading and unloading.

Furthermore, the red dashed line in Fig. 6(b) shows the behaviour prediction of the joint determined by following the analytical design procedure described in the last section. It can be seen that the proposed design equations can closely predict the behaviour of the joint. A similar close agreement between the analytical prediction and the experimental data was also observable for all other tests. This makes the designer capable of confidently predicting the hysteretic behaviour of the structure.

It should be noted that as the pre-stressing force in the bolts (and consequently F_{slip}) increases, the maximum displacement capacity of the joint decreases. This is because of the defined pre-compression force of the Belleville springs to provide the targeted slip force. Therefore, an optimized relationship between the slip force and the desired ultimate displacement should always be targeted in order to the have an efficient design for the connection. Another important observation from the test results is the stable behaviour of the connection. Flat slip friction connections, in which the external mild steel plates slide directly against the hard steel slotted centre plates, have previously demonstrated a good performance in terms of maintaining strength, stiffness and hysteretic stability [13,19]. The mentioned characteristics, which play significant roles when a damage avoidant seismic solution is aimed for, are observed as well for the RSF joint in addition to the self-centring behaviour. Taken together, these results suggests that RSF technology has a high potential for the application in seismic resistant structures specially when a resilient damage avoidant design is required in order to protect the structures from major seismic events and the associated aftershocks.

Fig. 7 shows the configuration of the tested RSF joint before and after slippage. It can be deduced that the compaction of the Belleville springs allows the device to be expanded (see Fig. 7(b)) and the preserved force

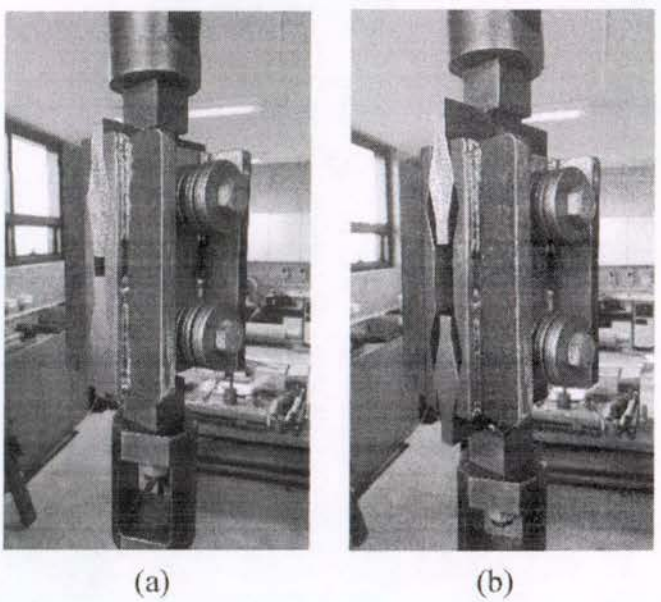

Fig. 7. Deformation of the tested RSF joint: a) At the zero displacement b) At the maximum displacement.

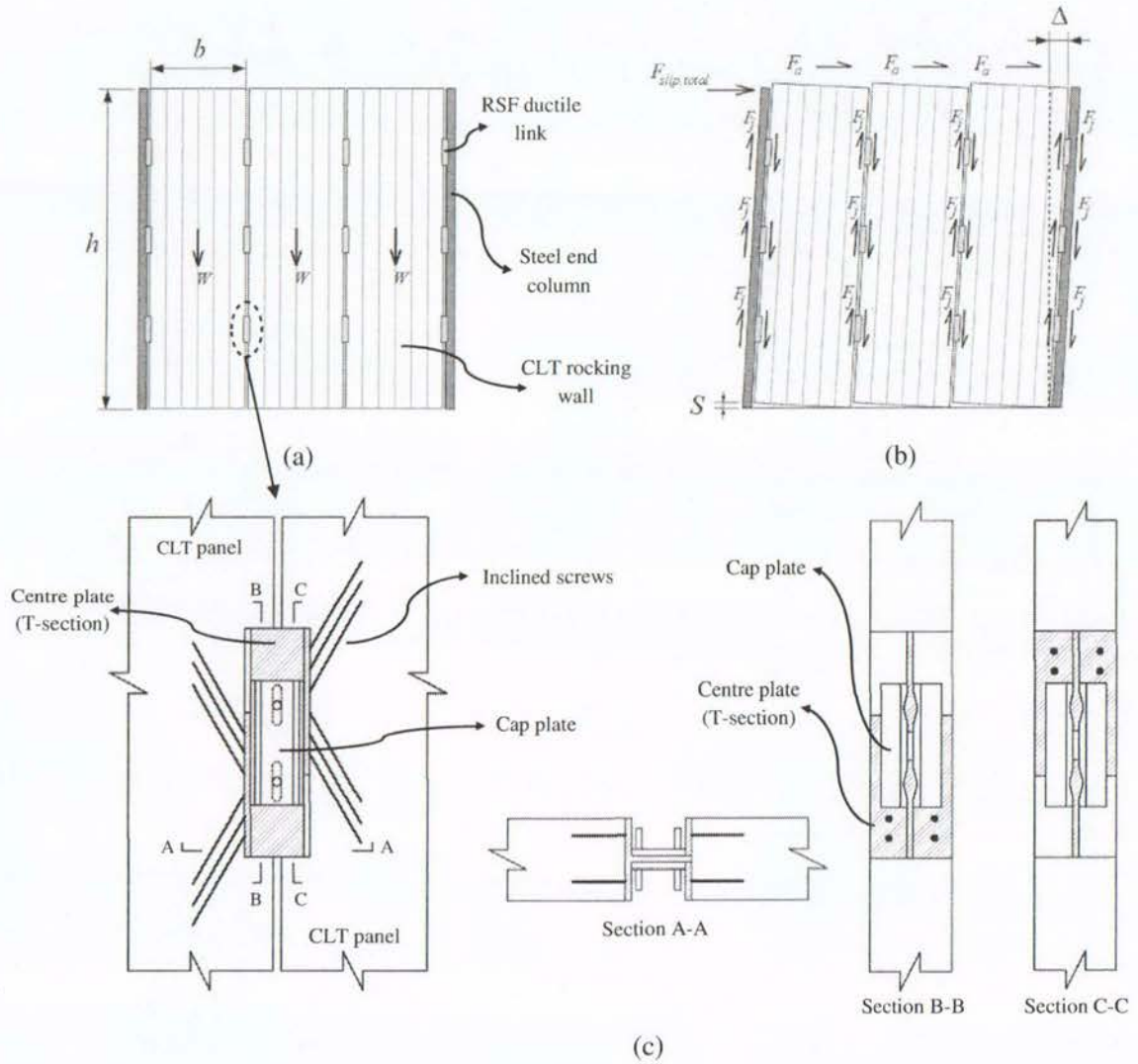

Fig. 8. CLT coupled walls with RSF joints: a) Before rocking b) After rocking c) RSF joint to CLT panel connection.

in the springs brings back the centre plates to their original position upon unloading.

4. Hybrid coupled wall system with RSF joint

4.1. The concept of hybrid CLT coupled walls with RSF joints

This section describes the concept of CLT coupled walls with RSF joints. The proposed system consists of coupled CLT walls, boundary steel columns and RSF joints as ductile links. The RSF joints connect the walls to any adjacent rocking CLT walls and/or the boundary columns. The steel columns are used to de-couple the perpendicular walls in-bidirectional rocking motion. Moreover, they can be used as the gravity load resisting members. A schematic view of the proposed concept is displayed in Fig. 8. It can be seen from the figure that the RSF joints are positioned in the notches within the CLT panels. The vertical slip in the connection between the RSF joints and the panels may affect the performance of the system. Hence, a rigid and non-slip connection is required to transfer the vertical forces from the wall panels to the RSF joints. In this case, self-tapping screws are recognised as one of the most efficient solutions. In the proposed approach for connecting the RSF joints to the CLT panels, steel flanges are attached to the two centre slotted plates to construct T-sections and then these flanges are connected the edge of the adjoining CLT walls by inclined screws (see Fig. 8(c)). The hatched parts in Fig. 8(c) indicate the T-sections. Note that the bolts and Belleville springs are not shown for better clarity. For the RSF joints connected to a boundary steel column, a welded connection between the flange and the column is considered. A similar configuration was previously proposed by the authors for connecting regular flat slip friction ductile links to CLT wall panels [15, 17].

On the brink of rocking, the acting forces on each wall include: the horizontal slip force applied at the top which triggers the sliding in the RSF joints and consequently rocking movement in the walls (F_a); the sum of RSF ductile link slip forces ($\sum F_j$); and the vertical loads (W). It should be pointed out that this concept is mainly proposed for structural systems where the lateral load resisting system is separated from the gravity load resisting members. Therefore, the only considered vertical load is the self-weight of the CLT walls. Nevertheless, the

Table 2
Design parameters for the Damper – Friction Spring Link element.

Parameter	Value
Loading slipping stiffness (N/mm)	833
Unloading slipping stiffness (N/mm)	276
Pre-compression displacement (mm)	−17.3
Stop displacement (mm)	30

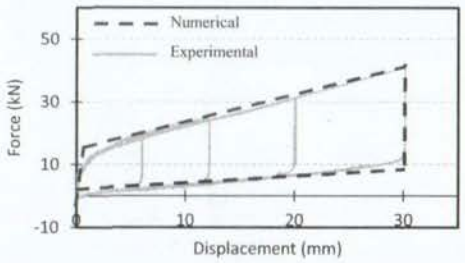

Fig. 9. Comparison of the numerical data obtained from the Damper - Friction Spring Link element in SAP2000 and the experimental results.

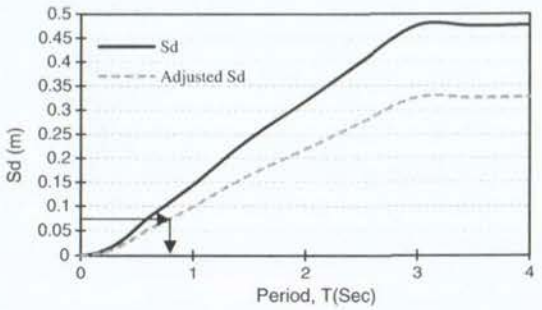

Fig. 10. The scaled displacement spectrum and the effective period (T_e = 1.1 s).

introduced system is able to mitigate all other types of the gravity loads including permanent and imposed loads.

Taking the moments about the rocking point of each wall, the sum of slip forces of the RSF joints ($\sum F_j$) can be determined by Eq. (5). In other words, the overturning moment in each wall which is induced by the applied lateral loads is resisted by the resistant moments produced by the RSF joints and the self-weight of the wall. In the case of the system shown in Fig. 8, the induced overturning moment (M_a) for each wall equals to the applied lateral load (F_a) multiplied by h. It should be noted that the total slip force ($F_{slip,total}$) is sum of the slip forces for each of the walls within the system. If the walls are not identical, the slip force for each one can be separately specified by following the same procedure with different h and b. In the case of a multi-story system, the total overturning moment is the sum of the moments produced by the lateral seismic forces in all story levels.

$$\Sigma F_j h = M_a - \frac{Wb}{2} \tag{5}$$

The relationship between the slip force (F_{slip}) and the maximum force in the joints ($F_{max,loading}$) depends on the type and properties of the employed Belleville springs and also the maximum desired deflection. Thus, a balanced relationship between the mentioned parameters is required to have an efficient design for the joints. An effective approach for determining the slip threshold for the system (M_a) is that when the applied lateral forces exceed the Ultimate Limit State (ULS) earthquake forces, the joints start to slide and the system starts to rock [23]. This philosophy will be used further in this paper for designing the joints within a coupled wall system. Note that the maximum stress at the compression toe of the CLT rocking walls should be limited below the allowable compressive stress of the wall material [6]. The connection between the RSF joints and the timber walls has to be designed with an over-strength factor to provide a relatively stiff connection to avoid any slipping during the rocking motion [24]. Moreover, the shear capacity of the CLT panel needs to be checked for the wall to be able to tolerate the shear stresses induced by the lateral loads. A special type of shear key should also be considered at the base of the walls to transfer the shear forces to the foundation while it is able to accommodate the uplift due to the rocking movement. Loo et al. proposed a shear key concept that can be considered as one possible solution [13].

Table 3
Design parameters for DBD approach [24,26].

Parameter	Value
Design inter-story drift	1%
Damping (elastic and hysteretic) (%)	13
Effective design displacement (m)	0.07
Effective mass (tonnes)	84
Effective height (m)	7.0
Effective stiffness (kN/m)	5042
Base shear (kN)	370
Base moment (kNm)	2630

The slot length for RSF ductile links connecting two adjacent walls has to be twice as it is for the RSF ductile links connecting a wall to a boundary column. The reason is that they are designed to slide in both upward and downward (tension and compression, respectively) directions while the RSF joints connecting the walls to the steel columns are only supposed to move upward (tension only). Accordingly, the slot length for the joints connecting the walls ($2S$) and ones connecting the walls to the columns (S) can be determined by Eq. (6) with respect to the required lateral displacement (Δ) (see Fig.8(b)). If the walls have different geometry, the slot lengths for the connections within each one of them should be calculated separately.

$$S = \Delta * \frac{b}{h} \tag{6}$$

4.2. Numerical modelling of the RSF joints using Damper – Friction Spring link element

In order to model the RSF load-displacement behaviour, the Damper – Friction spring Link element in SAP2000 software package is adopted [25]. For this link element, which is available in version 17 and above, several parameters need to be identified. In order to model the RSF hysteretic behaviour, these parameters should be accurately calibrated in accordance with the design parameters of the RSF joint such as slip force, loading stiffness, maximum loading force, maximum unloading force and the residual force. To verify the accuracy of this link element in the prediction of a RSF joint behaviour, a numerical model in SAP2000 is developed based on the experimental data of the tested RSF specimen with a slip force of 15 kN (see Fig. 6(b)). The calibrated parameters for the friction spring link element are presented in Table 2. These parameters were determined in accordance with the characteristics of the tested RSF joint and the specifications of the associated Belleville springs. The pre-compression displacement should be multiplied by the loading stifness to determine the slip force. The stop-displcement is the maximum deflection of the joint which is 30 mm for this case.

Table 4
Desing parameters for the RSF dcutile links.

Parameter	Value
Angle of the grooves (degrees)	15
Coefficient of friction	0.19
Number of bolts	2
Capacity of the Belleville washrs (kN)	110
Number of the springs per side per bolt	10
Total displacement of the joint (mm)	75
F_{slip} (kN)	32
$F_{ult,loading}$ (kN)	80
$F_{ult,unloading}$ (kN)	15
$F_{residual}$ (kN)	6
Maximum Top displacement (mm)	337.5
Slot length for the RSF joints connecting two walls (mm)	150
Slot length for the RSF joints connecting the walls to the columns (mm)	75

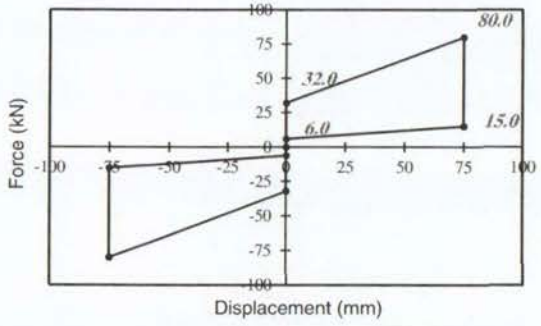

Fig. 11. The designed hysteresis for the RSF ductile links.

The numerically obtained hysteretic loop is compared with the experimental results, as shown in Fig. 9. It can be seen that the Damper – Friction Spring Link element can accurately predict the load-displacement behaviour of a RSF joint. As mentioned, a RSF joint can represent a similar behaviour in tension and compression (if it is designed for this purpose). In such case, the Damper – Friction Spring link element can accordingly be defined to respectively work in both directions.

4.3. Reversed cyclic quasi-static analysis of the hybrid CLT coupled walls with RSF joints

In order to study the seismic performance of the proposed coupled wall system, a three story building was considered as the case study prototype. It was assumed that the building had an approximate plan of 13 m in the longitudinal direction and 8 m in the transverse direction with an approximate floor area of 104 m^2 per floor. An overall height of 9 m with 3 m of height for each story was presumed. Also, the seismic weight assigned to each story was assumed as 320 kN. The Ultimate Limit State (ULS) earthquake forces were calculated using the Displacement Based Design (DBD) procedure [26] for soil type D (deep or soft soil) and 500 years of return period in Christchurch, New Zealand. The hazard factor (Z), the spectral shape factor (N) and the return period factor (R) were respectively determined as 3.0, 1.0 and 1.0 according to NZS1170.5 (New Zealand standard for earthquake actions [27]). Table 3 shows the calculated parameters based on the DBD method including the specified parameters for the equivalent single degree of freedom (SDOF) structure. Fig. 10 displays the scaled displacement spectrum and the resultant effective period of $T_e = 0.81$ s. Based on the described approach, the base shear of 370 kN and the base moment of 2630 kNm were found.

A system comprised of three 9 by 2 m CLT walls connected by RSF joints was assumed to be the main lateral load resisting system for the prototype building. The CLT panels were assumed to have five layers (three longitudinal layers and two transverse layers) with 40 mm thickness for each layer resulting in an overall thickness of 200 mm. Additionally, two 200 * 200 * 16 mm steel box columns were considered as the boundary elements at the two ends of the system (see Fig. 8). It was assumed that MSG8 (Machine Stress Graded timber with grade 8 [28]) is used for the timber boards within the CLT wall panels.

The RSF joints were designed with respect to Eq. (5) and considering the fact the three walls are identical and the total calculated overturning moment can be equally shared by them ($M_a = 2630 / 3 = 877$ kNm). Considering the density of MSG8 timber as 5.29 kN/m^3, the self-weight of each wall was found as $W = 19$ kN. By implementing three RSF ductile links up the height of the wall panels (similar to the schematic configuration shown in Fig. 8), a slip force of $F_{slip} = 32$ kN was found for the joints. In this study, F_{slip} is considered as 40% of the maximum load in the joint ($F_{max,loading}$). However, in general, the relationship between the slip force and the maximum force has to be defined in accordance with the ULS seismic forces (which indicate the slip threshold) and the maximum displacement of the exploited Belleville springs. Table 4 shows the design parameters for the RSF joints and Fig. 11 displays the designed hysteresis. The maximum top displacement was considered as 337.5 mm corresponding to 3.75% of lateral drift recommended by NZS1170.5 as the near collapse limitation [27]. The slot lengths for the RSF joints were determined by Eq. (6) ($2S$ for the joints connecting two wall panels and S for the joints connecting the walls to the boundary columns). The key parameters such as the angle of the grooves, the coefficient of friction and the springs were kept similar to the tested specimen described in Section 3.

Fig. 12(a) shows the general arrangement of the numerical model developed in SAP2000 for the described CLT coupled wall system. The RSF joints were modelled using the Damper – Friction Spring link element with the design parameters tabulated in Table 5. These parameters were calibrated in accordance with the design parameters

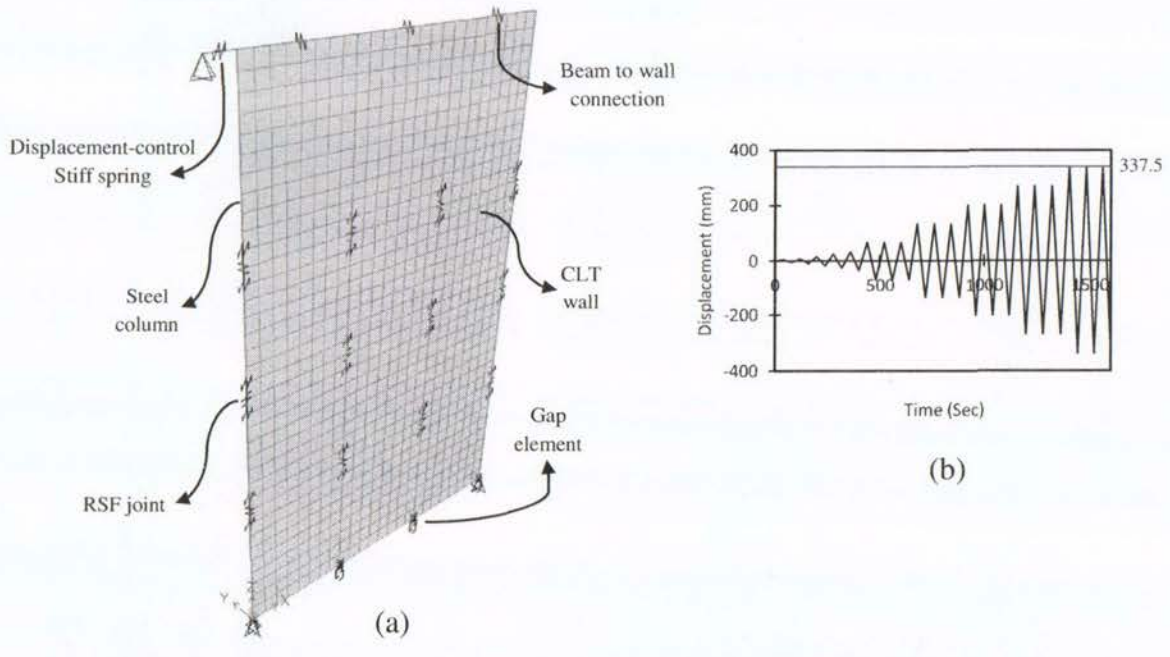

Fig. 12. Numerical model of the CLT coupled walls with RSF joints: a) General arrangement b) Displacement-control load schedule.

Table 5
Calibrated design parameters for the RSF ductile links.

Parameter	Value
Loading slipping stiffness (N/mm)	640
Unloading slipping stiffness (N/mm)	120
Pre-compression displacement (mm)	−50
Stop displacement (mm)	75

presented in Table 4. The CLT wall panels were modelled by layered shell element. The material properties of all layers were specified based on the mechanical properties of MSG8 timber. The arrangement of the layers were determined in a way that the longitudinal layers were oriented perpendicular to the direction of the applied lateral loads in order to increase the efficiency of the CLT panel for wall applications. Gap elements with a zero gap were used at the base of the walls to represent the foundation in which the walls are not allowed to move below that level. For each wall, the horizontal degree of freedom of the gap elements was restrained to represent the shear keys transferring shear forces to the foundation. A 10 mm intentional distance was considered between the walls and between the walls and the boundary steel columns to prevent them from pounding on each other during the rocking movement.

The modified version of the ISO 16670 loading protocol which was originally defined for shear walls was adopted for the quasi-static simulations [29]. The loading regime was applied through a displacement-control stiff spring at the top of the wall system to a stiff beam element representing the floor diaphragm and then through beam to wall connections which were able to transfer the forces to the wall panels in the horizontal direction.

The numerical response of the wall system subjected to cyclic quasi-static simulations is illustrates in Fig. 13. It can be seen that the RSF ductile links represent a flag-shaped hysteretic behaviour (see Section 3). It should be emphasized that the only considered vertical load in this model is the self-weight of the wall. This means that the provided self-centring behaviour does not rely on the gravity loads. This is particularly beneficial for the structural systems in which the lateral load resisting system is separated from the gravity load resisting system. By comparing Fig. 13(a) and (b), it is apparent that the joints connecting the walls to the boundary columns are working in one direction while the joints connecting two walls are working in both tension and compression. Therefore, when designing the joints, the dimensions of the ones connected to columns are less than those connecting two adjacent rocking walls.

Moreover, Fig. 13(c) evidently demonstrates the low damage characteristic of the introduced system as the lateral strength remained intact after numerous cycles of loading and unloading. Similar to what was observed during the joint component tests, the bounded area between the hysteretic loops (the absorbed energy through friction) steadily increased over time. This clearly represents a significant rate of energy dissipation which further confirms the potential to have a resilient and damage avoidant seismic solution. The presented system is applicable for both framed structures with shear walls as the lateral load resisting members and hybrid steel-timber panelised structures.

4.4. Non-linear dynamic time-history analyses of the hybrid CLT coupled walls with RSF joints

Non-linear dynamic time-history analyses were carried out on a numerical model similar to the one described in the last section (see Fig. 12(a)) without the displacement-control stiff spring, lateral load transferring beam and the beam to wall connections. Considering 320 kN of seismic weight for each story, a seismic mass of 10,900 kg was assigned to each of the walls at the three story levels. A suite of five conventional earthquake records were selected and scaled in accordance with NZS1170.5 [27] to match the Christchurch 500 year return period for ULS and 2500 year return period for the Maximum Credible Earthquake (MCE). Table 6 presents the selected seismic events and the associated scaled peak ground motions. The scaled acceleration records were applied at the base of the wall system.

The roof displacement responses for the five MCE simulations are shown in Fig. 14. It is evident that the structure returned to its initial

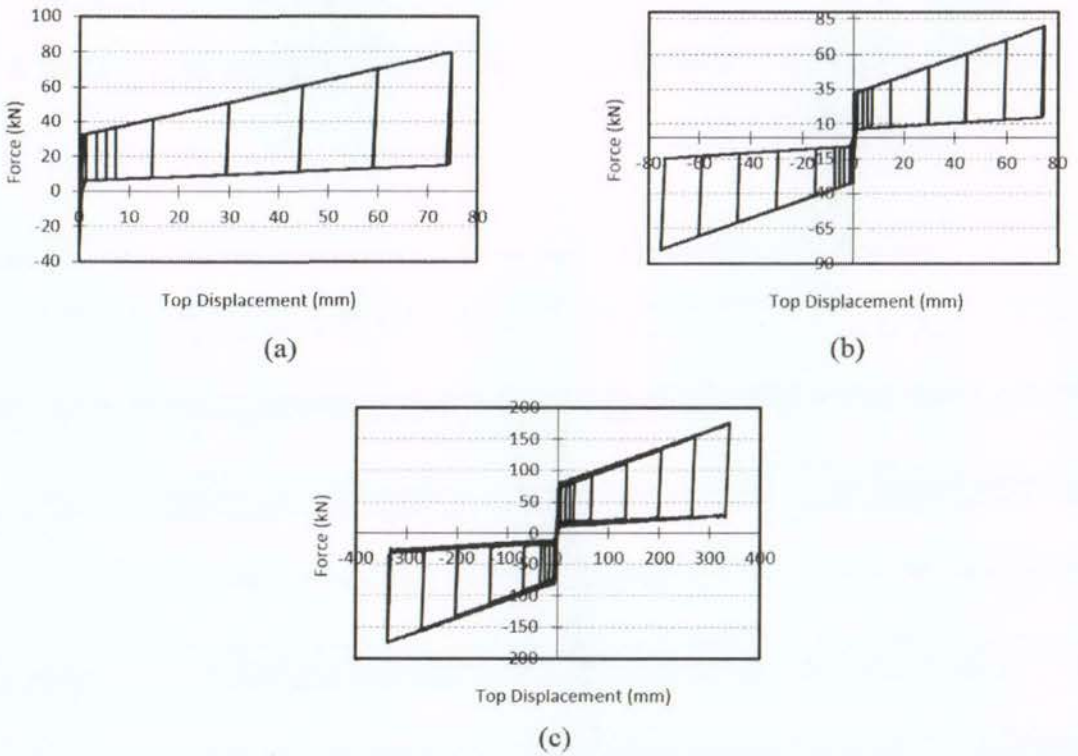

Fig. 13. Hysteretic response of the CLT coupled wall system with RSF joints: a) RSF joint connecting the walls to the boundary columns b) RSF joint connecting two walls c) Total system.

Table 6
The slected ground motions and scaling.

Event	Year	PGA (g)	Scaled PGA (ULS)	Scaled PGA (MCE)
El Centro	1940	0.31	0.31	0.56
Northridge	1994	0.23	0.33	0.59
Kobe	1995	0.82	0.41	0.74
Landers	1992	0.28	0.34	0.64
Christchurch	2011	0.48	0.38	0.53

position at the end of all simulations. This confirms the fully self-centring behaviour which can be attributed to the RSF joints implemented in the system. It should be emphasized that this behaviour is achieved without relying on any additional vertical loads such as the force from the post-tensioned cables [7] or the gravity loads [15].

The New Zealand standard recommends a drift of 2.5% as the upper bound limit for the structures subjected to ULS earthquakes [27]. It also suggests that this limit can be increased to 3.75% in case of a MCE event (with 1/2500 annual period of exceedance). These limitations are indicated in Fig. 15. From the figure, it is apparent that the maximum displacements for the MCE events are significantly higher than those for the ULS events. The uppermost recorded displacement among the MCE events is for Landers event which is approximately 3.4% of lateral drift. For ULS events, the maximum displacement was recorded for the Christchurch (2.3%). It can be seen that all of the recorded displacements are below the defined maximum allowable limits which indicates the efficiency of the proposed system in terms of mitigating the drift demands.

Fig. 16 shows the hysteretic response of one of the RSF ductile links subjected to the Landers MCE event. The joint was implemented between two of the adjoining CLT walls thus it is working in both tension and compression. It can be seen that the general hysteretic behaviour of the joint is consistent with results of the quasi-static analysis (see Fig. 13(b)). The maximum displacements are 33 mm in compression and 68 mm in tension which the latter is close to the designed capacity for the joint (75 mm). Furthermore, the figure confirms that the RSF joint maintained its stiffness during the numerous cycles of seismic loading and unloading. Also, the rate of absorbing the earthquake energy is amplified as the deflection in the joint increased. These facts strongly imply that the proposed lateral load resisting system has the potential to be further developed as an efficient solution for seismic resilient buildings.

5. Conclusions

From this study, it can be concluded that there is potential to significantly improve the seismic performance of hybrid timber-steel structures by using the innovative Resilient Slip Friction (RSF) joints. It is experimentally confirmed that this joint is able to provide a self-centring behaviour in addition to a significant rate of seismic energy dissipation through friction. Experimental joint component tests carried out on a RSF joint specimen with different levels of slip force exhibited stable flag-shaped hysteretic loops demonstrating the re-centering

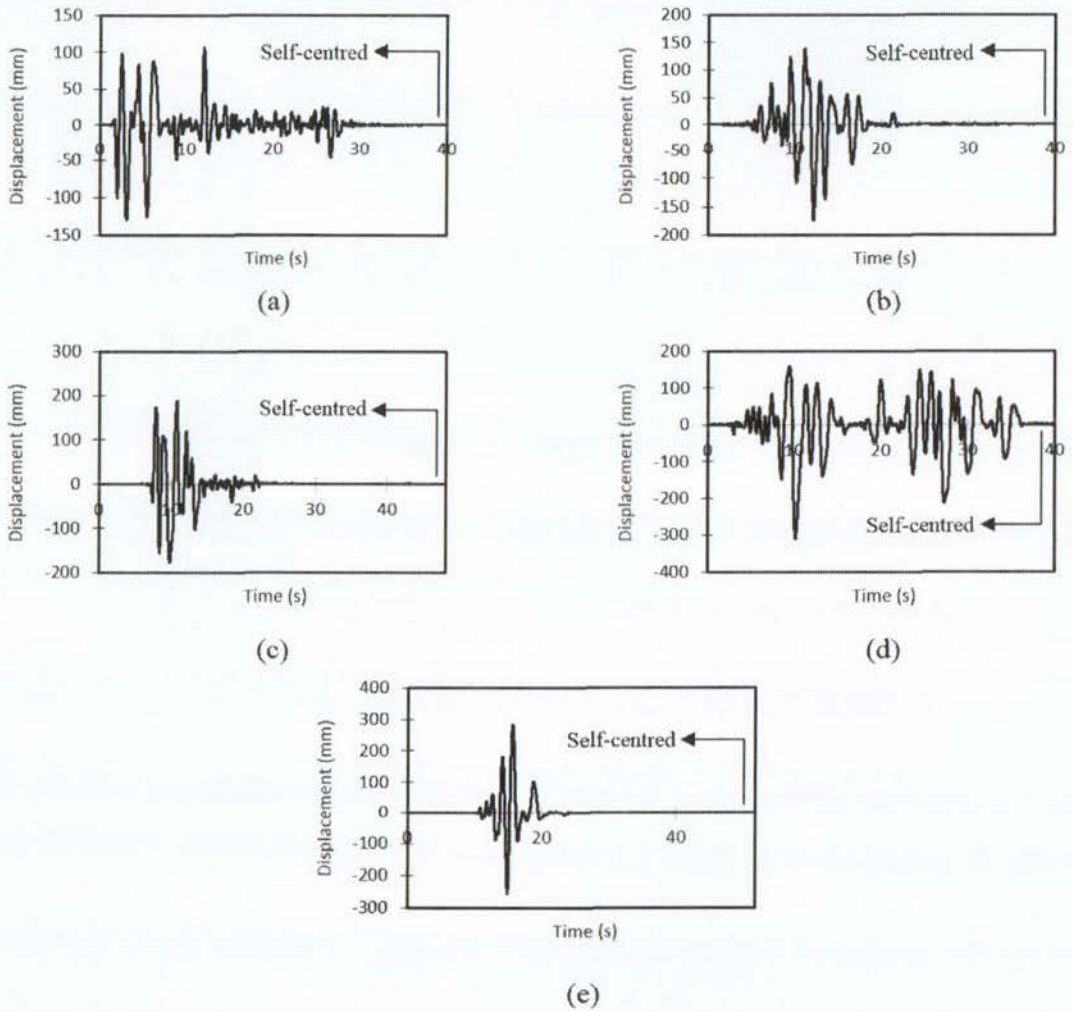

Fig. 14. Roof displacement response for MCE events: a) El Centro b) Northridge c) Kobe d) Landers e) Christchurch.

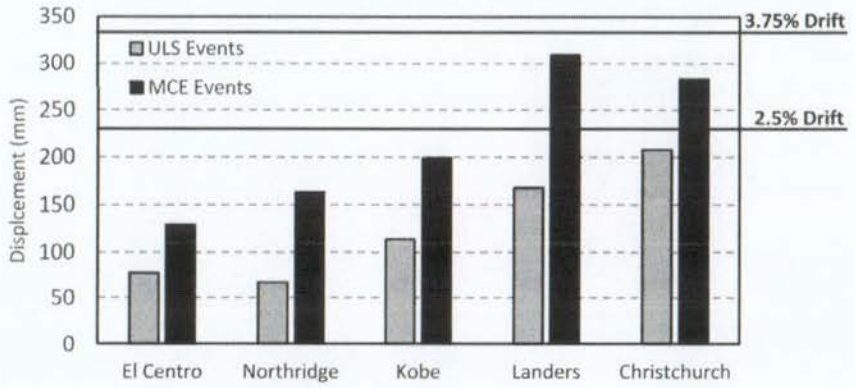

Fig. 15. Maximum roof displacement for MCE events: a) El Centro b) Northridge c) Kobe d) Landers e) Christchurch.

capacity. The Damper – Friction Spring link element in SAP2000 is adopted to represent the RSF joints in numerical modelling and its accuracy was validated by comparing the numerical results with the experimentally obtained data.

A new type of hybrid lateral load resisting system comprised of rocking CLT walls and RSF ductile links along the edge of the panels is introduced. This system also includes steel boundary columns to carry the gravity loads and also to de-couple the vertical movements of the perpendicular walls due to bi-directional rocking motion. The preliminary numerical results of displacement-control quasi-static analyses confirmed the potential to have a new resilient structural system for hybrid structures. Furthermore, non-linear time-history dynamic simulations on a three story prototype structure showed a fully self-centring behaviour as no residual damage was recorded. Moreover, the maximum displacements were within the thresholds indicated by the New Zealand standard for the Ultimate Limit State (ULS) seismic events and Maximum Credible Earthquake (MCE).

Owing to the reason that the resilience of the system is attributed to the hysteretic behaviour of the RSF joints, the proposed structural system can effectively be extended to steel and reinforced concrete structures. To augment the finding of this research, large scale experimental testing is planned to further investigate the performance of this new introduced seismic resistant hybrid coupled wall system.

Acknowledgement

The authors would like to thank the Earthquake Commission Research Foundation (EQC) of New Zealand for the financial support of the presented research under the project code "EQC 15/U710".

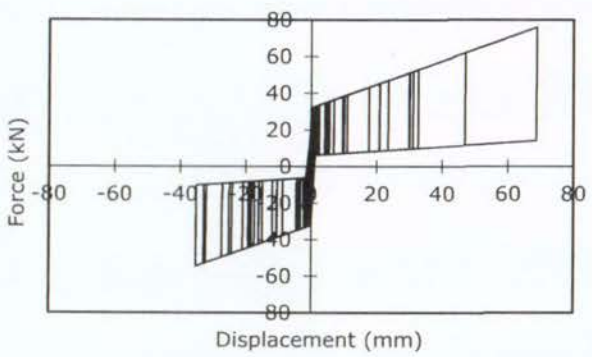

Fig. 16. Hysteretic response of the RSF ductile link subjected to the Landers event (MCE).

References

[1] S. Gagnon, C. Pirvu, CLT Handbook: Cross Laminated Timber, FPInnovations, 2011.
[2] M.J.N. Priestley, S. Sritharan, J.R. Conley, S. Pampanin, Preliminary results and conclusions from the PRESSS five-story precast concrete test building, PCI J. 44 (6) (1999) 42–67.
[3] A. Palermo, S. Pampanin, A.H. Buchanan, Experimental investigations on LVL seismic resistant wall and frame subassemblies, First European Conference on Earthquake Engineering and Seismology, 2006 (Geneva, Switzerland).
[4] A. Palermo, S. Pampanin, A. Buchanan, M. Newcombe, Seismic design of multi-storey buildings using laminated veneer lumber (LVL), New Zealand Society for Earthquake Engineering Conference (NZSEE), 2005 (Taupo, New Zealand).
[5] T. Smith, F. Ludwig, S. Pampanin, M. Fragiacomo, A. Buchanan, B. Deam, A. Palermo, Seismic response of hybrid-LVL coupled walls under quasi-static and pseudo-dynamic testing, New Zealand Society for Earthquake Engineering Conference (NZSEE), 2007 (Palmerston North, New Zealand).
[6] A. Iqbal, S. Pampanin, A. Palermo, A.H. Buchanan, Performance and design of LVL walls coupled with UFP dissipaters, J. Earthq. Eng. 19 (3) (2015) 383–409.
[7] F. Sarti, A. Palermo, S. Pampanin, Development and testing of an alternative dissipative posttensioned rocking timber wall with boundary columns, J. Struct. Eng. (2015) E4015011.
[8] A. Iqbal, T. Smith, S. Pampanin, M. Fragiacomo, A. Palermo, A.H. Buchanan, Experimental performance and structural analysis of plywood-coupled lvl walls, J. Struct. Eng. 142 (2) (2015) 4015123.
[9] E.P. Popov, C.E. Grigorian, T.S. Yang, Developments in seismic structural analysis and design, Eng. Struct. 17 (3) (1995) 187–197.
[10] G.C. Clifton, G.A. MacRae, H. Mackinven, S. Pampanin, J. Butterworth, Sliding hinge joints and subassemblies for steel moment frames, New Zealand Society for Earthquake Engineering Conference (NZSEE), 2007 (Palmerston North, New Zealand).
[11] H. Khoo, C. Clifton, G. MacRae, H. Zhou, S. Ramhormozian, Proposed design models for the asymmetric friction connection, Earthq. Eng. Struct. Dyn. 44 (8) (2015) 1309–1324.
[12] A. Filiatrault, Analytical predictions of the seismic response of friction damped timber shear walls, Earthq. Eng. Struct. Dyn. 19 (2) (1990) 259–273.
[13] W.Y. Loo, C. Kun, P. Quenneville, N. Chouw, Experimental testing of a rocking timber shear wall with slip-friction connectors, Earthq. Eng. Struct. Dyn. 43 (11) (2014) 1621–1639.
[14] W.Y. Loo, P. Quenneville, N. Chouw, A numerical study of the seismic behaviour of timber shear walls with slip-friction connectors, Eng. Struct. 34 (2012) 233–243.
[15] A. Hashemi, R. Masoudnia, P. Quenneville, A numerical study of coupled timber walls with slip friction damping devices, Constr. Build. Mater. 121 (2016) 373–385.
[16] A. Hashemi, W.Y. Loo, R. Masoudnia, P. Zarnani, P. Quenneville, Ductile cross laminated timber (CLT) platform structures with passive damping, World Conference of Timber Engineering (WCTE2016), 2016 (Vienna, Austria).
[17] A. Hashemi, R. Masoudnia, P. Quenneville, Seismic performance of hybrid self-centring steel-timber rocking core walls with slip friction connections, J. Constr. Steel Res. 126 (2016) 201–213.
[18] P. Zarnani, P. Quenneville, "A Resilient Slip Friction Joint," Provisional patent no. 7083, 2015.
[19] W.Y. Loo, P. Quenneville, N. Chouw, A new type of symmetric slip-friction connector, J. Constr. Steel Res. 94 (2014) 11–22.
[20] F. Wanninger, A. Frangi, M. Fragiacomo, Long-term behavior of posttensioned timber connections, J. Struct. Eng. 141 (6) (2014) 4014155.
[21] P. Zarnani, A. Valadbeigi, P. Quenneville, Resilient Slip Friction (RSF) joint: a novel connection system for seismic damage avoidance design of timber structures, World Conference of Timber Engineering (WCTE2016), 2016 (Vienna, Austria).
[22] A. Hashemi, P. Zarnani, A. Valadbeigi, R. Masoudnia, P. Quenneville, Seismic resistant cross laminated timber structures using an innovative resilient friction damping system, New Zealand Society for Earthquake Engineering Conference (NZSEE), 2016 (Christchurch, New Zealand).
[23] G.S. Djojo, G.C. Clifton, R.S. Henry, Rocking steel shear walls with energy dissipation devices, New Zealand Society for Earthquake Engineering Conference (NZSEE), 2014 (Palmerston North, Auckland).

[24] F. Sarti, A. Palermo, S. Pampanin, Quasi-static cyclic testing of two-thirds scale unbonded posttensioned rocking dissipative timber walls, J. Struct. Eng. 142 (4) (2015) E4015005.
[25] Computers and structures, SAP2000. (2011), 2011 (Berkeley, CA).
[26] M.J.N. Priestley, G.M. Calvi, Displacement-based Seismic Design of Structures, IUSS Press, Pavia, Italy, 2007.
[27] New Zealand Standard, Structural Design Actions (NZS 1170.5), 2004 (Wellington, New Zealand).
[28] A.H. Buchanan, N.Z.T.I. Federation, Timber design guide, New Zealand Timber Industry Federation, 1999.
[29] A.S.T.M. Standard, Stand. test methods cycl. load test shear resist. vert. elem. lateral force resist. syst (E2126), Build. West Conshohocken, PA Am. Soc. Test. Mater. 2009.

Experimental Testing of Rocking Cross-Laminated Timber Walls with Resilient Slip Friction Joints

Ashkan Hashemi[1]; Pouyan Zarnani[2]; Reza Masoudnia[3]; and Pierre Quenneville, M.ASCE[4]

Abstract: Allowing a wall to rock and uplift during a seismic event can cap the forces and minimize the postevent residual damage. Slip friction connections comprised of flat steel plates sliding over each other have been experimentally tested as the hold-down connectors in timber shear walls and performed well in terms of the hysteretic behavior and the energy dissipation rate. However, the main disadvantage of these joints is the undesirable residual displacements. In recognition of this fact, a novel type of friction joint called a resilient slip friction (RSF) joint is proposed. The innovative configuration of this joint provides the energy dissipation and self-centering behavior all in one compact package. This paper describes the large-scale experimental test conducted on a rocking cross-laminated timber (CLT) wall with RSF joints as the hold-down connectors. Additionally, a series of capacity equations are presented and validated by comparing the analytical results with the experimental data. The results confirmed that this technology has the potential to provide a robust solution for seismic-resilient structures. **DOI: 10.1061/(ASCE)ST.1943-541X.0001931.**

Author keywords: Rocking walls; Cross-laminated timber; Resilient slip friction (RSF) joints; Self-centering; Damage avoidance; Resilience; Shear key; Wood structures.

Introduction

Cross-laminated timber (CLT) is a relatively new engineered wood product made of several layers of timber boards stacked and glued crosswise (Gagnon and Pirvu 2011). This product was first developed in Austria in the 1990s and then in other parts of the world. Cross-laminated timber has many advantageous characteristics such as easy handling, high level of prefabrication, and a relatively higher strength-to-weight ratio compared with similar products made with other materials (such as precast concrete panels). Owing to these reasons, CLT has been becoming more well known in commercial and residential applications during the last two decades especially in midrise buildings. The common practice in CLT construction is the use of traditional steel connectors with mechanical fasteners such as nails, bolts, rivets, and screws. However, the latest research findings show that these connections are subjected to irrecoverable damage during an earthquake. The shake table tests on a 7-story building made of CLT panels proved that the serious damage in the connections, particularly in the hold downs, is likely to be the governing failure mode for the building (Ceccotti et al. 2013). Moreover, high response accelerations with a maximum of $3.8g$ were recorded during the tests, which confirmed the necessity of implementing additional damping devices to provide energy dissipation for the structure.

Ajrab et al. (2004) proposed the application of rocking walls in lieu of traditional fixed-base shear walls. They concluded that the use of rocking walls is the most suitable solution for low-rise to midrise buildings. However, this concept may be considered as an unreliable solution for high-rise structures owing to the lack of energy dissipation mechanism and the consequent large lateral displacements. The reason is that in a rocking wall, the force reactions are almost entirely taken by the connections and the rocking elements are designed to remain as elastic rigid bodies. Ajrab et al. (2004) also concluded that introducing supplementary damping devices to the system may overcome this deficit. Marriot et al. (2008) dynamically tested posttensioned precast concrete walls with mild steel elements as damping devices attached to the walls. Sarti et al. (2012) introduced and tested the concept of posttensioned timber shear walls with U-shaped flexural plates (UFPs) in addition to mild steel fuse type dampers at the base. The last two concepts demonstrated an acceptable seismic performance. Nevertheless, it should be noted that energy absorption occurs through plastic deformation or yielding of the devices. Thus, the dampers are most likely to be repaired or replaced, which adds to the cost and may be impossible depending on the physical location of the devices in the building. In recognition of this fact, damage-avoidant energy dissipaters such as slip friction connections or high-force-to-volume (HF2V) dampers were developed (Wrzesniak et al. 2016).

Loo et al. (2014b, 2015) introduced and tested slip friction connections as the hold-down connectors at the two base corners of a rocking laminated veneer lumber (LVL) wall. Friction devices date back to the 1980s (Baktash et al. 1983; Pall et al. 1980) and have been proven to have one of the most efficient energy dissipation mechanisms, which occurs due to sliding of flat steel plates (Bora et al. 2007; Khoo et al. 2015; MacRae et al. 2010; Popov et al. 1995). The experimental tests of Loo et al. (2014a) confirmed the previous findings. Nevertheless, such systems have a major

[1]Ph.D. Candidate, Dept. of Civil and Environmental Engineering, Faculty of Engineering, Univ. of Auckland, Private Bag 92019, Auckland 1142, New Zealand (corresponding author). E-mail: ahas439@aucklanduni.ac.nz

[2]Lecturer in Structural Engineering, Dept. of Built Environment Engineering, School of Engineering, Computer and Mathematical Sciences, Auckland Univ. of Technology, Private Bag 92006, Auckland 1142, New Zealand. E-mail: pouyan.zarnani@aut.ac.nz

[3]Ph.D. Candidate, Dept. of Civil and Environmental Engineering, Faculty of Engineering, Univ. of Auckland, Private Bag 92019, Auckland 1142, New Zealand. E-mail: rmas551@aucklanduni.ac.nz

[4]Professor of Timber Design and Head, Dept. of Civil and Environmental Engineering, Faculty of Engineering, Univ. of Auckland, Private Bag 92019, Auckland 1142, New Zealand. E-mail: p.quenneville@auckland.ac.nz

Note. This manuscript was submitted on February 16, 2017; approved on July 6, 2017; published online on November 10, 2017. Discussion period open until April 10, 2018; separate discussions must be submitted for individual papers. This paper is part of the ***Journal of Structural Engineering***, © ASCE, ISSN 0733-9445.

drawback, the undesired residual drifts after the earthquakes (Hashemi et al. 2016a, b; Loo et al. 2012). It means that an additional mechanism is required to bring back the structure to its initial position. Hashemi et al. (2016c) proposed the use of posttensioned beam-to-column joints to recenter the shear walls with slip friction connections. The most common solution is the use of posttensioned cable up the height of the timber walls, which was tested in several different configurations (Iqbal et al. 2015a, b; Sarti et al. 2015a; Smith et al. 2007). Nevertheless, the loss of posttensioning force due to shrinkage in timber potentially requires the restressing of the cables, which is always costly and only possible with a special type accessible anchorage (Wanninger et al. 2014). Wrzesniak et al. (2016) proposed the application of HF2V dampers for a glue-laminated timber wall. The results asserted the low damage characteristic; however, the self-centering behavior was lost for lateral drifts more than 1.3%.

This paper presents the results of displacement-control quasi-static experimental tests on a rocking CLT shear wall with new resilient slip friction (RSF) joints [P. Zarnani and P. Quenneville, "A resilient slip friction joint," U.S. Patent No. 7083 (2015)] as hold-down connectors. The RSF joint is a novel type of friction connection that, as a result of its special configuration, can provide energy dissipation in addition to self-centering behavior, all in one compact package with no postevent maintenance (Zarnani et al. 2016). This joint is able to offer a flag-shaped hysteresis representing fully self-centering behavior. A simple analytical procedure is described to predict the capacity of the proposed system. Moreover, a new type of shear transferring device is introduced and tested. This device was specially designed to effectively eliminate the slip between the wall and the foundation by mitigating the uplift occurring at the base of the rocking wall while efficiently transferring the shear forces to the foundation.

The main objectives of this study are (1) to investigate the efficiency of the proposed concept as the lateral load resisting system; (2) to study the hysteretic behavior of a rocking CLT wall with RSF joints; (3) to evaluate the feasibility and effectiveness of the adopted solution for connecting the RSF joints to the CLT wall; (4) to evaluate the performance of the proposed shear transferring device; (5) to investigate the accuracy of the proposed capacity equations for predicting the hysteretic behavior of the wall by comparing the experimental results with the analytically obtained hysteretic loops; and (6) to introduce and verify a numerical tool for modeling the structures containing the proposed concept.

RSF Joint and Design Equations

As can be seen in Fig. 1, a RSF joint is comprised of grooved outer cap plates and the center slotted plates clamped together by high-strength bolts and Belleville springs (conical disc springs) (Hashemi et al. 2016d; Zarnani et al. 2016). When the applied force to the joint overcomes the frictional resistance between the surfaces, the center slotted plates start to slip and energy will be dissipated over friction. The specific shape of the grooves together with the use of Belleville springs provide the self-centering characteristic. In other words, the reversing force due to compaction of the springs, which is higher than the friction force between the sliding surfaces, mobilizes the center plates and makes them return to their original position.

A series of capacity equations has been developed to predict the load-deformation behavior of the RSF joint. This paper focuses on the symmetric configuration of RSF joints to be used as hold-down connectors for a shear wall. Thus, only the capacity equations for symmetric RSF joints are described in this section. This concept is able to be used in asymmetric and combined symmetric-asymmetric configurations as well. Zarnani et al. (2016) gives more information about other applications of RSF joints and the associated design procedures. Fig. 2 shows the acting forces on a symmetric RSF joint before slipping and at the ultimate deflection. Based on the free body diagrams displayed in the figure, the slip force ($F_{RSF,slip}$) can be determined by Eq. (1)

$$F_{RSF,slip} = 2n_b F_{b,pr}\left(\frac{\sin\theta + \mu_s \cos\theta}{\cos\theta - \mu_s \sin\theta}\right) \tag{1}$$

in which θ = groove's angle; μ_s = coefficient of static friction; $F_{b,pr}$ = bolt clamping force as a result of being prestressed; and n_b = number of bolts on each splice (in Fig. 1, n_b equals 2). The residual force at the end of unloading ($F_{RSF,residual}$) is given by Eq. (2), where μ_k is the coefficient of kinetic friction, which can

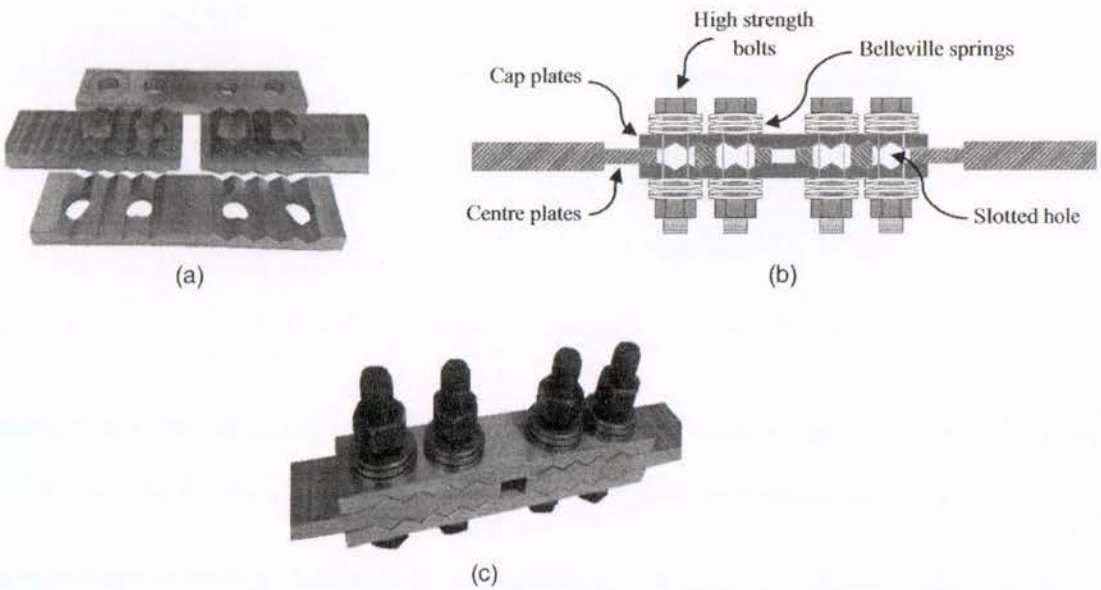

Fig. 1. RSF joint (data from Hashemi et al. 2016d; Zarnani et al. 2016): (a) cap plates and center slotted plates; (b) schematic longitudinal section view of the joint and the associated components; (c) assembly

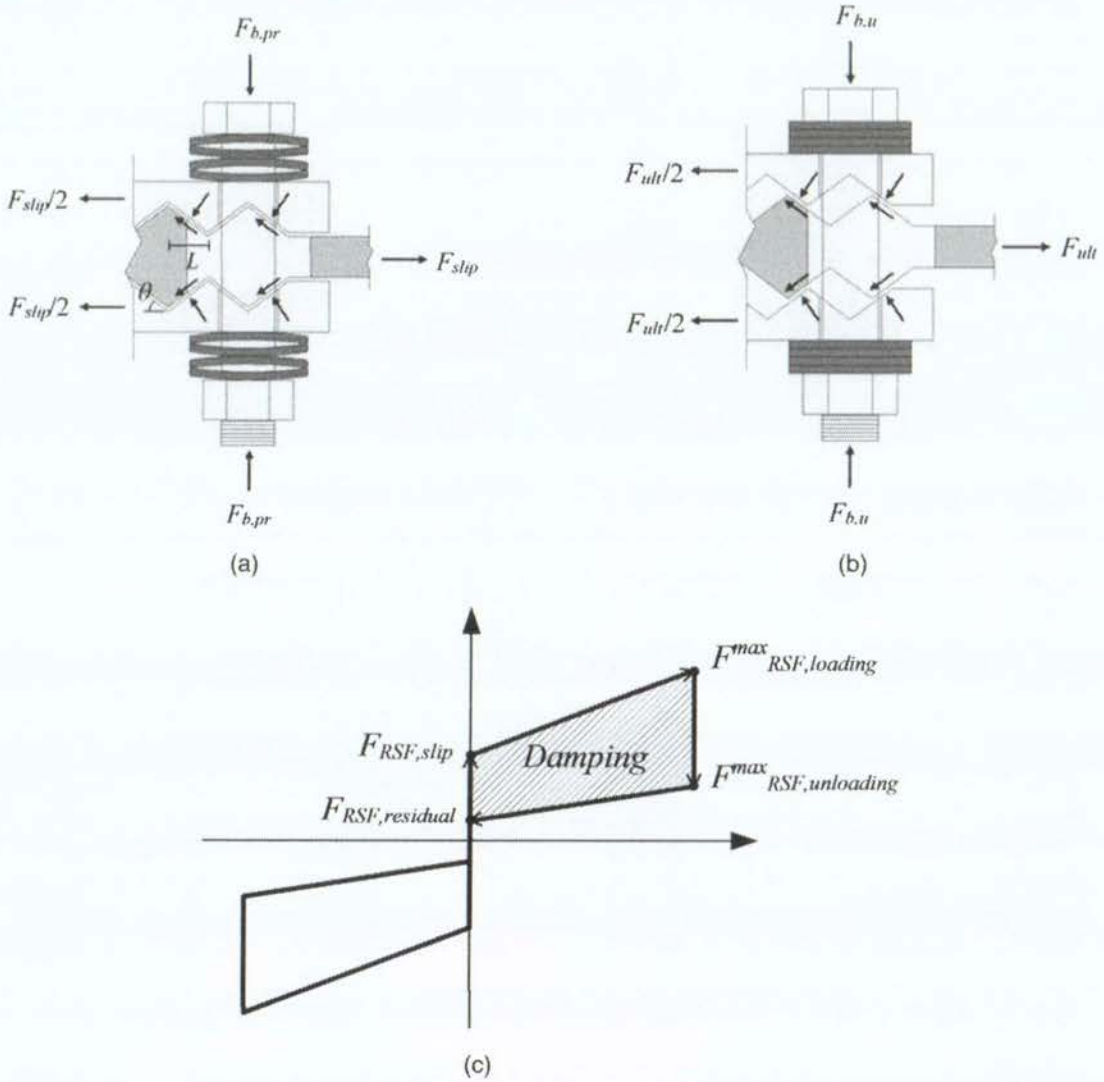

Fig. 2. Symmetric RSF joint: (a) acting forces before slipping; (b) acting forces at the end of slipping; (c) hysteresis

be assumed as $0.85\mu_s$ (Hashemi et al. 2017a). Fig. 2(c) illustrates the analytically predicted hysteresis for the RSF joint

$$F_{RSF,residual} = 2n_b F_{b,pr}\left(\frac{\sin\theta - \mu_k \cos\theta}{\cos\theta + \mu_k \sin\theta}\right) \tag{2}$$

The ultimate force on the bolt ($F_{b,u}$) is given by Eq. (3), in which k_s is the stiffness of the stack of springs on the bolt and Δ_s is the maximum possible deflection for them

$$F_{b,u} = F_{b,pr} + k_s \Delta_s \tag{3}$$

The maximum deflection in a RSF joint can be determined by Eq. (4), where n_j is the number of center plates acting in a series (e.g., n_j equals 1 for a single acting joint and equals 2 for a double acting one). To exemplify, the RSF joints shown in Fig. 1 contain two slotted center plates, thus $n_j = 2$

$$\delta_{\max} = n_j \frac{\Delta_s}{\tan\theta} \tag{4}$$

For the joint to be self-centered, it is essential to satisfy $\tan\theta > \mu_s$ and $L > \Delta_s/\tan\theta$, where L is the horizontal distance between the top and bottom of a groove. The first equation is to make sure that the force in the bolt due to the compaction of Belleville springs is sufficient to overcome the frictional resistance between the sliding surfaces and the second one is to check that the Belleville springs are fully compacted (and the RSF joint is locked) before the sliding plates reach the end of the ramp [Fig. 2(b)].

RSF Specimen and Joint Component Test

In the presented research, the RSF joints were meant to be used as replacements of traditional hold-down connectors for a CLT shear wall. For this purpose, two symmetric RSF joints were manufactured with two cap plates and two center plates made of mild steel Grade 350. The angle of the grooves was 15° and the slotted length for each of the two center plates was 35 mm, which led to a maximum displacement of 70 mm in tension (uplift). Additionally, a 20-mm gap was considered between the two center plates. In this way, the joint was able to accommodate up to 20 mm of deflection in compression [Fig. 4(b)]. The three-dimensional rendering and the geometry of the manufactured plates are shown in Fig. 3.

The Belleville springs had an outside diameter of 70 mm, an inside diameter of 21 mm, a thickness of 6.5 mm, a maximum deflection of 1.5 mm, and a maximum load capacity of 110 kN at the

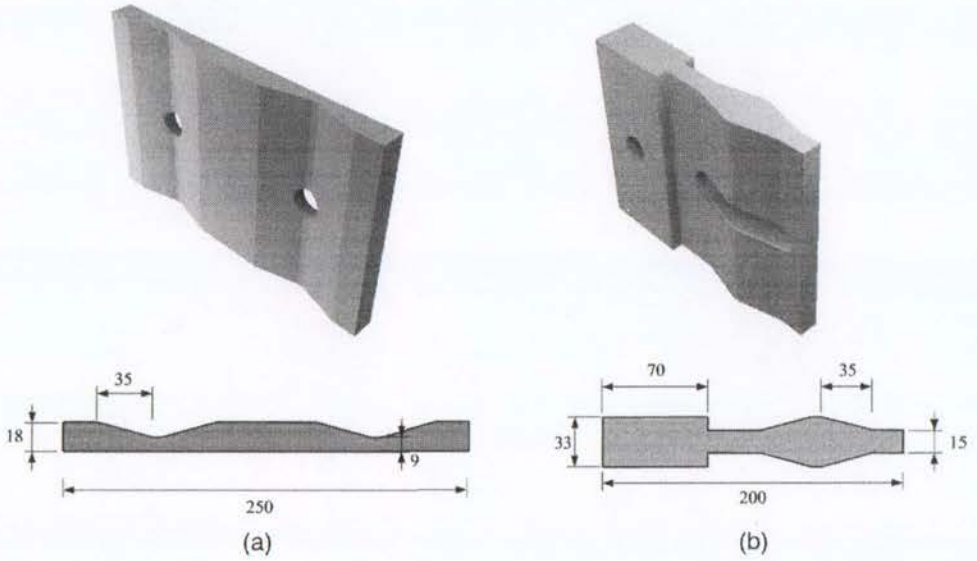

Fig. 3. Three-dimensional renderings and geometric properties of the manufactured RSF joints (dimensions in millimeters): (a) cap plate before attaching the stiffeners; (b) center slotted plate

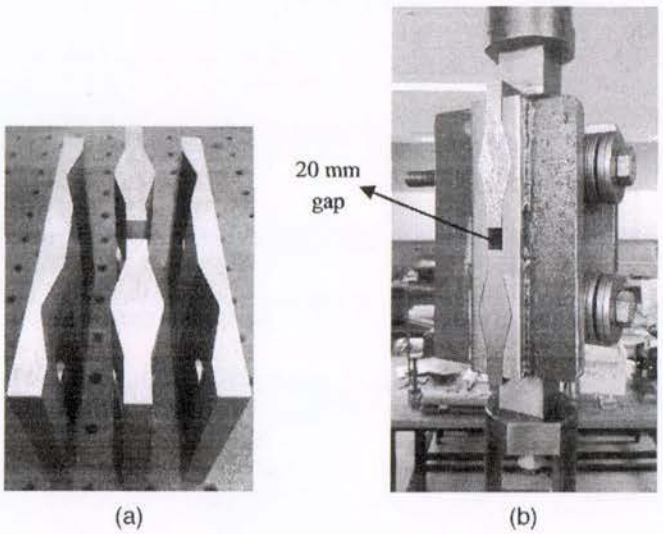

Fig. 4. RSF joint component test: (a) manufactured plates before attaching the stiffeners to the cap plates (b) test setup and assembly of the joint

flat state. Two 20-mm-diameter 8.8-grade bolts (with 800-MPa yield strength) with nine disc springs per bolt per side were used. The springs were stacked in a series arrangement to increase the total deflection while maintaining the desired tension in the bolts. Previous tests on the springs showed that they approximately represent a linear load-deformation behavior. Therefore, the turn-of-nut method was used to compact the springs. In this method, the number of rotations of the nut required to achieve a specific compaction level is specified by dividing the target deflection by the pitch of the threaded bolts. A depth micrometer device is also used to monitor the deflection of the stack of springs. A special type of grease (applicable for high pressures) was used between the sliding plates to control the possible galling effect.

The Instron (Melbourne, Australia) universal testing machine with a maximum load capacity of 100 kN was used for the experiments. The load was controlled by the machine's built-in load cell and the displacement was monitored by a LVDT fixed to the two cap plates. The loading heads were connected to the two cap plates. An average loading rate of 0.5 mm/s was adopted for all tests. Fig. 4 displays the manufactured plates and the test setup. Two $20 \times 50 \times 220$ mm mild steel stiffeners had later been attached to each cap plate to avoid the possible out-of-plane deformation.

Altogether, five tests were conducted. Fig. 5 shows the applied load schedule and the load-deformation behavior of the joint for one of the tests as a representative of the general performance of the RSF joint. Hashemi et al. (2017a) provides more information about the conducted joint component tests including all of the results and a detailed discussion.

The applied loading regime was based on previous experiments of Loo et al. (2014b) on conventional slip friction connections, which include three reversed displacement cycles at 20, 40, 67, and 100% of the ultimate deflection. As can be seen from Fig. 5(b), the maximum deformations of the joint in tension and compression are 40 and 15 mm, respectively, because the device is built to accommodate a relatively larger deflection in tension as would be the case for a hold-down connector. This will be further explained in "Testing Methodology."

With respect to the data in Fig 5(b), the joint performed as expected in accordance with the hysteresis predicted by the proposed capacity equations [Fig. 2(c)] (Hashemi et al. 2017b). Needless to say, the flag-shaped load-deformation curves demonstrate a fully self-centering behavior. Furthermore, stable and repeatable loops confirm the low damage characteristic because the joint maintained its strength over several displacement cycles. Although the ultimate displacement was different for tension and compression in the tested joint, it has been experimentally proven that the RSF joint can produce a symmetrical hysteresis if it is designed for such a purpose (Hashemi et al. 2016d).

Test Specimen and Details

Key Structural Elements

Fig. 6 shows the general arrangement of the test setup including a schematic view of the wall and a picture from the test setup.

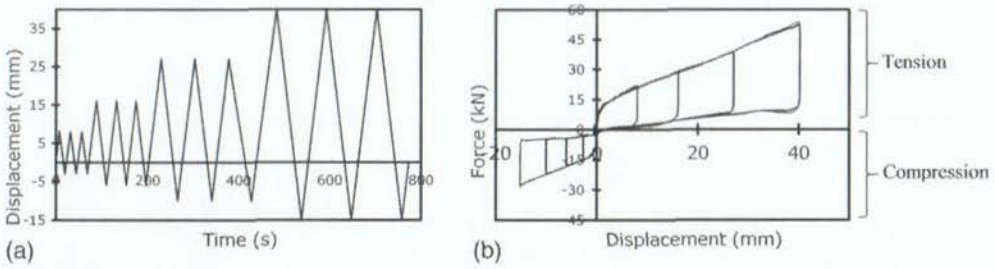

Fig. 5. Results of the RSF joint component test: (a) applied load schedule; (b) load-deformation behavior

This section describes the components of the test rig shown in Fig 6(b) and the instrumentation details.

CLT Wall

The CLT wall used for testing was a 5-layer panel 6 m high, 2,025 mm wide, and 200 mm thick. It had three vertically oriented longitudinal layers and two transverse layers. The width of the timber boards within the panel was 185 mm. The local CLT manufacturer who supplied the panel indicated an elastic modulus of 8,000 MPa [machine-graded timber with Grade 8 (MSG8)] (Buchanan 1999) for the longitudinal and transverse layers with a density of 510 kg/m^3 for all of the boards (corresponds to a total weight of 1,200 kg for the wall panel). In order to connect the RSF joints, two 480 by 345 mm blocks were removed from the corners of the wall and two steel brackets were positioned in the notches. To provide a rigid connection between the RSF devices and the wall, eight fully threaded self-tapping screws 550 mm long and 11 mm in diameter were inserted from beneath to attach the steel brackets to the wall. It was experimentally verified that this solution is capable of providing sufficient stiffness for the connection (Wrzesniak et al. 2016; Masoudnia et al. 2016). The RSF joints were pinned to the steel brackets later. Fig. 7 shows the schematic section of the tested CLT panel and the details of the screwed connection.

RSF Joints

Two identical RSF joints similar to the one that was subjected to joint components testing (described in "RSF Specimen and Joint Component Test") were used as the hold-down connectors for the CLT wall. In order to eliminate any bending moment induced on the joints, a double-pinned assembly was designed. For each RSF joint, two 20-mm high-strength steel pins were specified to connect the RSF joints to the top and bottom steel brackets. The top steel bracket was attached to the CLT panel by screws and the bottom steel brackets were bolted to the foundation plates [Fig. 8(c)].

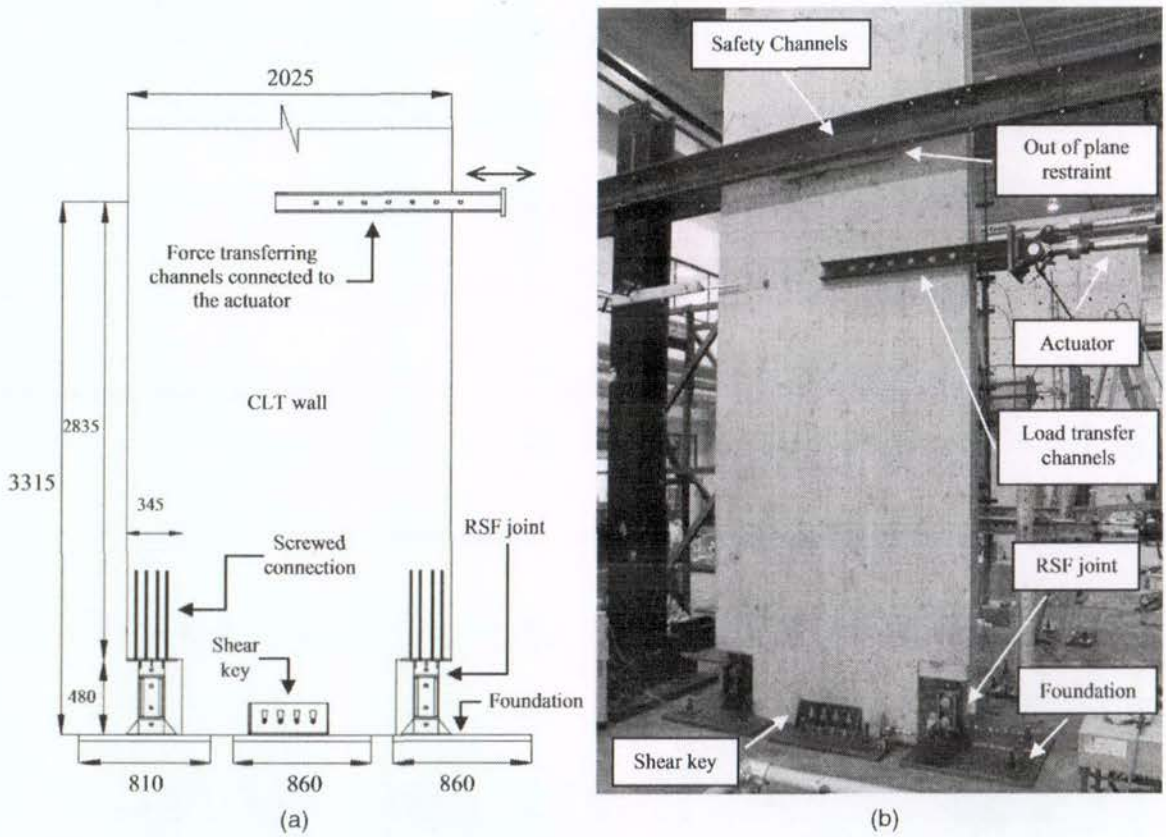

Fig. 6. CLT wall test with RSF joints (dimensions in millimeters): (a) elevation of the wall exhibiting the geometric properties of the test setup and configuration of the components; (b) general arrangement of the test setup

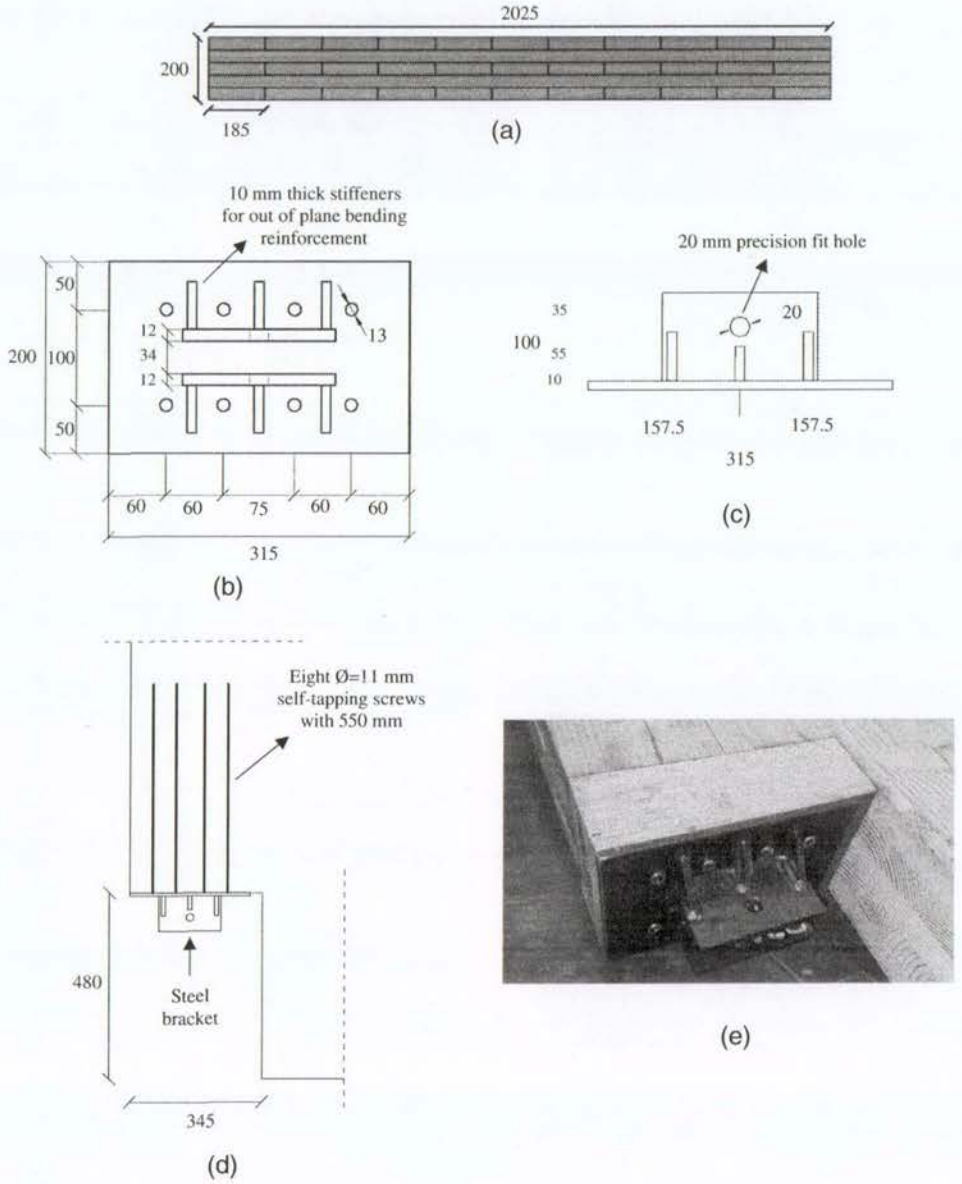

Fig. 7. Tested CLT specimen (dimensions in millimeters): (a) schematic cross section; (b) steel bracket connecting the RSF joint to the wall (plan view); (c) steel bracket connecting the RSF joint to the wall (side view); (d) position of the brackets at the notches and the screws; (e) assembly of the bracket connecting the RSF joint to the CLT panel

These hinges had an approximate tolerance of 0.02 mm between the pin and the pin hole to minimize any possible slopping effect during the tests. Fig. 8 shows the assembly of the RSF joints. Threaded holes had already been drilled in the steel foundation plates where the bottom steel brackets were positioned.

As mentioned in the previous section, the devices were manufactured in a way to be able to accommodate a maximum deflection of 70 mm in tension and 20 mm in compression. To be more specific, when the wall rotates in one direction, the deflection in the opposite joint is comparatively smaller, which is attributed to the lower eccentricity.

Three 36-mm-thick steel plates were used as the foundation under the wall. Each of the plates was anchored to the lab's strong floor by four 27-mm high-strength steel rods with an approximate posttensioning force of 100 kN. In this way, sufficient frictional resistance was provided between the lab's concrete strong floor and the foundation plates to avoid any possible sliding movement. Several threaded holes were created in the foundation to connect the RSF joints and the shear transferring devices to the foundation. The details of the foundation plates are displayed in Fig. 9. The position of the wall on the foundation was determined in accordance with the space limitations of the test hall.

Shear Transferring Devices

The full-scale experimental investigations of Popovski and Gavric (2015) and Yasumura et al. (2015) on CLT buildings built with conventional metal connectors demonstrated that the horizontal sliding between the CLT panel and the foundation (or the floor below) has the highest contribution in the horizontal deformation of the wall panel. This sliding movement, which usually is accompanied by irrecoverable damage in the connectors, significantly reduces the lateral strength of the system. Therefore, a special type of shear transferring device is required to not only eliminate the considerable contribution of the sliding movement in the overall lateral displacement but also to accommodate the uplift occurring at the base of the rocking wall. In recognition of this fact, different solutions

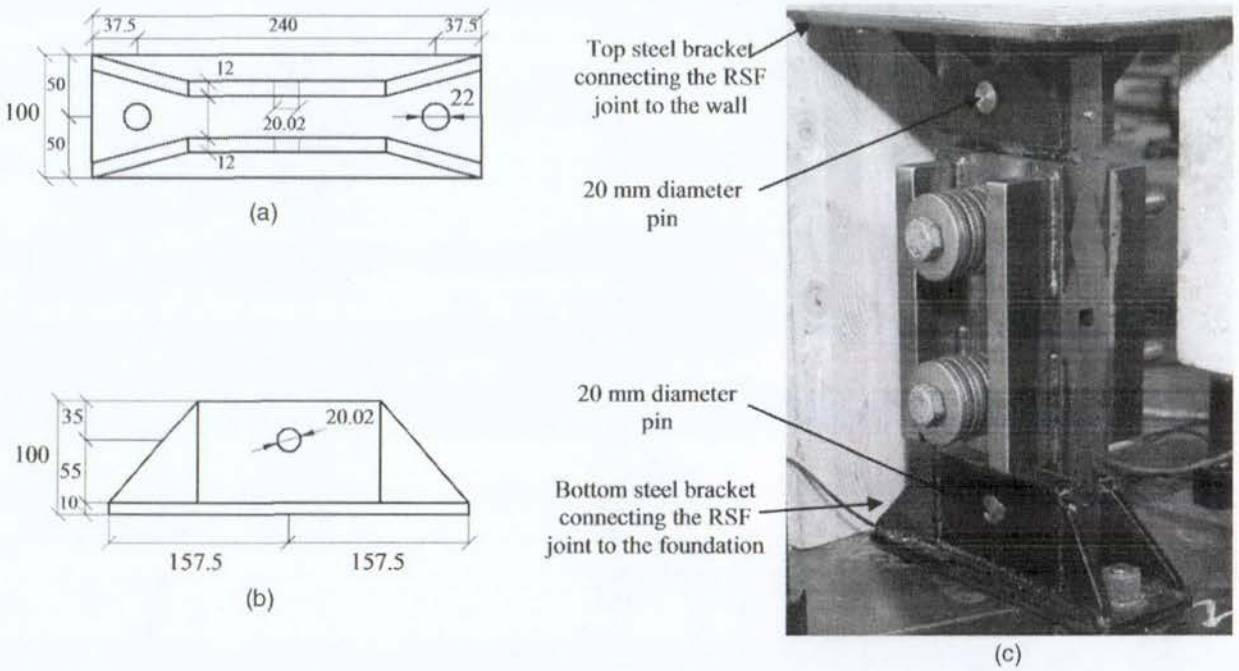

Fig. 8. RSF joint assembly (dimensions in millimeters): (a) steel bracket connecting the RSF joint to the steel foundation (plan view); (b) steel bracket connecting the RSF joint to the steel foundation (side view); (c) RSF joint assembly

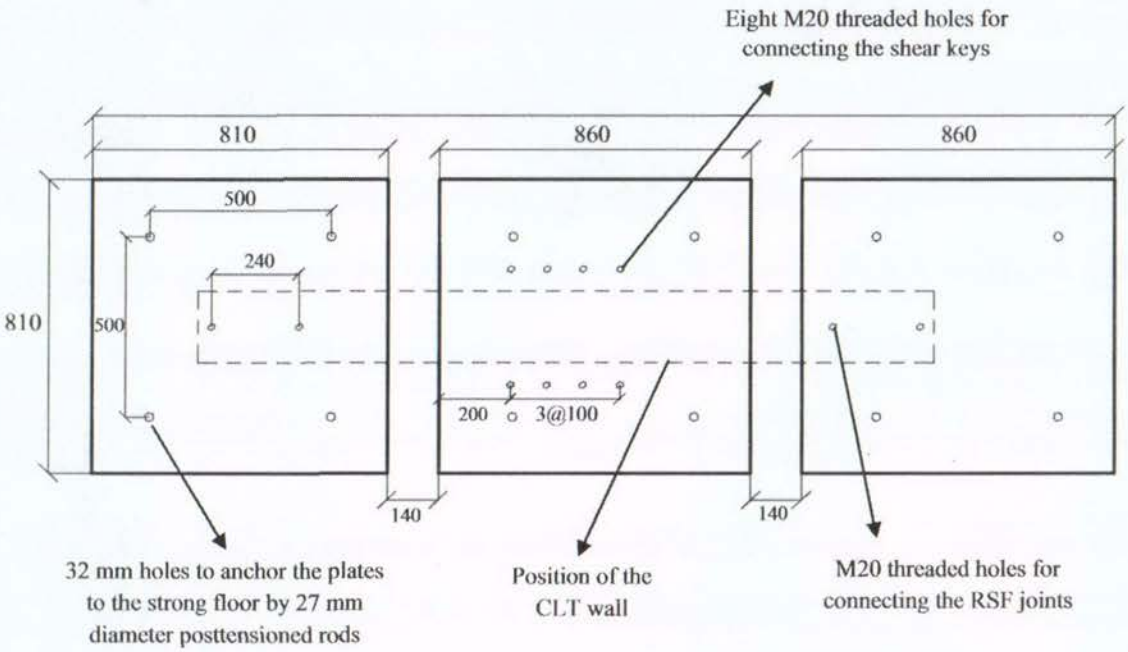

Fig. 9. General arrangement of the foundation plates (dimensions in millimeters)

for shear keys were adopted by researchers. Loo et al. (2014a) proposed and tested a new type of shear key comprised of steel plates attached to the foundation and steel rods attached to the wall to transfer the horizontal forces from the timber wall to the base. Wrzesniak et al. (2016) used steel angles at the corners of the wall to provide shear resistance. Sarti et al. (2015b) employed 40-mm-thick steel plates at the sides of the wall to prevent the in-plane sliding.

In this paper, a novel type of force-transferring device is presented to be used as the shear keys [A. Hashemi and P. Quenneville, "A shear anchor for a structural member," U.S. Patent No. 728725 (2017)]. The proposed device is comprised of conventional high-resistance bolts to transfer the horizontal loads from the wall to the foundation through a steel plate made of mild steel. Under loading, the device performs as intended, providing adequate lateral resistance, while at the same time allowing the wall to rock in the intended manner. The special shape of slots allows the wall to accommodate any uplift at the base level while the wall rocks. The bolts are connected to the timber wall and are always in contact with the slotted plate, making them capable of efficiently transferring the lateral loads to the base. The manufacturing cost of the proposed device is not much different from a regular bolted

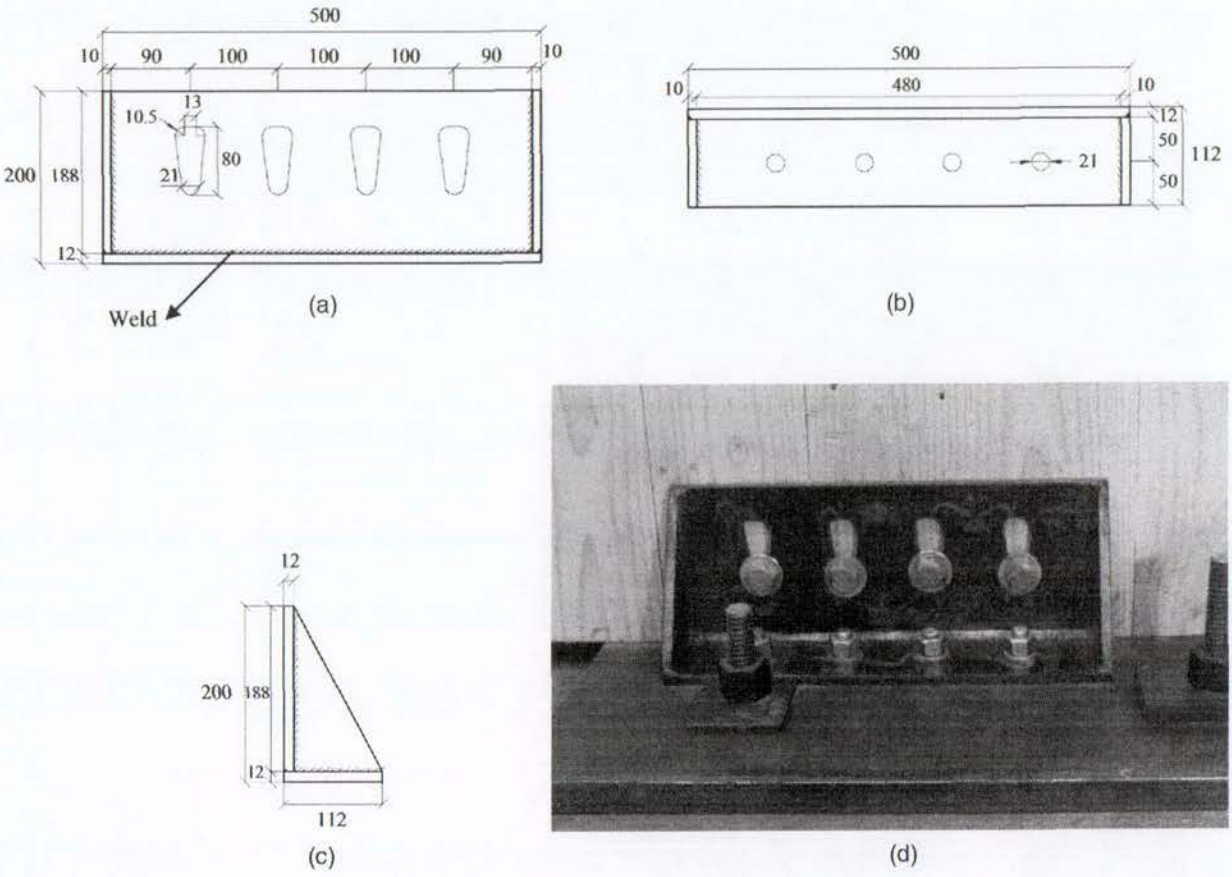

Fig. 10. Shear key [data from New Zealand Patent No. 728725 (2017)] (dimensions in millimeters): (a) front view; (b) top view; (c) side view; (d) image of the device

connection owing to the fact that no special or expensive component is employed.

The shape of the slots can be determined in accordance with the geometry of the rocking wall. The slots can be designed assuming the highest possible lateral drifts (4–5%) to make sure that the bolts do not touch the end of the slot unless in extreme situations, for instance, when a maximum credible earthquake (MCE) takes place (New Zealand Standards 2004). Fig. 10 shows the shear key designed and manufactured for the current test. The shape of the slots corresponds to 5% of lateral drift for the wall. Two devices were used on the two sides of the CLT wall and four M20 bolts were implemented through the wall and the devices to transfer the horizontal forces from the wall to the foundation. The devices were in contact with the CLT wall; however, the contact surfaces were lubricated with grease to avoid any extra frictional resistance while the wall was rocking. Additionally, the same type of lubrication was used in the contact surface between the bolts and the slots.

Experimental Facilities and Equipment

A hydraulic actuator with a maximum stroke of 250 mm was employed to apply the lateral force to the wall at a vertical distance of 3,315 mm from the foundation [Fig. 6(a)]. The force from the actuator was transferred to the CLT panel by two 1,400 by 125 by 65 mm steel channels with 4.7-mm web thickness. The load-transferring channels were connected to the CLT wall by six M24 bolts. To avoid slopping, the bolts were subjected to tensile forces on one side by implementing Belleville springs with 50-kN capacity. The bolts were tightened until the springs became flat, resulting in a frictional resistance of 227 kN between the channels and the wall (static coefficient of friction between wood and steel was assumed as 0.65), which is approximately five times higher than the maximum expected lateral force. For safety reasons, the wall was placed between two steel channels that were bolted to a strong column themselves [Fig. 6(b)]. In order to restrain the out-of-plane movement of the wall, two pieces of 120 by 1,200 mm sawn timber were positioned between the safety channels and the CLT wall. These timber members were bolted to the safety channels and a commercial grease was used in the contact surface between them and the CLT panel to avoid any unpredicted frictional resistance during rocking. Fig 11 shows the load-transferring channels and out-of-plane restraints.

Fig. 12 shows a diagram of the instruments used to measure force and displacements during the test. The experiment was a displacement-control setup in which a 300-kN load cell integrated with the actuator was employed to measure the applied racking force. A LVDT capable of recording deflections up to 150 mm was used to measure the main horizontal displacement of the CLT wall at the height at which the racking force was applied. In addition, a string pot device was used as the backup instrument for the top LVDT. The vertical uplift occurring at the toes of the wall (where the RSF joints are positioned) was gauged by two spring-loaded LVDTs attached to the surface of the CLT panel. Another two LVDTs were employed to monitor the horizontal slip between the CLT wall and the steel foundation, which were placed as close as possible to the shear keys. Fig. 12 displays the instruments and their positions. In addition to the previously mentioned devices, two displacement gauges were also placed where the top steel brackets

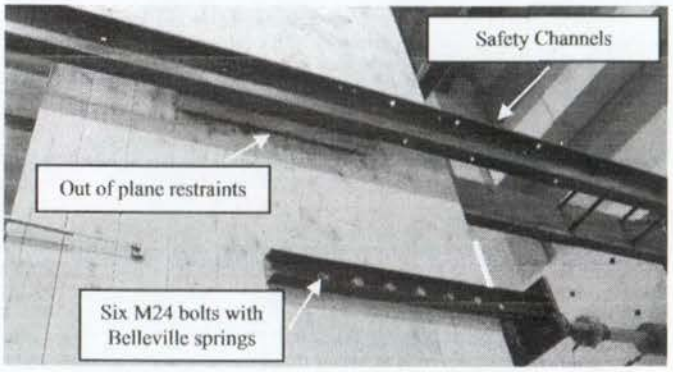

Fig. 11. Load-transferring channels and out-of-plane restraints

were screwed to the CLT panels with the purpose of measuring the possible deformation of the screwed connections.

Testing Methodology

Altogether, seven tests were carried out on the CLT wall with RSF joints in which the joints had two different arrangements with 9 or 11 Belleville springs per bolt on each side. The general configuration of the RSF joints was similar to the tested specimen described in "RSF Specimen and Joint Component Test." The tests were conducted by applying different prestressing forces to the springs to evaluate the performance of the system in different circumstances. Table 1 shows the test matrix including the prestressing forces and the number of disc springs. The stack heights presented in the table were measured by the depth micrometer device.

The adopted displacement schedule was comprised of three reversed cycles applied at increasing amplitudes of 15, 45, 70, and 100% of the ultimate targeted lateral deflection. The maximum displacement was specified as 100 mm, which corresponds to 3% of lateral drift for the wall at the same height where the hydraulic

Table 1. Test Matrix

Test code	Number of springs per bolt on each side	Initial stack height (mm)	Stack height after prestressing (mm)	Slip force for the wall (kN)
Test 1	11	88.0	76.5	11
Test 2	11	88.0	69.7	16
Test 3	11	88.0	59.0	24
Test 4	9	72.0	72.0	2.5
Test 5	9	72.0	60.5	13
Test 6	9	72.0	56.0	17
Test 7	9	72.0	47.2	25

actuator was positioned. This threshold was determined to satisfy most of the building codes around the world including the New Zealand standard, which indicates 2.5% drift as the upper-bound limit for ultimate limit state (ULS) design (New Zealand Standards 2004). Nevertheless, it should be pointed out that the RSF joints can be designed to achieve higher lateral drifts providing that other parts of the building can accommodate those deflections. Fig. 13 illustrates the applied displacement schedule. The adopted loading rate was approximately 0.5 mm/s, which was manually maintained by controlling the oil pressure within the hydraulic actuator.

Results and Discussions

Analytical Prediction for the Lateral Strength of a Rocking CLT Wall with RSF Joints

Fig. 14 shows the acting forces on a rocking CLT wall with RSF joints and the predicted hysteretic behavior for the hold downs. It can be seen that the deflection of the joints corresponds to their lever arm, which is the horizontal distance between the centroid of the RSF joints to the rotating edge of the wall panel. Thus,

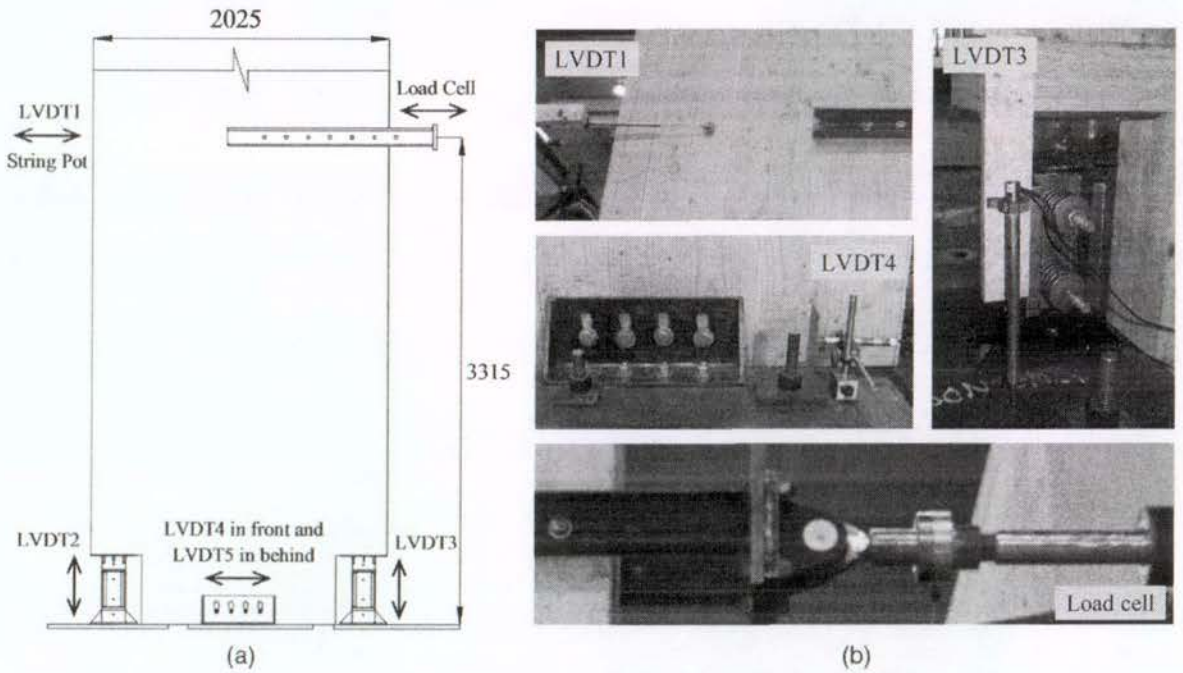

Fig. 12. Instrumentation: (a) schematic configuration; (b) location of the devices

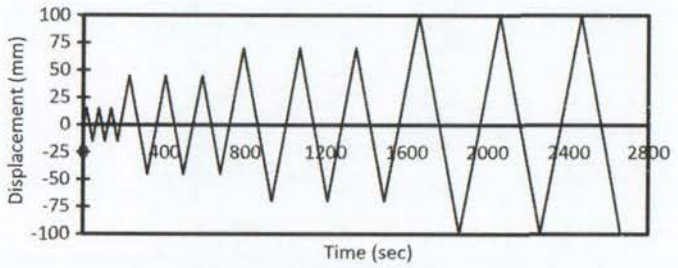

Fig. 13. Applied displacement schedule

$\Delta_{RSF,1}/\Delta_{RSF,2} = L_1/L_2$, where Δ_{RSF} and L are, respectively, the deflection within the RSF joints and the associated lever arms [Fig. 14(a)].

Taking the moments about the rotating point, the horizontal force applied at the top which triggers the rocking movement ($F_{top,slip}$) can be determined by Eq. (5), where H is the height of the wall, W is the applied vertical loads, L_W is the lever arm for the vertical loads, and $F_{RSF,slip}$ is the slip threshold of the RSF joints. It is assumed that the employed RSF joints are identical

$$F_{top,slip} = \frac{1}{H}[WL_W + F_{RSF,slip}(L_1 + L_2)] \tag{5}$$

After slippage, the force within the RSF joints corresponds to the deflection within them. Therefore, the lateral strength of the wall can be accordingly specified by Eq. (6), where $F_{RSF,1}$ and $F_{RSF,2}$ are the forces within the ascending and descending RSF joints, respectively. The relationship between $F_{RSF,1}$ and $F_{RSF,2}$ can be determined by Eq. (7) during the loading of the wall. During the unloading of the wall, this relationship can be calculated using the same equation [Eq. (7)], with $F_{RSF,slip}$ replaced with $F_{RSF,residual}$. The value of $F_{RSF,residual}$ is equal for the two RSF joints. For the lateral direction of movement indicated in Fig. 14(a), the ascending RSF joint is in tension and the descending one is in compression. The schematic hysteretic curves are illustrated in Figs. 14(b and c). By employing Eqs. (6) and (7), the overall load-deformation behavior of the wall can be determined

$$F_{top} = \frac{1}{H}(WL_W + F_{RSF,1}L_1 + F_{RSF,2}L_2) \tag{6}$$

and during the loading of the RSF joints

$$F_{RSF,2} = \frac{L_2}{L_1}(F_{RSF,1} - F_{RSF,slip}) + F_{RSF,slip} \tag{7}$$

The residual force in the wall ($F_{top,residual}$) can be determined by Eq. (5) by replacing $F_{RSF,slip}$ with $F_{RSF,residual}$. The described analytical approach is based on the assumption that the wall panel represents a rigid body during the rocking motion. In other words, it was presumed that the screwed connection is sufficiently rigid and the bending and shear deformation of the CLT panel can be neglected when compared with the overall displacement of the wall. The correctness of these assumptions are investigated in the following section.

Hysteretic Behavior of the CLT Wall

Fig. 15 shows the obtained load-deformation behavior from the seven conducted tests. In all diagrams, the horizontal force measured by the load cell is plotted against the displacement measured by LVDT1 (Fig. 12). As can be seen, the stability of the peak forces (slip force and ultimate force) is excellent in all cases and the forces were capped under the predicted levels. It is apparent from the figures that the wall exhibited a flag-shaped hysteretic behavior demonstrating a fully self-centering characteristic.

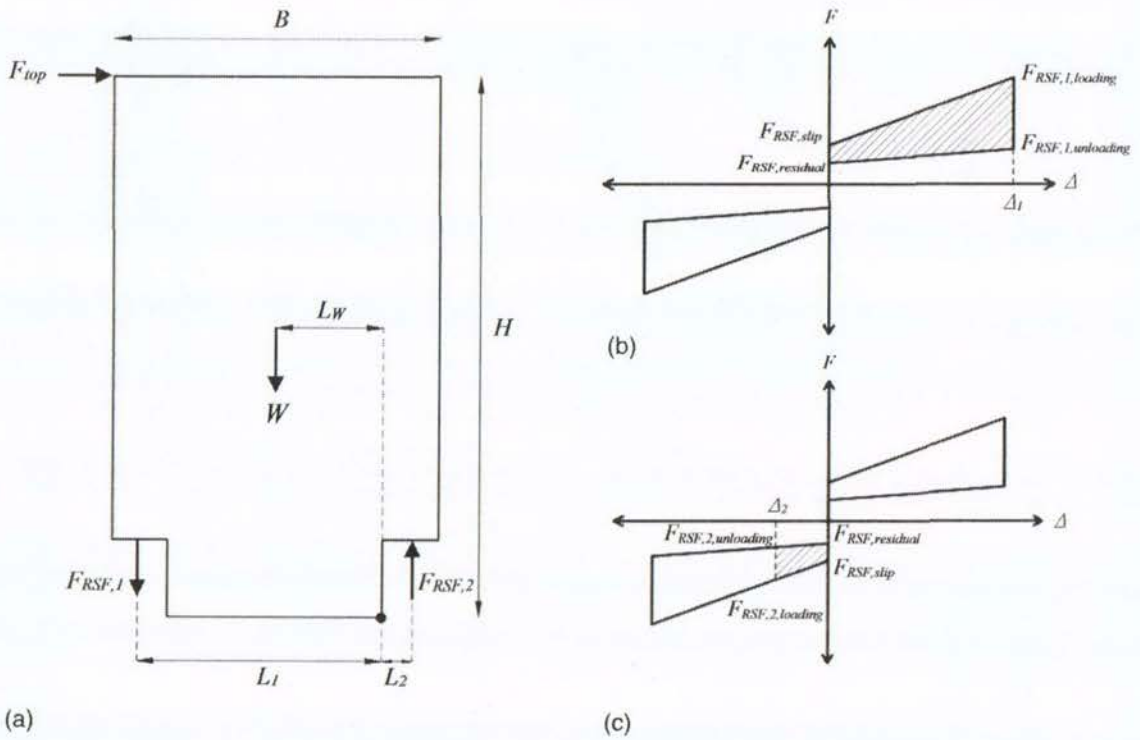

Fig. 14. Rocking CLT wall with RSF joints: (a) acting forces; (b) left RSF joint hysteresis (for the left to right direction of rocking); (c) right RSF joint hysteresis

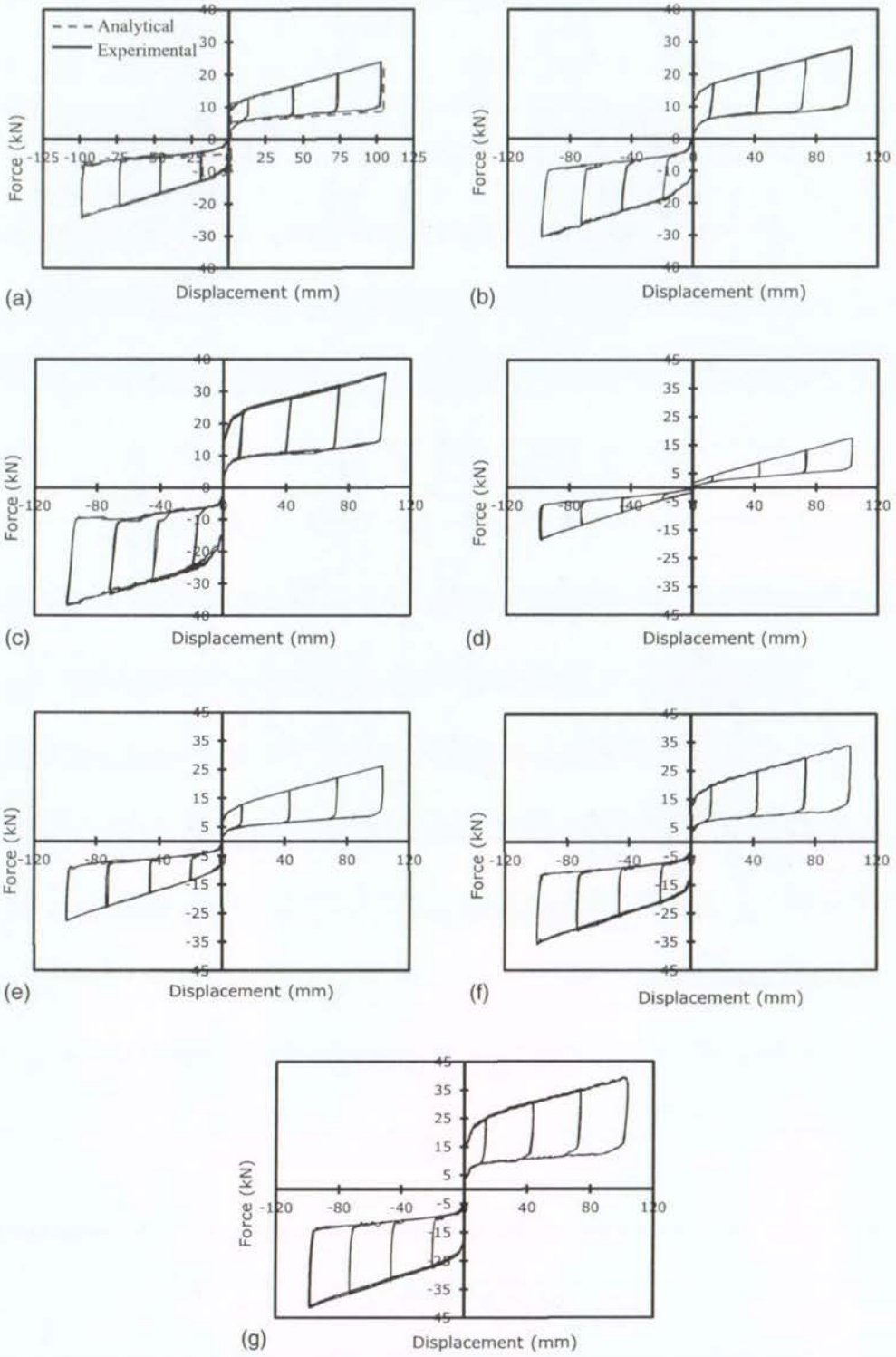

Fig. 15. Experimental results of the quasi-static tests: (a) Test 1; (b) Test 2; (c) Test 3; (d) Test 4; (e) Test 5; (f) Test 6; (g) Test 7

This was achieved respecting the fact that the only vertical loads applied to the wall were the self-weight of the CLT panel, half of the weight of the actuator, and the weight of the actuator steel parts (12.5 kN in total measured). This clearly confirms the significance of the proposed concept because in similar concepts, the re-centering behavior has always been reliant on additional vertical loads, which could be the gravity loads (Loo et al. 2015) or the load produced by the posttensioned cables (Sarti et al. 2015b).

The maximum top wall displacement for all tests was 100 mm, which corresponds to a drift level of 3%. This threshold was determined mainly because of the size of the CLT panel and the constraints within the test hall. Nevertheless, it should be noted that the system could be redesigned to achieve a higher drift level if it is required for a specific structure.

The CLT wall was monitored during all tests and no damage or unanticipated behavior was observed. Moreover, the wall did not exhibit any ratcheting effect. This phenomenon usually takes place

Table 2. Specified Parameters for Test 1

Description	Item	Value
Geometric properties of the system	H (height of the wall)	3,315 mm
	B (width of the wall)	2,025 mm
	L_1 (lever arm for the ascending RSF joint)	1,522 mm
	L_2 (lever arm for the descending RSF joint)	188 mm
	L_W (lever arm for the gravity loads)	668 mm
Target RSF joint specifications	$F_{RSF,slip}$ (slip force of the RSF joints)	16.5 kN
	$F^{max}_{RSF,loading}$ (maximum force of the RSF joints upon loading)	47 kN
	$F^{max}_{RSF,unloading}$ (maximum force of the RSF joints upon unloading)	11.2 kN
	$F_{RSF,residual}$ (residual force of the RSF joint)	5.1 kN
	Δ^{max}_{RSF} (maximum deflection of the RSF joint)	46 mm
Target hysteretic parameters for the wall	$F_{top,slip}$ (horizontal slip force of the wall)	11 kN
	$F^{max}_{top,loading}$ (maximum horizontal force of the wall upon loading)	25.2 kN
	$F^{max}_{top,unloading}$ (maximum horizontal force of the wall upon unloading)	8 kN
	$F_{top,residual}$ (horizontal residual force of the wall)	5.2 kN
	Δ^{max}_{top} (maximum deflection of the RSF joint)	100 mm

when the applied vertical loads (gravity loads or the forces from the posttensioned elements) are relatively low and the wall panel rises on the dampers (Wrzesniak et al. 2016). This damper ratcheting phenomenon is typically prevented by inclusion of additional vertical loads in the design. However, in this study, the self-centering characteristic offered by the RSF joints efficiently prevented this phenomenon, which affirms the efficiency of the proposed lateral load resisting system.

It can be seen from the figures that the largest racking force applied to the wall was nearly 35 kN, and for a 3,315 by 2,025 mm CLT wall with layer arrangement described in "Key Structural Elements" and the self-weight of 12.5 kN, the sum of elastic bending and shear deformation is approximately 0.5 mm, which can be ignored when compared with the overall horizontal displacement of the wall (100 mm). This confirms the validity of the rigid body motion assumption for the CLT wall, and as a result the hysteretic behavior of the wall can be presumed to be almost entirely dependent on the behavior of the RSF joints. For the proposed system, higher lateral resistances are achievable by increasing the capacity of the RSF joints. At 100 mm of horizontal displacement, a small vertical force is created due to the slight rotation of the hinge at the actuator level (Fig. 6). This small amount of force does not affect the overall performance of the system and can be ignored.

In order to verify the accuracy of the analytical approach described in the last section, the hysteretic parameters for Test 1 were determined using Eqs. (6) and (7). Table 2 presents the geometric properties of the tested wall system, the target hysteresis for the RSF joints, and the analytically calculated hysteretic parameters for the wall. Similar to the joint component tests, the turn-of-nut method was employed to achieve the target hysteresis for the RSF joints.

Fig. 15(a) compares the analytically obtained load-deformation behavior for the wall with the experimental data. It is apparent from the figure that the provided capacity equations are capable of accurately predicting the hysteretic behavior of the rocking CLT wall with RSF joints. This makes the engineer able to confidently determine the behavior of such a system. The horizontal reaction in the shear key is slightly above the foundation level (90 mm). The small moment caused by this eccentricity does not affect the overall behavior of the system and can be neglected.

Overall, from observations of the hysteresis curves, it is concluded that the energy dissipation potential of the RSF joints and the self-centering behavior offered by the system are promising.

Performance of the RSF Joints

The stable hysteretic behavior of the wall panel, as shown in Fig. 15, attests to the fact that the RSF joint performed as expected with excellent preservation of both stiffness and strength. The nearly symmetrical hysteretic curves confirm that the use of the turn-of-nut method allowed the RSF joints to achieve very similar strengths, which confirms the efficiency of the adopted technique.

Fig. 16 shows the deformed shape of the RSF joints in tension and in compression. As expected, due to the relatively larger level arm, the deflection in tension is substantially higher when compared with the deformation in compression. The horizontal distance between the cap plates increases as the joints deform. For the adopted configuration in this study, no physical barrier existed to interfere with this deformation. However, this geometric tolerance needs to be taken into account when implementing RSF joints in real structures.

Fig. 17 illustrates the vertical displacements recorded by LVDT2 and LVDT3 in Test 6 (as a representation for all tests), which, respectively, correspond to the left and right RSF joints [Fig. 12(a)]. It can be seen that the joints deformed as expected in accordance with the displacement schedule applied to the top (Fig. 13). More to the point, the figure demonstrates that the damper ratcheting effect has effectively been prevented because the ascending and descending RSF joints are deforming as predicted in a stable and continuous manner.

Despite the large cumulative traveling distance of the RSF joints during the tests, which was approximately 19 m for each joint (including the joint component tests, the trial tests, and the final tests in which the results are presented), they still performed as predicted by the end of the last test. No significant damage was observed to the slipping surfaces with no galling or wearing effect.

The behavior of the screwed connections was observed during and after the experiments, and no damage or slip was noticed. Furthermore, the displacement gauges attached to the screwed connections have not recorded any significant deformation, which highlights that the connection used was able to provide sufficient rigidity. However, some minor rotation of the upper center plate (relative to the cap plates) was observed, which can be attributed to the frictional resistance between the pin and the hole in the upper hinge. This extra resistance can be effectively prevented by using a lubricant between them. Nevertheless, the observed rotation has not affected the overall behavior of the joint.

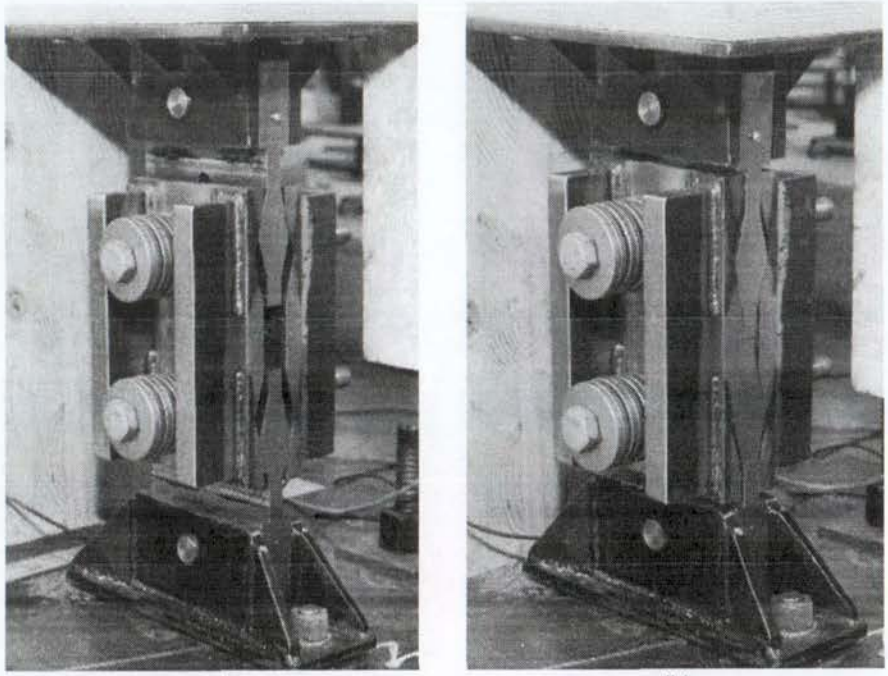

(a) (b)

Fig. 16. RSF joints in deformation: (a) tension; (b) compression

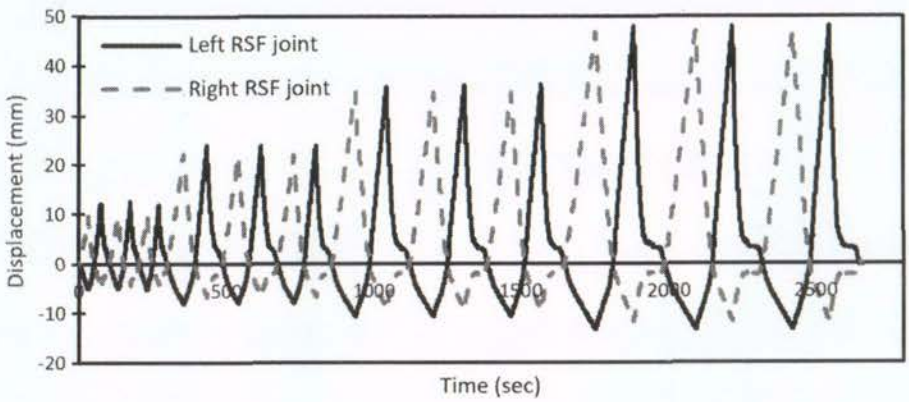

Fig. 17. Vertical displacements at left and right RSF joints for Test 6

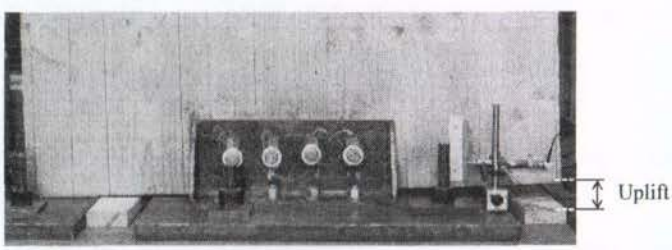

Fig. 18. Deformed shape of the shear key

Performance of the Shear Keys

Fig. 18 shows the deformed shape of the shear key while the CLT wall rocks. It is apparent that the device was able to efficiently accommodate the uplift occurring as a result of the rocking motion. Furthermore, the maximum horizontal slip recorded by either LVDT4 or LVDT5 [Fig. 12(a)] was slightly under 2.5 mm, which clearly highlights the effectiveness of the proposed solution. In other words, the shear key provided adequate lateral resistance while at the same time it allowed the CLT wall to rock in the anticipated manner.

Moreover, the deformation of the shear keys was closely monitored and no damage or inconsistency in either the timber wall or the device itself was observed. At the end of the tests, the bolts were removed and inspected and no damage was noticed in them. In fact, the shear keys performed as expected with a behavior similar to a conventional timber-bolted connection. Overall, the experimental results suggest that the proposed shear transferring device has the potential for application in rocking structures as a simple, efficient, and economical solution.

Numerical Modeling

A numerical model was developed in the *SAP2000* software package in order to investigate the seismic performance of the

Table 3. Design Parameters for the Damper-Friction Spring Link Elements

Parameter	Value
Loading slipping stiffness	663 N/mm
Unloading slipping stiffness	133 N/mm
Precompression displacement	−24.9 mm
Stop displacement	46 mm

introduced wall system. The damper-friction link element, which is available in *SAP2000* or above, was adopted to model the RSF joints. This element has been proven to be able to accurately predict the hysteretic behavior of the RSF joint. Hashemi et al. (2017b) provides more details. The parameters for the RSF joints were calibrated to represent a similar configuration to the joints in Test 1 (Table 3). Fig. 9(a) shows the general arrangement of the developed numerical model. The CLT panel was modeled using the layered shell element with the mechanical characteristics of MSG8 timber as the material properties (Buchanan 1999). Gap elements with zero gaps were considered at the toes to define the foundation level which the wall is not allowed to move below. The displacement schedule in Fig. 13 (which was also used for the experimental tests) was applied to the top of the wall through a displacement-control stiff spring. The horizontal degree of freedom of the middle joint of the CLT panel at the base level was restrained to represent the shear keys. Because the height of the tested CLT panel was 6,000 mm, the unit weight of the timber was increased to 9.6 kN/m^3 to take the self-weight of rest of the panel (above the 3,350-mm height) into account and to achieve a total self-weight of 12.5 kN, which is the overall weight considered in the experiments.

The results of the quasi-static simulations are shown in Figs. 19(b and c). As can be seen, the RSF joints performed as expected and the hysteretic behavior of the wall [Fig 19(c)] is consistent with the experimental data, which highlights the reliability of the developed numerical model. The presented numerical technique for modeling the wall system with RSF joints is extendable for other types of structural systems that involve RSF technology. This allows the designer to be able to model, analyze, and design the desired structure with a commonly used numerical software package such as *SAP2000*.

Conclusions

This paper highlighted the experimental results of a series of displacement-control quasi-static tests on a rocking CLT wall with innovative RSF joints as the hold-down connectors installed at the corners of the wall panel. Furthermore, a new type of shear transferring device is proposed to transfer the horizontal shear forces from the wall to the foundation while accommodating the uplift

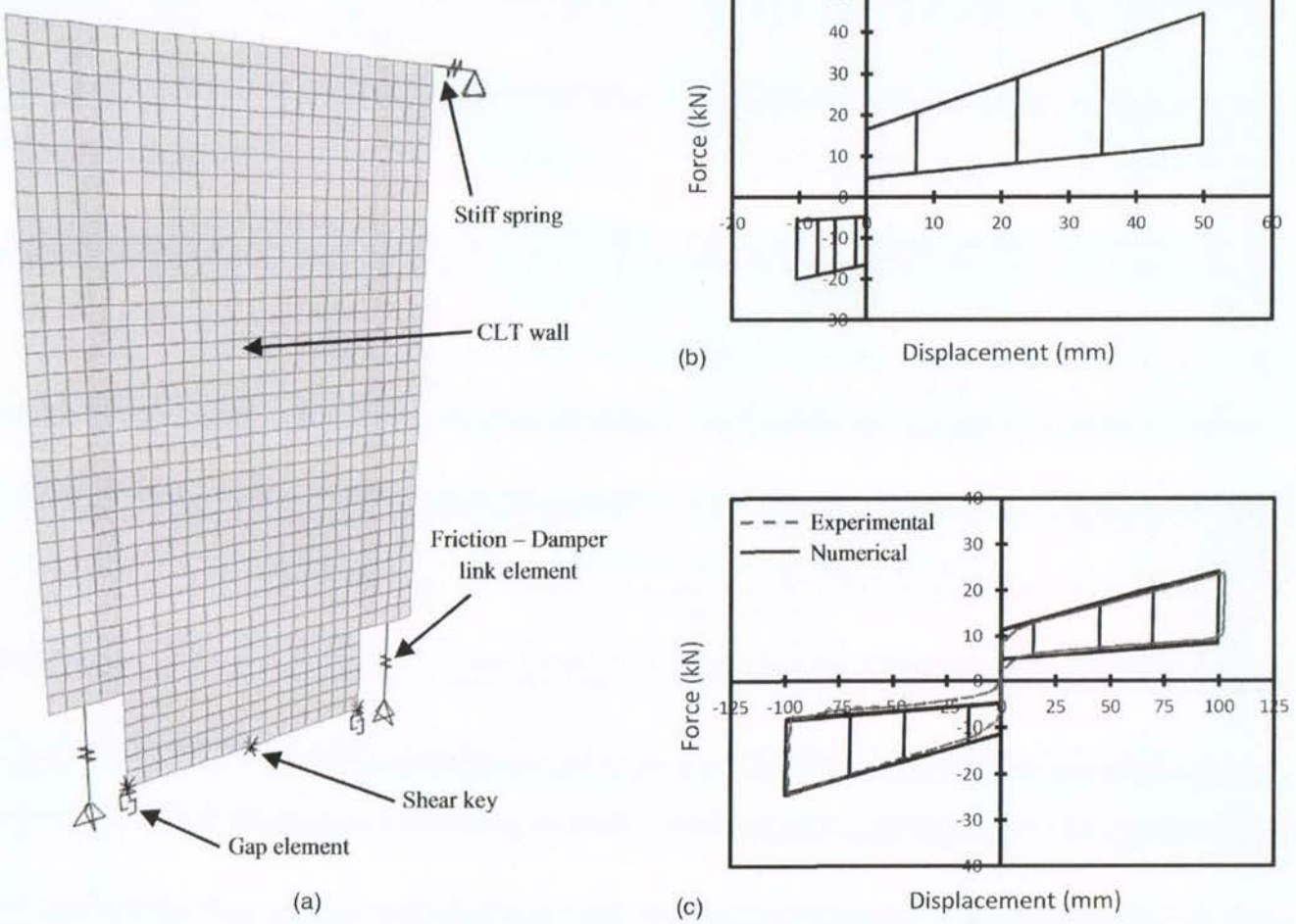

Fig. 19. Numerical modeling and results of the quasi-static simulations: (a) general arrangement; (b) RSF joint hysteresis; (c) total system hysteresis in comparison with the experimental data

occurring at the base of the wall due to the rocking motion. Several tests were conducted, and in spite of large travel distance of the sliding surfaces, no damage was observed in the CLT panel or in the RSF joints.

The experimental results confirmed that the proposed system can provide a robust solution when a seismic resilient design is aimed for. Despite the fact that the no additional vertical load was applied to the wall, the wall achieved a fully self-centering behavior that can be attributed to the unique characteristic of the RSF joints. Moreover, the stable hysteretic response of the system demonstrated a significant rate of energy dissipation through friction, which cumulatively increases as the deflection in the joints increases. The damper ratcheting effect, which is a common and undesirable phenomenon in structural walls with dampers, has efficiently been prevented by the use of RSF joints. Self-tapping screws were employed to connect the RSF joints to the CLT panel and the experimental data confirmed the effectiveness of this solution because it was able to provide sufficient rigidity.

The shear keys performed as predicted, allowing the wall panel to move in the intended manner, while the shear forces were efficiently transferred to the foundation. The performance of the shear keys was similar to a conventional bolted connection, thus representing an efficient yet economical solution for application in rocking structural members.

A series of analytical equations were proposed for designing the rocking walls with RSF joints. The analytical results were compared with experimental data and it was proven that the provided equations can accurately predict the lateral strength of the system. Additionally, a numerical model in the *SAP2000* software package was developed and validated to be used for numerical modeling of similar systems.

Future research will involve testing a similar configuration with higher loading rates to evaluate the performance of the system in rapider movement. Overall, the proposed concept showed an excellent behavior, which suggests potential for application in seismic-resilient structures when a damage-avoidant design philosophy with no postevent maintenance is considered.

Acknowledgments

The authors would like to thank the Earthquake Commission Research Foundation (EQC) of New Zealand for the financial support of the presented research under the Grant EQC 15/U710.

References

Ajrab, J. J., Pekcan, G., and Mander, J. B. (2004). "Rocking wall-frame structures with supplemental tendon systems." *J. Struct. Eng.*, 10.1061/(ASCE)0733-9445(2004)130:6(895), 895–903.

Baktash, P., Marsh, C., and Pall, A. (1983). "Seismic tests on a model shear wall with friction joints." *Can. J. Civ. Eng.*, 10(1), 52–59.

Bora, C., Oliva, M. G., Nakaki, S. D., and Becker, R. (2007). "Development of a precast concrete shear-wall system requiring special code acceptance." *PCI J.*, 52(1), 122–135.

Buchanan, A. H. (1999). *Timber design guide*, New Zealand Timber Industry Federation, Wellington, New Zealand.

Ceccotti, A., Sandhaas, C., Okabe, M., Yasumura, M., Minowa, C., and Kawai, N. (2013). "SOFIE project—3D shaking table test on a seven-storey full-scale cross-laminated timber building." *Earthquake Eng. Struct. Dyn.*, 42(13), 2003–2021.

Gagnon, S., and Pirvu, C. (2011). *CLT handbook: Cross-laminated timber*, FPInnovations, Vancouver, Canada.

Hashemi, A., Loo, W. Y., Masoudnia, R., Zarnani, P., and Quenneville, P. (2016a). "Ductile cross laminated timber (CLT) platform structures with passive damping." *World Conf. on Timber Engineering (WCTE2016)*, Vienna Univ. of Technology, Vienna, Austria.

Hashemi, A., Masoudnia, R., and Quenneville, P. (2016b). "A numerical study of coupled timber walls with slip friction damping devices." *Constr. Build. Mater.*, 121(1), 373–385.

Hashemi, A., Masoudnia, R., and Quenneville, P. (2016c). "Seismic performance of hybrid self-centring steel-timber rocking core walls with slip friction connections." *J. Constr. Steel Res.*, 126(1), 201–213.

Hashemi, A., Zarnani, P., Masoudnia, R., and Quenneville, P. (2017a). "Seismic resistant cross laminated timber (CLT) structures with innovative resilient slip friction (RSF) joints." *World Conf. on Earthquake Engineering (16WCEE)*, Chilean Association of Seismology and Earthquake Engineering, Santiago, Chile.

Hashemi, A., Zarnani, P., Masoudnia, R., and Quenneville, P. (2017b). "Seismic resistant rocking coupled walls with innovative Resilient Slip Friction (RSF) joints." *J. Constr. Steel Res.*, 129(1), 215–226.

Hashemi, A., Zarnani, P., Valadbeigi, A., Masoudnia, R., and Quenneville, P. (2016d). "Seismic resistant cross laminated timber structures using an innovative resilient friction damping system." *Proc., New Zealand Society for Earthquake Engineering (NZSEE) Conf.*, New Zealand Society for Earthquake Engineering, Wellington, New Zealand.

Iqbal, A., Pampanin, S., Palermo, A., and Buchanan, A. H. (2015a). "Performance and design of LVL walls coupled with UFP dissipaters." *J. Earthquake Eng.*, 19(3), 383–409.

Iqbal, A., Smith, T., Pampanin, S., Fragiacomo, M., Palermo, A., and Buchanan, A. H. (2015b). "Experimental performance and structural analysis of plywood-coupled LVL walls." *J. Struct. Eng.*, 10.1061/(ASCE)ST.1943-541X.0001383, 4015123.

Khoo, H., Clifton, C., MacRae, G., Zhou, H., and Ramhormozian, S. (2015). "Proposed design models for the asymmetric friction connection." *Earthquake Eng. Struct. Dyn.*, 44(8), 1309–1324.

Loo, W. Y., Kun, C., Quenneville, P., and Chouw, N. (2014a). "Experimental testing of a rocking timber shear wall with slip-friction connectors." *Earthquake Eng. Struct. Dyn.*, 43(11), 1621–1639.

Loo, W. Y., Quenneville, P., and Chouw, N. (2012). "A numerical study of the seismic behaviour of timber shear walls with slip friction connectors." *Eng. Struct.*, 34(1), 233–243.

Loo, W. Y., Quenneville, P., and Chouw, N. (2014b). "A new type of symmetric slip-friction connector." *J. Constr. Steel Res.*, 94(1), 11–22.

Loo, W. Y., Quenneville, P., and Chouw, N. (2015). "Rocking timber structure with slip-friction connectors conceptualized as a plastically deformable hinge within a multistory shear wall." *J. Struct. Eng.*, 10.1061/(ASCE)ST.1943-541X.0001387, E4015010.

MacRae, G. A., Clifton, G. C., Mackinven, H., Mago, N., Butterworth, J., and Pampanin, S. (2010). "The sliding hinge joint moment connection." *Bull. N. Z. Soc. Earthquake Eng.*, 43(3), 202–212.

Marriott, D., Pampanin, S., Bull, D., and Palermo, A. (2008). "Dynamic testing of precast, post-tensioned rocking wall systems with alternative dissipating solutions." *2008 New Zealand Society for Earthquake Engineering (NZSEE) Conf.*, New Zealand Society for Earthquake Engineering, Wellington, New Zealand.

Masoudnia, R., Zarnai, P., and Quenneville, P. (2016). "Evaluation of effective flange width in the CLT composite T-beams." *World Conf. on Timber Engineering WCTE2014*, Vienna Univ. of Technology, Vienna, Austria.

New Zealand Standards. (2004). "Structural design actions." *NZS 1170.5*, Wellington, New Zealand.

Pall, A. S., Marsh, C., and Fazio, P. (1980). "Friction joints for seismic control of large panel structures." *PCI J.*, 25(6), 38–61.

Popov, E. P., Grigorian, C. E., and Yang, T.-S. (1995). "Developments in seismic structural analysis and design." *Eng. Struct.*, 17(3), 187–197.

Popovski, M., and Gavric, I. (2015). "Performance of a 2-story CLT house subjected to lateral loads." *J. Struct. Eng.*, 10.1061/(ASCE)ST.1943-541X.0001315, E4015006.

SAP2000 version 17 [Computer Software]. Computer and Structures, Inc., Berkeley, CA.

Sarti, F., Palermo, A., and Pampanin, S. (2012). "Design charts and simplified procedures for post-tensioned seismic resistant timber walls."

World Conf. on Timber Engineering WCTE2012, New Zealand Timber Design Society, Wellington, New Zealand.

Sarti, F., Palermo, A., and Pampanin, S. (2015a). "Development and testing of an alternative dissipative posttensioned rocking timber wall with boundary columns." *J. Struct. Eng.*, 10.1061/(ASCE)ST.1943-541X.0001390, E4015011.

Sarti, F., Palermo, A., and Pampanin, S. (2015b). "Quasi-static cyclic testing of two-thirds scale unbonded posttensioned rocking dissipative timber walls." *J. Struct. Eng.*, 10.1061/(ASCE)ST.1943-541X.0001291, E4015005.

Smith, T., et al. (2007). "Seismic response of hybrid-LVL coupled walls under quasi-static and pseudo-dynamic testing." *2007 New Zealand Society for Earthquake Engineering (NZSEE) Conf.*, New Zealand Society for Earthquake Engineering, Wellington, New Zealand.

Wanninger, F., Frangi, A., and Fragiacomo, M. (2014). "Long-term behavior of posttensioned timber connections." *J. Struct. Eng.*, 10.1061/(ASCE)ST.1943-541X.0001121, 4014155.

Wrzesniak, D., Rodgers, G. W., Fragiacomo, M., and Chase, J. G. (2016). "Experimental testing of damage-resistant rocking glulam walls with lead extrusion dampers." *Constr. Build. Mater.*, 102(1), 1145–1153.

Yasumura, M., Kobayashi, K., Okabe, M., Miyake, T., and Matsumoto, K. (2015). "Full-scale tests and numerical analysis of low-rise CLT structures under lateral loading." *J. Struct. Eng.*, 10.1061/(ASCE)ST.1943-541X.0001348, E4015007.

Zarnani, P., Valadbeigi, A., and Quenneville, P. (2016). "Resilient slip friction (RSF) joint: A novel connection system for seismic damage avoidance design og timber structures." *World Conf. on Timber Engineering WCTE2014*, Vienna Univ. of Technology, Vienna, Austria.

Construction and Building Materials 149 (2017) 432–443

Contents lists available at ScienceDirect

Construction and Building Materials

journal homepage: www.elsevier.com/locate/conbuildmat

Seismic resilient lateral load resisting system for timber structures

Ashkan Hashemi [a,*], Pouyan Zarnani [b], Reza Masoudnia [a], Pierre Quenneville [a]

[a] Department of Civil and Environmental Engineering, Faculty of Engineering, The University of Auckland, Private Bag 92019, Auckland 1142, New Zealand
[b] Department of Built Environment Engineering, School of Engineering, Computer and Mathematical Sciences, Auckland University of Technology, Private Bag 92006, Auckland 1142, New Zealand

ARTICLE INFO

Article history:
Received 26 February 2017
Accepted 9 May 2017

Keywords:
Damage avoidant
Rocking walls
Low damage
RSF joints
Self-centring
Resilience
Energy dissipation
Damping
Friction

ABSTRACT

Conventional light timber frame buildings made with metal fasteners such as nails, screws, rivets or bolts usually use traditional plywood sheathed shear walls as the main lateral load resisting members. During an earthquake, these structures are prone to large inelastic deformations in the fasteners which lead to drastic stiffness degradation for the system. A damage avoidant seismic solution is being developed to provide the required lateral drift capacity while mitigating the damage through controlled rocking motion. This system includes lateral load resisting members consist of rocking timber panels made of Laminated Veneer Lumber (LVL) and innovative Resilient Slip Friction (RSF) joints as the hold-down connectors at the base. Moreover, a novel type of shear key is introduced to transfer the lateral forces to the foundation. A prototype building is designed and numerically modelled. To investigate the seismic performance, non-linear dynamic time-history simulations were carried out on the system and on similar systems with existing seismic solutions. The results confirm a promising seismic performance in terms of ductility, energy dissipation and self-centring behaviour.

1. Introduction

Convectional timber framed buildings made with metal fasteners such as nails, screws, rivets or bolts containing traditional plywood sheathed shear walls as the main lateral load resisting members are designed to allow for inelastic damage in the connections and crushing in the wood fibres as long as the collapse of the building is prevented. The permitted damage is expected to be repaired. However, it may not be possible (due to accessibility issue of the damaged components) or it might be possible but would be highly uneconomical. Moreover, the damage occurred during a major seismic event significantly reduces the strength and stiffness of the building making it considerably vulnerable to the aftershocks. The results of the shake table tests on a seven story timber panelised structure made with the traditional steel connections asserted to the fact that these connections are prone to irrecoverable plastic deformation [1]. Additionally, high acceleration recorded at top stories (up to 3.85 g) highlighted the need for supplementary damping devices in the system to absorb the seismic energy. These facts have motivated many researchers to start developing alternative solutions that can provide adequate ductility while dissipating the seismic energy through fuses implemented throughout the structure.

Iqbal et al. studied the application of U-shaped Flexural Plates (UFPs) as supplementary damping devices in post-tensioned LVL timber coupled rocking walls [2]. The concept had later been experimentally investigated and a design procedure for a prototype building was proposed [3]. The test results demonstrated an efficient energy absorption rate through inelastic deformation of the UFPs. Sarti et al. experimentally investigated the seismic performance of hybrid rocking walls with end steel columns [4]. The experimental results highlighted the flexibility and acceptable seismic performance of the system accompanied by stable load-deformation behaviour with minor stiffness degradation in the dissipaters. Iqbal et al. tested coupled posttensioned rocking LVL walls with sacrificial nailed plywood sheets as hysteretic dampers [5]. Although the system did not provide a stability similar to UFPs, it was concluded that it could be considered as a low cost alternative solution. Kramer et al. tested rocking Cross Laminated Timber (CLT) walls with steel energy dissipaters at the base and post-tensioned cables up the height of the wall panels [6]. Loo et al. introduced and experimentally investigated the application of slip friction connections as hold-downs for a rocking LVL wall [7]–[9]. The experimentally obtained data highlighted the efficiency of the system since it exhibited a stable hysteresis close to an elastic-perfectly-plastic one. However, it was proven that the

* Corresponding author.
E-mail address: ahas439@aucklanduni.ac.nz (A. Hashemi).

http://dx.doi.org/10.1016/j.conbuildmat.2017.05.112
0950-0618/

system requires an additional mechanism such as gravity loads to self-centre the wall panel at the end of a seismic event [10]. Hashemi et al. further developed the concept into a coupled wall system. Their numerical studies showed that such system is likely to exhibit considerable residual displacements especially in absence of gravity loads [11,12]. Wrzeniak tested damage-resistant glue laminated timber walls with High Force to Volume (HF2V) dampers at the base [13]. The results confirmed the low damage characteristic. Nevertheless, the self-centring was lost for lateral drifts more than 1.3%. Hashemi et al. introduced rocking core walls in which the energy is dissipated by slip friction connections while self-centring is provided by post-tensioned beam to column connections [14].

This study seeks to develop a seismic resilient solution for timber and hybrid timber-steel structures. The proposed system includes rocking wall panels with Resilient Slip Friction (RSF) joints [15] (as the hold-down connectors) and load-bearing components on the two sides of wall panels. This system offers adequate ductility for the building while energy dissipations and self-centring are provided by the RSF joints. Additionally, the rocking walls are anchored to the foundation by a new type of shear transferring device. This paper presents a preliminary design procedure for the proposed system based on the Displacement Based Design (DBD) approach. To further investigate the seismic performance of this system, non-linear dynamic time-history simulations were carried out and the results are compared with those obtained from similar models in which the RSF joints are replaced with conventional connectors.

2. Rocking timber wall with RSF joints

Conventional friction dampers with flat plates slipping on each other have always been renowned for having one of the most efficient energy dissipation mechanisms. The provided hysteresis which is close to an elastic-perfectly-plastic one combined with the cost effectiveness of these devices has made them very favourable. Nevertheless, the lack of self-centring behaviour is a major disadvantage for the structures containing these dampers which may result in considerable residual displacement after an earthquake. To compensate this issue, a novel energy dissipation device entitled Resilient Slip Friction (RSF) joint is developed. The components of the RSF joint are configured in a way that energy dissipation and self-centring can be achieved all in one compact device. Fig. 1 shows the components and assembly of a RSF joint. The angle of the ridges is designed in a way that at the time of unloading, the reversing force caused by the elastically compacted Belleville springs is larger than the resisting friction force between the surfaces. Thus, the slotted plates are re-centred to their original position while energy dissipates over sliding. RSF joint exhibits a flag-shaped hysteresis which is experimentally confirmed by the authors [14,16]. Fig. 1(d) displays the theoretical hysteretic loop of the RSF joint. The slip force and the residual force in the joint can be determined by Eqs. (1) and (2).

$$F_{slip} = 2n_b F_{b,pr}\left(\frac{\sin\theta + \mu_s\cos\theta}{\cos\theta - \mu_s\sin\theta}\right) \tag{1}$$

$$F_{residual} = 2n_b F_{b,pr}\left(\frac{\sin\theta - \mu_k\cos\theta}{\cos\theta + \mu_k\sin\theta}\right) \tag{2}$$

where $F_{b,pr}$ is the clamping force in the bolts originated from the pre-stressing of the Belleville springs, n_b is the number of bolts, θ is the angle of the ridges, μ_s is the static coefficient of friction and μ_k is the kinetic coefficient of friction which can be assumed as 0.85 μ_s [14,16]. The ultimate force in loading ($F_{ult,loading}$) and unloading ($F_{ult,unloading}$) can be calculated by replacing μ_s and $F_{b,pr}$ in Eqs. (1) and (2) by μ_k and $F_{b,u}$, respectively. The ultimate force in the bolts ($F_{b,u}$) can be determined by Eq. (3) in which k_s and Δ_s are respectively the total stiffness of the stack of springs and the maximum deflection when they become flat. These equations are analytically derived which the details can be found in [17].

$$F_{b,u} = F_{b,pr} + k_s\Delta_s \tag{3}$$

Experimental tests were carried out by Hashemi et al. on a CLT wall with RSF joints as the hold-down connectors. A summary of the test setup and an example of the obtained results are presented in order to demonstrate the functionality of the proposed concept. More details about the experiments can be found in [18]. Two identical RSF joints were installed in the notches at the bottom corner of the CLT wall. Each joint consists of two centre slotted plates and two cap plates made with mild steel grade 350. The angle of

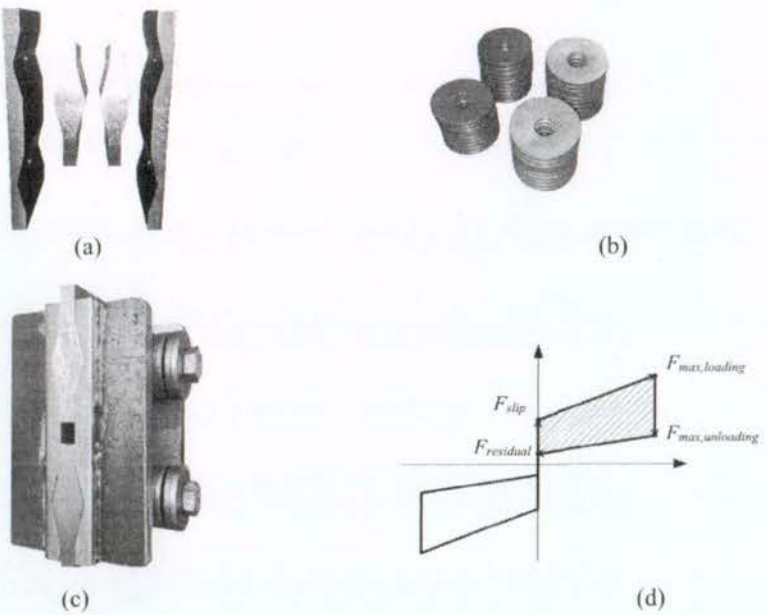

Fig. 1. RSF joint: (a) Cap plates (before attaching the stiffeners) and centre slotted plates (b) Belleville springs (c) Assembly (d) Theoretical hysteresis.

the ridges was 15 degrees and two 220 mm by 50 mm by 20 mm stiffener plates had later been welded to the cap plates to reinforce them against out of plane bending (see Fig 1(c)).

Fig. 2 shows the general arrangement of the test setup. The RSF joints were designed and fabricated to be able to accommodate a maximum displacement of 65 mm in tension and 15 mm in compression. This was because of the relatively larger displacement demand in tension compared to compression in a hold-down connector. The tested CLT panel had five 40 mm thick layers made of MSG8 timber [19] (200 mm of thickness in total). Each RSF joint had two bolts and 11 Belleville springs per bolts per side. The springs had a maximum load capacity of 110 kN and a maximum displacement capacity of 1.5 mm at flat state [14]. The loading protocol displayed in Fig. 2(a) was applied to the wall at the height of 3350 mm with an approximate loading rate of 1.25 mm/s. To demonstrate the performance of the proposed concept, a maximum drift amplitude of 3% was considered.

During the tests, no damage was observed to the wall with no evidence of deterioration in strength or stiffness of the RSF joints. Fig. 3(b) shows the typical hysteresis for the wall as a representative for the test results. As can be seen, the pre-stressing force is approximately 50% of the maximum force. The flag-shaped hysteresis in Fig. 3(b) clearly highlights the self-centring behaviour. It should be pointed out that the self-centring was independent from the gravity loads considering the fact that the only applied vertical load was the self-weight of the panel.

3. General concept of rocking timber wall with RSF joints

This section describes the general concept of rocking timber walls with RSF joints as lateral load resisting members for seismic resilient structures. It should be emphasized that this study focuses on timber buildings, however, the proposed concept can be adopted for other types of structures including reinforced concrete. Fig. 4 schematically illustrates the concept. It includes a rocking timber wall panel connected to the foundation by RSF joints as hold-down connectors. In addition, lateral load bearing components are considered to transfer the lateral shear forces from the columns to the wall panel. It should be remembered that these devices may develop a frictional resistance while transferring the lateral forces. Despite the fact that this frictional resistance might increase the energy absorption rate of the system, they may behave unstable or unpredictable. Therefore, they can affect the overall behaviour of the system and even endanger the self-centring behaviour. To avoid this, a nearly frictionless configuration is required. Sarti et al. used a shear transferring device

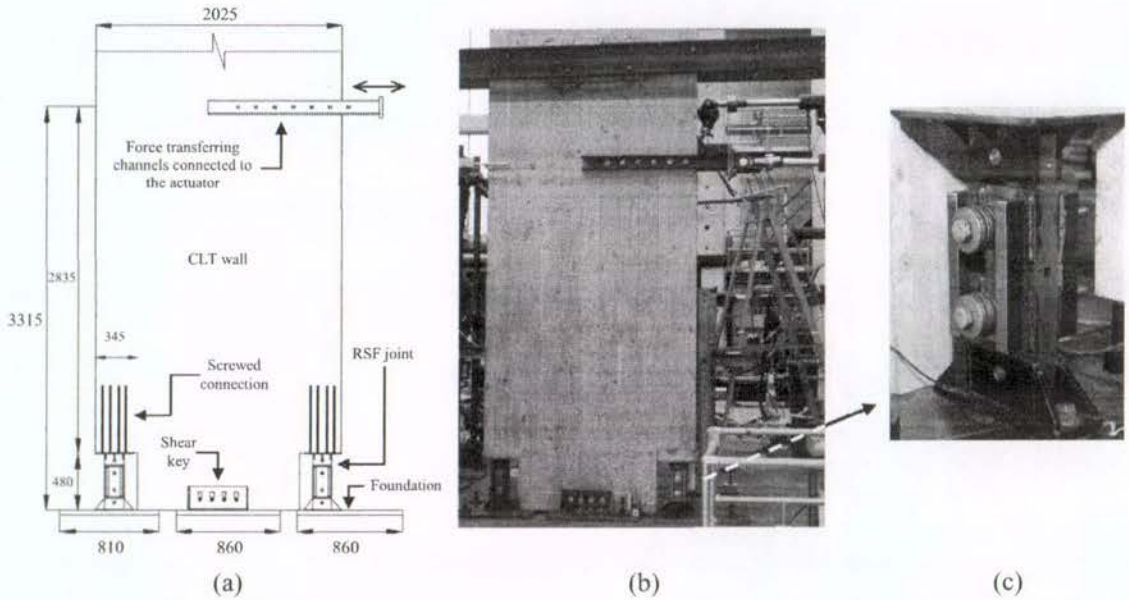

Fig. 2. Experimental testing of a rocking CLT wall with RSF joints [18]: (a) General arrangement (b) An image of the test setup (c) RSF joint as a hold-down connector.

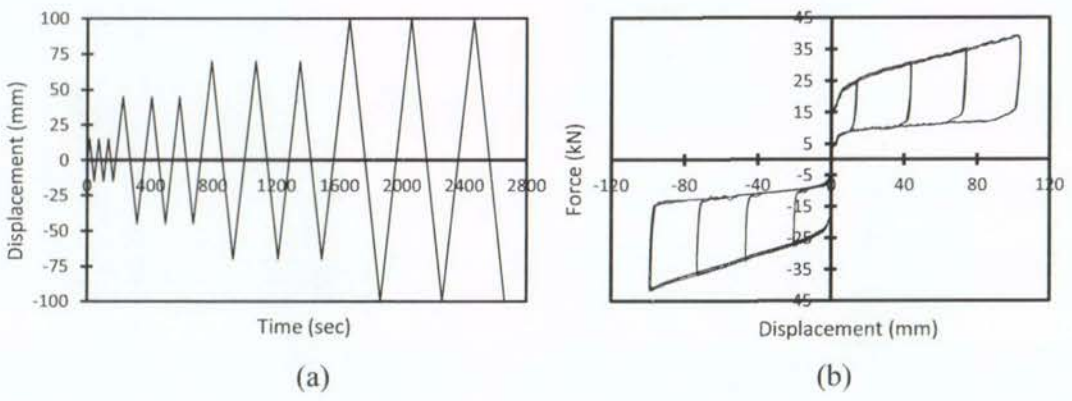

Fig. 3. Experimental results [18]: (a) Applied displacement schedule (b) Load-deformation behaviour.

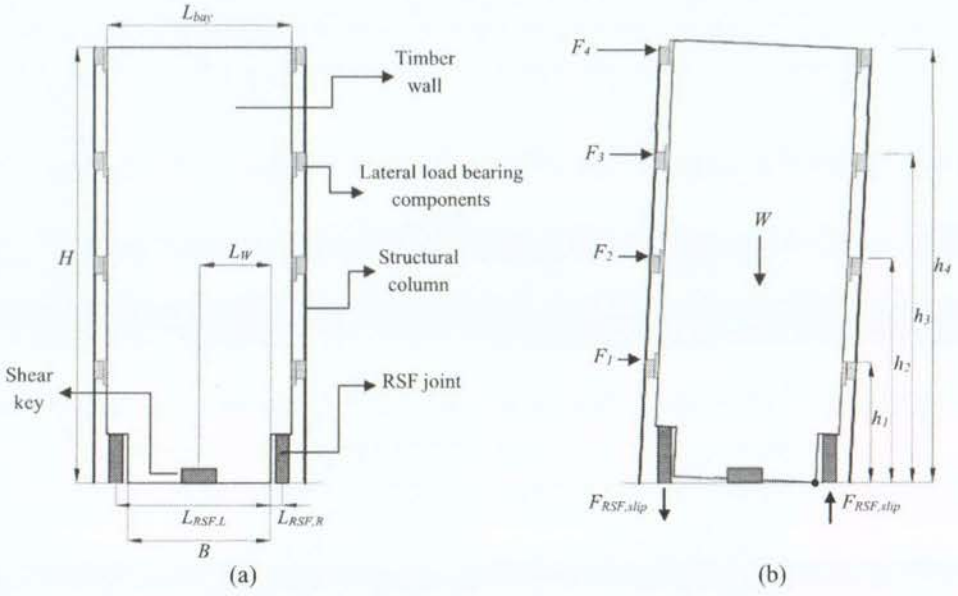

Fig. 4. The concept of rocking timber wall with RSF joints: (a) Before rocking (b) After rocking.

consisting of a LVL block connected to the column and a high density polyethylene sheet attached to the wall to decrease the friction in the devices as much as possible [4]. A similar solution can be adopted here as well.

In Fig. 4, L_{bay} is the width of the wall at top, H is the height of the wall, B is the width of the wall at the base level, W is the self-weight of the wall panel, $F_{RSF,L}$ and $F_{RSF,R}$ are respectively the force produced by the left and right RSF joints, $L_{RSF,L}$ and $L_{RSF,R}$ are respectively the lever arm for the left and right RSF joints (the horizontal distance of the centroid of the RSF joints from the rocking pivot), L_W is the lever arm for W and F_1 to F_4 are the lateral seismic forces. The philosophy adopted in this study is that the RSF joints should start to slide and the wall start to rock when an Ultimate Limit State (ULS) earthquake takes place. Therefore, the overturning moment triggering the movement in the system equals $\sum_{i=1}^{n} F_i h_i$ where F_i represents the ULS earthquake force applied at each story level and n is number of stories. Taking the moment about the rocking pivot, the slip force within the RSF joints can be found by Eq. (4). Note that it is assumed that the two RSF joints are identical.

$$F_{RSF,slip} = \frac{\sum_{i=1}^{n} F_i h_i - W L_W}{L_{RSF,L} + L_{RSF,R}} \tag{4}$$

It should be pointed out that the wall is isolated from the floors. Otherwise, the vertical displacement incompatibility occurring at the wall to floor connections may severely damage the floor diaphragms [20].

A novel type of shear key is considered at the base of the wall to transfer the shear forces from the wall to the foundation [21]. This device is capable to efficiently transfer the shear forces while accommodating the uplift caused by the rocking movement. As can be seen in Fig. 5, the bolts are installed in the timber wall while the slotted plate is attached to the foundation. When the rocking motion initiates, the bolts are dragged by the wall but the special shape of the slotted holes allow the bolts to stay in contact with the slotted surfaces during the rocking movement. Thus, the device is able to transfer shear forces with a mechanism similar to a conventional bolted connection.

4. Prototype building

To demonstrate the behaviour of a structure containing the proposed concept, a prototype building is considered. This structures is a five-story residential building designed for a shallow soil (type C) based on New Zealand standard for structural design actions

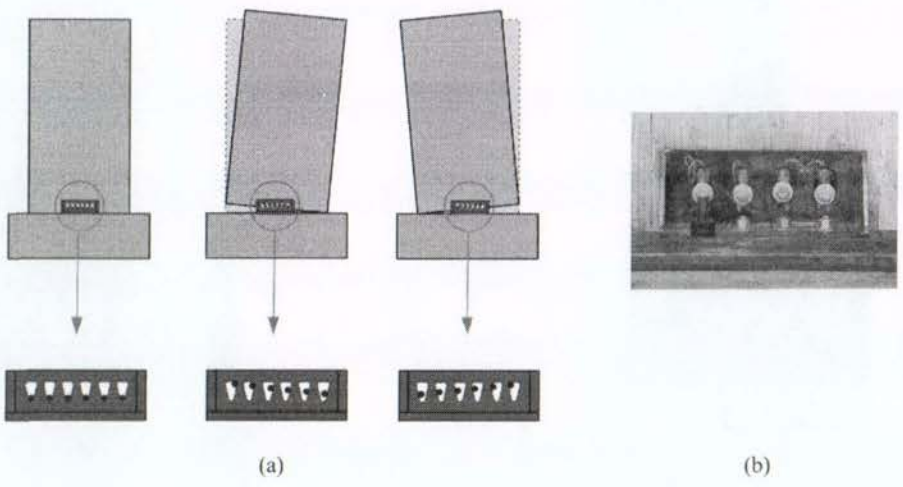

Fig. 5. The shear key [21]: (a) The concept (b) The manufactured device for large scale testing.

[22]. The overall height of the building is 15.5 m with 3.5 m of height for the first story and 3 m of height for the other four stories. As can be seen in Fig. 6, the building has six spans with 6 m of span length in each direction. A series of simplifying assumptions were made to evaluate the gravity loads and associated seismic masses. The building is assumed to be a hybrid framed building with steel hollow section columns, LVL beams and light timber floors. The permanent loads including ceiling, services, light partitions, workstations, floor panels (made with plywood sheets and light timber box joists), self-weight of the exterior walls, the weight of the beams and the weight of the columns are considered as 1.35 kPa for the first level, 1.25 kPa for levels two to four and 0.84 kPa for the roof. The imposed loads are assumed as 2 kPa for the first level, 1.5 kPa for levels two to four and 0.5 kPa for the roof [22]. The associated seismic masses are $2.24 * 10^5$ kg, $1.78 * 10^5$ kg and $1.14 * 10^5$ kg for the first story, stories two to four and the roof, respectively. Eight rocking walls with RSF joints made with 240 mm thick LVL panels with the arrangement outlined in Fig. 6 are considered to be used as the lateral load resisting members. The LVL members were assume as LVL 13.2 [19] with a density of 5.31 kN/m^3.

The ULS seismic forces (with a return period of 500 years) were calculated for the prototype building using the Displacement Based Design (DBD) method targeting 2% design drift and soil type C (shallow soil) located in Christchurch, New Zealand [10,23]. The design specifications are shown in Table 1.

With respect to the symmetric arrangement of the building plan and shear walls, the centre of mass and the centre of resistance are assumed to be coincident. Thus, only 10% of accidental eccentricity was considered for calculating the lateral forces applied to the shear walls. Table 2 shows the calculated seismic forces applicable for each wall.

Fig. 6(b) illustrates the configuration considered for the rocking walls. From the figure, $L_{RSF,R}$ = 4.7 m, $L_{RSF,L}$ = 0.2 m and L_W = 2.25 m. The self-weigh of the wall is calculated as W = 104.8 kN. Following Eq. (4) and with respect to the forces specified in Table 2, the slip force for the RSF joints is specified as $F_{RSF,slip}$ = 420.54 kN. Other design parameters for the RSF joint (Table 3) are determined based on Eqs. (1) to (3) with regard to the specifications of the tested Belleville springs (see Section 2). In this design, the slip force is considered as 30% of the maximum force upon loading. Nevertheless, the relationship between the slip force and the maximum force has to be determined according to the ULS seismic forces (which dictates the slip threshold) and the maximum deflection of the disc

Table 1
Design specifications for the prototype building.

Parameter	Value
Design inter-story drift	2%
Damping (%)	13
Effective design displacement (m)	0.21
Effective mass (tonnes)	713.9
Effective height (m)	10.70
Effective stiffness (kN/m)	3348
Effective period (sec)	2.90
Base shear (kN)	715.6

Table 2
Calculated seismic forces applied to a wall.

Story	Height (m)	Force (kN)	Base moment (kNm)
5	15.5	56.43	874.65
4	12.5	53.58	669.74
3	9.5	40.72	386.84
2	6.5	27.86	181.10
1	3.5	18.89	66.12
Sum		197.48	2178.45

Table 3
Design parameters for the RSF hold-downs.

Parameter	Value
Angle of the ridges (degrees)	15
Coefficient of friction	0.18
Number of bolts	2
Number of Belleville springs per bolt per side	23
Maximum displacement of the joint in tension (mm)	183
Maximum displacement of the joint in compression (mm)	8
Slip force in tension and compression (kN)	421.6
Maximum force for loading in tension (kN)	1351.5
Maximum force for unloading in tension (kN)	258
Maximum force for loading in compression (kN)	462.3
Maximum force for unloading in compression (kN)	88.3
Residual force in tension and compression (kN)	80.5

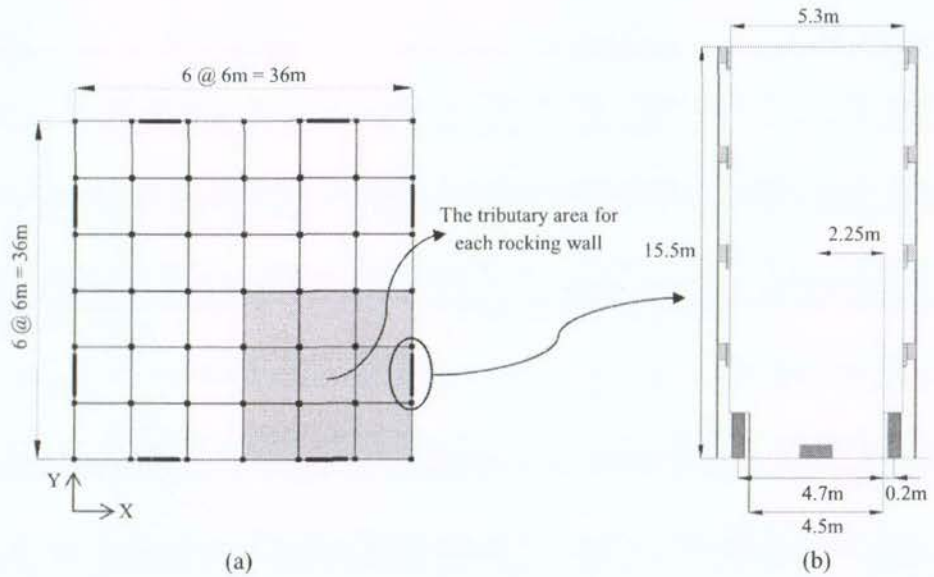

Fig. 6. The prototype building: (a) Plan view (b) Specifications of the rocking walls.

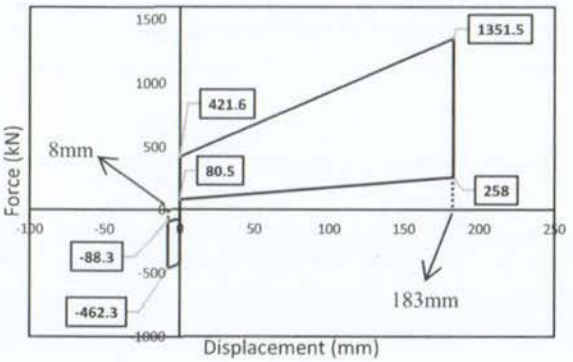

Fig. 7. The designed hysteresis for the RSF joints.

Table 4
Calibrated design parameters for the Damper – Friction Spring link element.

Parameter	Value
Loading slipping stiffness (N/mm)	5087
Unloading slipping stiffness (N/mm)	972
Pre-compression displacement (mm)	−82.9
Stop displacement (mm)	183

springs. The maximum displacement of the RSF joints (183 mm) is specified to meet the 3.75% of lateral drift which is recommended by the New Zealand standard as the near collapse limit. Note that 183 mm displacement in tension in the right RSF joint corresponds to approximately 8 mm of deflection in compression in the left one (see Fig. 5(b)). Thus, the maximum displacement capacity of the RSF joints in compression is specified as 8 mm. The coefficient of friction was considered as 0.18 which is experimentally obtained by the authors [24]. Fig. 7 shows the designed hysteresis.

5. Numerical modelling of the rocking timber walls with RSF joints

This section describes the numerical model developed for the rocking timber walls with RSF joints and compares it with similar systems where the RSF joints are replaced with conventional connectors. The LVL wall is modelled in SAP2000 [25] software package as a 15.5 m high by 4.5 m width shell element with the material properties related to LVL13.2 (E_{LVL} = 13,200 MPa [19]). The RSF joints were modelled by "Damper – Friction spring" link element which is available in SAP2000 version 17 and above. Hashemi et al. showed that this link element is able to accurately predict the hysteretic behaviour of the RSF joint. This was confirmed by comparing the RSF joint component test results with the numerical data [26]. The calibrated parameters for the design specifications in Table 3 are shown in Table 4. A series of Gap elements (compression-only link elements) with the gap set to zero were employed to represent the lateral load bearing components. Similar Gap elements were used at the rocking pivots (at the base of the wall) to represent the

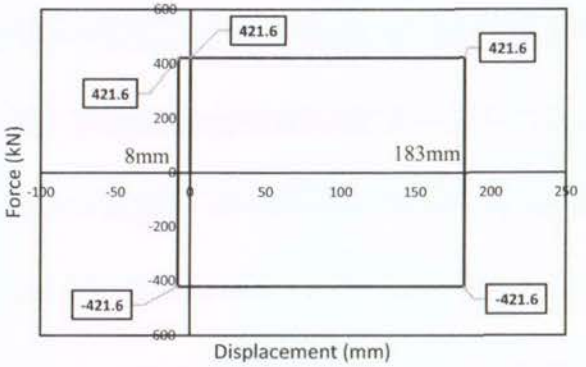

Fig. 9. The designed hysteresis for the symmetric friction dampers.

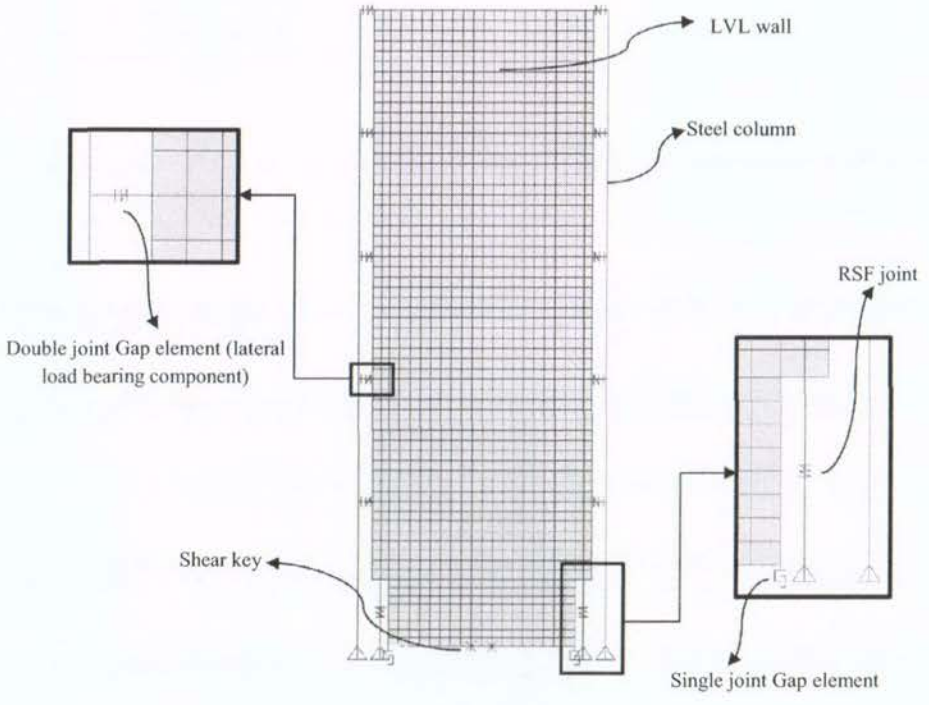

Fig. 8. General arrangement of the numerical model developed for the timber rocking wall with RSF joints.

foundation level. The boundary steel columns were modelled as mild steel box members with 400 mm * 400 mm * 12 mm section for the first three stories and 350 mm * 350 mm * 10 mm section for the two upper stories. The shear key is modelled by restraining the horizontal degree of freedom for the two of the nodes at the base level. Fig. 8 shows the general arrangement of the developed numerical model.

In the numerical models, the only non-linear behaviour is in the RSF joints and the lateral load bearing components. The rest of the structural members were modelled as linear elastic elements.

The application of symmetric friction dampers in rocking timber structures was comprehensively studied by Loo et al. with rigorous numerical analyses and large scale experimental tests [7,8,10,27]. They concluded that the systems containing symmetric

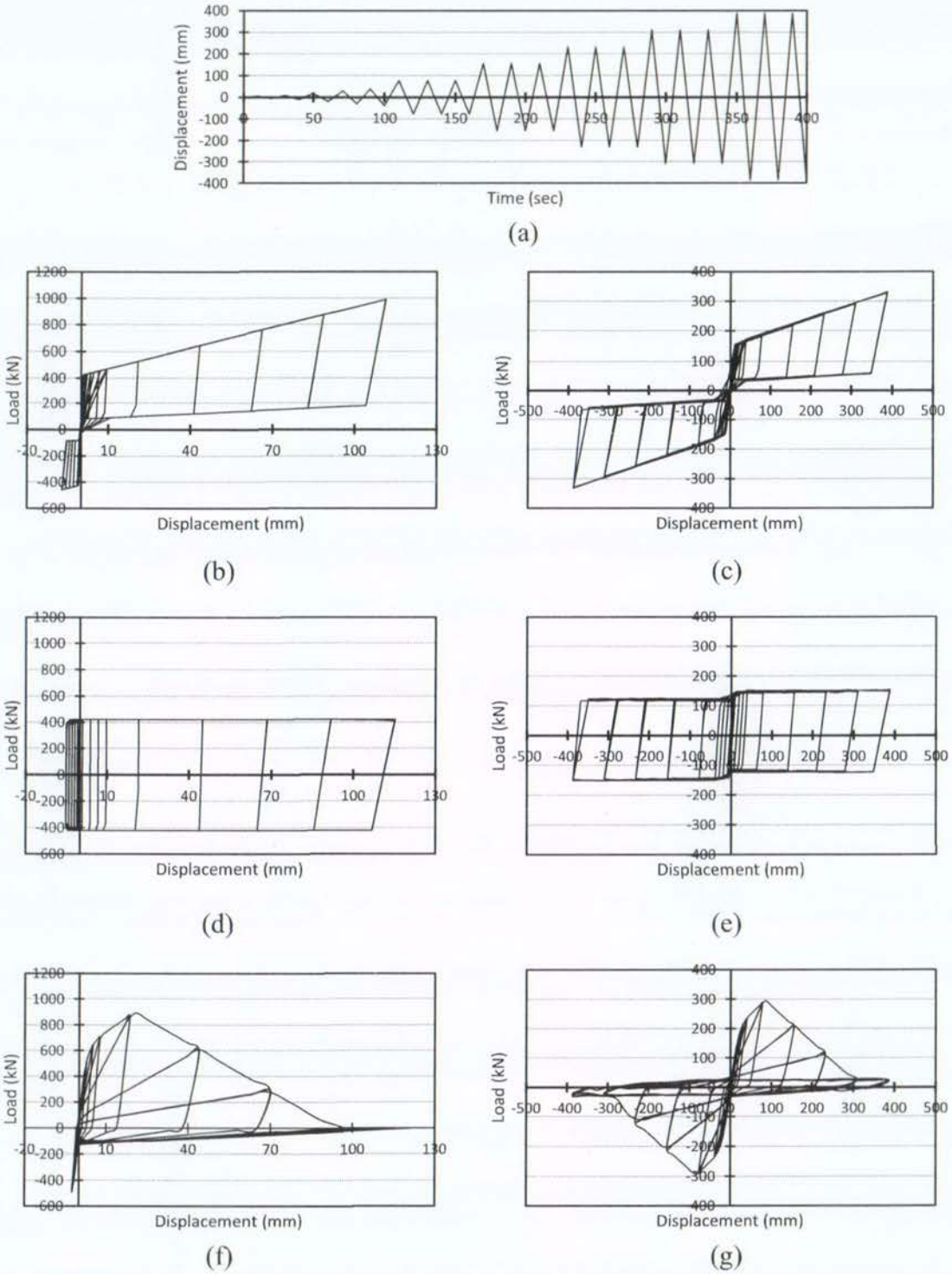

Fig. 10. Numerical results for the quasi-static simulations: (a) Applied displacement schedule (b) RSF joint hysteresis (c) Hysteresis for the total system with RSF joints (d) Symmetric friction damper hysteresis (e) Hysteresis for the total system with symmetric friction dampers (f) Traditional connection hysteresis (g) Hysteresis for the total system with traditional connections.

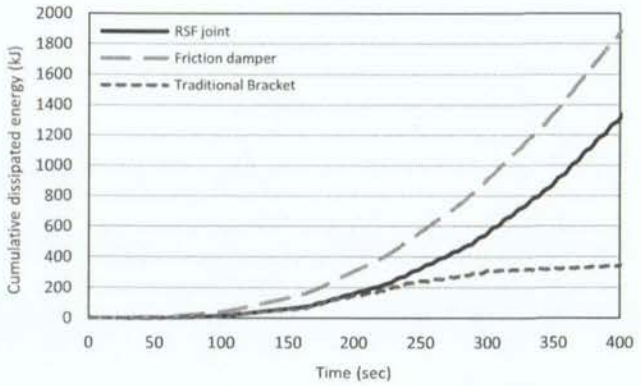

Fig. 11. The dissipated energy for the quasi-static simulations.

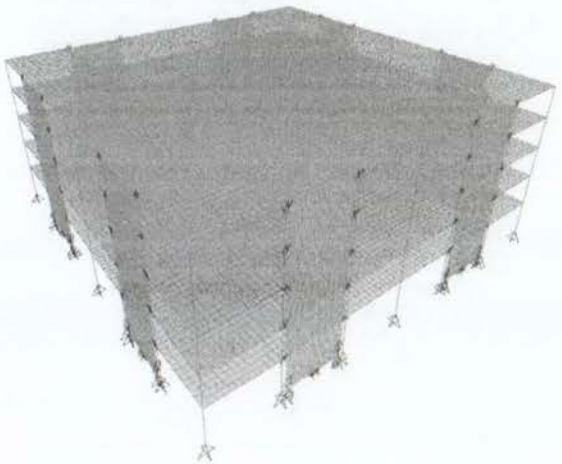

Fig. 12. The general arrangement of the numerical model for the five story prototype building.

friction dampers can confidently be considered as low damage structures. However, the system lacked self-centring behaviour. In order to compare the performance of the introduced concept as a damage avoidant seismic solution with similar systems which contains conventional connectors, another two numerical models were developed with the RSF joints replaced with equivalent symmetric friction dampers (as a well-known low damage concept) in one model and equivalent traditional nailed connections (as a high damage concept) in the other one. The slip threshold and the slot length of the symmetric friction dampers was considered as same as they were for the RSF joints. The reader is referred to [11] for more details about the numerical modelling of symmetric friction dampers and nailed connections.

Symmetric friction dampers were modelled using multi-linear plastic elements with a kinematic hysteresis type. This numerical technique has previously been validated by Loo et al. [10,28]. To model the traditional nailed connections, multi-linear plastic links with pivot hysteresis type were adopted. Hashemi et al. validated this technique by comparing the numerical results with the experimentally obtained data [11]. The hysteresis of the dampers used in the second model is shown in Fig. 9. Since one of the major objectives of this study was to develop a system in which the lateral load resisting members are isolated form the gravity load resisting components, the only considered vertical load was the self-weight of the LVL panel.

The three described models were subjected to quasi-static displacement-control simulations by applying the load protocol in Fig 10(a) at the top of the wall. This load schedule is based on ISO16670 standard for reversed cyclic tests of vertical shear resistant elements [29]. The maximum applied displacement is 387.5 mm which corresponds to 2.5% of lateral drift required for the ULS seismic design [22]. With a load rate of 6 mm/s, the simulations had a total length of 400 s.

Fig 10(b) and (c) show the hysteresis for one of the RSF joints and the total system, respectively. As can be seen, the RSF joint performed as anticipated with an approximately 115.2 mm displacement in tension and 7.07 mm in compression. These displacements are consistent with the analytically calculated displacements (117.5 mm and 8 mm, respectively) which confirms the nearly rigid body motion of the LVL wall. The flag-shaped hysteresis in Fig. 10(c) highlights the self-centring behaviour for the system. Furthermore, it is observable that the system retained its stiffness and strength during 400 s of loading and unloading. Minor fluctuations in the curves are associated with the elastic deflection of the LVL panel which can be ignored when compared with the displacements due to the rocking movement. Note that the maximum force within the RSF joint (see Fig. 10(b)) is less than the maximum capacity (1351.5 kN) because the latter corresponds to 3.75% of lateral drift while the quasi-static simulation targeted 2.5% which relates to the ULS demand.

Fig 10(d) and (e) respectively illustrate the hysteresis for one of the hold-down connections and the total system when the RSF joints are replaced with symmetric friction dampers. The data suggests that the maximum force in the hold-down is capped under a certain limit which is the slip force of the dampers. The nearly elastic-perfectly-plastic hysteretic loops for the wall (Fig. 10(e)) asserts to the fact that the system lacks self-centring behaviour and requires an additional mechanism (such as gravity loads or the force produced by previously implemented post-tensioned cables) to bring it back to its original position. This will be further investigated in the next section. Similar to the system with RSF joints, general stability and minor fluctuations are observable in the hysteretic loops. Accordingly, the system maintained its stiffness and strength which demonstrates the low damage characteristic.

Fig 10(f) and (g) display the hysteretic loops for the third model where the traditional nailed connections were used as hold-downs.

Table 5
The selected ground motions and scaling [30].

Event	Year	PGA (g)	Scaled PGA (ULS)	Scaled PGA (MCE)
El Centro	1940	0.31	0.25	0.47
Northridge	1994	0.23	0.28	0.48
Kobe	1995	0.82	0.24	0.41
Landers	1992	0.28	0.28	0.51
Christchurch	2011	0.48	0.24	0.48
San Fernando	1971	0.21	0.29	0.55
Loma Prieta	1989	0.53	0.21	0.42
Chi Chi	1999	0.23	0.30	0.55
Chihuahua	1979	0.25	0.25	0.45

From these figures it is apparent that when the displacement increases, the stiffness of the system deteriorates and the strength of the wall significantly reduces in comparison with the first two models. This is evidently because of the pinching phenomena usually occurred at the traditional nailed connections. The maximum provided lateral strength in the third model (Fig. 8(g)) is comparable to what was observed in the first model (Fig. 8(c)). Nevertheless, it rapidly dropped when the displacement in the system increased.

Fig. 11 demonstrates the cumulative dissipated energy for the three developed numerical models. The dissipated energy is found by calculating the total area enclosed by the hysteretic curves. It can be seen that the energy dissipation rate is steady for the first two models with RSF joints and friction dampers which is due to low damage characteristic of these devices. However, for the system with traditional hold-downs, the rate of energy dissipation is dramatically decreased after 200 s. This is the result of severe stiffness degradation in the system due to pinching behaviour.

As anticipated, the cumulative dissipated energy in the system containing RSF joints is less than the system with symmetric friction dampers (almost 500 kJ lower). This is because of the fact that flag-shaped hysteresis of the first model covers two of the quadruplets in the load-deformation diagram while the symmetric friction dampers cover all four quadruplets (although with a lower force). It should be pointed out that this comparison is for the RSF joints with $F_{slip}/F_{max,loading} = 0.33$. If this ratio is subjected to change, the energy dissipation rate would be altered.

6. Non-linear dynamic time-history analyses of the prototype building

A suite of nine ground motions scaled to ULS and MCE (Maximum Credible Earthquake) were selected for non-linear dynamic time-history simulations (18 analysed cases in total). They are scaled to match the Christchurch 500 year return period for ULS and 2500 year return period for MCE. Table 5 tabulates the earthquakes and the scaled peak ground motions.

Similar to the rocking wall models described in Section 5, three numerical models were developed for the prototype building in which the only difference between them was the type of the hold-down connectors. RSF joints, symmetric friction dampers and traditional nailed connections were employed as hold-downs in the three developed numerical models, respectively. Fig. 12 illustrates the general arrangement of the numerical models. The beams were modelled as 63 mm * 400 mm timber beams made with LVL13.2. The columns were modelled as mild steel boxes with a 400 mm * 400 mm * 12 mm section for the first three story and a 350 mm * 350 mm * 10 mm section for the upper two stories. The floors were modelled as 150 mm thick shell members with the material properties specified to represent the assumed light timber flooring system described in Section 4. The rocking walls were modelled similar to the ones explained for quasi-static simulations (see Section 5).

The records were applied to the three developed models in the two major directions. Fig. 13 shows the peak roof drifts of the ULS and MCE events. Generally, it can be seen that the peak roof drifts of the building with RSF joints are slightly higher than the one with

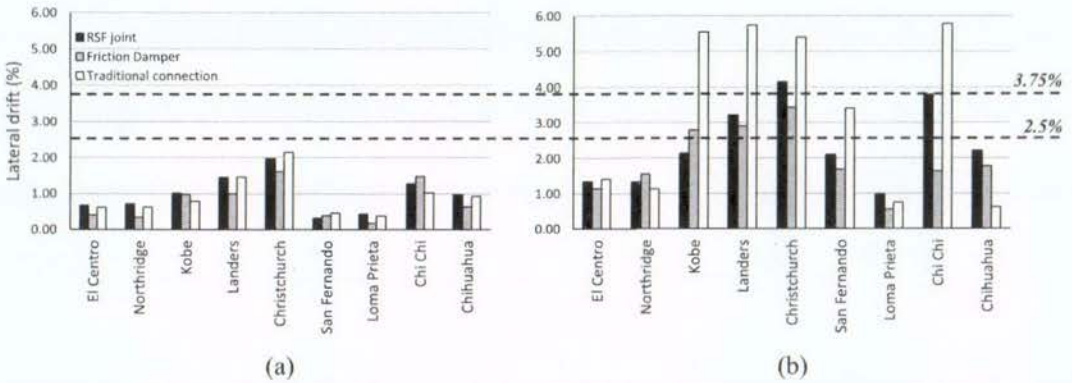

Fig. 13. Peak roof drifts: (a) ULS events (b) MCE events.

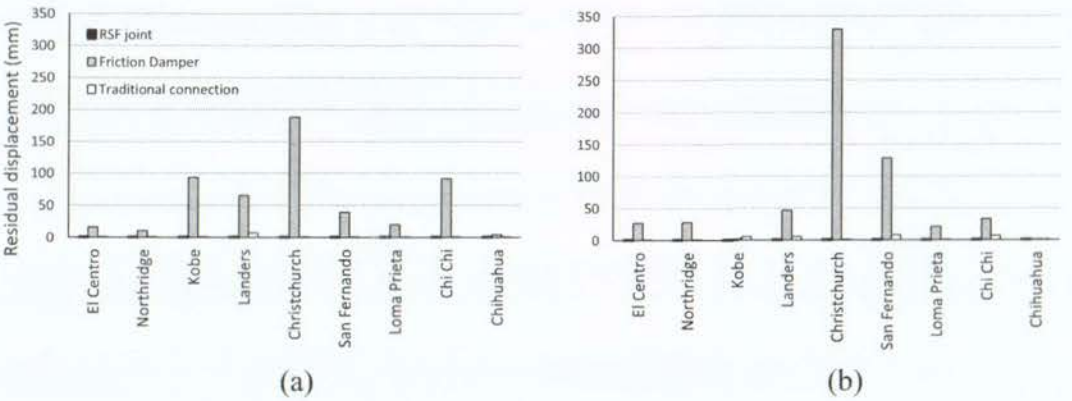

Fig. 14. Residual displacements in the roof: (a) ULS events (b) MCE events.

symmetric friction dampers. For ULS events, none of the structures demonstrated a drift more than 2.5% which is the recommended limitation for the ULS seismic design [22]. The maximum drift was for the model with traditional connections subjected to Christchurch event which is slightly higher than 2%. For MCE events, the structure with traditional connections experienced peak roof drifts as high as 5.8% which probably would result in global collapse of the building in a real case. This can be attributed to the significant stiffness degradation in the connections due to pinching phenomena. For the structures with RSF joints, the peak roof drifts remained under the recommended limit (3.75%) except for the Christchurch and Chi Chi which the difference is under 8% and may be considered as acceptable. None of the structures with symmetric friction dampers experienced peak roof drifts more than 3.45% which can be the results of the relatively higher energy dissipation ratio in the dampers. In terms of maximum lateral drift, it can be concluded that structures with RSF joints and symmetric friction dampers performed well while the buildings with traditional connections are prone to collapse specially when a MCE event takes place.

Fig. 14 displays the residual displacements for the ULS and MCE events. As can be seen, the residual displacements for the structure with asymmetric friction dampers are drastically higher than the other two models. This asserts to the fact that the considerable post-event displacements for these dampers is a major disadvantage which may cause severe damage to structural and non-structural elements. The highest residual displacement is for the Christchurch which is 251 mm for ULS and 535 mm for MCE (corresponding to 1.61% and 3.45% of lateral drift). It should be emphasized that even in cases where the building is not highly damaged, the dampers may need to be opened up for the structural elements to return to their original position. This procedure is likely to be extremely costly and involves many uncertainties. On the contrary, the systems with RSF joints exhibited no residual displacements which was expected due to the flag-shaped hysteretic behaviour of the joints. The systems with traditional connections demonstrated insignificant levels of residual displacements. It was also expected because of the fact that the stiffness of the structure considerably reduces in each cycle and as a consequence, the restoring forces from seismic excitations and self-weight of the lateral load resisting members are sufficient to re-centre the building.

Fig. 15 illustrates the peak roof accelerations. Despite the fact that it has previously been proven that timber structures with traditional connections may demonstrate an acceptable seismic performance, the peak roof accelerations for them are much higher than those with dissipative devices such as RSF joints or symmetric friction dampers. During the shake table tests within the SOFIE project, it was concluded that additional energy dissipation devices are required to decrease the earthquake induced accelerations [1]. In average, the results in Fig. 15 confirms that the use of RSF joints

Table 6
The applied seismic sequences.

Analyze case	Events
Sequence 1	Christchurch (ULS) – Christchurch (MCE)
Sequence 2	Kobe (ULS) – Kobe (MCE)
Sequence 3	Chi Chi (ULS) – Chi Chi (MCE)
Sequence 4	Landers (ULS) – Landers (MCE)
Sequence 5	San Fernando (ULS) – San Fernando (MCE)
Sequence 6	Christchurch (ULS) – San Fernando (MCE)
Sequence 7	Kobe (ULS) – Christchurch (MCE)
Sequence 8	Chi Chi (ULS) – San Fernando (MCE)
Sequence 9	Landers (ULS) – Chi Chi (MCE)
Sequence 10	San Fernando (ULS) – Christchurch (MCE)

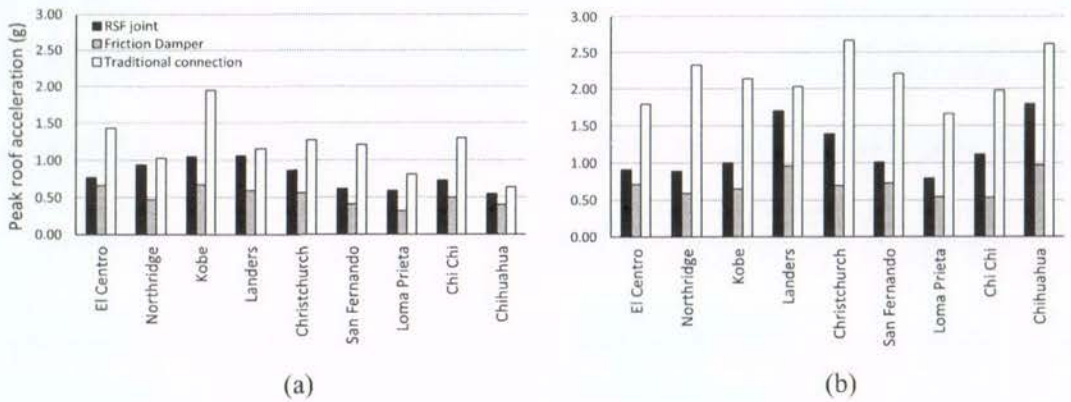

Fig. 15. Peak roof accelerations: (a) ULS events (b) MCE events.

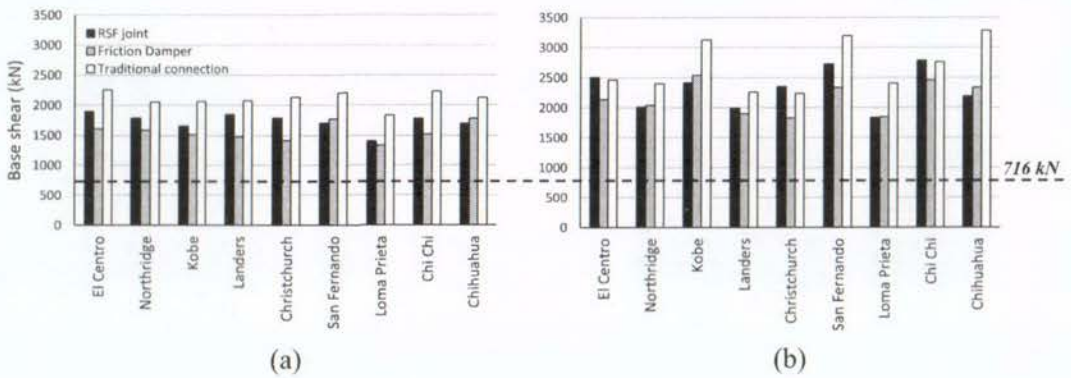

Fig. 16. Base shear: (a) ULS events (b) MCE events.

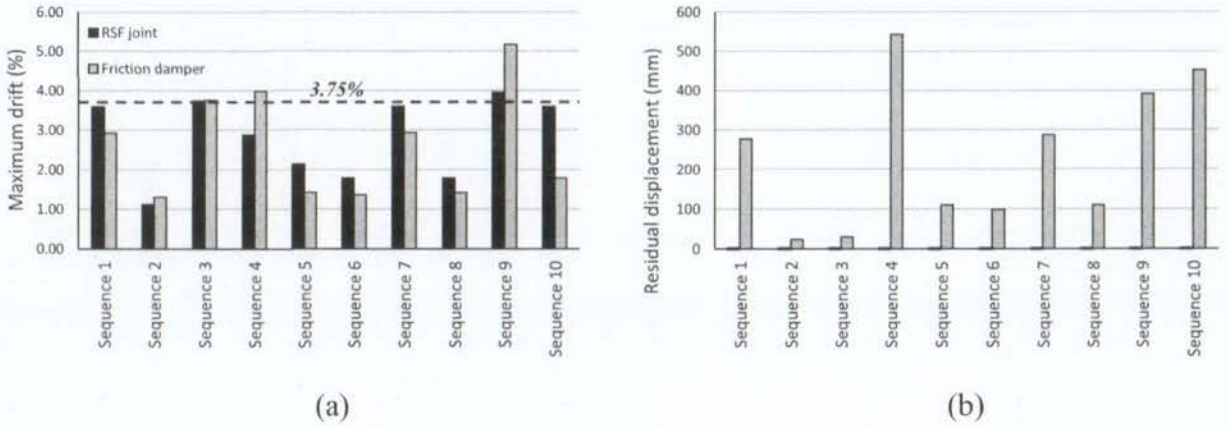

Fig. 17. Numerical results for the sequences of earthquakes: (a) Maximum drifts (b) Residual displacements.

and symmetric friction dampers contribute to 41% and 58% reduction in the peak roof accelerations, respectively. It can be seen that for the structures with traditional connections subjected to MCE events, the recorded peak roof accelerations are much higher than those with RSF joints or symmetric friction dampers. Undoubtedly, this is owing to the dramatic decrease in the lateral stiffness of the building through the excitations. From the numerical data in Fig. 15, it can be concluded that the use of more advanced connectors such as RSF joints or symmetric friction dampers can highly decrease the seismic induced accelerations.

Fig. 16 shows the base shear in the X direction of the prototype building models (see Fig. 6(a)). It is observable that the recorded base shears are higher than the analytically calculated one (715.6 kN) which is consistent with the findings of Loo et al. for timber rocking walls with friction dampers [10]. More to the point, a dynamic amplification factor needs to be considered to account for the effect of higher modes of vibration when designing the structural members. As can be seen from the figure, a base shear dynamic amplification factor of 2.5 can be suggested for the systems containing rocking walls with RSF joints.

An important motivation for developing damage avoidant seismic solutions is the fact that the structure should tolerate multiple seismic events. In fact, if the lateral strength of a structure dramatically decreases in a severe earthquake, even a minor aftershock may contribute to collapse of the building. In order to further investigate the seismic performance of the systems described in this study, the models were subjected to sequences of earthquakes. Each sequence included an ULS earthquake followed by a MCE event. This situation is similar to what happened in Christchurch, New Zealand in 2010 and 2011. Table 6 shows the selected sequences.

Since it was affirmed that the models with traditional connections can barely survive the MCE events, the sequence of earthquakes were applied only to the two first models (the models with RSF joints and symmetric friction dampers). Fig. 17 shows the obtained results for maximum lateral drifts and maximum residual displacements at the top. It can be seen that the average of maximum drifts for the model with RSF joints is still under the indicated threshold. However, for the symmetric friction dampers, it reached a peak of 5.2% which is far above the allowed limitation. This observation confirms that a system with symmetric friction dampers can exhibit unfavourable seismic performance in spite of having a relatively high energy dissipation rate.

For the structures with friction dampers, significant residual displacements were recorded for most of the seismic sequences. The maximum is for sequence 4 which is 665 mm (corresponds to 4.29% of lateral drift). For sequence 9 and sequence 10, the residual displacement is close to 400 mm (corresponding to 2.58%). It can be concluded that a structure with friction dampers that already reached a considerable residual displacement is likely to yield even more residual displacement under the second seismic event.

On the contrary, the model with RSF joints resulted in no residual displacement confirming the self-centring behaviour under sequences of earthquakes. From the numerical results, it is hard to escape the obvious conclusion that the structural system including symmetric friction dampers yield poor seismic performance in terms of post-event residual displacements and the associated damage. The systems with RSF joints maintained their efficiency and robustness during single and multiple seismic events.

7. Conclusions

This paper explains the development of a new type of lateral load resisting system which includes rocking timber walls and Resilient Slip Friction (RSF) joints as hold-down connections. This system provides self-centring in addition to energy dissipation. Non-linear cyclic and dynamic simulations were performed to demonstrate the seismic performance of the introduced system. In order to evaluate the efficiency of the proposed concept on the system level, a five story prototype building was designed based on the Displacement Based design (DBD) procedure. To compare the concept with existing seismic solutions, another two numerical models were developed with RSF joints replaced with equivalent symmetric friction dampers and traditional nailed connections. The results of the time-history simulations highlighted the good seismic performance of the proposed concept in terms of maximum lateral drifts, residual displacements and peak roof accelerations. On the contrary, the systems with traditional connections exhibited significant reduction in lateral strength and the systems with symmetric friction dampers revealed notable residual displacement which even increased after applying sequences of seismic events to the model. Overall, the results of this preliminary study confirmed that the proposed concept has the merit to be considered as a damage avoidant seismic solution. Further experimental investigations may be required in future to confirm the findings of this study for new seismic resilient structures or for retrofitting existing buildings.

Acknowledgement

The authors would like to thank the Earthquake Commission Research Foundation (EQC) of New Zealand for the financial sup-

port of the presented research under the grant number "EQC 15/U710".

References

[1] A. Ceccotti, C. Sandhaas, M. Okabe, M. Yasumura, C. Minowa, N. Kawai, SOFIE project–3D shaking table test on a seven storey full scale cross laminated timber building, Earthq. Eng. Struct. Dyn. 42 (13) (2013) 2003–2021.

[2] A. Iqbal, S. Pampanin, A. Buchanan, and A. Palermo, Improved seismic performance of LVL post-tensioned walls coupled with UFP devices, in: 8th Pacific conference on earthquake engineering, Singapore, 2007.

[3] A. Iqbal, S. Pampanin, A. Palermo, A.H. Buchanan, Performance and design of LVL walls coupled with UFP dissipaters, J. Earthq. Eng. 19 (3) (2015) 383–409.

[4] F. Sarti, A. Palermo, S. Pampanin, Development and testing of an alternative dissipative posttensioned rocking timber wall with boundary columns, J. Struct. Eng. (2015) E4015011.

[5] A. Iqbal, T. Smith, S. Pampanin, M. Fragiacomo, A. Palermo, A.H. Buchanan, Experimental performance and structural analysis of plywood-coupled LVL walls, J. Struct. Eng. 142 (2) (2015) 4015123.

[6] A. Kramer, A.R. Barbosa, A. Sinha, Performance of steel energy dissipators connected to cross-laminated timber wall panels subjected to tension and cyclic loading, J. Struct. Eng. 142 (4) (2015) E4015013.

[7] W.Y. Loo, Rocking Structures with Passive Energy Dissipaters: An Approach in Timber, The University of Auckland, 2016.

[8] W.Y. Loo, C. Kun, P. Quenneville, N. Chouw, Experimental testing of a rocking timber shear wall with slip-friction connectors, Earthq. Eng. Struct. Dyn. 43 (11) (2014) 1621–1639.

[9] W.Y. Loo, P. Quenneville, N. Chouw, A new type of symmetric slip-friction connector, J. Constr. Steel Res. 94 (2014) 11–22.

[10] W.Y. Loo, P. Quenneville, N. Chouw, Rocking timber structure with slip-friction connectors conceptualized as a plastically deformable hinge within a multistory shear wall, J. Struct. Eng. (2015) E4015010.

[11] A. Hashemi, R. Masoudnia, P. Quenneville, A numerical study of coupled timber walls with slip friction damping devices, Constr. Build. Mater. 121 (2016) 373–385.

[12] A. Hashemi, W.Y. Loo, R. Masoudnia, P. Zarnani, P. Quenneville, Ductile Cross Laminated Timber (CLT) Platform Structures with Passive Damping, in: World Conference of Timber Engineering WCTE2016, Vienna, Austria, 2016.

[13] D. Wrzesniak, G.W. Rodgers, M. Fragiacomo, J.G. Chase, Experimental testing of damage-resistant rocking glulam walls with lead extrusion dampers, Constr. Build. Mater. 102 (2016) 1145–1153.

[14] A. Hashemi, P. Zarnani, R. Masoudnia, P. Quenneville, Seismic resistant rocking coupled walls with innovative Resilient Slip Friction (RSF) joints, J. Constr. Steel Res. 129 (2017) 215–226.

[15] P. Zarnani, P. Quenneville, A Resilient Slip Friction Joint, Provisional patent no. 7083, 2015.

[16] A. Hashemi, P. Zarnani, R. Masoudnia, P. Quenneville, Seismic Resistant Cross Laminated Timber (CLT) Structures with Innovative Resilient Slip Friction (RSF) Joints, in: World Conference of Earthquake Engineering (16WCEE), 2017.

[17] P. Zarnani, A. Valadbeigi, P. Quenneville, Resilient slip friction (RSF) joint: a novel connection system for seismic damage avoidance design og timber structures, in: World Conference of Timber Engineering WCTE2014, Vienna, Austria, 2016.

[18] A. Hashemi, P. Zarnani, A. Valadbeigi, R. Masoudnia, P. Quenneville, Seismic Resistant Timber Walls with New Resilient Slip Friction Damping Devices, Int. Netw. Timber Eng. Res. Conf, Graz, Austria, 2016.

[19] A.H. Buchanan, N.Z.T.I. Federation, Timber design guide, New Zealand Timber Industry Federation, 1999.

[20] F. Sarti, A. Palermo, S. Pampanin, Design and testing of post-tensiond timber wall systems, in: World Conference of Timber Engineering WCTE2014, Qubec city, Canada, 2014.

[21] A. Hashemi, P. Quenneville, A shear anchor for a structural member, Provisional Patent no. 728725, 2017.

[22] New Zealand Standards, Structural Design Actions (NZS 1170.5), 2004. Wellington, New Zeal..

[23] M.J.N. Priestley, G.M. Calvi, Displacement-Based Seismic Design of Structures, IUSS Press, Pavia, Italy, 2007.

[24] A. Hashemi, P. Zarnani, A. Valadbeigi, R. Masoudnia, P. Quenneville, Seismic resistant cross laminated timber structures using an innovative resilient friction damping system, in: Proceedings of New Zealand Society for Earthquake Engineering Conference (NZSEE), Christchurch, New Zealand, 2016.

[25] Computers and Structures, SAP2000 Ver. 19 (2017), Berkeley, CA, 2017.

[26] A. Hashemi, R. Masoudnia, P. Quenneville, Seismic performance of hybrid self-centring steel-timber rocking core walls with slip friction connections, J. Constr. Steel Res. 126 (2016) 201–213.

[27] W.Y. Loo, P. Quenneville, N. Chouw, A numerical study of the seismic behaviour of timber shear walls with slip friction connectors, Eng. Struct. 34 (2012) 233–243.

[28] W.Y. Loo, P. Quenneville, N. Chouw, A numerical approach for simulating the behaviour of timber shear walls, Struct. Eng. Mech. 42 (3) (2012) 383–407.

[29] ASTM Standard, "E2126", Stand. test methods Cycl. load test Shear Resist. Vert. Elem. lateral force Resist. Syst. Build. Am. Soc. Test. Mater., West Conshohocken, PA, 2009.

[30] PEER, NGA Database, Pacific Earthquake Engineering Research Center, Univ. California, Berkeley, USA, 2006. http//peer. berkeley. edu/nga.

Construction and Building Materials 121 (2016) 373–385

Contents lists available at ScienceDirect

Construction and Building Materials

journal homepage: www.elsevier.com/locate/conbuildmat

A numerical study of coupled timber walls with slip friction damping devices

Ashkan Hashemi *, Reza Masoudnia, Pierre Quenneville

Department of Civil and Environmental Engineering, Faculty of Engineering, The University of Auckland, Private Bag 92019, Auckland 1142, New Zealand

HIGHLIGHTS

- Coupled timber walls with slip-friction connections were introduced and numerically modelled.
- The response of the system to quasi-static and time-history dynamic loading was studied.
- The efficiency of the proposed system is compared with a similar system with equivalent nailplates.
- Timber coupled walls with slip friction connections enhance the ability of walls to absorb the seismic energy.
- Timber coupled walls with slip friction connections represent a feasible low damage solution for rocking timber structures.

ARTICLE INFO

Article history:
Received 30 January 2016
Received in revised form 24 May 2016
Accepted 26 May 2016

Keywords:
Timber walls
Cross Laminated Timber
Slip friction
Low damage
Energy dissipation

ABSTRACT

In rocking timber structures, the traditional connections such as nailplates may need to be replaced by damping devices to provide the required lateral resistance and dissipate the seismic energy. This study seeks to investigate the seismic behaviour of coupled timber walls with slip friction connections. Slip friction connections present a low damage solution as they do not suffer from stiffness degradation and can be used after a seismic event. The seismic response of the described system is compared to those with equivalent nailplates. Displacement control quasi-static and also dynamic time-history analyses showed that the performance of the systems with friction devices is significantly improved under seismic loading compared to similar systems with equivalent nailplate connections. The systems with nailplates incurred significant inelastic damages while the systems with friction devices exhibited superior performance in terms of strength degradation and absorbed seismic energy. The introduced concept presents a feasible solution for timber structures when a low damage design is targeted.

1. Introduction

The potential for structural systems with prefabricated members in seismic applications has significantly increased in the last two decades. This was mostly due to the introduction of jointed ductile connections in precast concrete. In the United States in the early 1990's, the PRESSS (PREcast Seismic Structural Systems) program was initiated in order to develop design recommendations for precast construction in seismic zones and also to introduce novel concepts and technologies in precast concrete structures [1]. As an important outcome of the program, precast concrete walls were recognised as being significantly effective lateral load resisting members. Later, in order to minimise the observed residual damage during the experiments, a coupled wall system with energy dissipative devices was introduced as another part of the program [2].

In a typical coupled wall system, two or more prefabricated walls are connected to each other with special energy dissipative connectors along the vertical edges. In a seismic event, the walls are allowed to rock restrictedly at the base and then return to their initial position. The vertical joints dissipate energy by experiencing inelastic deformations under lateral forces. The system can accommodate large lateral drifts while residual damages are minimised. This concept has later been adapted to timber structures by Palermo et al. [3]. Iqbal et al. [4] further developed the concept and tested coupled timber walls with mild steel U-shaped Flexural Plates (UFPs) as the vertical joints. They concluded that the U-shaped plates offer an effective energy absorption mechanism through metal yielding during rocking of the walls.

Passive friction-based energy dissipater devices were originally utilised for steel structures. Popov et al. [5] introduced the

* Corresponding author.
E-mail address: ahas439@aucklanduni.ac.nz (Ashkan Hashemi).

http://dx.doi.org/10.1016/j.conbuildmat.2016.05.160
0950-0618/

symmetric slotted bolted connection which dissipates energy through friction during equilateral tension and compression cycles. It consists of a main plate sandwiched by two outer plates connected together by bolts. The connection is designed such that at a predestined force, sliding will be initiated. The slippage force is function of both the clamping force of the bolts and the coefficient of friction of the surfaces enclosed by the two outer plates.

Clifton et al. [6] proposed the *Asymmetric* sliding hinge joint for steel moment resisting frames which had non-rectangular yet stable hysteretic behaviour. In the asymmetric assembly, when the applied force rises above the frictional resistance of the first surface, sliding will be triggered while the bottom plate remains still for a short period of time. Subsequently, the bottom plate starts to slip and the sliding shear and the stiffness of the connection will be doubled. Therefore, bolts are forced into a double curvature state and the joint renders a pinched hysteretic behaviour [7]. This is advantageous for minimising the post-seismic residual drifts but it is not beneficial for stiffness retention after a seismic event. Khoo et al. [8] developed the design models for asymmetric slotted bolted connections based upon numerous experiments and also rigorous analyses.

For timber structures, Most of the proposed seismic solutions were based on energy dissipation through deformation and yielding of the fasteners (such as nails or screws) and crushing of the wood fibres [9–12]. Filiatrault [13] utilised friction dampers for timber sheathed shear walls. The analytical studies demonstrated a noticeable improvement in the hysteretic behaviour of the walls compared to traditional timber shear walls. Large amount of dissipated energy was also observed at different lateral drifts up to 1.5%. Loo et al. [14,15] investigated the application of slip friction connections as a replacement of traditional hold-downs for timber Laminated Veneer Lumber (LVL) walls. Their experiments showed significantly improved seismic performance compared to traditional systems in terms of hysteretic behaviour stability and residual deflections [16]. Additionally, and most importantly, the timber wall remained in the elastic region after several quasi-static and dynamic numerical analyses that was also confirmed by experimental tests.

This study seeks to investigate the application of sliding frictions passive dampers (slip friction connections) in coupled timber walls. Towards this purpose, a new configuration is proposed. The slip friction connections developed and tested by Loo et al. [14,15] are used as hold-down connectors. Additionally, a new type of slip friction connector for vertical joints inspired by previously proposed slip friction hold-downs is presented. A symmetric configuration is considered for both hold-downs and vertical joints between the adjacent walls. Nonetheless, the asymmetric concept undoubtedly has the potential for further studies in timber structures. General arrangement of the proposed system is shown in Fig. 1.

In order to determine the slip force which triggers the rocking movement in the system, a numerical simulation has been conducted on the timber walls. Henceforth, the efficiency of the proposed coupled wall system is investigated through displacement control quasi-static and dynamic time-history analyses. To compare the seismic performance of the introduced concept with the conventional systems, similar numerical models with equivalent nailplate connections in lieu of slip friction devices are developed and analysed.

2. Lateral resistance of Cross Laminated Timber (CLT) and Laminated Veneer Lumber (LVL) walls

Cross laminated timber is a new generation of engineered wood product which was firstly developed in Europe in the 1990s and then adopted in other parts of the world [17]. It consists of typically three, five, or seven layers of dimensioned lumber oriented orthogonally to each other and then glued to create a structural panel. It is a strong, sustainable and dimensionally stable wood product. It offers almost similar characteristics to that of a precast concrete panel yet has a much more advantageous strength to weight ratio. More than that, efficient planning during construction and a high level of prefabrication are the two key advantages which significantly accelerate the construction process. Thus, CLT has been notably gaining popularity among the building owners and the designers around the world and numerous CLT buildings have been built in different countries during the last decade.

Generally, in all low damage timber structural systems, the key point is that timber elements must remain in the elastic region and any possible pinching phenomena in the connections which may cause non-recoverable plastification in the wood should be avoided. Thus, the first step in design and modelling of CLT shear walls with slip friction connections is to decide on a rational method to determine the maximum tolerable lateral force (and the consequent overturning moment) at which the wall can remain in the elastic region (F_E). If a lateral force is applied to the top of a rocking CLT wall (see Fig. 3(b)), the movement should be initiated before the stress in any of the timber boards exceeds the allowable characteristic strength. Loo et al. used a similar approach to specify the slip threshold for a rocking LVL wall with slip friction hold-downs [15].

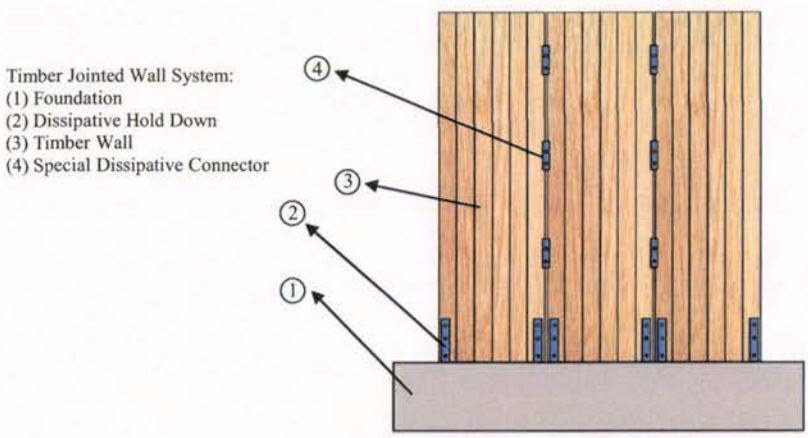

Fig. 1. The concept of coupled timber walls with slip friction connections.

While there are numerous analytical methods or numerical models for analysing LVL walls (and consequently determining F_E), there is a lack of research studies about CLT walls under lateral forces with the focus on the timber boards. Most of the previous numerical models for CLT panels were focused on the behaviour of the connections rather than the panel itself. Bogensperger et al. proposed a cubic numerical model to assess the bearing capacity of the CLT panels [18]. Fragiacomo et al. developed a numerical model for CLT floors containing two isotropic materials for layers parallel and perpendicular to the main floor direction [19]. Pozza et al. used a simplified two dimensional assembly to analyse the hysteretic behaviour of CLT shear walls with traditional connections [20]. Yasumura et al. developed a numerical model for a three story CLT building which the CLT panels and the connections were expressed as shell and spring elements, respectively [10].

In this paper, series of finite element analyses on different configurations for CLT walls have been carried out using the ABAQUS software package [21]. In each wall, the lateral force applied at the top is increased until the normal stress in one of the timber boards exceeds its permissible characteristic strength indicated in Table 1. Additionally, three LVL wall models with different widths were investigated to look over the benefits of a hybrid CLT-LVL coupled wall system.

A five layer CLT panel with three 40 mm thickness longitudinal layers and two 40 mm thickness transverse layers with 200 mm width for all boards is assumed in all models. To optimise the efficiency of CLT wall applications, panels have been placed with their outer layers parallel to the gravity loads [17]. The elastic modulus parallel to grain of all the boards within the CLT members was set to 8000 MPa and the elastic modulus of LVL veneers was set to 13,200 MPa [22] (see Table 1 for more details). The mechanical properties are assigned to timber boards according to the principal axes illustrated in Fig. 2.

Six different height to width ratios for CLT panels and four for LVL walls were analysed. In the numerical models, 8-node solid element C3D8R (a linear 3D hex-structured shape element) was adopted for timber boards [23]. In Fig. 3, the numerical assembly of the CLT wall and the stress distribution are shown. In addition to the self-weight of the walls, a 25 kN per wall's width vertical load is applied to the models at two elevations as an approximate estimation for permanent and live loads for a timber shear wall. Details of different wall configurations and the results are given in Table 2. In this table, Δ_E represents the elastic deformation at the top due to the corresponded F_E.

As expected, F_E for the LVL walls is approximately 40 to 50% higher than that of the CLT walls with the same geometry (see Fig. 4). This may be beneficiary for coupled timber walls comprised of different engineered wood panels (CLT-LVL) when geometric limitations are restricting the designer. Furthermore, it can be derived from Fig. 4 that while the thickness of the CLT panel remains constant, the lateral elastic stiffness has almost a linear relationship with the height to width ratio. In this study, these results are used to determine the slip threshold for the slip friction connections, however, there is still room to investigate the relationship between the lateral stiffness of CLT walls with different arrangement of the layers or with different material properties for the timber boards.

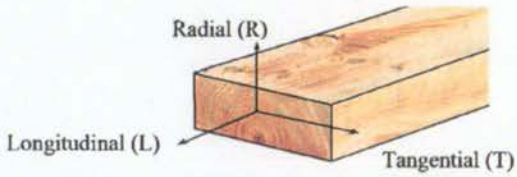

Fig. 2. Principal axes of a single timber board within the CLT numerical model.

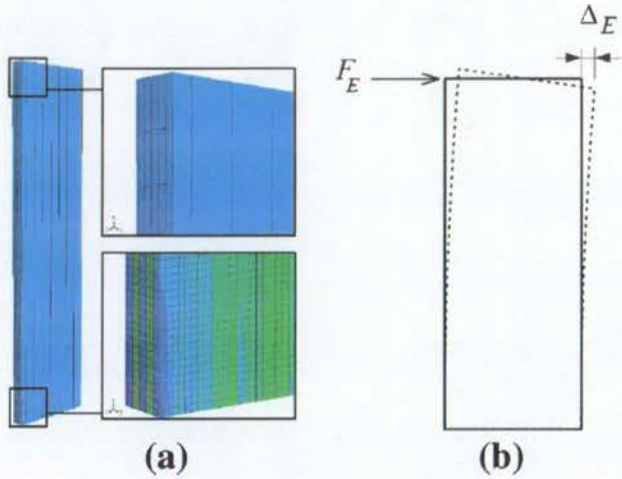

Fig. 3. CLT Numerical model: a) Numerical assembly b) Wall elastic deformation.

3. Proposed configuration for coupled timber wall system with slip friction connections

Fig. 5 illustrates a schematic view of the proposed configuration for the coupled timber wall system with slip friction connections. The components of the system transfer the lateral forces to the foundation while providing the required ductility at a given drift. The walls are typically made of CLT or LVL panels which the type is generally determined based on the required lateral resistance. The bottom connections are Slip Friction Hold-downs (SFH) comprised of several parts (Fig. 5(c)). The centre plate (the wall embedded plate) is attached to the timber wall with mechanical fasteners. The connection between the timber wall and the centre plate is meant to be very stiff since the inelastic behaviour of the system is provided by the slippage of the friction devices. It has been analytically and experimentally verified that rivets can provide such stiffness with their relatively higher load per unit transfer capacity in comparison to bolts or screws. Furthermore, no timber cross section reduction needs to be considered for the rivet hole which in this case, with respect to the number of friction joints, will indubitably be an advantage [24].

Table 1
Material properties of the LVL member and CLT boards [22].

Component	E_L	E_R	E_T	ν_{LT}	ν_{TL}	ν_{LR}	ν_{RL}	ν_{TR}	ν_{RT}	f_c	f_t
LVL	13,200	600	600	0.35	0.030	0.35	0.030	0.35	0.35	45	33
CLT boards (MSG8*)	8000	363	363	0.20	0.018	0.15	0.018	0.21	0.18	18	6

E = Elastic Modulus.
ν = Poison's ratio.
MPa for all modulus for LVL and CLT.
* MSG8 refers to grade 8 machinery graded sawn timber [22].

Table 2
Configuration of the wall models and results.

Material	Model number	Height	Width	Thickness	Width to Height Ratio	Axial load	F_E	Δ_E
CLT	C01	6000	2400	200	1/2.5	60	49.7	18.3
	C02	6000	2000	200	1/3	50	39.4	19.3
	C03	6000	1600	200	1/3.75	40	29.3	20.9
	C04	6000	1500	200	1/4	37.5	26.5	21.2
	C05	6000	1200	200	1/5	30	19.4	23.1
	C06	6000	1000	200	1/6	25	14.7	23.7
LVL	L01	6000	1600	200	1/3.75	40	51.5	10.7
	L02	6000	1500	200	1/4	37.5	46.9	10.9
	L03	6000	1200	200	1/5	30	33.4	12.2
	L04	6000	1000	200	1/6	25	25.1	13.7

Millimetres for all dimensions and displacements.
kN for all loads and forces.

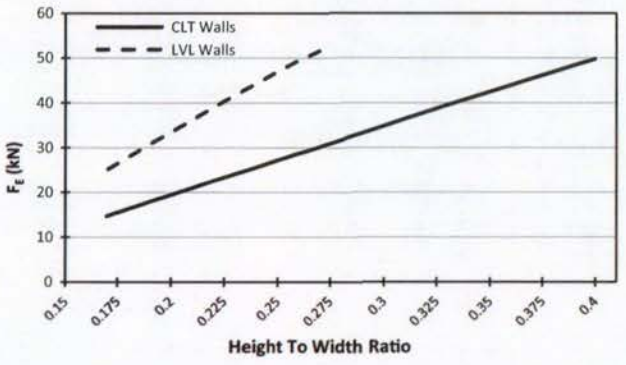

Fig. 4. F_E for the CLT and LVL walls.

The three plates within the SFH (the two outer plates and the centre plate) are bolted in a manner that the centre plate is sandwiched by the outer plates. When the imposed vertical force to the hold-down overcomes the frictional resistance between the two surfaces, the centre plate starts to move and energy will be dissipated through sliding. The efficiency of this connector has been experimentally validated in timber shear walls [16] and also in precast concrete structures [25].

In the proposed system, two or more rocking walls with above-mentioned configuration will be connected together by special ductile links which are the source of significant energy dissipation from the relative vertical movement between the adjoining walls. In this study, a new type of Slip Friction Joint (SFJ) is proposed. Similar to SFHs, three plates are bolted and clamped together in a way that the centre slotted plate is attached to one of the walls by using a steel flange (see Fig. 5(b)). The two outer plates are connected to the other wall with a similar assemblage. When the vertical force at one direction exceeds the frictional resistance between the two surfaces, the centre plate starts to slide and energy will be dissipated over the joint. Correspondingly, for the other direction, the centre plate remains still and cover plates will be dragged along by the friction bolts. The slip threshold for the SFH or the SFJ is given by Eq. (1) where μ is the coefficient of friction between the two surfaces, n_b is the number of bolts and T_b is the tension force in each bolt.

$$F_{slip} = 2\mu n_b T_b \tag{1}$$

The purpose of slip friction connectors is to protect the wooden members from inelastic damage while the ductility of the system is provided by rocking behaviour. Towards this purpose, F_E for each wall has been determined in accordance with the numerical results

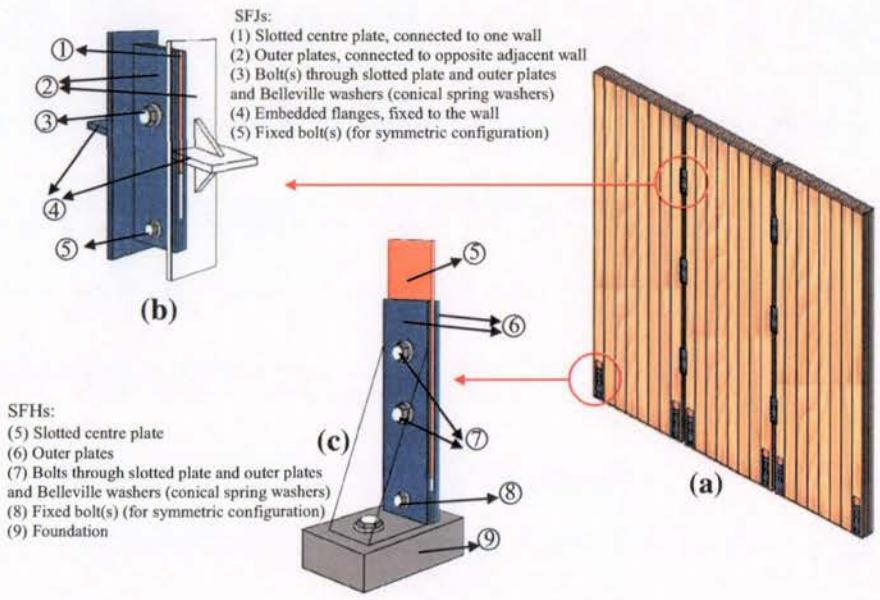

Fig. 5. Proposed configuration for a coupled timber wall system with slip friction connections: a) General arrangement b) Slip friction joints (SFJs) c) slip friction hold-downs (SFHs).

from Section 2. By that, the slip threshold for all connectors (which are acting together) is defined in a way that the resultant applied force on the top of each timber wall is limited to F_E.

As shown in Fig. 6(a), the acting forces on each wall within a system comprised of three identical walls are slip friction hold-down force (F_H), the sum of slip friction joint forces ($\sum F_j$) and the vertical loads (W). $F_{E,t}$, $F_{E,i}$ and $F_{E,l}$ in Fig. 6(a) are the maximum tolerable forces at the top of each wall for the trailing wall, the intermediate wall and the leading wall for the left to right direction of rocking. It should be noted that at the opposite direction, the roles of the leading wall and the trailing wall are reversed (thus, the acting forces on them are also reversed) while the role of the intermediate wall(s) does not change. Providing that the walls are identical, $F_{E,t} = F_{E,i} = F_{E,l}$. Taking the moments about the rocking point of each wall and assuming that the slip force (F_{slip}) is set in a manner that sliding will be triggered when the lateral force applied at the top of the wall is equal to its F_E, the gross slip force in the connections ($F_H + \sum F_j$) can be calculated from Eq. (2).

$$F_H + \sum F_j = F_E \frac{h}{b} - \frac{W}{2} \tag{2}$$

where W includes the applied gravity loads and the self-weight of the wall. The stiffness of a slip friction connection is as same as a rigid connection before sliding. Therefore, the system performs as a wide single shear wall before slippage. As the applied lateral force exceeds the slip force of the system (sum of slip forces of all of the walls), the devices are mobilised and the walls rock (Fig. 6(a)). During the rocking motion, the system provides a stable lateral resistance owing to the reason that the force within each of the friction connectors remains constant.

The friction devices can be designed by Eq. (2) taking into account the fact that for each wall, the sum of slip friction joint strengths ($\sum F_j$) ought to be equal or less than the slip friction hold-down force (F_H). Otherwise, the sliding would firstly initiate in the hold-downs and the adjacent walls may be locked together. If there is more than one intermediate wall in the system, the sliding force is equal for all of them provided that the geometry and material properties, thus F_E, for all are the same. For the trailing wall, only F_H is acting as the friction force and as a result, it has a lower lateral resistance compared to the leading and intermediate walls. If the walls in the system have different geometry or material properties, the slip force for each one can be separately derived by following the same procedure with different h and b for each one of them.

Note that the slot length for SFJs has to be twice as it is for the SFHs for the reason that they are designed to slide in both upward and downward directions while SFHs are supposed to move only upward. In other words, if the centre plate in a SFJ moves upward in one direction of rocking, in the opposite direction, it stays still whilst the outer plates are dragged downward by the friction bolts. Fig. 6(b)–(d) shows the position of the centre plate and the friction bolts before and after rocking.

Since the elastic lateral deformation of the timber walls itself is much lower than the lateral displacement due to the sliding of the connections (see Table 2), it can be neglected. Accordingly, the slot length for all SFHs (S) and SFJs ($2S$) for each wall can be determined by Eq. (3) with respect to the required lateral displacement (Δ) (see Fig. 6(a)). If the walls have different geometry, the slot lengths for the connections within each one of them should be calculated separately.

$$S = \Delta * \frac{b}{h} \tag{3}$$

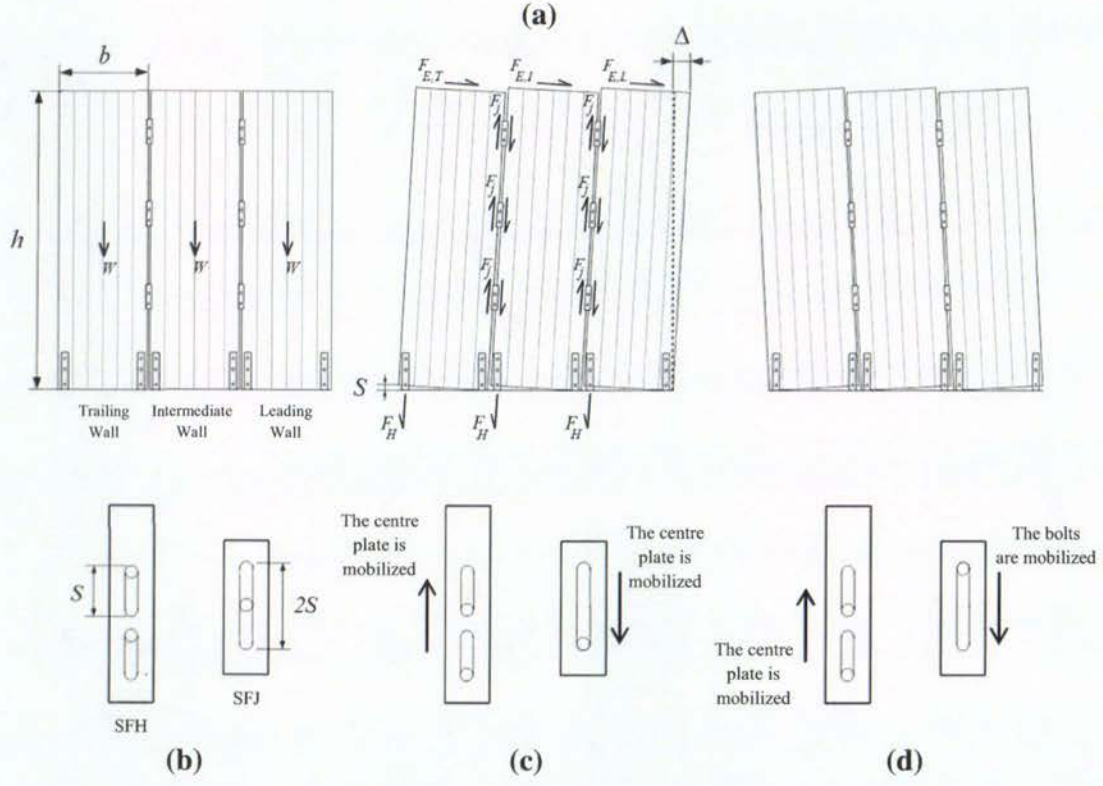

Fig. 6. Coupled timber wall system: a) Acting forces and rocking movement b) Position of the centre plate and the friction bolts before rocking c) Position of the centre plate and the friction bolts after rocking in one direction d) Position of the centre plate and the friction bolts after rocking in the opposite direction.

4. Numerical modelling of coupled timber walls with slip friction connections and nailplates

The method which has been developed by the authors for numerical modelling of coupled timber walls with slip friction connections is described here. To model the hysteretic behaviour of the slip friction hold-downs in the SAP2000 software package [26], different link elements have been employed [15]. For SFHs, a multi linear plastic link with a kinematic hysteresis is used to represent the hysteretic behaviour of a symmetric friction connection without stiffness degradation through the cycles of loading and unloading. A gap element (with zero gap) is employed to prevent the connection from moving below the base. Additionally, a hook element is considered to restrict the maximum displacement to the calculated slot length.

A similar method is used to model the SFJs. However, because the upward and downward displacements of the SFJs are equal in both rocking directions, the connection is allowed to positively and negatively deform through gap and hook elements. For CLT walls, layered shell element is employed to model a five layer section with three longitudinal layers in the vertical direction. The standard material properties of MSG8 timber is used for each layer as indicated in Table 1. For the LVL panels, standard linear shell element is employed (Fig. 7).

To compare the efficiency of the proposed system as a low damage option with a similar system including common available metal connections (as a high damage solution), another series of numerical models is also developed for coupled timber walls with nailplates in lieu of SFHs and SFJs. In other words, slip friction connectors are replaced with equivalent nailplates to compare the seismic performance of the two options.

In 2012, Loo et al. proposed a methodology for the numerical modelling of nail-slip behaviour [14] based on the use of hysteretic parameters obtained from previous test data [27]. In this study, an analogous methodology has been adopted to model the nailplate connections with the same capacity as their equivalent slip friction connections. The developed model is similar to the one in Fig. 7 but with the slip friction link elements replaced by nailplate link elements. The timber elements for both models are identical. For the multilinear plastic link, a pivot hysteresis has been selected representing the stiffness degradation of the nails under the cycles of loading and unloading. In Fig. 8, the hysteretic curves obtained from the developed numerical model for a nailplate hold-down comprised of twelve nails with 4 by 60 mm dimensions are compared with the experimental data [12].

5. Cyclic response of timber coupled wall system

It should be admitted that there is a higher level of interest in the use of CLT in design and construction of multi-storey timber buildings compared to LVL. However, owing to the higher

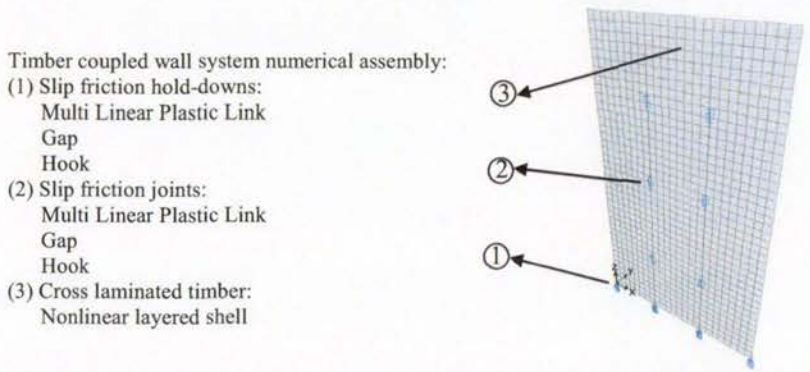

Fig. 7. Numerical model for a coupled timber wall system with slip friction connections.

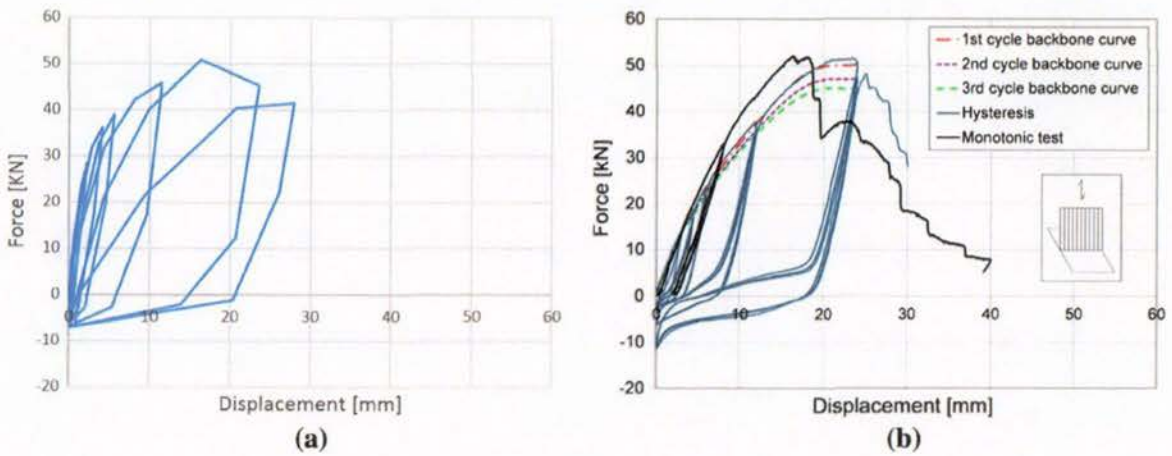

Fig. 8. Force-displacement curve for a naiplate hold-down: a) Numerical model b) Experimental data (Garvic et al. [12]).

Table 3
Configuration of the model wall systems.

Item	Value	
	S1	S2
Arrangement		
Total height	6000	6000
Width of the leading wall	1200	1000
Width of the intermediate wall	1200	1600
Width of the trailing wall	1200	1000
Thickness	200	200

Millimetres for all dimensions.

Table 4
Slip force calculations for the friction connections.

Item	Value	
	S1	S2
Self-weight of the side walls	7.6	6.35
Self-weight of the intermediate wall	7.6	12.24
Gravity loads on the side walls	30	25
Gravity loads on the intermediate wall	30	40
F_H for the side walls	54	32
F_H for the intermediate wall	54	127
Number of joints between the adjacent walls	3	3
F_j	8	13.33
Required lateral drift	4%	4%
Ultimate displacement	240	240
Slot length (S) for the side walls	48	40
Slot length (S) for the intermediate wall	48	64

Millimetres for all dimensions.
kN for all loads and forces.

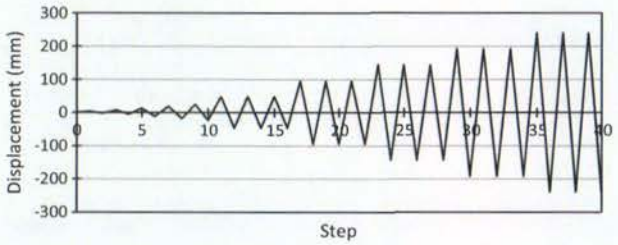

Fig. 9. Displacement-control loading regime for the quasi-static analyses.

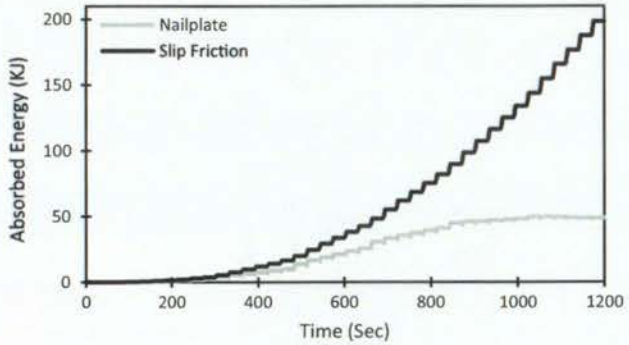

Fig. 11. Comparison of the dissipated energy for the S1 system with different connectors.

resistance of LVL, it may have a potential in hybrid CLT-LVL wall applications. This is more important when the architectural limitations enforce the designer to keep the member sizes under a certain level. The specifications of the two numerically investigated coupled wall arrangements are presented in Table 3. The S1 system is comprised of three identical CLT walls (C05 model in Table 2) while the S2 system includes two CLT side walls (C06 model in Table 2) and one LVL intermediate wall (L01 model in Table 2).

For the S1 model, all SFHs are identical and the slip threshold for them is determined with respect to Table 1 and Eq. (2). For the S2 system, the slip forces are calculated in the similar way but this time the calculated F_H for hold-downs are different for CLT and LVL walls because of the different characteristics of the wall panels. Three SFJs are positioned between any two adjacent walls for both systems and their slip force is specified by Eq. (2). The resultant forces are provided in Table 4. Note that for both systems, an intentional 10 mm gap is considered between any two walls in to avoid any undesirable frictional resistance due to a possible panel to panel contact.

The modified ISO16670 loading protocol for reversed cyclic tests for shear resistance of vertical elements (Fig. 9) was adopted for the quasi-static analyses [28]. The only modification is that the 120% of the ultimate displacement which is recommended by the protocol is ignored here. This is because the slot length of all slip friction connections is determined in accordance with the required ultimate displacement (Eq. (3)) and all timber elements are meant to represent rigid bodies during rocking. Considering 4% lateral drift for all simulations, the ultimate displacement at the top of the walls has been limited to 240 mm.

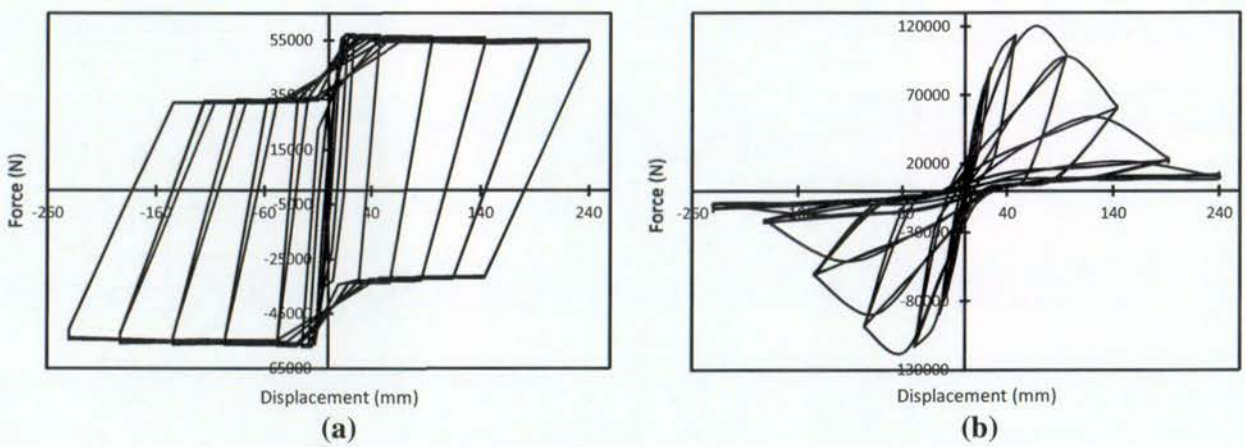

Fig. 10. Hysteresis curves for the S1 system with: a) Slip friction connections b) Nailplates.

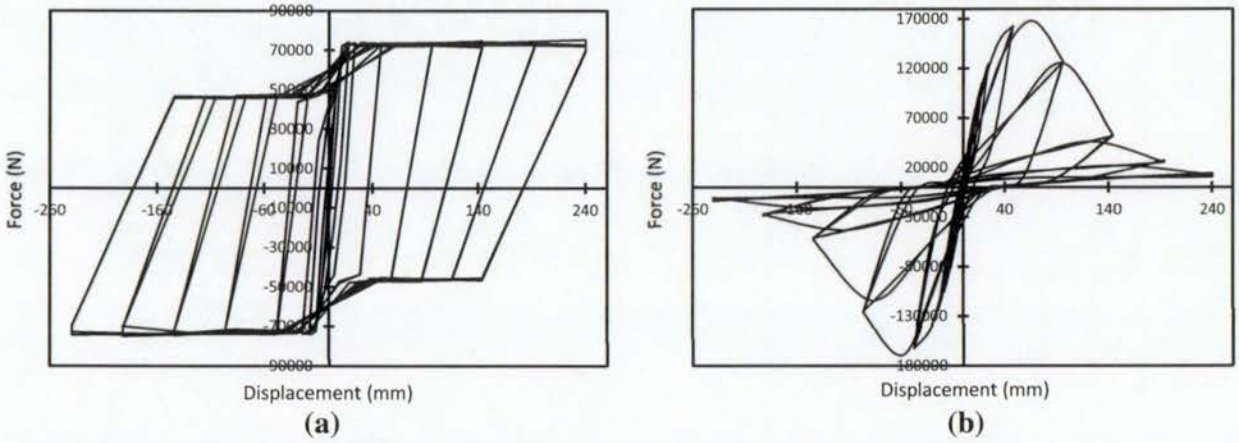

Fig. 12. Hysteresis curves for the S2 system with: a) Slip friction connections b) Nailplates.

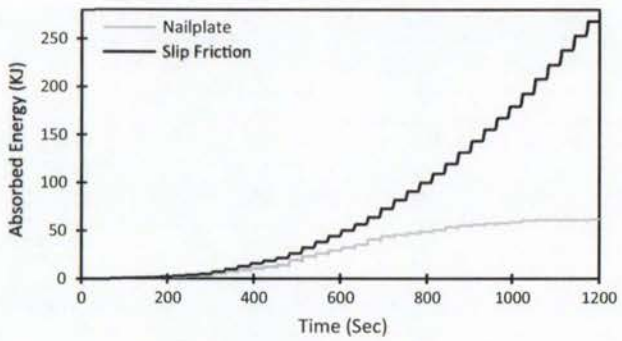

Fig. 13. Comparison of the dissipated energy for the S2 system with different connectors.

Fig. 10 compares the cyclic behaviour (applied force at the top against the base shear) of the S1 model with slip friction connections with a similar model with nailplates. Fig. 10(a) readily demonstrates that the S1 system with slip friction connections maintained its strength through several cycles of loading and unloading. Furthermore, the maximum lateral force within the system is kept under a certain level which makes the designer capable of predicting the behaviour of the system at a targeted lateral drift.

The quasi-static simulation on the S1 system with nailplate connections (Fig. 10(b)) clearly shows that the connection layout governs the cyclic behaviour of a coupled wall system. The hysteretic loops are found to evidently exhibit the "pinching" behaviour in addition to large inelastic deformations. It can be seen as the displacement increases, the stiffness of the system expeditiously deteriorates.

Fig. 11 compares the cumulative absorbed energy for the S1 system with different connectors. It is observable that the wall system with nailplate connections reached in relatively higher resistance, nevertheless, on the ground of severe stiffness degradation, its absorbed energy is much lower than the one with slip friction connections. It should be emphasised that for the system with slip friction devices, the higher rate of damping is provided without any substantial damage. This is the key characteristic of a low damage system such as the one which has been introduced by the authors.

Fig. 12 illustrates the quasi static response of the S2 system subjected to the displacement control load protocol in Fig. 9. Similar to the S1 system, it can be seen that the system with slip friction

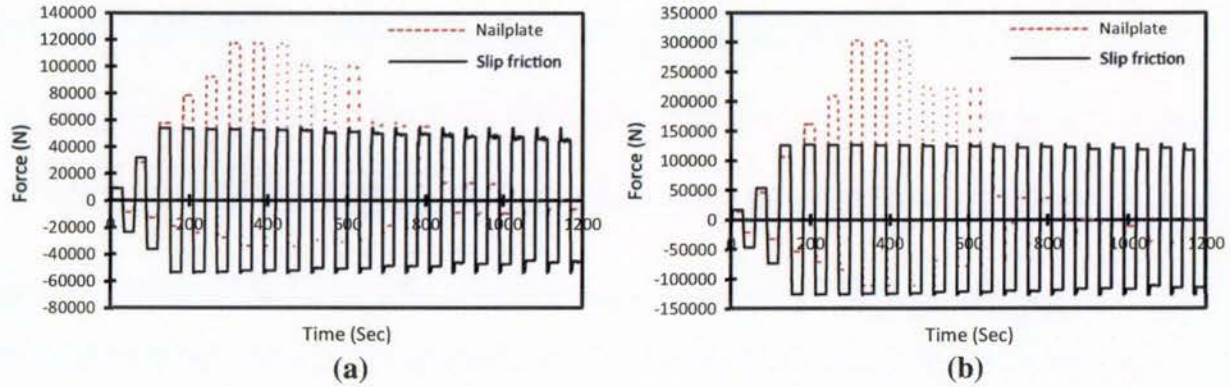

Fig. 14. Force in the middle wall's hold-down for: a) S1 system b) S2 system.

connections demonstrated a stable quadrangular cyclic behaviour while the classic "pinching" phenomena is observable for the system with nailplates. Note that this phenomena causes non-recoverable crushing in the wood fibres which is exceedingly unfavourable for a low damage seismic solution. In comparison to the S1 system, the maximum forces (for both connection layouts) is relatively higher owing to the premier lateral elastic resistance, therefore higher slip force, for the intermediate LVL wall.

Similar to the S1 system, the cumulative absorbed energy for the S2 system with slip friction connections is notably higher than the one with nailplates (almost 4 times). This significant difference can be attributed to severe rate of stiffness degradation in the nailplates which drastically reduces the area bounded by the hysteretic loops (see Fig. 13).

In Fig. 14, the force in the slip friction hold-down of the middle wall for both S1 and S2 systems is compared with the force in the equivalent nailplate. It can be seen that the maximum forces within the slip friction connections (which affects the wall) is limited to the slip threshold of the connections (54 kN and 127 kN for S1 and S2 systems, respectively). However, for the nailplates, the maximum forces are as high as 117 kN for S1 system and 302 kN for the S2 system. These relatively higher forces cause pinching phenomena accompanying by irrecoverable damage to the nails and also crushing in the timber.

6. Seismic response of coupled timber walls

6.1. Timber coupled walls under earthquake loading

In this section, the seismic response of the introduced timber coupled wall systems (S1 and S2) with slip friction connections are compared to those with equivalent nailplates. A seismic mass of 11,000 kg are assigned to all walls in the S1 model at two elevations up the height of the walls (top and middle). For the S2 system, seismic masses of 7000 kg to the CLT side walls and 13,000 kg to the LVL middle wall have been assigned. The slip thresholds of 76 kN and 102 kN are respectively determined for the S1 system and the S2 system by following the procedure described in Section 3.

Four conventional time-history acceleration records were chosen for the earthquake loading. In accordance with NZS1170 [29], each record was scaled to match the Christchurch 2500 year return period for Maximum Credible Earthquake (MCE) and 500 year return period for Ultimate Limit state (ULS). A type C soil (shallow soil site) was selected for ground motion scaling. Scale factors were determined with regards to numerically obtained fundamental period of 0.37 s for the S1 system and 0.31 s for the S2 system. The fundamental frequencies were determined as 2.68 Hz and 3.16 Hz, respectively. The scaled peak ground motions for both systems are presented in Table 5. An equivalent viscous damping of 2% was adopted for all modes of vibration to represent a massive timber structure [30].

Table 5
Earthquake records and scaling [31].

Event	Year	PGA (g)	Scaled PGA (ULS) for S1	Scaled PGA (MCE) for S1	Scaled PGA (ULS) for S2	Scaled PGA (MCE) for S2
El Centro	1940	0.313	0.251	0.407	0.251	0.407
Northridge	1994	0.231	0.278	0.508	0.303	0.531
Kobe	1995	0.821	0.246	0.575	0.325	0.655
Christchurch	2011	0.438	0.219	0.526	0.262	0.569

6.2. Force-displacement behaviour

Considering the lateral stiffness of the system as a damage index, Fig. 15 clearly demonstrates that the S1 system with nailplates suffered from large amount of stiffness degradation (thus significant inelastic damage) while in case of slip friction connections, the initial stiffness remained almost intact and the systems approximately exhibited elasto-perfectly-plastic behaviour with nearly square shaped force-deformation loops. For the S1 system with nailplates, some elastic behaviour is noticeable in the first cycles of excitements for El Centro and Northridge events. Nevertheless, the system incurred significant damage at the end. For Kobe and Christchurch events, less elastic behaviour is noticeable and the system experienced prompt decline in strength just after a few cycles and the extensive loss of stiffness resulted in relatively large displacements.

Despite the acceptable rate of energy absorption of the coupled wall systems with nailplates (which is however lesser than those with slip friction connections) they cannot be comparatively considered as reliable since the nails would almost certainly need to be replaced after a severe seismic event mainly because of the drastic reduction in their characteristic strength.

The seismic response of the S2 system with nailplate connections is similar to the S1 one. However, a higher lateral resistance is achieved that can be attributed to the high contribution of the middle LVL wall to the total lateral resistance of the system (Fig. 16). In other words, the stiffer middle wall with greater fundamental frequency (and higher slip force) predominantly governs the seismic response.

Both S1 and S2 systems with slip friction connections performed as expected under MCE loadings. They maintained their lateral stiffness to end of the seismic event. This means the connectors remain operational and a structure built with these devices can quickly be reoccupied even after a severe earthquake.

Lateral resistance of the systems were restricted to the certain level which can be determined by the formulas in Section 3. The S2 system behaves in a very similar manner to the S1 one. However, the hysteretic loops for S1 under all load cases contain lower shear forces compared to the S2 curves. Likewise, the superior contribution of the centre LVL wall is likely to be the main reason for that.

6.3. Maximum and residual displacements

The maximum horizontal displacements at the top of the wall systems are shown in Fig. 17. In accordance with NZS1170.5, the maximum deformation limit of 2.5% is the reference upper bound applicable to the ultimate limit state (1/500 annual period of exceedance for ordinary structures) for all buildings. This limit is imposed to minimise the probability of any instability in a structural system. For the conventional buildings under the MCE (with a 1/2500 annual period of exceedance), the deflection limit is recommended to be increased to 3.75% [29] to represent the near collapse limitation. These deformation limits are indicated in Fig. 17.

Fig. 17 shows that both S1 and S2 systems with nailplate connections have met the criteria for the ultimate limit state drift threshold (2.5%). For the systems with slip friction connections, the criteria is satisfied for all cases except for the Christchurch event for the S2 system which the difference is within 5% and can be considered as acceptable. For MCE events, none of the systems with nailplate connections reached the threshold. However, for the S1 system with slip friction connections under the Kobe event, the lateral displacement met the drift limit as it is almost 3.75%. For the S2 system, it is slightly beyond the limit. Neverthe-

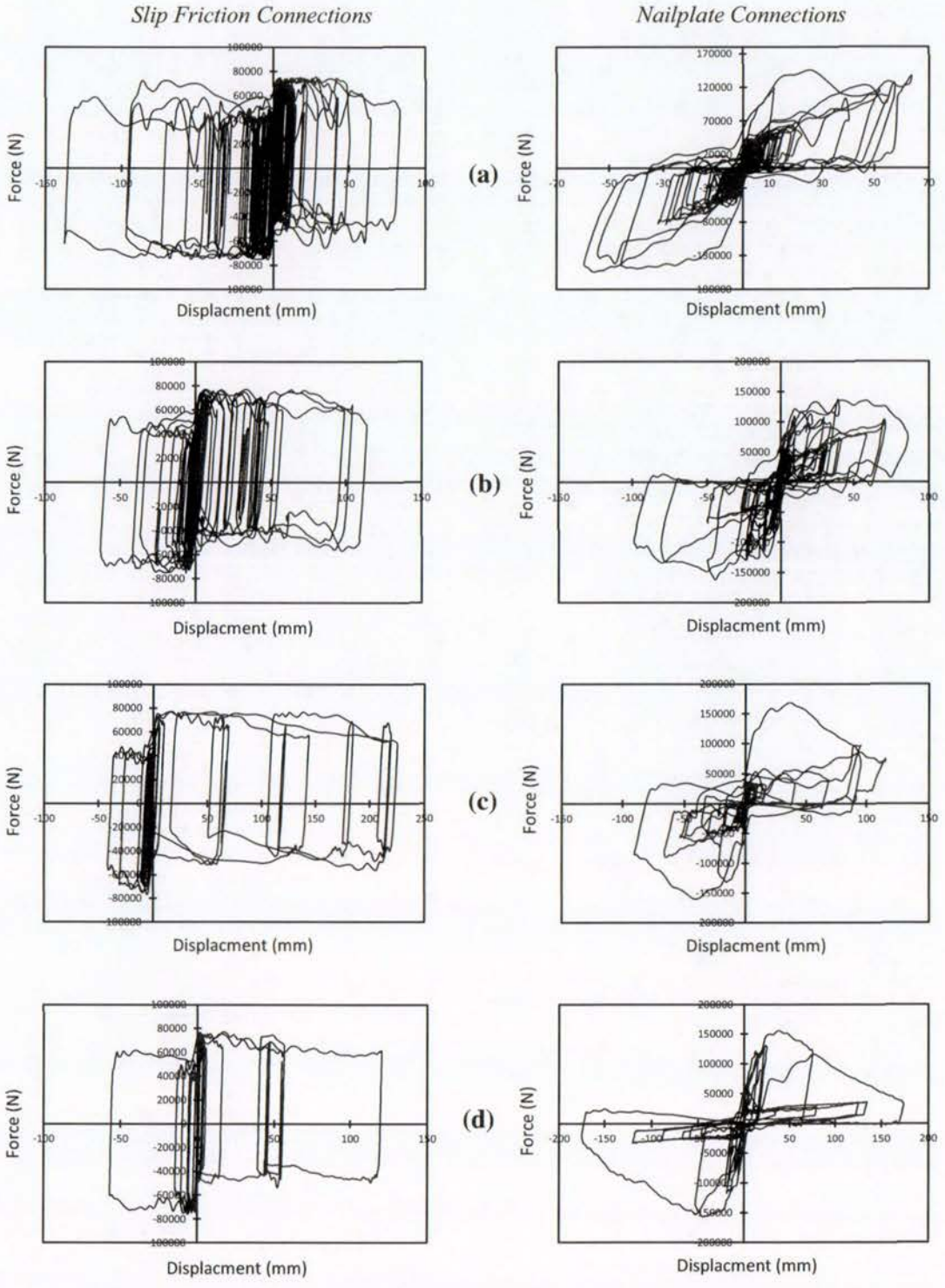

Fig. 15. Seismic response of the S1 system under MCE events: a) El Centro b) Northridge c) Kobe d) Christchurch.

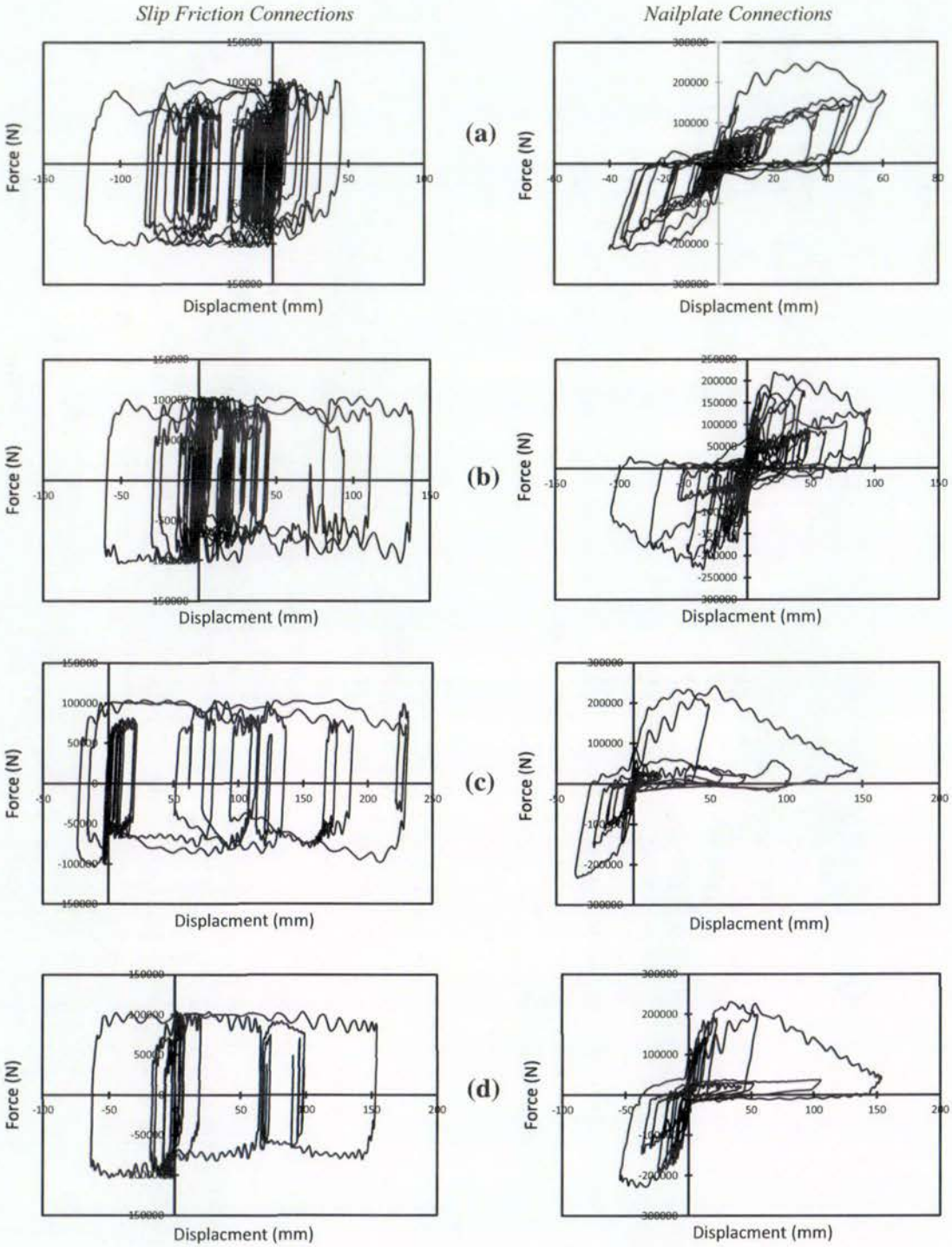

Fig. 16. Seismic response of the S2 system under MCE events: a) El Centro b) Northridge c) Kobe d) Christchurch.

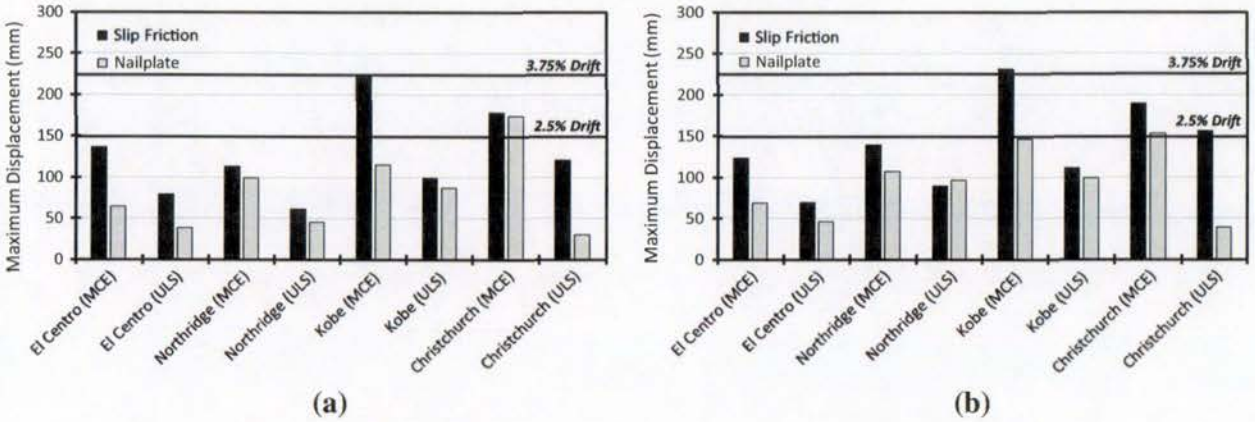

Fig. 17. Maximum displacements under seismic loading: a) S1 system b) S2 system.

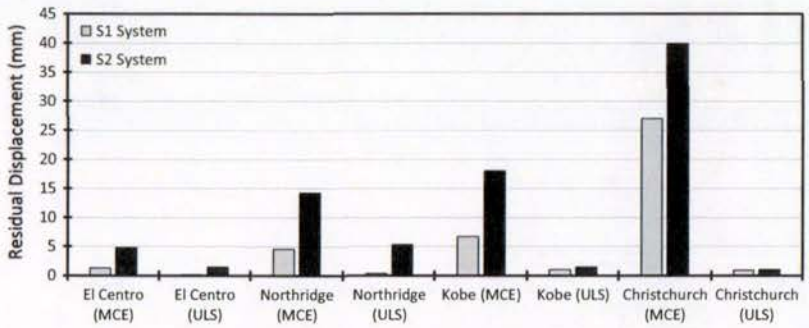

Fig. 18. Residual displacements under seismic loading.

less, the variation is within 5% and it can be considered as satisfactory. In general, the systems with slip friction connections (the low damage solution) have shown more flexibility compared to the high damage systems with traditional nailed connections.

Fig. 18 illustrates the horizontal residual displacements. The worst case is for the Christchurch event which is 27 mm (0.45% drift) for the S1 system and 39 mm (0.65% drift) for the S2 system. For the other load cases, the residual displacement is under 20 mm (0.3% drift). It should be noted that the residual drift (representing the self-centring behaviour) is highly dependent on the vertical loads and greater vertical loads compared to those in the models presented in this paper are highly probable in real structures. Therefore, even lower residual drifts can be expected for a real situation. In other words, to achieve a self-centring system, a balanced relation between the total slip force and the vertical loads should be aimed for.

7. Conclusions

The potential for structural systems with prefabricated members in seismic applications has significantly increased in the last two decades due to the introduction of jointed ductile coupled walls. In this system, two or more single prefabricated walls are connected to each other with special energy dissipative connectors along the vertical joints. In a seismic event, the walls are allowed to rock restrictedly at the base and then return to their initial position.

In this study, the application of passive sliding friction dampers (slip friction connections) in coupled timber walls is introduced. A new configuration comprised of symmetric slip friction devices as hold-down connectors and also as vertical joints between the adjacent walls were presented. To compare the seismic performance of the proposed system with the conventional timber wall systems, another series of numerical models were developed with the slip friction connections replaced with equivalent nailplates.

The results of the numerical analyses evidently proved that the slip friction connections can notably improve some aspects of the seismic performance of coupled timber walls. The quasi-static cyclic simulations showed that the systems with slip friction connections efficiently limit the stresses in the timber members below a certain level thus protecting them from non-repairable inelastic damage. From the dynamic time-history analyses, it can be noticed that the earthquake performance of coupled timber walls will significantly be improved by replacing the traditional nailed connections with slip friction devices. Under the selected earthquake loadings, the wall systems with nailplate connections incurred significant inelastic damage while the same systems with slip friction devices, were able to avoid those notable inelastic deformations while maintaining their stiffness during the seismic event.

Overall, the results represent the potential for a highly damage avoidant structural system in timber buildings. The coupled walls with slip friction connections exhibited considerably lower stiffness degradation, extremely more stable hysteretic behaviour and significantly higher rate of energy absorption. They remain operational even after a severe seismic event. Thus a structure built with connectors can be quickly reoccupied and business disruption is minimised.

Further experimental investigations are required to confirm the efficiency of the proposed system in real applications and to identify its potential limitations.

Acknowledgements

The authors would like to thank the Earthquake Commission Research Foundation (EQC) for the financial support of this research, and the three anonymous reviewers for their valuable comments which have improved the clarity of this paper.

References

[1] M.J. Nigel Priestley, S. Sritharan, J.R. Conley, S. Pampanin, Preliminary results and conclusions from the PRESSS five-story precast concrete test building, PCI J. 44 (6) (1999) 42–67.
[2] S.D. Nakaki, J.F. Stanton, S. Sritharan, An overview of the PRESSS five-story precast test building, PCI J. 44 (2) (1999) 26–39.
[3] A. Palermo, S. Pampanin, A. Buchanan, M. Newcombe, Seismic design of multi-storey buildings using laminated veneer lumber (LVL), in: Proceedings of New Zealand Society for Earthquake Engineering Conference NZSEE, Taupo, New Zealand, 2016.
[4] A. Iqbal, S. Pampanin, A. Palermo, A.H. Buchanan, Performance and design of LVL walls coupled with UFP dissipaters, J. Earthquake Eng. 19 (3) (2015) 383–409.
[5] E.P. Popov, C.E. Grigorian, T.S. Yang, Developments in seismic structural analysis and design, Eng. Struct. 17 (3) (1995) 187–197.
[6] G.C. Clifton, G.A. MacRae, H. Mackinven, S. Pampanin, J. Butterworth, Sliding hinge joints and subassemblies for steel moment frames, Palmerston North, New Zealand: Proc of New Zealand Society for Earthq Eng Conf, 2007.
[7] S. Ramhormozian, G.C. Clifton, G. A. MacRae, The Asymmetric Friction Connection with Belleville springs in the Sliding Hinge Joint, NZSEE Conference, Towards Integrated Seismic Design, 2014.
[8] H. Khoo, C. Clifton, G. MacRae, H. Zhou, S. Ramhormozian, Proposed design models for the asymmetric friction connection, Earthquake Eng. Struct. Dyn. (2014).
[9] M. Popovski, E. Karacabeyli, Seismic behaviour of cross-laminated timber structures, in: Proceedings of the World Conference on Timber Engineering, Auckland, New Zealand, 2012.
[10] M. Yasumura, K. Kobayashi, M. Okabe, T. Miyake, K. Matsumoto, Full-scale tests and numerical analysis of low-rise CLT structures under lateral loading, J. Struct. Eng. (2015) E4015007.
[11] A. Ceccotti, C. Sandhaas, M. Okabe, M. Yasumura, C. Minowa, N. Kawai, SOFIE project – 3D shaking table test on a seven-storey full-scale cross-laminated timber building, Earthquake Eng. Struct. Dyn. 42 (13) (2013) 2003–2021.
[12] I. Gavric, M. Fragiacomo, A. Ceccotti, Cyclic behaviour of typical metal connectors for cross-laminated (CLT) structures, Mater. Struct. 48 (6) (2014) 1841–1857.
[13] A. Filiatrault, Analytical predictions of the seismic response of friction damped timber shear walls, Earthquake Eng. Struct. Dyn. 19 (2) (1990) 259–273.
[14] W.Y. Loo, P. Quenneville, N. Chouw, A numerical approach for simulating the behaviour of timber shear walls, Struct. Eng. Mech. 42 (3) (2012) 383–407.
[15] W.Y. Loo, P. Quenneville, N. Chouw, A numerical study of the seismic behaviour of timber shear walls with slip-friction connectors, Eng. Struct. 34 (2012) 233–243.
[16] W.Y. Loo, C. Kun, P. Quenneville, N. Chouw, Experimental testing of a rocking timber shear wall with slip-friction connectors, Earthquake Eng. Struct. Dyn. 43 (11) (2014) 1621–1639.
[17] S. Gagnon, C. Pirvu, CLT Handbook: Cross-Laminated Timber. FPInnovations, 2011.
[18] T. Bogensperger, M. Augustin, G. Schikhofer, Properties of CLT-panels exposed to compression perpendicular to their plane, in: At the Conference. International Council for Research and Innovation in Building and Construction, Working Commission W18-Timber Structures, vol. 28, 2011, pp. 1–15.
[19] M. Fragiacomo, A. Menis, I. Clemente, G. Bochicchio, B. Tessadri, Experimental and numerical behaviour of cross-laminated timber floors in fire conditions, in: World Conference on Timber Engineering, 2012. pp. 177–178.
[20] L. Pozza, R. Scotta, D. Trutalli, M. Pinna, A. Polastri, P. Bertoni, Experimental and numerical analyses of new massive wooden shear-wall systems, Buildings 4 (3) (2014) 355–374.
[21] Hibbitt, Karlsson, Sorensen, ABAQUS, Standard User's MANUAL, Hibbitt, Karlsson & Sorensen, 2014. vol. 1.
[22] A.H. Buchanan, N.Z.T.I. Federation, Timber design guide, New Zealand Timber Industry Federation, 1999.
[23] A. Hashemi, P. Zarnani, A. Valadbeigi, R. Masoudnia, P. Quenneville, Seismic resistant cross laminated timber structures using an innovative resilient friction damping system, Proceedings of New Zealand Society for Earthquake Engineering Conference (NZSEE), Christchurch, New Zealand, 2016.
[24] P. Zarnani, P. Quenneville, Strength of timber connections under potential failure modes: an improved design procedure, Constr. Build. Mater. 60 (2014) 81–90.
[25] C. Bora, M.G. Oliva, S.D. Nakaki, R. Becker, Development of a precast concrete shear-wall system requiring special code acceptance, PCI J. 52 (1) (2007) 122.
[26] Computers and Structures, SAP2000. (2011), Berkeley, CA, 2011.
[27] J.D. Dolan, B. Madsen, Monotonic and cyclic nail connection tests, Can. J. Civ. Eng. 19 (1) (1992) 97–104.
[28] A. Standard, "E2126", Stand. test methods Cycl. load test Shear Resist. Vert. Elem. lateral force Resist. Syst. Build. West Conshohocken, PA Am. Soc. Test. Mater., 2009.
[29] Standards New Zealand, NZS1170. Structural Design Actions Part 5, 2004.
[30] W.Y. Loo, P. Quenneville, N. Chouw, Rocking timber structure with slip-friction connectors conceptualized as a plastically deformable hinge within a multistory shear wall, J. Struct. Eng. (2015) E4015010.
[31] P. Peer, NGA Database, Pacific Earthquake Engineering Research Center, Univ. California, Berkeley, USA, 2015.

Journal of Constructional Steel Research 126 (2016) 201–213

Contents lists available at ScienceDirect

Journal of Constructional Steel Research

Seismic performance of hybrid self-centring steel-timber rocking core walls with slip friction connections

Ashkan Hashemi *, Reza Masoudnia, Pierre Quenneville

Department of Civil and Environmental Engineering, Faculty of Engineering, The University of Auckland, Private bag 92019, Auckland 1142, New Zealand

ARTICLE INFO

Article history:
Received 14 April 2016
Received in revised form 12 July 2016
Accepted 13 July 2016
Available online xxxx

Keywords:
Rocking core walls
Cross Laminated Timber
Slip friction
Low damage
Energy dissipation
Self-centring
Steel strands

ABSTRACT

While structures with conventional lateral force resisting systems are designed to meet the life safety criteria for the residents during and after a seismic event, they are allowed to tolerate the expected structural damage. This damage might be because of the residual displacements after the earthquake or the lack of ductility in the system. Despite the fact that the allowable damages are intended to be repairable, however, in most cases the repairs are highly uneconomical. A self-centring hybrid steel-timber rocking core wall system (SC-RW) is developed to provide sufficient ductility in addition to a significant amount of energy dissipation while it limits the residual drift and the associated damage. This system is comprised of one or more rocking cross laminated timber (CLT) walls with slip friction connections as the main lateral resisting system and steel beams and columns to resist against gravity loads. Horizontally oriented post-tensioned strands through the beams provide additional moment resistance at the beam-column interface to re-centre the structure after the earthquake. The efficiency of the proposed system is investigated under cyclic and seismic loading regimes. Furthermore, a preliminary displacement based design approach for a SC-RW system is introduced. Dynamic time-history simulations confirm an excellent behaviour in terms of drift capacity, residual displacement and peak roof accelerations.

1. Introduction

Structural walls provide excellent seismic resistance and are commonly used as the main lateral resisting system in buildings. During the past seismic events, these walls were found to represent superior seismic performance compared to other alternative structural members [1–3]. Those walls constructed with prefabricated components have additional advantages including offsite fabrication, improved quality and speed of construction. During the 1994 Northridge earthquake, several commercial precast parking structures experienced significant damage [2], however, this damage was mainly because of incompatibilities between the lateral and gravity resisting systems and no considerable damage was observed in the walls themselves. Furthermore, during the 1995 Kobe earthquake, precast concrete buildings with structural wall systems performed well with negligible post-earthquake damages.

Recently, there has been an extensive interest towards the design and construction of multi-story timber structures with engineered wood products such as Cross Laminated Timber (CLT) and Laminated Veneer Lumber (LVL) panels. However, the application of these products in seismic regions as the primary lateral resisting system was limited firstly due to the lack of information about their seismic behaviour, secondly the subsequent restrictions imposed by the design codes and thirdly because of their non-ductile behaviour which leads to relatively high response accelerations. During the large-scale experimental investigation of a seven story building made of CLT panels within the SOFIE project, accelerations as high as 3.8 g were recorded [4]. Despite the fact that these accelerations may be acceptable for human health, they are uncomfortable and unpleasant for the habitants. As an important outcome of the SOFIE project, other research studies were commenced in order to mitigate the earthquake damage by developing new solutions to absorb the seismic energy and decrease the ensuing response accelerations.

This study seeks to develop an innovative steel-timber rocking core as the main lateral force resisting system to efficiently lessen the post-earthquake damage. This system includes supplementary slip friction dampers to dissipate the seismic energy along with high strength post-tensioned steel strands through the beams to self-centre the structure after the earthquake. The efficiency of this system is inspected through displacement control quasi-static analyses. Furthermore, a displacement based design approach is introduced to design the system in accordance with the induced seismic loads. Finally, the designed system is subjected to dynamic time-history simulations to investigate its seismic performance in terms of provided ductility, self-centring capacity and the peak roof accelerations.

2. Research background

Rocking mechanism for earthquake protection dates back to the Greek era, where segmental construction of columns led to gap opening

* Corresponding author.
E-mail address: ahas439@aucklanduni.ac.nz (A. Hashemi).

http://dx.doi.org/10.1016/j.jcsr.2016.07.022
0143-974X/

at the joints when exposed to seismic activity. However, it was not until 1950s that it had been studied for application in seismic resistant structures. Housner is recognized as the first researcher to investigate the rocking behaviour to describe why many slender and tall structures survived the 1960 Chilean earthquake [5]. Palermo et al. proved that utilizing the "controlled rocking" concept in bridge systems is an effective alternative for the traditional systems [6]. The possibility of accommodating the inelastic demand at the specific elements (mild steel bars in that case) when rocking takes place, led to a significant damage reduction in the pier component. Ma et al. proposed simplified mathematical expressions derived from the equation of motion [7]. As a practical example of the application of rocking behaviour in seismic resistance structures, the South Rangitikei rail viaduct in New Zealand can be mentioned [8,9]. That structure was designed to allow for rocking of the piers on the pile cap which resulted in notable decrease in the base shear demand.

Henry et al. proposed the PreWEC system (precast concrete wall with end columns) for earthquake resistant structures [10]. This system comprised of single or multiple precast concrete walls attached to end columns with special energy dissipative connectors. The efficiency of the proposed system has later been validated by experimental tests [11]. Iqbal et al. studied the application of U-shaped Flexural Plates (UFPs) as supplementary damping devices in post-tensioned LVL timber coupled rocking walls [12]. The system had later been experimentally investigated and a design procedure was proposed [13]. Sarti et al. tested coupled LVL walls with UFP connectors and also with fuse type damping devices at the base of the walls [14]. The results was promising in terms of energy dissipation rate and the residual damage.

Loo et al. introduced the application of symmetric slip friction hold-downs for LVL rocking timber shear walls [15]. A symmetric slip friction hold-down offers a bidirectional hysteretic behaviour results in efficient energy dissipation. Furthermore, it provides constant resistance force against the overturning moment. The proposed configuration had later been experimentally tested and demonstrated a stable hysteretic behaviour which is the key characteristic of a low damage system [16].

After the Northridge earthquake, multiple new concepts for steel frames were developed which were intended to lessen the onsite welding as much as possible and also to avoid high inelastic deformations caused by the yielding of the members [17]. Ricles et al. proposed an alternative moment connection for steel structures with significant reduction in residual damage in the beams and little remaining lateral drift after an earthquake [18]. In the proposed concept, high strength steel strands are employed to self-centre the structure. Additionally, the inelastic deformations were localized at the connections by the opening of the gap in the beam-column contact surface. This concept was further developed by several researchers on account of its simplicity and excellent behaviour under quasi-static and dynamic loads in terms of stiffness, strength and deformation capacity. Garlock et al. introduced a step by step design approach for steel PT frames based on the lateral applied forces [19]. Tsai el al. designed and tested four PT steel moment frames under cyclic loads [20]. They reported stable and efficient performance providing that the lateral drift is under 5%. Kim et al. combined the PT frames with frictions dampers installed on the top and bottom flanges of the beams [21]. The experimental results exhibited stable cyclic response, insignificant strength degradation and almost no residual drift. Lin et al. developed and tested a full scale PT steel moment frame with friction dissipative devices attached to the bottom flange of the beams [22].

Most of the previously developed self-centring mechanisms for hybrid rocking walls were focused on the application of vertical post-tensioned cables up the height of wall while they are anchored to the foundation. Although this system demonstrated a promising self-centring behaviour, however, the relaxation of the cables because of the imminent creep in the wood lessens the efficiency of the system [23,24]. This study presents an alternative low damage rocking core wall system that can efficiently absorb the seismic energy through slip friction damping devices. Additionally, the system is able to accommodate the uplift and rotation incompatibility at the floor to wall connection which might cause a substantial damage to the floor diaphragm.

3. Self-centring Rocking Wall (SC-RW) system with friction dampers

In this paper, a novel system consisting of rocking timber walls with slip friction damping devices and beam to column post-tensioned connections is proposed. As Fig. 1 shows, the Self-centring Rocking wall system, referred in short as SC-RW system, is comprised of different structural components: (i) rocking timber walls which normally are massive wooden panels such as Cross Laminated Timber (CLT) or Laminated Veneer Lumber (LVL) (they are the main lateral load resisting elements in the system) (ii) slip friction connections which connects the wall to the base and to the adjacent walls or columns (these connections absorb the energy through sliding) (iii) special steel beam (or floor) to wall connection which transfers the horizontal loads from the diaphragm to the walls yet is isolated from relative vertical movement between the floor and the rocking wall. These connections can accommodate the displacement incompatibility between the floors and the walls during rocking (iv) steel columns designed to resist the gravity loads transferred through steel beams (they are pin jointed to the base) (v) post-tensioned connections between the beams and

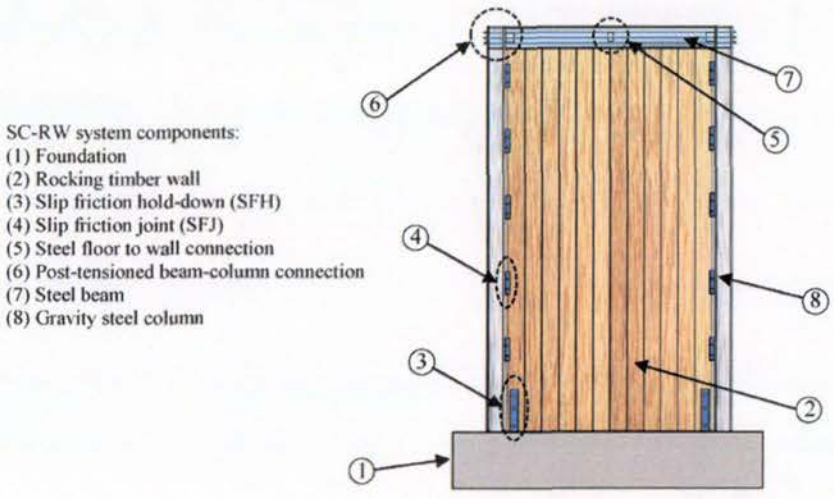

Fig. 1. General arrangement of the SC-RW system.

columns to re-centre the structure by the generated moments due to gap opening in the connection and elongation of the strands.

While there is no limitation on the panel length, however, it is recommended that the aspect ratio of the panels be restricted to minimum value of 2.0 to ensure the flexural behaviour is the dominating mechanism [11]. When wider walls are required, two or more walls can be used with or without steel columns between them. In that case, dissipative friction devices can be placed between any two adjacent panels.

Fig. 2 displays the details of each component within the SC-RW system. An assemblage introduced and tested by Loo et al. for LVL rocking walls is employed in the system for the Slip Friction Hold-downs (SFHs) [15,16].

In the SFH, the outer plates are clamped down on the centre slotted plate with Belleville washers (conical disc springs). When the imposed axial force to the SFH dominates the frictional resistance between the two clamped surfaces, the centre plate starts to move and the energy will be absorbed by friction through cycles of sliding (see Fig. 2(a)). A symmetric force-displacement behaviour for SFHs is considered to minimize the stiffness degradation. By that, the friction bolts are in tension only. This is different from the asymmetric configuration where bolts are in tension and shear [25]. Refer to [16] for more details about the differences between the symmetric and asymmetric slip friction connections. A similar arrangement is assumed for the slip friction joints (SFJs). SFJs are installed between the wall panels and columns or between the adjoining panels. Similar to the SFHs, three plates are bolted and clamped together with Belleville washers in a manner that the centre slotted plate is attached to the wall with a steel flange and the two outer plates are connected to the column (or the other wall). When the vertical force at one direction exceeds the frictional resistance between the two surfaces, the centre plate starts to move and energy will be dissipated over the joint. In the other direction, the centre plate remains still and exterior plates will be dragged along by the bolts (see Fig. 2(b)). The slip threshold for SFH or SFJ is given by Eq. (1) where μ is the coefficient of friction between the two surfaces, n_b is the number of friction bolts and T_b is the tension force in each bolt.

$$F_{slip} = 2\mu n_b T_b \tag{1}$$

When uplift occurs at the foundation of a rocking wall, the floor diaphragms are not able to accommodate this uplift if they are rigidly connected to the wall. In such case, floors are subjected to severe inelastic damage which significantly influences the seismic performance of the structure [26,27]. In recognition of this issue, the connection between the wall and the floor has to be designed to mitigate the displacement

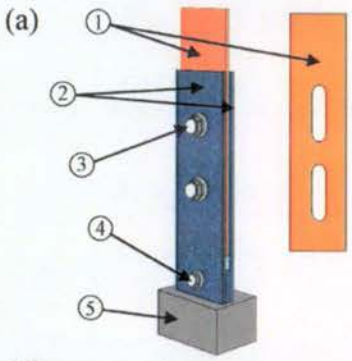

SFHs:
(1) Slotted centre plate
(2) Outer plates
(3) Friction bolts with Belleville washers through the slotted plate and the outer plates
(4) Fixed bolt(s) (for symmetric configuration)
(5) Foundation

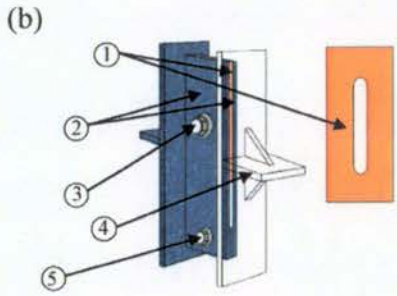

SFJs:
(1) Slotted centre plate, connected to one wall
(2) Outer plates, connected to the opposite adjacent wall
(3) Friction bolt(s) with Belleville washers through the slotted plate and the outer plates
(4) Embedded flanges, fixed to the wall
(5) Fixed bolt(s) (for symmetric configuration)

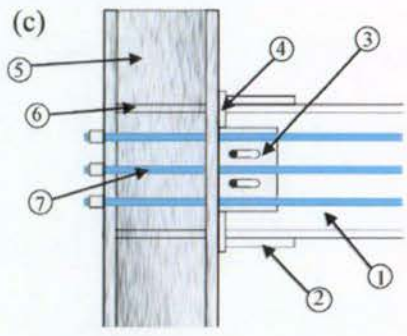

PT connection:
(1) Steel beam
(2) Reinforcing plate
(3) Shear slotted plate
(4) Bearing plate
(5) Steel column
(6) Column stiffener
(7) High strength post-tensioned strands

Special steel beam to wall connection [26]:
(1) Slotted steel plate (connected to the wall)
(2) Slotted steel plate (connected to the beam or the floor)
(3) Round-square-round steel dowel

Fig. 2. The components of the SC-RW system: a) slip friction hold-down (SFH) b) slip friction joint (SFJ) c) beam to column post-tensioned connection d) steel beam to wall connection.

incompatibility. It has to be able to transfer the horizontal forces from the floor (or the beam) to the wall while it de-couples the diaphragm from the rotation and uplift of the wall. The behaviour of the wall should be predictable and any damage to the floor diaphragm should be prevented. Moroder et al. experimentally investigated the behaviour of seven different floor to wall connections in timber structures subjected to lateral loading [26]. The seven different types of tested connections were: two types of bolted connections with different arrangements, external timber blocks pushing against the edge of the wall, two types of round steel pin, a steel comb with slotted holes and a steel to steel connection with a round-square-round steel dowel in a slotted hole. Although each option represented various advantages and drawbacks, the last configuration exhibited the best results in terms of the relative rotation between the beam and the wall and also the relative vertical movement between the beam and the wall. No rotation and/or displacement incompatibility between the beam and the wall is observed and the system strength remained almost unaltered during the cyclic tests. In this configuration, a 40 mm diameter round-square-round steel pin in a slotted hole was used. The slotted hole in the wall was designed in way that when the wall rocks, the square-shaped part of the pin was able to vertically slide in the hole to accommodate the mentioned vertical displacement and rotation incompatibility between the beam and the wall. (see Fig. 2(d)). This configuration is considered as an effective solution for the wall to floor connection within the introduced SC-RW system as its efficiency has been experimentally validated.

Fig. 2(c) schematically illustrates the post-tensioned connection within the proposed concept. The PT beam-column connection consists of a vertically oriented slotted plate welded to the column flange and bolted to the beam web to transfer the shear forces. The slot length is determined to accommodate the horizontal displacement which is the result of the gap opening in the connection. The PT strands run parallel to the beam across single or multiple bays. The reinforcing plates are attached to the outside surfaces of the beam to inhibit yielding near the PT strand holes [22]. In this system, rocking walls are the main lateral resisting elements and PT strands provide sufficient resistance to re-centre the structure.

4. Cyclic behaviour of the SC-RW system with slip friction connections

The acting forces on a SC-RW system with one rocking wall are shown in Fig. 3. On the brink of rocking, taking the moments about the rocking point, the gross force at the top of the wall (F_a), which triggers the movement in the system, can be calculated from Eqs. (2) and (3).

$$F_{slip-total} = (F_H + \sum F_j)\frac{b}{h} \tag{2}$$

$$F_a = F_{slip-total} + \frac{Wb}{2h} + \frac{M_{pt,i}}{h} \tag{3}$$

where $F_{slip\text{-}total}$ is the applied force at the top of the wall which overcomes the frictional resistance of the dissipative devices, F_H is the slip friction hold-down force, F_j is the slip friction force for the joints between the wall and the columns (or between the adjacent walls), W is the self-weight of the wall and $M_{pt,i}$ is the gross resisting moment of the all PT joints in the system (There are two of them in this case). Assuming the top of the beam as the point of rotation and the middle of the beam's depth as the centroid of the PT strands, the moment capacity of a PT connection can be determined by Eq. (4) [22].

$$M_{pt} = F_{pt,i}.d \tag{4}$$

where $F_{pt,i}$ is the initial post-tensioning force in the strands and d is the distance of the centroid of the strands from the point of rotation which is equal to the half of the beam depth. For the SC-RW system in Fig. 3, two PT joints are acting; thus, the total resisting moment in the system ($M_{pt,i}$) is the sum of the induced moments in the two joints (see Fig. 3(b)). Note that Fig. 3(c), (d) schematically show the beam to floor connection in the proposed concept before and after rocking. This configuring is adopted from the one described in Fig. 2(d) with the timber beam replaced with the steel beam.

If the initial PT force in the strands ($F_{pt,i}$) is set equal to $(\frac{F_{slip-total}h}{d} - \frac{Wb}{2d})$, the hysteretic loop of the proposed system has *five phases*. Under the lateral loading, each beam-column connection has an initial stiffness similar to a rigid connection because of the moment capacity of the PT strands (Eq. (4)). When the applied lateral force (P) overcomes the sum of these moments ($M_{pt,i}$), the decompression of the beam flange from the column face is initiated (end of *phase 1* in Fig. 4). As the applied force increases, the rocking movement of the wall (and the rotation of the connection) is resisted by the slip friction devices and the self-weight of the wall until the applied force negates them (end of *phase 2* in Fig. 4). The gap opening in the PT joint is imminent once P is equal to $2F_{slip\text{-}total}$ which is the sum of provided resistances

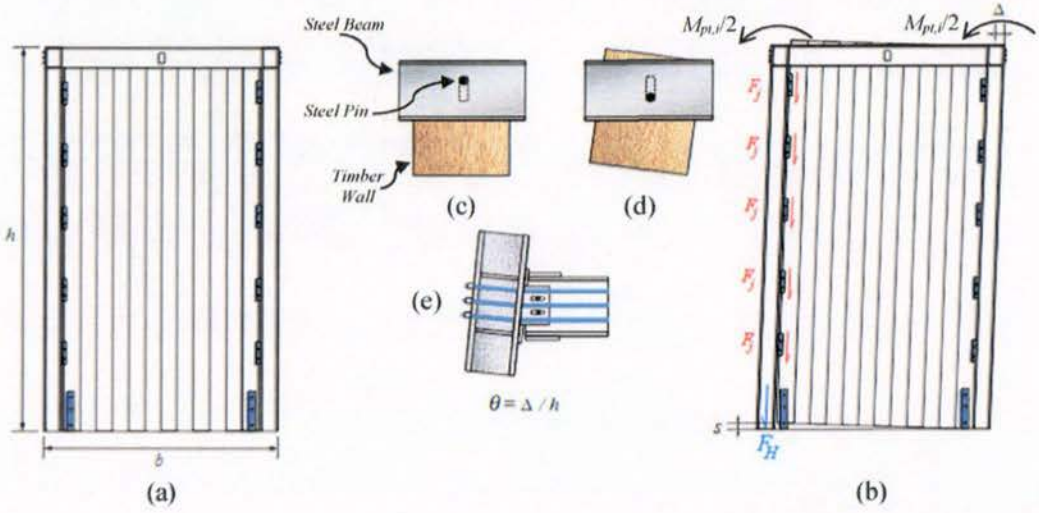

Fig. 3. A SC-RW system with a single rocking wall: a) before rocking b) after rocking c) beam to wall connection before rocking d) beam to wall connection after rocking e) gap opening in the post-tensioned beam-column connection.

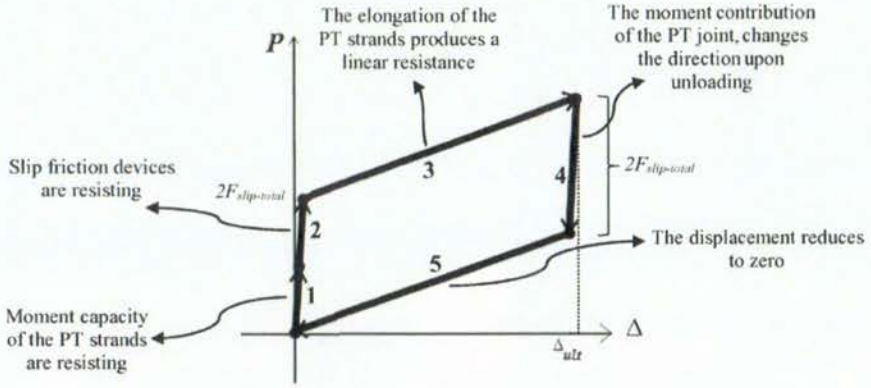

Fig. 4. Schematic hysteretic loop of a SC-RW system.

by the PT connections, the slip friction devices and the self-weight of the wall (*Phase 3* in Fig. 4). In this phase, the stiffness of the connection depends on the elastic stiffness of the PT strands. As the applied load rises, the elongation of the strands generates an additional resisting force until the point with the ultimate lateral drift (end of the *phase 3* in Fig. 4). Analytical and experimental studies of by Iyama et al. [28] and Wolski et al. [29] indicated that the moment (and resultant force) in a PT beam-column system with friction dampers in 2.5% of rotation is approximately 50% higher than the moment immidiately before the gap starts to open. It should be emphasized that the yielding of the strands should not happen before this point. Experimental investigations of Lin et al. showed that the stands can normally stay in the elastic region for 2.5% to 4% rotation in the PT joint [22]. The produced force by the PT strands can be calculated as follows [19,22]:

$$F_{pt} = F_{pt,i} + \theta d k_{PT-joint} \tag{5}$$

and

$$k_{PT-joint} = \frac{k_s\, k_b}{k_s + k_b} \tag{6}$$

where, θ is the rotation at the joint. $k_{PT-joint}$, k_s and k_b are respectively the total axial stiffness of the PT joints, the axial stiffness of the strands and the axial stiffness of the beam (i.e., AE/L). During the unloading at *phase 4*, the moment contribution of the PT connection changes the direction of the rocking wall as a result of a reversal friction force. In *phase 5*, the lateral displacement reduces to zero and the beam flange returns in contact with the column. A similar loop is expected in the opposite direction providing that the PT strands remain elastic and the preserved PT force will re-centre the system upon unloading.

The SC-RW system in Fig. 3 was modelled in SAP2000 [30] with the assumed specifications in Table 1. The five layer CLT wall was modelled using the layered shell element with three longitudinal layers of standard MSG8 sawn timber boards and two transverse layers of MSG6 boards. The mechanical properties of CLT are specified in Table 1 [31] where *L*, *R* and *T* axes refer to *z*, *y* and *x* global axes in the model (see Fig. 5(a)). To optimize the efficiency of CLT wall applications, wall elements have been placed with their outer layers parallel to the gravity loads.

The maximum tolerable horizontal force applied at top of the wall (providing that all of the timber boards within the CLT panel remain in the elastic region) was found as 65 kN from a numerical analysis similar to the one in Fig. 10 [15,32]. The sliding threshold for the slip friction devices (SFHs and SFJs) are determined in such the slippage starts before the applied load at the top exceeds 65 kN (see Eq. (2) and Table 2). Considering the self-weight of the wall $W = 19$ kN, $F_{slip\text{-}total} = 60.25$ kN is accordingly determined. Assuming the initial PT force in the strands $F_{pt,i} = 3310$ kN (equal to $(\frac{F_{slip-total}h}{d} - \frac{Wb}{2d})$), the gap opening starts when the applied load is 120.5 kN ($2F_{slip\text{-}total}$) which is the start of *phase 3* in Fig. 4. Note that since two PT joints are acting, the resultant PT forces were divided by two in the numerical model.

The SFHs were simulated using a multi-linear plastic link with a kinematic hysterestic type (which does not allow stiffness degradation) in addition to a gap element with zero initial gap representing the base level which the wall is not allowed to move below. A hook element is considered as well to restrict the maximum displacement of the hold-down. The SFJs were modelled similarly but the initial gap was set equal to the slot length as the connection is allowed to symmetrically move upward and downward. Hence, the slot length of the SFJs are twice as the SFHs. This numerical approach for modelling of the slip friction connections has been experimentally validated by Loo et al. [15,16,33]. The slot length (s) is specified in accordance with the required lateral drift and the geometry of the wall (see Fig. 3(b)).

Table 1
Material properties of the CLT.

Element	E_L	E_R	E_T	ν_{LT}	ν_{TL}	ν_{LR}	ν_{RL}	ν_{TR}	ν_{RT}
Longitudinal layers (MSG8[a])	8000	363	363	0.2	0.018	0.15	0.018	0.21	0.18
Transverse layers (MSG6[a])	6000	272	272	0.15	0.015	0.15	0.015	0.15	0.15

E = Elastic Modulus.
ν = Poison's ratio.
MPa for all modulus.
[a] MSG8 and MSG6 refer to grade 8 and grade 6 machine graded sawn timber, respectively [31].

Table 2
Specification of the numerical model of the SC-RW system.

Item	Value
Height of the wall	6000
Width of the wall	3000
Self-weight of the wall (W)	19
F_H	60.5
Number of the joints between the wall and the column	6
F_j	10
Column section	BOX220 • 220 • 16
Beam section	IPE200
Gravity distributed load	20
$F_{slip\text{-}total}$	60.25
$F_{pt,i}$	3330
Slot lentgh for the SFHs	112.5
Slot lentgh for the SFJs	225

Millimetre for all dimensions.
kN for all loads and forces.
N/mm for the stiffness and distributed loads.

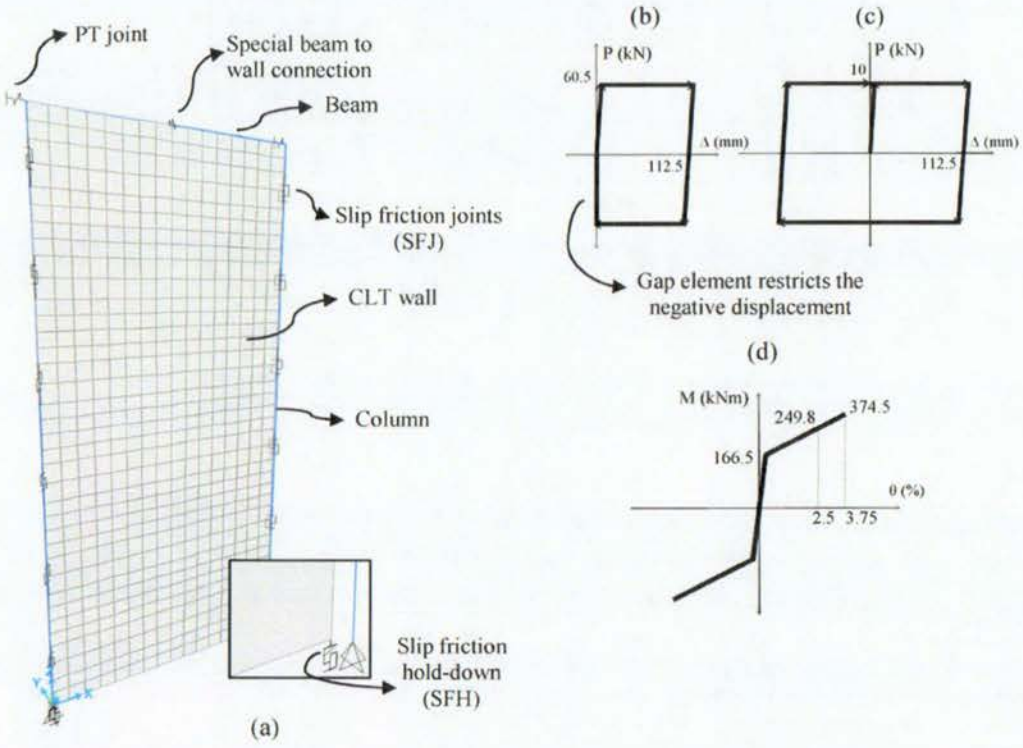

Fig. 5. Numerical model for the SC-RW system: a) numerical assembly b) schematic SFH hysteresis c) schematic SFJ hysteresis d) PT strands hysteresis.

A multi-linear rotational elastic link is employed to simulate the PT strands in the beam-column connection. This type of element is selected to represent the bi-linear elastic moment-rotation behaviour of the beam-column PT connections [18,21,22,28,29] (see Fig. 5(c)). The pre-stressed moment for each of the two PT joints is 165.5 kNm and the stiffness of the second line within the link is specified in such the moment at 2.5% of rotation is 50% higher than the pre-stressed moment (see Fig. 5(d)). The columns are pin jointed to the foundation. The movement of the wall is constrained to the beam in the x and y directions but the vertical translational degree of freedom in the z direction is freed to represent the mentioned special beam to wall connection. The gravity loads were assigned to the beams. Fig. 5 shows the numerical assembly of the model. The maximum drift of 3.75% (225 mm) is selected which is recommended by the New Zealand standard as the ultimate near collapse limit [34]. The cyclic response of the system under the ISO16670 loading protocol (applied at the top of the wall) is shown in Fig. 6 [35]. The numerical results show the gap opening in the PT connections and the consequent rocking movement of the wall starts when the applied force is 120.5 kN. From that point, the elongation of the PT stands produce a linear resistance up to the point with the maximum displacement (225 mm). Because the PT strands remain elastic during cycles of loading and unloading, the system exhibits symmetrical and stable load-deflection curves under the applied cyclic loading regime. The *flag shape* hysteresis in Fig. 6(d) evidently represents the self-centring behaviour. Although the described SC-RW system has been investigated for the first time in this paper, however, the concept of beam to column PT connections with slip friction devices has been experimentally investigated by several researchers before [22,28,36] and their obtained load-deformation loops are all flag shaped curves similar to the one in Fig. 6(b). Refer to the mentioned publications to compare the presented hysteretic loop with the experimentally obtained ones.

5. Displacement based design (DBD) procedure for SC-RW system

The described SC-RW as an in-plane system can be extended to core walls. Core walls are generally used as the primary lateral load resisting

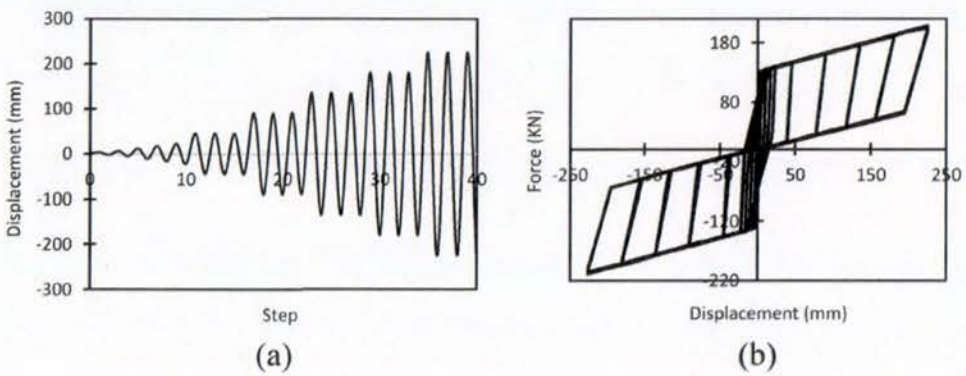

Fig. 6. Hysteretic behaviour of the SC-RW system: a) loading regime b) load-deflection loops of the system.

system for multi-story buildings. The use of SC-RW core has many notable benefits. The most important one is involved with seismic mitigation. Multi-directional earthquake loads can cause extensive damage particularly at the corners. High ductility of the proposed system combined with the remarkable energy dissipation rate of the friction dampers can efficiently mitigate the potential seismic loss.

For the elastic structures, the earthquake induced actions are directly related to the stiffness and strength of the system. That is the reason why the majority of the traditional earthquake design procedures were found on forces rather than displacements. However, for the inelastic systems, strength has a lesser significance because other factors such as ductility can extremely influence the behaviour of the system.

Priestly et al. addressed some of the fundamental problems of the traditional forced-based design approach [37,38] and proposed the direct displacement based design approach for the seismic design of ductile structures. They asserted that if the displacements are within a certain limit state, seismic damage can be efficiently avoided.

Loo et al. used a tentative displacement based design procedure for the walls with slip friction connections [33]. By the reason of the similarities between the SC-RW system behaviour to what loo et al. carried out, a similar step by step design procedure is used in this study. A six story SC-RW system with 18 m height and 6 m width is designed for soil type D (deep soil) in Christchurch with a 500 year return period. A five layer CLT for the first four floors and a three layer CLT for the two upper floors are considered. Thickness of all the layers of the CLT panels was assumed as 200 mm. MSG8 (Machine Graded Timber with grade 8) is selected for all the longitudinal and transverse layers (see Table 1). The density of the timber is assumed as 550 kg/m^3.

Step 1) determine the required drift limit and displacement profile

NZS1170.5 suggests a maximum inter-story deformation limit of 2.5% as the reference upper bound limit applicable to the ultimate limit state to minimize the probability of instability in a structure [34]. Therefore, a total target drift limit of $\theta = 2.5\%$ with 0.25% for elastic deflection is chosen. For simplicity, a linear distribution up the height of the structure is assumed. Thus, the displacement for each story can be determined as follows:

$$\Delta_i = h_i(\theta_{rot,max} + \theta_{el,y}) \tag{7}$$

where $\theta_{rot,max}$ and $\theta_{el,y}$ are the maximum rotation of the wall due to the rocking and the elastic deflection, respectively.

Step 2) determine the characteristics of the idealized equivalent single degree of freedom (SDOF) structure

The design displacement (Δ_d), the effective mass (m_e) and the effective height (H_e) can be determined as follow:

$$\Delta_d = \frac{\sum_{i=1}^{n} m_i \Delta_i^2}{\sum_{i=1}^{n} m_i \Delta_i} \tag{8}$$

$$m_e = \frac{\sum_{i=1}^{n} m_i \Delta_i}{\Delta_d} \tag{9}$$

$$H_e = \frac{\sum_{i=1}^{n} m_i \Delta_i h_i}{\sum_{i=1}^{n} m_i \Delta_i} \tag{10}$$

Calculated values based the assumed seismic masses for each story are presented in Table 3.

From Eqs. (8) to (10) and the data in Table 3, the equivalent SDOF structure has a design displacement $\Delta_d = 0.28$ m, an effective mass $m_e = 66.34$ tonnes and an effective height $H_e = 11.08$ m.

Table 3
Characterisitics of the idealized equivalent SDOF structure.

Story	Height (h_i)	Mass (m_i)	Δ_i	$m_i\Delta_i$	$m_i\Delta_i^2$	$m_i\Delta_i h_i$
6	18	2	0.45	2.25	1.013	40.5
5	15	10	0.375	3.75	1.406	56.25
4	12	15	0.3	4.5	1.35	54
3	9	15	0.225	3.375	0.759	30.375
2	6	20	0.15	3	0.45	18
1	3	20	0.075	1.5	0.113	4.5
Sum				18.375	5.09	203.625

Meters for heights and displacements.
Tonnes for masses.

Step 3) calculate the equivalent viscous damping

The equivalent viscous damping (ξ_{eq}) is comprised of the elastic damping (ξ_{el}) and the hysteretic damping (ξ_{hyst}):

$$\xi_{eq} = \xi_{el} + \xi_{hyst} \tag{11}$$

The hysteretic damping can be determined by Eq. (12), where A_1 is the area of the hysteric loop (Fig. 7 exhibits the ideal hysteresis loop for the SC-RW system) and A_2 is the area restricted by the elastic-perfectly-plastic loop [33,39] (The area within the dotted rectangle).

$\Delta_{He,y}$ can be specified by multiplying the $\theta_{el,y}$ (which is 0.25% from step 2) by the effective height. Therefore, $\Delta_{He,y}$ is equal to 30.4 mm. The ductility factor (μ) can now be determined:

$$\mu = \frac{\Delta_d}{\Delta_{He,y}} \tag{13}$$

From Fig. 7, A_1 and A_2 can be calculated as follows:

$$A_1 = 2F_{slip-total}(2\Delta_d - 3\Delta H_{e,y}) \tag{14}$$

$$A_2 = 12F_{slip-toal}\Delta_d \tag{15}$$

It should be pointed out that in the proposed design procedure, $F_{slip\text{-}total}$ should be assumed in this step and the procedure has to be iteratively repeated until the convergence is attained. In this case, assuming the $F_{slip\text{-}total}$ as 59 kN, the hysteretic damping is found as 17.8%. Adopting 2% for the elastic damping [33], the total equivalent viscous damping is accordingly determined as 19.8%.

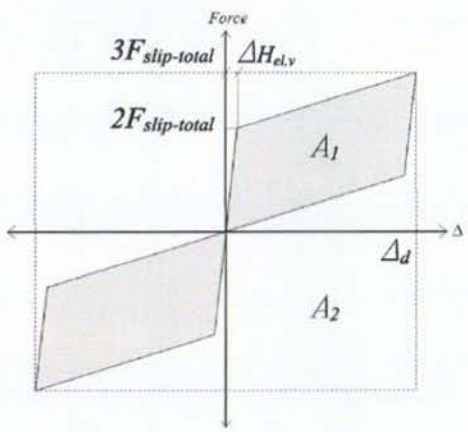

Fig. 7. Determination of the ideal hysteretic damping for the SC-RW system..

$$\xi_{hyst} = \frac{2A_1}{\pi A_2}$$

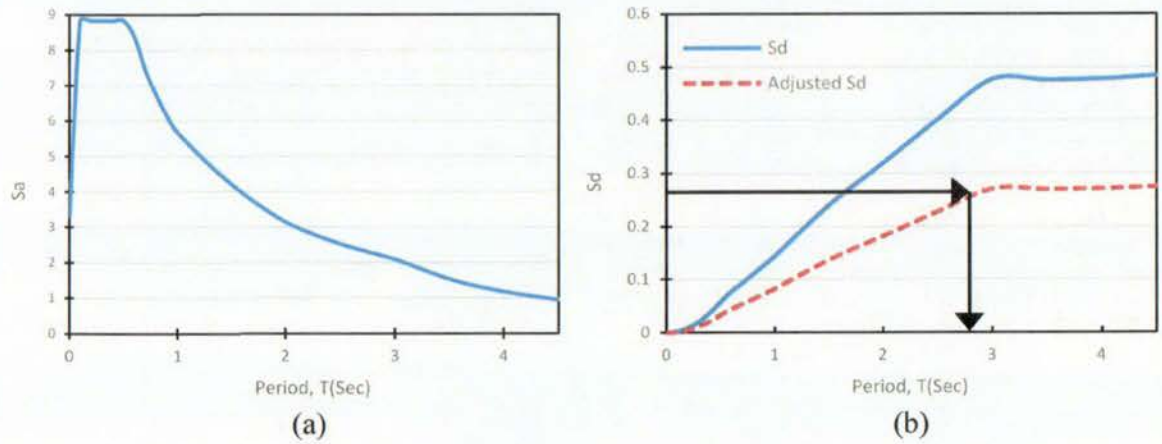

Fig. 8. Response spectrums: a) the acceleration spectrum b) the displacement spectrums.

Step 4) determine the effective period from the reduced design displacement spectrum

Referring to NZS1170.5 [34], the acceleration spectrum can be defined as shown below:

$$S_a = C_h(T)ZRN \tag{16}$$

where, Z is the hazard factor, $C_h(T)$ is the spectral shape factor and N is the near fault factor. In this structure Z, R and N are determined as 0.3, 1.0 and 1.0, respectively. The displacement spectrum can consequently be specified from the acceleration spectrum:

$$S_d = \frac{T^2}{4\pi^2} S_a \tag{17}$$

The scale factor to be applied to the design displacement spectrum (usually with 5% damping) is defined as:

$$R_{eq} = \left(\frac{7}{2+\xi_{eq}}\right)^{0.5} \tag{18}$$

In Fig. 8, the acceleration spectrum, the displacement spectrum and the corresponding adjusted displacement spectrum are illustrated. Accordingly, the effective period $T_e = 2.8$ s is found.

Step 5) obtain the equivalent lateral stiffness

The equivalent lateral stiffness can be specified as follows:

$$K_e = \frac{T^2}{4\pi^2} S_a \tag{19}$$

With the effective period of 2.8 s, the effective stiffness is calculated as 334.03 kN/m.

Step 6) determine the base shear and distribute the forces

The base shear and the distribution of the forces up the height of the structure can be specified from Eqs. (20) to (22).

$$V_b = K_e \Delta_d \tag{20}$$

$$F_i = 0.92 V_b \frac{m_i \Delta_i}{\sum_{i=1}^{n} m_i \Delta_i} \text{(for all stories except the roof)} \tag{21}$$

$$F_i = 0.08 V_b + 0.92 V_b \frac{m_i \Delta_i}{\sum_{i=1}^{n} m_i \Delta_i} \text{(for the roof)} \tag{22}$$

Note that the extra 8% of the based shear is added to the roof level to consider the effect of higher modes. The base shear $V_b = 101.97$ kN is found from Eq. (20). The distribution of the lateral forces and the corresponding overturning moments are listed in Table. 4.

Step 7) determine the slip thresholds and the PT forces

The total overturning moment from the seismic forces can be calculated as:

Table 4
Distribution of the forces.

Story	Height (h_i)	F_i	V_i	M_i
6	18	16.78	16.78	302.1
5	15	17.37	34.16	260.59
4	12	20.85	55.01	250.16
3	9	15.64	70.64	140.72
2	6	13.90	84.53	83.39
1	3	6.95	91.49	20.85

Meters for heights.
kN for forces.
kNm for the moments.

$$M_r = \sum_{i=1}^{n} F_i h_i \tag{23}$$

From Table 4, $M_r = 1057.8$ kNm. It should be noted that on the brink of rotation, the resisting force against the overturning moment is equal to $2F_{slip\text{-}total}$ (starting point of the *phase 3* in Fig. 4). Thus, the $F_{slip\text{-}total}$ can be determined via moment equilibrium (see Eq. (24)).

$$F_{slip-total} = \frac{M_r}{2h} \tag{24}$$

If there are n identical rocking walls in the system, the resultant $F_{slip\text{-}total}$ is equally shared between them:

$$\left(F_H + \sum F_j\right)\frac{b}{h} = \frac{1}{n} F_{slip-total} \text{ (For each CLT wall)} \tag{25}$$

In this structure, $F_{slip\text{-}total} = 59$ kN (at the top of the wall system) is shared equally between the two jointed CLT walls. If the walls had different mechanical or geometric characteristics, the proportion of the $F_{slip\text{-}total}$ would depend on the lateral stiffness of each one of them. By

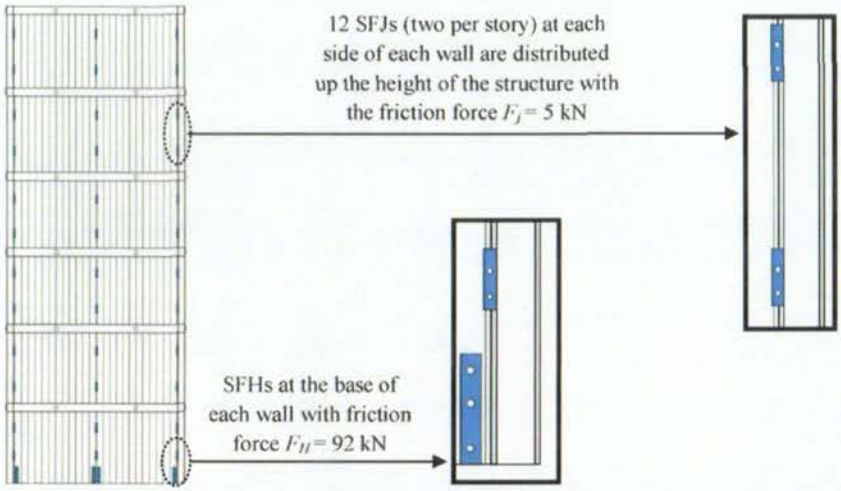

Fig. 9. General arrangement of the slip friction connections within the designed SC-RW system.

Table 5
Initial PT forces.

Story	Height (h_i)	d_i	$F_{pt,i(i)}$
6	18	100	171
5	15	100	177
4	12	100	212
3	9	120	132
2	6	120	117
1	3	140	51

Meters for all heights.
Millimetres for all dimensions.
kN for all forces and loads.

considering 12 SFJs on each side of each wall, $F_H = 92$ kN and $F_j = 5$ kN are determined from Eq. (25). Fig. 9 shows the schematic arrangement of the slip friction connections.

Considering the fact that two PT connections are acting at each elevation, post-tensioned forces can be specified as:

$$M_{pt-total} = F_{slip-total}h - \frac{Wl}{2} \tag{26}$$

$$F_{pt,i(i)} = \frac{f_i}{2\sum_{i=1}^{n} f_i} \frac{M_{pt-total}}{d_i} \tag{27}$$

The coefficient of 1/2 in Eq. (27) represents the two acting PT joints per bay. From Eq. (26) and the self-weight of $W = 99$ kN, $M_{pt\text{-}total} = 186$ kNm is found. The results of step 7 calculations are summarized in Table 5.

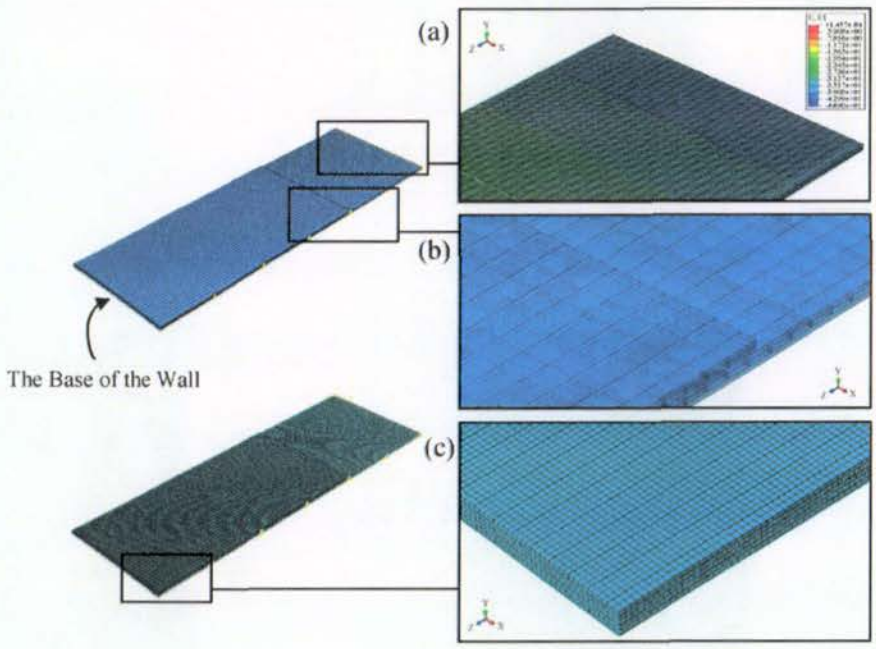

Fig. 10. Numerical model of the six story CLT wall: a) elastic deflection b) numerical assembly c) numerical mesh.

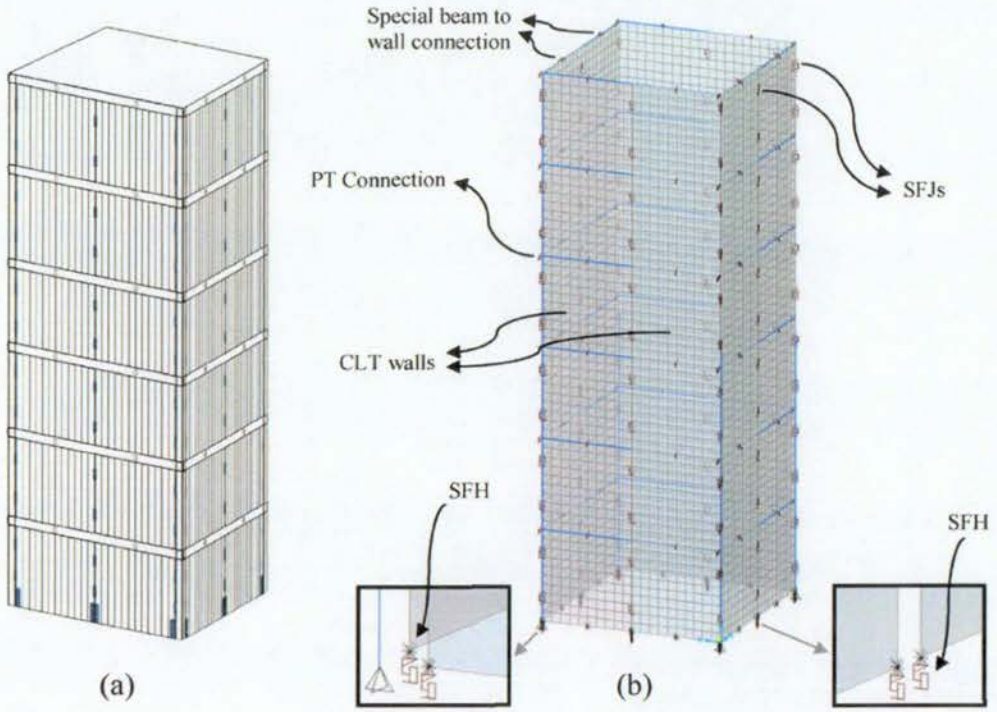

Fig. 11. SC-RW core system: a) schematic view b) numerical model.

Table 6
Earthquake records and scaling [42].

Event	Year	PGA (g)	Scale factor for ULS	Scale factor for MCE
El Centro	1940	0.313	1.2	2.1
Northridge	1994	0.231	1.6	3.0
Kobe	1995	0.821	0.5	0.8
Christchurch	2011	0.483	0.8	1.3
Landers	1992	0.280	1.5	2.6

Step 8) check the elastic deflection

Based on the resultant forces in Table 5, the elastic deflection of the structure should be checked for any difference from what is assumed in step 2. If the difference is significant, the procedure should be repeated from step 2 until the convergence is reached.

Because CLT is a highly non-uniform material, there is lack of knowledge in determining the equivalent elastic modulus. Thus, it is hard to accurately specify the elastic deformation of a CLT member. In this

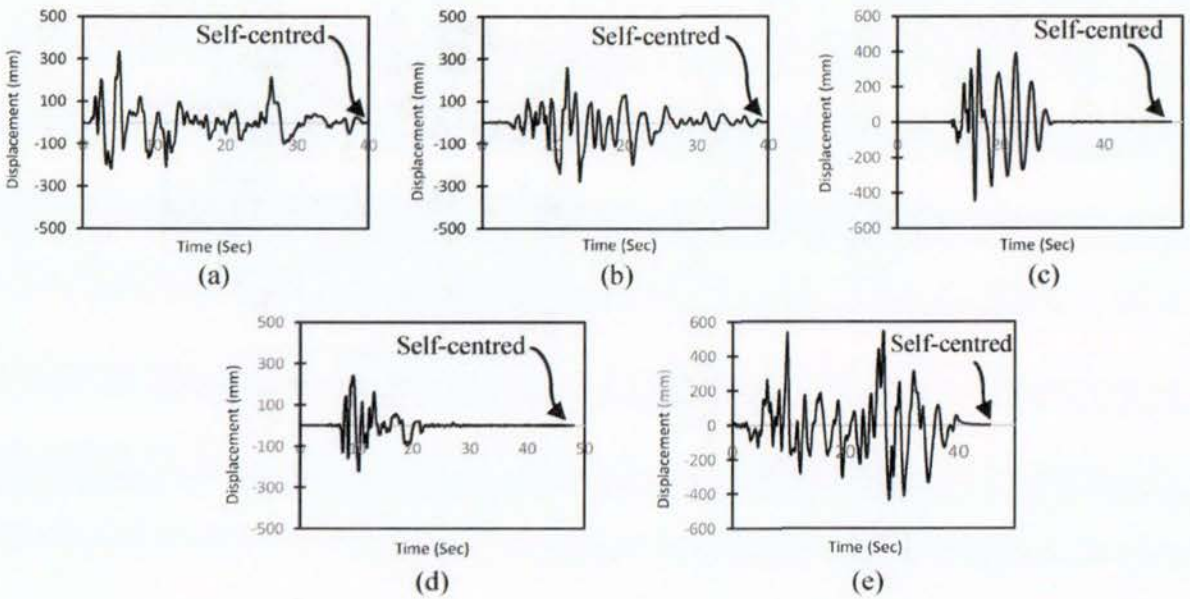

Fig. 12. Displacement response to MCE events: a) El Centro b) Northridge c) Kobe 4) Christchurch 5) Landers.

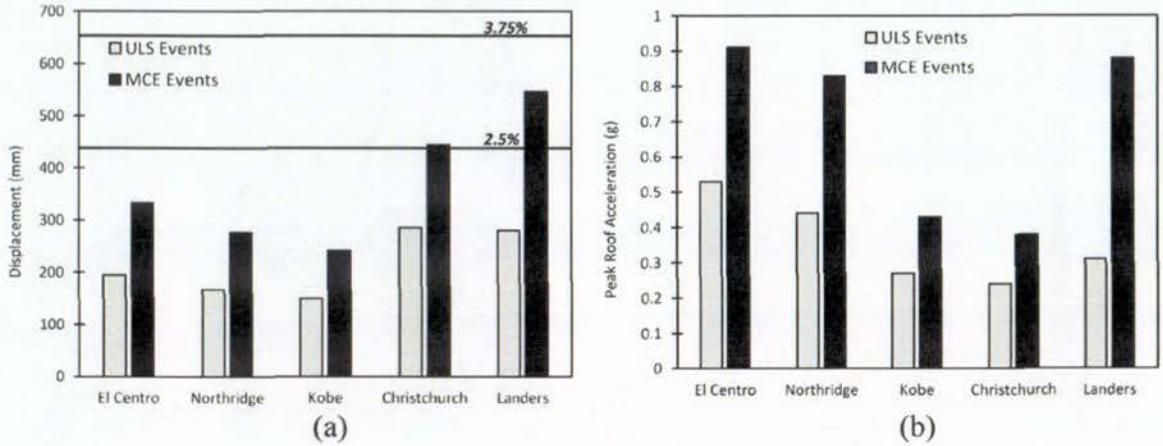

Fig. 13. Seismic response of the SC-RW core system: a) Maximum displacements b) Peak roof accelerations.

study, a numerical model using ABAQUS software package is developed to determine the lateral elastic deflection of the wall. However, an accurate yet simple method to predict the equivalent mechanical properties of CLT panels is absolutely necessary. This would make the designer capable of calculating the deflections by commonly used methods such as the moment area theory. In Fig. 10, the numerical assembly for the two 18 m by 3 m CLT walls with the assumed specifications in Section 5 is displayed. The two walls are tied together at every meter up the height of the structure representing the slip friction joints before slippage. From the numerical simulation, the elastic deflection of the top due to the applied calculated seismic forces was 47 mm ($\theta_{el,y} = 0.26\%$) which is not considerably different from what is assumed earlier. Therefore, the assumption for the elastic deflection in step 2 ($\theta_{el,y} = 0.25\%$) can be confidently accepted. It should be noted that the wall model in Fig. 10 is shown flipped over for better clarity. This numerical technique has previously been used and validated by the authors for a different wall application [40].

Step 9) apply a dynamic amplification factor

The numerical investigations of Loo et al. proved that the shear demand of a rocking wall with slip friction connections has to be multiplied by the dynamic amplification factor to consider the effect of the higher modes of vibration. This factor can be calculated with the proposed formula by Kelly [41]:

$$\omega_v = 1 + a_{vn}\mu \tag{28}$$

where μ can be determined by Eq. (13) ($\mu = 10$) and a_{vn} is the shear amplification factor. According to Loo et al., this factor can be considered as $a_{vn} = 0.9$ for CLT rocking walls with friction devices. Hence, $\omega_v = 10$ should be multiplied by the resultant base shear from step 6 and the CLT walls should be accordingly designed for the increased shear demand.

6. Seismic response of the self-centring rocking core system

Nonlinear dynamic numerical simulations were carried out using SAP2000 [30] for a core comprised of two previously designed identical SC-RW wall system in each direction (x and y). The modelling procedure is similar to what is described in Section 4. The CLT walls are modelled by nonlinear layered shell elements. The slip friction hold-downs are modelled as multi-linear plastic link elements with a gap element with zero gap representing the foundation level and a hook element to restrict the upward movement of the hold-downs. Similar assembly is used for the slip friction joints but with the gap and hook element openings equal to the slot length which demonstrates the slot length for the SFJs are twice as the one for SFHs. Two multi-linear elastic rotational links were used in each level at each direction to represent the calculated PT forces in Table 5. The stiffness of the second linear part of these links was specified in such the moment at 2.5% of rotation is 50% higher than the pre-stressed moment. In Fig. 11, the schematic view and the numerical assembly for the SC-RW core system are displayed. The floors are assumed to be rigid diaphragms in plane.

A suite of five ground motions were selected for earthquake simulations. The scale factors are calculated in accordance with NZS1170.5 to match the Christchurch 2500 year return period for the Maximum Credible Earthquake (MCE) and 500 year return period for the Ultimate Limit state (ULS). A type D soil (deep soil site) is selected for the ground motion scaling. The scaled peak ground motions are presented in Table 6. An equivalent viscous Damping of 2% was adopted for all modes of vibration [15,33]. The scaled accelerations are applied to the structure in both directions.

The floor displacement time-histories at the roof level for different MCE event simulations are shown in Fig. 12. The most imperative observation from this figure is that all floor displacement returned to zero at the end of the simulations. There is nearly no recognizable residual drift which perfectly demonstrates the self-centring behaviour. Fig. 13 summarized the simulation results including the maximum roof displacement and the peak roof accelerations. NZS1170.5 restricts the maximum inter-story deformation limit to 2.5% as the reference upper bound limit applicable to all ULS events (1/500 annual period of exceedance for ordinary buildings). However, for the MCE events with much lower annual probability of exceedance (1/2500), the deflection limit has been increased to 3.75% which represents the near collapse limits for common structural forms [34]. Both limits are marked in Fig. 13(a). On average, displacements for the MCE events are significantly higher than ULS events. None of the ULS maximum displacements surpasses the 2.5% limit. The highest recorded displacements are for the Landers and Christchurch events which was approximately 1.56%. For the MCE events, only the displacement of the Landers event exceeds 2.5% and none of them reached 3.75%.

Fig. 13(b) illustrates the peak recorded response accelerations at the roof level. It is observable that the maximum acceleration is 0.91 g for the El Centro event. Despite the fact that the shake table tests within the SOFIE project were conducted on a seven story CLT building, However, the maximum accelerations obtained in this study can be compared to what was recorded in the SOFIE project (3.8 g) to generally demonstrate the efficiency of the response system in decreasing the response accelerations [4]. This considerable reduction can be attributed to the significant energy dissipation rate of the slip friction connections.

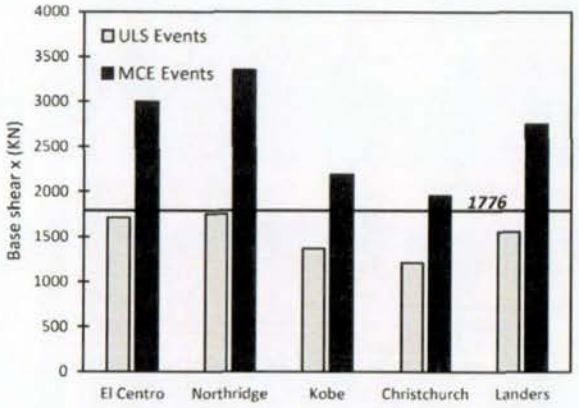

Fig. 14. Maximum base shear in *x* direction for ULS and MCE events.

Fig. 14 shows the peak base shears for the ULS and MCE events. The total intensified base shear value from the last step of the design procedure is 1776 kN to include the effect of higher modes of vibration. It is observable that the base shear demand for the ULS events does not exceed the indicated value, however, all of the MCE events surpassed the limit. The maximum recorded shear force is for the Northridge event which is approximately 1.8 times higher than what is calculated by the Kelly's formulae [41] (Eq. (28)). The studies of Loo et al. demonstrates that proposed formulae for the amplification factor is accurately applicable for timber walls with slip friction connections [33]. Nevertheless, for the SC-RW system, there is still room to investigate the effect of higher modes on the base shear. It is recognizable from Fig. 14 that the Kelly's equation is accurate for ULS events but it is non-conservative for MCE events.

7. Conclusions

This study describes the development of a new type of self-centring rocking timber wall (SC-RW) system capable of providing elastoplastic behaviour and ductility while limiting the residual drift and peak roof accelerations. In this system, rocking Cross Laminated Timber (CLT) walls are the main lateral resisting system while steel beams and columns are resisting gravity loads. Horizontally oriented post-tensioned steel strands through the beams provide moment resistance at the beam-column interface to self-centre the structure after the earthquake. Nonlinear cyclic and dynamic simulations were carried out to investigate the efficiency of the proposed system. The system exhibited a flag shape hysteresis which confirms the self-centring behaviour. Furthermore, a displacement based design approach was presented to design the SC-RW system in accordance with the targeted lateral drift. The designed system were subjected to numerous dynamic Ultimate Limit State and Maximum Credible Earthquake time-history simulations. No significant residual displacement was observed in the dynamic analyses indicating that the system is self-centring. Moreover, the maximum displacements were within the recommended limits by the New Zealand Standard. The recorded peak acceleration at the roof level for the six story prototype structure was 0.91 g which is remarkably lesser than what was documented during the shake table tests within the SOFIE project. This is the result of the significant rate of energy absorption in the slip friction damping devices. The recorded maximum base shears show that the Kelly's formulae for the dynamic amplification factor is accurate for the ULS event, however, it is non-conservative for the MCE events.

This preliminary study demonstrated that the hybrid self-centring rocking core system can be an efficient low damage lateral force resisting system compared to existing rocking timber wall systems with different types of dampers that are highlighted in the research background section.

References

[1] A.M. Rahman, J.I. Restrepo-Posada, Earthquake Resistant Precast Concrete Buildings: Seismic Performance of Cantilever Walls Prestressed Using Unbonded Tendons, 2000.
[2] J.K. Iverson, N.M. Hawkins, Performance of precast/prestressed building structures during northridge earthquake, PCI J. 39 (2) (1994).
[3] M. Fintel, Performance of buildings with shear walls in earthquakes of the last thirty years, PCI J. 40 (3) (1995) 62–80.
[4] A. Ceccotti, C. Sandhaas, M. Okabe, M. Yasumura, C. Minowa, N. Kawai, SOFIE project–3D shaking table test on a seven-storey full-scale cross-laminated timber building, Earthq. Eng. Struct. Dyn. 42 (13) (2013) 2003–2021.
[5] G.W. Housner, The behavior of inverted pendulum structures during earthquakes, Bull. Seismol. Soc. Am. 53 (2) (1963) 403–417.
[6] A. Palermo, S. Pampanin, The Use of Controlled Rocking in the Seismic Design of Bridges(Doctorate Thesis) Tech. Inst. Milan, Milan, 2004.
[7] Q.T. Ma, J.W. Butterworth, A generalised mathematical model for controlled rocking systems, 4th International Conference on Earthquake Engineering, Taipei, Taiwan, October 12–13, 2006.
[8] M. ElGawady, A.J. Booker, H.M. Dawood, Seismic behavior of posttensioned concrete-filled fiber tubes, J. Compos. Constr. 14 (5) (2010) 616–628.
[9] L.G. Cormack, The Design and Construction of the Major Bridges on the Mangaweka Rail Deviation, 1988.
[10] S. Sritharan, S. Aaleti, R.S. Henry, K.-Y. Liu, K.-C. Tsai, Introduction to PreWEC and key results of a proof of concept test, MJ Nigel Priestley Symposium 2008, pp. 95–106.
[11] S. Sritharan, S. Aaleti, R.S. Henry, K. Liu, K. Tsai, Precast concrete wall with end columns (PreWEC) for earthquake resistant design, Earthq. Eng. Struct. Dyn. 44 (12) (2015) 2075–2092.
[12] A. Iqbal, S. Pampanin, A. Buchanan, A. Palermo, Improved seismic performance of LVL post-tensioned walls coupled with UFP devices, 8th Pacific Conference on Earthquake Engineering, Singapore, 2007.
[13] A. Iqbal, S. Pampanin, A. Palermo, A.H. Buchanan, Performance and design of LVL walls coupled with UFP dissipaters, J. Earthq. Eng. 19 (3) (2015) 383–409.
[14] F. Sarti, A. Palermo, S. Pampanin, Design and testing of post-tensioned timber wall systems, World Conference of Timber Engineering, Qubec City, Canada, 2014.
[15] W.Y. Loo, P. Quenneville, N. Chouw, A numerical study of the seismic behaviour of timber shear walls with slip-friction connectors, Eng. Struct. 34 (2012) 233–243.
[16] W.Y. Loo, C. Kun, P. Quenneville, N. Chouw, Experimental testing of a rocking timber shear wall with slip-friction connectors, Earthq. Eng. Struct. Dyn. 43 (11) (2014) 1621–1639.
[17] C.W. Roeder, S.A.C.J. Venture, State of the art report on connection performance, Report No. FEMA-355D, Federal Emergency Management Agency (FEMA), Washington (DC), 2000.
[18] J.M. Ricles, R. Sause, M.M. Garlock, C. Zhao, Posttensioned seismic-resistant connections for steel frames, J. Struct. Eng. 127 (2) (Feb. 2001) 113–121.
[19] M.M. Garlock, R. Sause, J.M. Ricles, Behavior and design of posttensioned steel frame systems, J. Struct. Eng. 133 (3) (2007) 389–399.
[20] K.C. Tsai, C.-C. Chou, C.-L. Lin, P.-C. Chen, S.-J. Jhang, Seismic self-centering steel beam-to-column moment connections using bolted friction devices, Earthq. Eng. Struct. Dyn. 37 (4) (2008) 627–645.
[21] H.-J. Kim, C. Christopoulos, Friction damped posttensioned self-centering steel moment-resisting frames, J. Struct. Eng. 134 (11) (2008) 1768–1779.
[22] Y.C. Lin, R. Sause, J.M. Ricles, Seismic performance of steel self-centering, moment-resisting frame: hybrid simulations under design basis earthquake, J. Struct. Eng. 139 (11) (2013) 1823–1832.
[23] H.W. Morris, M. Zhu, M. Wang, The long-term instrumentation of the NMIT Arts Building–EXPAN shear walls, N. Z. Timber Des. J. 20 (1) (2011) 13–24.
[24] F. Wanninger, A. Frangi, M. Fragiacomo, Long-term behavior of posttensioned timber connections, J. Struct. Eng. 141 (6) (2014) 4014155.
[25] W.Y. Loo, P. Quenneville, N. Chouw, A new type of symmetric slip-friction connector, J. Constr. Steel Res. 94 (2014) 11–22.
[26] D. Moroder, F. Sarti, A. Palermo, S. Pampanin, A.H. Buchanan, Experimental investigation of wall-to-floor connections in post-tensioned timber buildings, New Zealand Society of Earthquake Engineering Conference. Auckland, New Zealand, 2014.
[27] R.S. Henry, Self-Centering Precast Concrete Walls for Buildings in Regions with Low to High Seismicity, 2011 (PhD Thesis).
[28] J. Iyama, C.Y. Seo, J.M. Ricles, R. Sause, Self-centering MRFs with bottom flange friction devices under earthquake loading, J. Constr. Steel Res. 65 (2) (2009) 314–325.
[29] M. Wolski, J.M. Ricles, R. Sause, Experimental study of a self-centering beam–column connection with bottom flange friction device, J. Struct. Eng. 135 (5) (2009) 479–488.
[30] Computers and Structures, "SAP2000. (2011)", 2011 (Berkeley, CA).
[31] A.H. Buchanan, N. Z. T. I. Federation, Timber Design Guide, New Zealand Timber Industry Federation, 1999.
[32] A. Hashemi, R. Masoudnia, P. Quenneville, A numerical study of coupled timber walls with slip friction damping devices, Constr. Build. Mater. 121 (2016) 373–385.
[33] W.Y. Loo, P. Quenneville, N. Chouw, Rocking timber structure with slip-friction connectors conceptualized as a plastically deformable hinge within a multistory shear wall, J. Struct. Eng. (2015) E4015010.
[34] N. Z. Standard, NZS1170. 5: 2004, Struct. Des. Actions Part, vol. 5, 2004.
[35] A. Standard, "E2126," Stand. Test Methods Cycl. Load Test Shear Resist. Vert. Elem. Lateral Force Resist. Syst. Build. West Conshohocken, PA Am. Soc. Test. Mater, 2009.
[36] C.C. Chou, Y.J. Lai, Post-tensioned self-centering moment connections with beam bottom flange energy dissipators, J. Constr. Steel Res. 65 (10) (2009) 1931–1941.
[37] M.J. Kowalsky, M.J. Priestley, G.A. Macrae, Displacement-based design of RC bridge columns in seismic regions, Earthq. Eng. Struct. Dyn. 24 (12) (1995) 1623–1643.

[38] M.J.N. Priestley, G.M. Calvi, M.J. Kowalsky, Direct displacement-based seismic design of structures, 2007 NZSEE Conference, 2007.
[39] F. Mazza, A. Vulcano, Equivalent viscous damping for displacement-based seismic design of hysteretic damped braces for retrofitting framed buildings, Bull. Earthq. Eng. 12 (6) (2014) 2797–2819.
[40] A. Hashemi, P. Zarnani, A. Valadbeigi, R. Masoudnia, P. Quenneville, Seismic resistant cross laminated timber structures using an innovative resilient friction damping system, Proceedings of New Zealand Society for Earthquake Engineering Conference (NZSEE), Christchurch, New Zealand, 2016.
[41] T.E. Kelly, Tentative seismic design guidelines for rocking structures, Bull. N. Z. Soc. Earthq. Eng. 42 (4) (2009) 239.
[42] P. PEER, NGA Database, Pacific Earthquake Engineering Research Center, Univ. California, Berkeley, USA, (http://peer.berkeley.edu/nga), 2012.

Seismic resistant cross laminated timber structures using an innovative resilient friction damping system

A. Hashemi[1], A. Valadbeigi[3], R. Masoudnia[4] & P.Quenneville[5]

Department of Civil and Environmental Engineering, The University of Auckland, Auckland.

P. Zarnani[2]

Department of Built Environment Engineering, Auckland University of Technology, Auckland.

2016 NZSEE Conference

ABSTRACT: Multi-storey timber structures are becoming progressively desirable owing to their aesthetic and environmental benefits and to the high strength to weight ratio of timber. A recent trend in timber building industry is toward cross laminated timber (CLT) panelized structures. The shake table tests within the SOFIE project have shown that the CLT buildings constructed with traditional methods can experience high damage especially at the connections which generally consist of hold-down brackets and shear connectors with mechanical fasteners such as nails or bolts. Thus, current construction methods are not recognised as reliable in seismic prone areas. The main objective of this project is to develop a new low damage structural concept using innovative resilient slip friction (RSF) damping devices. The component test results demonstrate the capacity of this novel joint for dissipating earthquake energy as well as self-centring to minimize the damage and the residual drift after a severe event. The application of RSF joints as hold-down connectors for walls were investigated through numerical studies. Moreover, a core wall system comprised of cross laminated timber and RSF connectors is subjected to time-history earthquake simulations. The numerical results exhibit no residual displacement alongside a significant reduction in peak acceleration which can be attributed to significant amount of dissipated seismic energy over the RSF joints within the system.

1 INTRODUCTION

Structural walls offer outstanding seismic resistance compared to other structural systems and are commonly employed as the main lateral resisting system. Structural walls constructed with prefabricated components have additional advantages including offsite fabrication, improved quality and speed of construction. Recently, there has been a tremendous interest towards design and construction of multi-storey timber structures with engineered wood products such as Cross Laminated Timber (CLT) and Laminated Veneer Lumber (LVL) panels. Nevertheless, the application of these products in seismic regions as the primary lateral resisting system was limited by codes firstly because of insufficient technical information about their dynamic behaviour and secondly the non-ductile nature of them which leads to high response accelerations especially in high-rise buildings. During the large-scale experiments of a seven story building made of CLT panels within the SOFIE project, high accelerations with a maximum of 3.8 g in higher floors were recorded (Ceccotti et al. 2013). Despite the fact that these accelerations may be acceptable for human health, they are uncomfortable and displeasing for the habitants. As an important outcome of the SOFIE project, other research studies were started with the aim of developing new seismic solutions for timber industry to absorb the seismic energy, decrease the subsequent response accelerations and minimize the residual damage.

During the PRESS (PREcast Seismic Structural Systems) program in the early 1990's, hybrid wall systems were recognized as relatively efficient lateral load resisting members (Priestley et al. 1999). The tested hybrid system comprised of unbonded post-tensioned tendons with dissipative devices such

as grouted longitudinal post-tensioned bars. While the dissipating devices absorb the seismic energy, the post-tensioned tendons provide self-centring behaviour (Palermo et al. 2005). The concept had later been extended to reinforced concrete jointed walls. In such system, two or more single prefabricated walls are connected to each other with special energy dissipative connectors as ductile links along the vertical joints between the adjoining walls. Similar assembly is employed for timber coupled walls. The experimental investigation on coupled post-tensioned LVL walls with internal mild steel bars as the energy dissipater devices demonstrated promising results in terms of ductility and residual displacements (Palermo et al. 2005). Similar systems were developed and tested with external fuse type longitudinal threaded steel rods as the connection between the wall and the base (Smith et al. 2007).

Iqbal et al. studied the application of U-shaped Flexural Plates (UFPs) as supplementary damping devices in post-tensioned LVL timber coupled rocking walls (Iqbal et al. 2007). The system had later been experimentally investigated and a design procedure was proposed (Iqbal et al. 2015). The test results confirmed an efficient energy dissipation mechanism over yielding the UFPs during the earthquakes. Sarti et al. tested coupled LVL walls and UFP connectors with fuse type damping devices at the base of the walls (Sarti et al. 2014). Despite the fact that all mentioned wall systems represented relatively superior seismic behaviour compared to traditional systems, however, because the energy absorption is through yielding of metal members, large amount of stiffness degradation occurs in them during and after a sever seismic event. Thus, such system cannot be accredited as a low damage solution.

Loo et al. introduced the application of symmetric slip friction hold-downs for LVL rocking timber shear walls. The symmetric slip friction hold-down offers a rectangular load-deflection curve which means efficient energy dissipation. Furthermore, it provides constant resistance force against overturning moment. The proposed configuration later had been experimentally tested and demonstrated a stable hysteresis with minimum stiffness degradation which is the key characteristic of a low damage system (Loo et al. 2014). Although the energy dissipation mechanism of slip friction connections is one of the most efficient amongst passive damping devices, however, the lack of self-centring in these joints requires the use of an additional system (such as post-tensioned tendons) to bring back the structure to its initial position after an earthquake if the self-weight is not sufficient.

In this paper, a new structural wall system based on a novel friction joint is presented. The components of this joint are formed and arranged so that the self-centring capacity as well as energy absorption is achieved all in one connection system. This new Resilient Slip Friction (RSF) joint invented by Zarnani and Quenneville (Zarnani et al. 2015) could have a considerable impact on the building industry as it is exactly aligned with the high demand for cost-efficient low damage systems.

2 RESILIENT SLIP FRICTION (RSF) JOINT

Figure 1 shows the components and assemblage of the RSF joint. The grooved plates are bolted and clamped in a manner that the centre slotted plates are sandwiched by the cap plates. When the imposed force to the joint overcomes the frictional resistance between the surfaces, the centre plate starts to slide and energy will be dissipated through cycles of sliding. The frictional resistance is a function of the pre-stressed force of the bolts, the coefficient of friction between the surfaces and the angle of the grooves. The specific shape of the grooves along with the use of Belleville washers (or equivalent die springs) and high strength bolts provide the desirable self-centring characteristic.

Figure 1: RSF joint: a) Components b) Assemblage

The angle of the grooves is designed in such a way that at the time of unloading, the reversing force induced by the elastically compacted Belleville washers is larger than the resisting friction force acting

between the plates surfaces. Hence, the system is re-centred by the reversing force upon unloading. In addition, the lateral resistance of this new joint is relatively higher than the conventional friction joints for a similar clamping force provided by the high strength bolts. It should be pointed out that Figure 1(a) displays a double acting RSF joint which two centre slotted plates are employed within the connection.

3 RSF JOINT DESIGN PROCEDURE

A design procedure has been developed for the capacity prediction of this new joint based on the free body diagrams shown in Figure 2 (Zarnani et al. 2015). The slip force (F_{slip}) for a symmetric configuration can be determined by Equation 1.

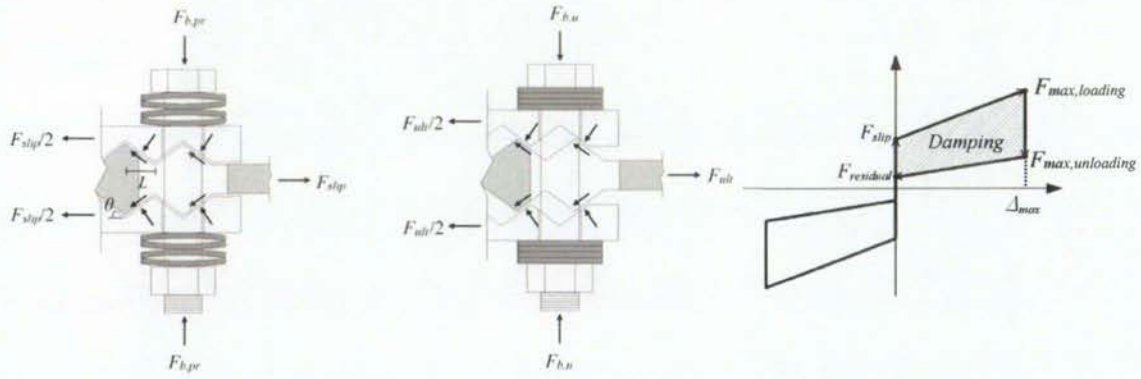

(a) (b) (c)

Figure 2: Schematic illustration of the symmetric RSF joint: a) Friction plates before slip b) Friction plates at ultimate deflection c) Schematic hysteretic loop

$$F_{slip} = 2n_b F_{b,pr}\left(\frac{\sin\theta + \mu_s \cos\theta}{\cos\theta - \mu_s \sin\theta}\right) \tag{1}$$

Where $F_{b,pr}$ is the bolt clamping force as a result of being pre-stressed, n_b is the number of bolts, θ is the angle of the grooves and μ_s is the coefficient of static friction. The residual force in the device at the end of unloading is calculated by Equation 2 where μ_k is the coefficient of kinetic friction which can be assumed as $0.85\mu s$

$$F_{residual} = 2n_b F_{b,pr}\left(\frac{sin\theta - \mu_k cos\theta}{\cos\theta + \mu_k sin\theta}\right) \tag{2}$$

The ultimate capacity at loading ($F_{ult,loading}$) and unloading ($F_{ult,loading}$) can be determined by replacing the μs and $F_{b,pr}$ in Equation 1 and Equation 2 with μ_k and $F_{b,u}$, respectively. The ultimate force on the bolt ($F_{b,u}$) is given by Equation 3 in which k_s and Δ_s are the stiffness of the stack of washers on the bolt and the maximum deflection of them in the fully compressed state, respectively.

$$F_{b,u} = F_{b,pr} + k_s \Delta_s \tag{3}$$

It should be emphasized that in an asymmetric configuration, the friction bolts in the connection need to transfer the applied force through shear and tension. Therefore, they should be designed for both. Refer to (Loo et al. 2014) for more details about the differences between symmetric and asymmetric friction connections.

$$\delta_{\max} = n_j \frac{\Delta_s}{\tan\theta} \tag{4}$$

Where n_j is the number of joints acting in a series (e.g. n_j equals to 1 for a single acting joint and equals to 2 for a double acting connector). The connection exhibits self-centring behaviour providing that the following considerations are taken into account.

$$\mu_s < \tan\theta \tag{5}$$

$$L > \frac{\Delta_s}{\sin\theta} \tag{6}$$

Where L is the horizontal distance between the top and bottom of the groove.

4 EXPERIMENTAL INVESTIGATION OF THE RSF JOINT CYCLIC BEHAVIOUR

In order to experimentally investigate the hysteretic behaviour of the RSF joint, a double acting symmetric RSF joint was fabricated and tested with a 100 kN Instron Machine. Cap plates were manufactured with mild steel grade 300 and slotted centre plates with bisalloy grade 400. Four high strength bolts with minimum of 830 MPa tensile strength were employed (Two bolts in each side). The stack of Belleville washers on each side of each bolt comprised of four series springs with 38 kN of load at flat position. The pre-stressed force of each bolt ($F_{b,pr}$) was 5 kN. It should be noted that for a double acting RSF joint, the number of bolts in Equation 1 (n_b) refers to the number of bolts in one of the slotted plates which equals to 2 in this case. The stacks of Belleville washers were placed under the nuts of the bolts and the nuts were tightened until the desired pre-stressed force (5 kN) per bolt is achieved. A specific lubricant is used between the cap plates and centre plates to increase the durability of the friction surfaces by controlling the possible galling and rusting. Figure 3 shows the test setup and the experimentally obtained hysteresis for the RSF joint prototype.

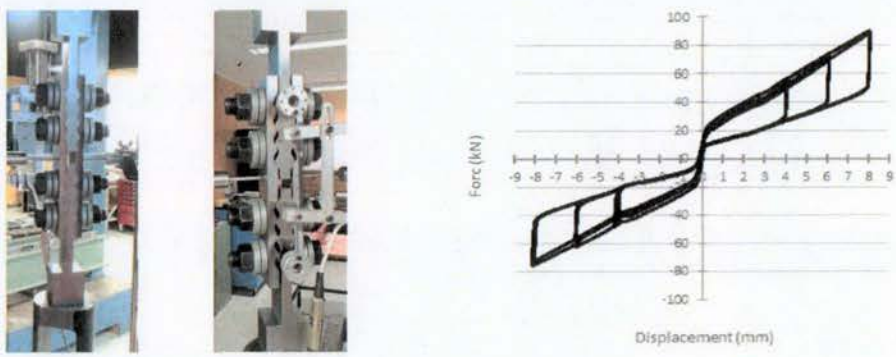

(a) (b)

Figure 3: Experimental test of a double acting RSF joint a) Test setup b) Hysteresis loops

The flag shape hysteresis in Figure 3(b) demonstrates the fully self-centring behaviour of the system. It shows that the system returned to its initial position after cycles of loading and unloading. The coefficient of friction was obtained as 0.18 for the specified surfaces with the special lubrication. The maximum displacement for this preliminary experiment was 8 mm. Further experimental tests and in-depth numerical simulations are being carried out by the authors at The University of Auckland to further investigate the dynamic behaviour and different applications of the proposed concept.

5 NUMERICAL MODELLING OF CLT WALLS WITH RSF CONNECTIONS

A numerical analysis is carried out in SAP2000 (CSI 2011) to investigate the cyclic behaviour of the CLT rocking walls with double acting symmetric RSF hold-downs. A 6 m by 1.5 m CLT wall with five layers of 40 mm thick MSG8 (Machine Graded Timber – Grade 8) boards is considered (Buchanan 1999). The width of the boards is assumed as 200 mm. The CLT is modelled using layered shell elements to represent the longitudinal and transverse layers. To optimize the efficiency of the

wall, the three longitudinal layers have been placed perpendicular to the applied lateral load. Defining a reasonable approach to determine the slip threshold for the rocking timber walls is extremely imperative. In all low damage structural concepts in timber structures, the wooden elements should remain elastic and the elastoplastic behaviour is provided by the connections. In this case, the wall needs to rock before the stress in any of the timber boards within the CLT wall exceeds the allowable elastic tension or compression stresses. CLT is a highly non-uniform engineered wood product which makes is extremely hard to accurately define its lateral resistance by using conventional analytical methods. In order to specify the maximum tolerable force applied to the top of the wall (F_E) before the timber goes beyond the elastic region, a numerical model is developed in ABAQUS (Hibbitt et al. 2014) software package (see Figure 4(b)). The numerical assembly and the normal stress distribution are shown in Figure 4. The density of the timber is considered as 540 kg/m^2. The F_E of 26.5 kN was found from the numerical analysis. In Figure 4(a), the wall is shown flipped over horizontally for better clarity.

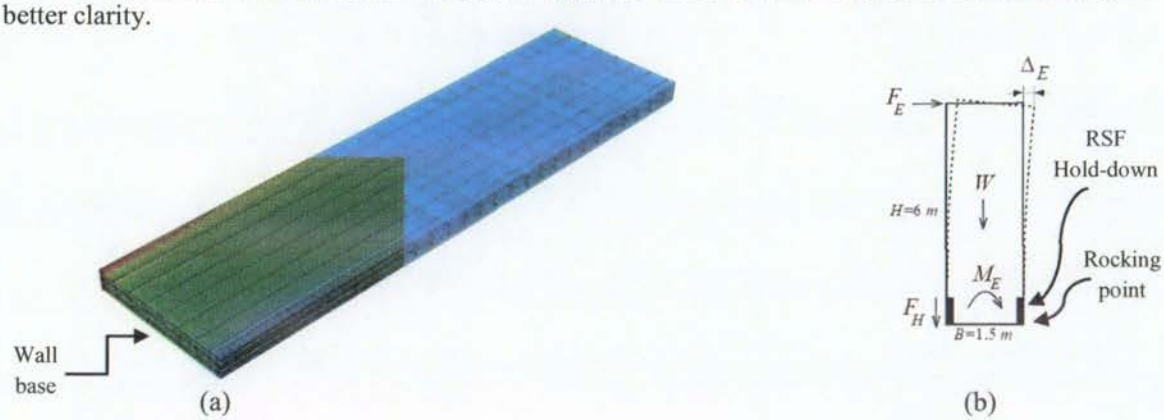

Figure 4: Numerical modelling of a CLT wall a) Assembly and stress distribution b) Elastic deflection of the wall

Taking the moments about the rocking point (Figure 5(c)), the force of the hold-down connector (F_H) can be calculated by Equation 7 for a determined F_E.

$$(F_H + W/2)B = F_E H \tag{7}$$

With reference to Figure 2(c) and F_H = 100kN from Equation 7, the maximum load within the RSF connection ($F_{max,loading}$) is determined as 100 kN. The hold-down is designed by following the proposed design procedure in section 3. The calculated design parameters for the Belleville washers (or equivalent die springs) and the sliding plates are presented in Table 1. The slot length should be determined in accordance with the 2.5% of the lateral drift at the top of the wall as the target limit. This limit is recommended by The New Zealand Standard as the reference upper bound limit for ultimate limit state considerations for all buildings (NZS1170.5 2004).

Table 1. Design parameters for the RSF hold-down

n_b	θ	μ_s	Washer Thickness (mm)	Washer Height (mm)	Washer Capacity (kN)	Number of Washers Per bolt	$F_{b,pr}$ (kN)	Slip Distance (mm)
2	15	0.18	6.47	1.75	55	6	27	39.9

From Equation 1 and substituting the μ_s and $F_{b,pr}$ with μ_k and $F_{b,u}$, the RSF joint has a slip threshold of F_{slip} = 50.8 kN and the maximum force of $F_{max,loading}$ = 96.5 kN which is within the acceptable range (less than 100 kN). The clamping force of $F_{b,pr}$ = 27 kN for each bolt is determined to achieve the mentioned sliding and maximum forces. From Equation 2, the residual force at the end of unloading $F_{residual}$ = 9.7 kN is specified. The RSF hold-down is modelled in SAP2000 using a Damper-Friction Spring link element to represent the proposed hysteretic behaviour (see Figure 2(c)). A gap element is

used as well to simulate the foundation level which the wall cannot move below. The displacement loading regime of Figure 5(b) is applied at the top of the wall. A 40 mm slot length is considered for the joint with respect to the target lateral drift and the designed slip distance for the connection. The cyclic behaviour of the system (the applied load at the top vs. base shear) displayed in Figure 5(c) demonstrates that RSF connectors can effectively retain the forces on shear walls below the destined level, thereby protecting them from inelastic damage. The reason is that the force in each of the connections does not exceed $F_{max,loading}$ which is the force that the joint is designed for it. Furthermore, the flag shape hysteretic loops represent the self-centring behaviour as an important performance criterion for RSF joints.

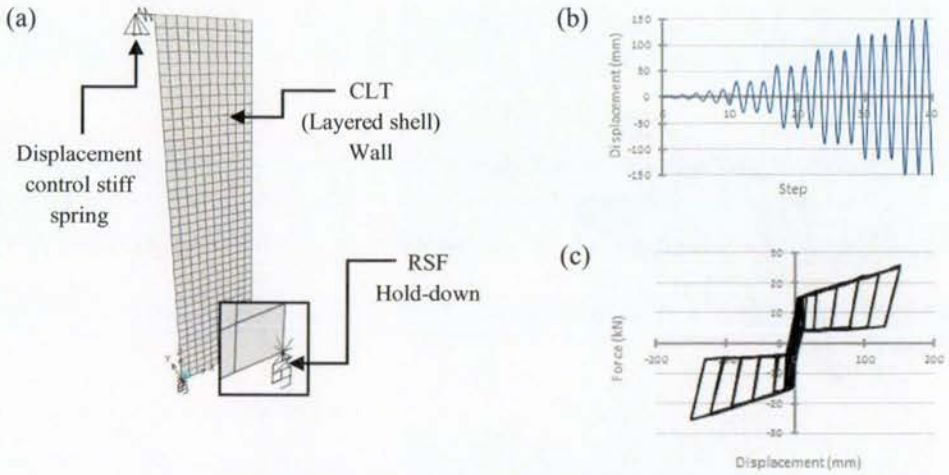

Figure 5: Numerical analysis of CLT wall with RSF joints a) Numerical model b) Loading regime c) Force-displacement loops

6 DYNAMIC TIME-HISTORY ANALYSIS OF CLT CORE SYSTEM WITH RSF JOINTS

Rocking CLT walls with RSF connections can efficiently be extended to core wall applications. Core walls are typically known as the primary lateral load resisting element in the multi-residential buildings. High ductility of the proposed system in conjunction with significant energy absorption rate and self-centring characteristic of the RSF joints make the core capable of effectively mitigating the potential seismic loss and post-earthquake residual damage.

Nonlinear dynamic time-history analyses were carried out on a rocking CLT core wall with RSF connections in SAP2000. The core included two identical wall systems in each direction with each system comprised of two 15 m by 2.5 m CLT walls. The arrangement of the layers and the material properties of the timber boards within the CLT walls are as defined in section 5. RSF hold-downs are used to anchor the walls to the foundation while each wall is connected to the adjacent walls or columns by slotted plate ductile links. These links are meant to transfer the horizontal forces while de-coupling the vertical movement of the walls during rocking. Steel columns are placed at the corners of the core to de-couple the perpendicular walls in bi-directional rocking. Nonlinear layered shell element and Damper-Friction Spring link element are used to model the CLT wall and the RSF joints, respectively. Ductile vertical links are modelled as linear stiff springs with zero stiffness in the vertical direction.

A numerical analysis of a five layer 15 m by 2.5 m CLT wall in ABAQUS shows that the maximum overturning moment providing that all timber boards in the CLT panels stay elastic is M_E = 215 kNm and as a result, $F_{max,loading}$ = 36 kN is found for the RSF joints using Equation 7. Consequently, the design parameters of the RSF joints within the proposed system are determined by following the design procedure introduced in section 3 (see Table 2).

Table 2. Design parameters for the RSF hold-downs in the core system

n_b	θ	μ_s	Washer Thickness (mm)	Washer Height (mm)	Washer Capacity (kN)	Number of Washers Per bolt	$F_{b,pr}$ (kN)	Slip Distance (mm)
2	15	0.18	6.47	1.75	38	8	10	94.6

The slot length for the RSF hold-downs is designed with a 3.75% maximum target drift at the top. It should be noted that the slot length for the vertical ductile links is twice as the hold-down as the connection has to accommodate the corresponding displacements in both upward and downward directions. Four earthquake acceleration records were selected for dynamic time-history loading (PEER 2006). The records were scaled for type D (deep soil) in Christchurch with 500 year return period for Ultimate Limit State (ULS) and 2500 year return period for Maximum Credible Earthquake (MCE). The scale factors were calculated based on numerically determined fundamental period and fundamental frequency of 0.66 seconds and 1.51 Hz, respectively. The scaled factors are presented in Table 3.

Table 3. Considered earthquakes for time-history analysis

Event	El Centro (1940)	Northridge (1994)	Kobe (1995)	Landers (1992)
PGA (g)	0.31	0.23	0.82	0.28
Scale factor (ULS)	1.0	1.6	0.4	1.1
Scale factor (MCE)	1.7	2.9	0.6	2.0

Seismic masses of 7500 kg for the roof and 14000 kg for other four stories were assigned to the structure to represent a five story panelized timber structure. It should be pointed out that in the proposed system, the core is the main lateral load resisting system and the gravity loads are carried by other perimeter CLT walls. The elastic viscous damping of 2% is adopted for all modes of vibration.

Figure 6(a) shows the numerical model of the proposed core system. In Figure 6(b) a possible solution for vertical ductile links is exhibited as the connection can transfer horizontal loads while is free to move upward or downward during the wall's rocking.

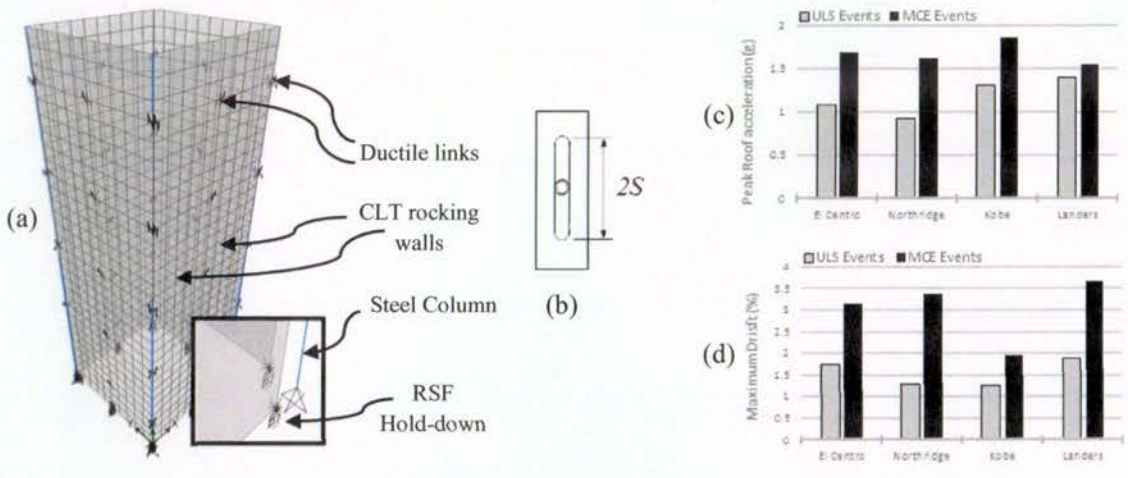

Figure 6: Numerical analysis of the CLT core with RSF joints a) Numerical model b) slotted plate ductile link c) Maximum lateral drifts d) Peak roof accelerations

The numerical results showed that the structure returned to its initial position at the end of earthquake for all ULS and MCE events. This exhibits the self-centring behaviour which can be attributed to the RSF connections within the system. Figure 6(c) compares the maximum horizontal drift at the roof

level for the two limit states. For ULS events, the peak drift is for the Landers event which is less than 2%. It should be noticed that none of the maximum ULS drifts exceeds 2.5% limit indicated by most of the building codes around the world. NZS1170.5 suggests that the deflection limit for 1/2500 annual period of exceedance (MCE events) can be increased to 3.75% (NZS1170.5 2004). For the MCE events, the most significant drift is for the Landers event (3.6%) which is still within the acceptable range.

The peak response accelerations at the roof level are displayed in Figure 6(d). The recorded accelerations are between 0.9 g to 1.8 g for the ULS and MCE events. This should be compared to observed accelerations as high as 3.8 g in the shake table tests of a 7-story CLT building within the SOFIE project (Ceccotti et al. 2013). This significant reduction can be attributed to the large amount of dissipated seismic energy through RSF joints.

7 CONCLUSIONS

Latest research findings have shown that CLT buildings constructed with traditional connections such as nailplates or bolts can experience high damage during and after a severe earthquake. In this paper a new type of low damage CLT wall system with innovative resilient slip friction (RSF) joints is introduced. The component test results in conjunction with numerical cyclic analyses demonstrate the capacity of this system for dissipating seismic energy as well as self-centring behaviour. The numerical time-history seismic analyses on a core system with RSF connections exhibited the efficiency of the proposed system in terms of ductility, energy dissipation and self-centring behaviour as key factors for providing a low damage seismic design.

REFERENCES

Buchanan, A., 1999. Timber Design Guide. *New Zealand Timber Industry Federation.*

Computers and Structures, Inc, 2011. SAP2000: Structural Analysis Program, USA.

Hibbitt, K., 2014. ABAQUS. *Standard User's Manual.* V. 6.13

Iqbal, A., Pampanin, S., Buchanan, A., Palermo, A., 2007. Improved Seismic Performance of LVL Post-Tensioned Walls Coupled with UFP Devices. *8th Pacific conference on earthquake engineering,* Singapore.

Iqbal, A., Pampanin, S., Palermo, A, Buchanan, A., 2015. Performance and Design of LVL Walls Coupled with UFP Dissipaters. *Journal of Earthquake Engineering* 19 (3): 383-409.

Loo, W., Kun, C., Quenneville, P., Chouw, N., 2014. Experimental Testing of a Rocking Timber Shear Wall with Slip-friction Connectors. *Earthquake Engineering & Structural Dynamics* 43 (11): 1621-1639.

Loo, W., Quenneville, P., Chouw, N., 2014. A New Type of Symmetric Slip-Friction Connector. *Journal of Constructional Steel Research* 94: 11-22.

Priestley, N., Sritharan, S., Conley, J., Pampanin, S. 1999. Preliminary Results and Conclusions from the PRESSS Five-Story Precast Concrete Test Building. *PCI Journal* 44 (6): 42-67.

NZS1170. 5, 2004. Structural Design Actions, Part 5: Earthquake Actions. *New Zealand Standards.*

Palermo, A., Pampanin, S., Buchanan, A., Newcombe, M. 2005. Seismic Design of Multi-Storey Buildings using Laminated Veneer Lumber (LVL). *Planning and Engineering for Performance in Earthquakes conference*, Taupo, New Zealand.

PEER, 2006. NGA Database, Pacific Earthquake Engineering Research Centre. *University of California, Berkeley,* USA.

Sarti, F., Palermo, A., Pampanin, S., 2014. Design and testing of post-tensioned timber wall systems. *World conference on timber engineering*, Quebec, Canada.

Smith, T., Ludwig, F., Pampanin, S., Fragiacomo, M., Buchanan, A., Deam, B., Palermo, A., 2007. Seismic Response of Hybrid-LVL Coupled Walls under Quasi-Static and Pseudo-Dynamic Testing. *Performance by design NZSEE conference,* Palmerston North, New Zealand.

Zarnani, P., Quenneville, P., 2015. A Resilient Slip Friction Joint. *Provisional Patent no. 7083.*

16th World Conference on Earthquake, 16WCEE 2017
Santiago Chile, January 9th to 13th 2017
Paper N° 4595 (Abstract ID)
Registration Code: S-N1463119628

SEISMIC RESISTANT CROSS LAMINATED TIMBER (CLT) STRUCTURES WITH INNOVATIVE RESILIENT SLIP FRICTION (RSF) JOINTS

A. Hashemi[1], P. Zarnani[2], R. Masoudnia[3] , P. Quenneville[4]

[1] Department of Civil and Environmental Engineering, The University of Auckland, Auckland, New Zealand, ahas439@aucklanduni.ac.nz
[2] Department of Built Environment Engineering, Auckland University of Technology, Auckland, New Zealand, pouyan.zarnani@aut.ac.nz
[3] Department of Civil and Environmental Engineering, The University of Auckland, Auckland, New Zealand, rmas551@aucklanduni.ac.nz
[4] Department of Civil and Environmental Engineering, The University of Auckland, Auckland, New Zealand, p.quenneville@auckland.ac.nz

Abstract

Multi-story timber structures are becoming progressively desirable for engineers and building owners owing to their aesthetic and environmental benefits and to their higher strength to weight ratio compared to other construction materials. Moreover, there is an increasing public pressure to have low damage structural systems to minimize the earthquake destruction after moderate to severe seismic events. This is important as the building could be reoccupied quickly with minimal business interruption and repair costs. A recent trend in timber building industry is toward cross laminated timber (CLT) panelised structures. CLT is a relatively novel engineered wood based product well suited for multi-story structures. Due to the precise prefabrication and easy installation of CLT panels, there is an increasing trend towards construction of timber panelised structures using them. Latest research findings have shown that CLT buildings constructed with traditional methods can experience high damages especially at the connections which generally consist of hold-down brackets and shear connectors with nails, screws, rivets or bolts. Several research studies have proven that friction joints can provide a perfectly elastoplastic behaviour alongside a stable hysteretic response under severe seismic excitations. Up until now, the main disadvantage of the frictions joints has been the undesirable residual displacements after a seismic event. The main objective of this study is to develop a ductile low-damage structural system for multi-story residential and commercial timber buildings using the innovative Resilient Slip Friction (RSF) joint. The proposed system includes resilient coupled walls and end column as the main lateral load resisting members. RSF joints are used as hold-down connectors which connects the wall to the foundation and also as ductile links between the adjacent walls or between the walls and steel end columns. The ductility and resilience of such system is provided by the RSF joints.

A series of joint component test has been conducted to experimentally evaluate the hysteretic behaviour of the RSF joints. The test results demonstrated a stable flag-shaped hysteresis which readily exhibits the self-centring behaviour and also a significant rate of energy dissipation representing the damping capacity of the joint. The Damper – Friction Spring Link element function in SAP2000 was used and proved to be able to accurately represent the load-deformation behaviour of a RSF joint. Additionally, displacement-control cyclic analyses of CLT coupled walls with RSF joints showed that this innovative system definitely has the potential to be recognized as an efficient resilient structural systems for timber construction which could be extended to steel and reinforced concrete buildings as well.

Keywords: Resilience; Cross Laminated Timber; Low damage; Energy dissipation

1. Introduction

Multi-story timber structures are becoming progressively desirable for engineers and building owners because of their aesthetic and environmental benefits and further for the higher strength to weight ratio of the wood and

engineered wood products. More than that, there is an increasing public pressure to have low damage structural systems in order to minimize the earthquake destruction after moderate to severe seismic events. This is important as the building could be reoccupied quickly with minimal business interruption and repair costs.

Cross laminated timber (CLT) is a new generation of engineered wood product which was firstly developed in Europe in the 1990s and then in other parts of the world [1]. It is a strong, sustainable and dimensionally stable product that offers structural characteristics similar to that of a pre-cast concrete panel yet has relatively higher strength to weight ratio. More than that, CLT structures offer flexible planning and high level of prefabrication which significantly accelerate the construction progress and reduce the overall cost. Thus, CLT has been notably gaining popularity among building owners and designers and numerous CLT buildings have been built in different countries during the last decade.

During the PRESS (PREcast Seismic Structural Systems) program in the early 1990's, a new design approach for structural walls was introduced [2]. It was based on dry joints between the prefabricated panels to localize the inelastic deformation in addition to unbounded posttensioned members to provide re-centring behaviour. The dissipation capacity of such system highly depends on the type of the dissipaters, or sacrificial fuses, between the walls. For timber structures, Palermo et al. conducted preliminary experimental tests on laminated veneer lumber (LVL) walls with different types of fuses [3,4]. The results confirmed the enhanced performance of the system because of the jointed ductile connections. Smith et al. further extended the concept into coupled wall systems [5]. They proved that the design flexibility of the hybrid coupled wall systems combined with the speed of erection creates a significant potential for the construction of multi-story buildings. Iqbal et al. studied the application of U-shaped Flexural Plates (UFPs) as supplementary damping devices in post-tensioned LVL timber coupled rocking walls [6]. That concept had later been experimentally investigated and a design procedure was proposed [7]. The test results demonstrated an efficient energy dissipation mechanism over yielding the UFPs during the earthquakes. Sarti et al. experimentally investigated the seismic performance of the hybrid rocking walls with end columns [8]. Iqbal et al. tested coupled posttensioned rocking LVL walls with sacrificial nailed plywood sheets as hysteretic dampers [9]. The experimental results affirmed the performance of the system. Nevertheless, relatively lower hysteretic stability was observed compared to the similar systems with UFPs.

Passive friction based damping devices were originally proposed for steel structures. Popov et al. introduced symmetric slotted bolted connections which dissipates energy through friction during equilateral tension and compression cycles [10]. Popov's comprehensive experiments showed a stable rectangular shape hysteresis. Clifton et al. proposed the asymmetric sliding hinge joint for steel moment resisting frames which had non-rectangular yet stable force-deformation behaviour [11]. Khoo et al. developed design models for the asymmetric slotted bolted connections based upon numerous experiments and rigorous analyses [12].

For the first time in timber structures, Filiatrault used friction dampers in timber sheathed shear walls [13]. The results exhibited a significant improvement in hysteretic behaviour of the walls while large amount of seismic energy was absorbed. Loo et al. investigated the application of slip friction connections as a replacement of traditional hold-downs in LVL rocking walls [14,15]. The experiments showed excellent seismic performance in terms of hysteretic behaviour and minimized residual deflections. Additionally, and most importantly, the timber wall remained in the elastic region after several quasi-static tests and dynamic numerical analysis.

This paper presents research into CLT coupled rocking walls with innovative Resilient Slip Friction (RSF) joints [16] as the hold-down connections and ductile links between the adjacent walls or columns. A simple procedure to design the system is described and the results of RSF joint component tests are presented. Furthermore, a numerical model is developed to demonstrate the seismic performance of the proposed system. To investigate the seismic performance, the model is subjected to quasi-static displacement control cyclic loads.

1. Resilient Slip Friction (RSF) Joint

The concept of slip friction connections using flat steel plates sliding over each other has already been confirmed as an effective structural damping solution [11,17], [18]. The energy absorption mechanism of friction joints is one of the most efficient amongst passive devices. Nevertheless, the lack of re-centring behaviour in these joints

requires the use of an additional system to bring back the structure to its initial position after a seismic event, which is always costly. One of the common techniques for providing self-centring is the use of post-tensioned tendons which has two major drawbacks. Firstly, approximately 30% (or even more in some cases) of tendon force losses can occur during the service life of the structure which considerably decreases the efficiency of the system [19]. To reduce the total loss, restressing of the cables is required which is only possible with a special type of accessible anchorage. Secondly, the post-tension force is highly depended on the humidity of the environment. Although controlling the humidity reduces the losses, however, it is not possible to control it in all situations.

In this paper, a novel friction joint is presented in which the components are formed and arranged in a way that the self-centring behaviour is achieved as well as damping, all in one device. Fig.1 shows the components and the assembly for the Resilient Slip Friction (RSF) joint [16]. The specific shape of the grooves combined with the use of Belleville washers (conical disc springs) and high strength bolts provide the desirable self-centring behaviour. The angle of the grooves is designed in such a way that at the time of unloading, the reversing force induced by the elastically compacted Belleville washers is larger than the resisting friction force between the surfaces. As a consequence, the elastic force of the washers re-centres the slotted plate to its initial position. Note that Fig.1 exhibits a double acting RSF joint in which two centre slotted plate are used.

(a) (b) (c)

Fig. 1 – RSF joint: a) Cap plates and slotted centre plates b) Belleville washers and high strength bolts c) Assembly

A design procedure has been developed for the capacity prediction of the RSF joint based on the free body diagrams shown in Fig.2 [16,20]. The slip force (F_{slip}) for a symmetric configuration can be determined by Eq. (1). Note that this design procedure is for the symmetric configuration for slip friction connections. Refer to [21] for more information about the differences between symmetric and asymmetric concepts in friction joints. The slip force (F_{slip}) for a symmetric configuration can be determined by Eq. (1).

(a) (b)

Fig. 2 – Free body diagrams for a symmetric RSF joint: a) Before slippage b) Ultimate deflection state

$$F_{slip} = 2n_b F_{b,pr}\left(\frac{\sin\theta + \mu_s \cos\theta}{\cos\theta - \mu_s \sin\theta}\right) \quad (1)$$

Where $F_{b,pr}$ is the clamping force in the bolt due to pre-stressing of the Belleville washers, n_b is the number of bolts, θ is the angle of the grooves and μ_s is the static coefficient of friction. Fig.3 shows the schematic hysteretic loop for a RSF joint. The residual force in the joint at the end of the unloading can be determined by Eq. (2) where μ_k is the kinetic coefficient of friction which can be assumed as $0.85\mu_s$.

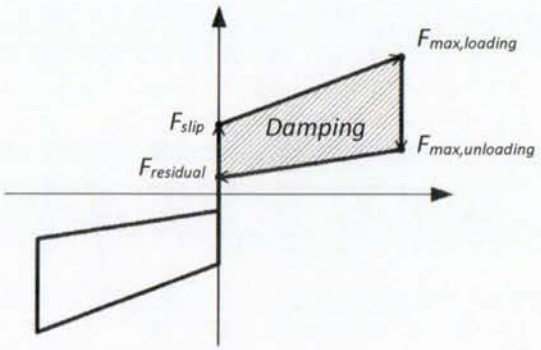

Fig. 3 – Schematic load-deformation loop for RSF joint

$$F_{residual} = 2n_b F_{b,pr}\left(\frac{sin\theta - \mu_k cos\theta}{\cos\theta + \mu_k sin\theta}\right) \quad (2)$$

The ultimate force upon loading ($F_{ult,loading}$) and unloading ($F_{ult,unloading}$) can be calculated by replacing μ_s and $F_{b,pr}$ in Eq. (1) and Eq. (2) with μ_k and $F_{b,u}$, respectively. The ultimate force in the bolt ($F_{b,u}$) can be specified by Eq. (3) in which k_s and Δ_s are respectively the total stiffness of the of washers and their maximum deflection when they are fully compressed (the washers become flat).

$$F_{b,u} = F_{b,pr} + k_s \Delta_s \quad (3)$$

The maximum deflection in a RSF joint is given by Eq. (4) where n_j is the number of joints acting in a series (e.g. n_j equals to 1 for a single acting joint and equals to 2 for a double acting one).

$$\delta_{\max} = n_j \frac{\Delta_s}{\tan\theta} \quad (4)$$

The joint offers a self-centring characteristic providing that Eq. (5) and Eq. (6) are satisfied. In Eq. (6), L represents the horizontal distance between the top and bottom of a groove.

$$\mu_s < \tan\theta \quad (5)$$

$$L > \frac{\Delta_s}{\sin\theta} \quad (6)$$

3. Resilient Slip Friction (RSF) Joint Component Test

In order to experimentally investigate the hysteretic behaviour of the RSF joint, a series of joint component tests were conducted. Fig.4 displays the components and the assembly of the manufactured specimen which was a symmetric double acting RSF joint comprised of two centre slotted plate and two cap plates. The cap plates were manufactured using mild steel grade 350 and the centre plates were fabricated with high strength Bisplate 80 steel. The angle of the grooves was 15 degrees in order to maximize the deformation capacity of the joint. Two 220 mm by 75 mm mild steel stiffener plates had later been welded to the cap plates to restrain them against out of plane bending.

(a) (b) (c) (d)

Fig. 4 – RSF joint specimen: a) Cap plates and centre plates b) Belleville washers c) Assembly d) Test setup

The Belleville washers (conical disk springs) have maximum capacity of 110 kN and maximum deflection of 1.5 mm at the flat state. Two high strength 8.8 grade bolts with nine spring washers per side (washers were a series arrangement) are used. Table 1 presents the calculated design parameters and the capacity of the RSF prototype based on the described design procedure in the previous section.

Table 1 – Characteristics of the tested RSF joint

Item	n_b	μ_s	Washer Thickness (mm)	Washer Height (mm)	Washer Capacity (kN)	Number of Washers Per bolt
Value	2	0.19	6.5	8.0	110	18

For the tests of this section, a maximum connector deformation of 30 mm was used. The displacement schedule (see Fig.5(a)) was based on that adopted by Loo et al. [17] and only allowed upward movement as would be the case if the device were implemented as a hold-down connection for a shear wall. It should be pointed out that the previous experimental tests on different configurations of RSF joints have shown that this device can perfectly exhibit similar behaviour in both negative and positive displacements if it is designed for such as purpose [20].

The machine that was used for the tests was the Instron Universal Test Machine capable of performing both low and high force testing up to 100 kN. The load cell is mounted on the crosshead above the RSF prototype while the displacement was measured using a Linear Variable Differential Transducer (LVDT) device

attached to the cap plates. To avoid a possible overpowering of the Instron machine, a maximum loading rate of 0.5 mm/s was adopted.

Altogether three tests were carried out on the RSF joint with 15, 24 and 31 kN of slip force (F_{slip}). In order to achieve these forces, the Belleville spring washers were compacted using the turn-of-nut method, in which the number of rotations of the nut required to achieve a targeted deflection was determined by dividing this deflection to the pitch of the threaded bolts. The resultant load-deformation curves for the three conducted tests are illustrated in Fig.5. Note that a specific lubricant is used between the cap plates and centre plates to increase the durability of the friction surfaces by controlling the possible galling and rusting. In this way, the static coefficient of 0.19 was found for the tested device.

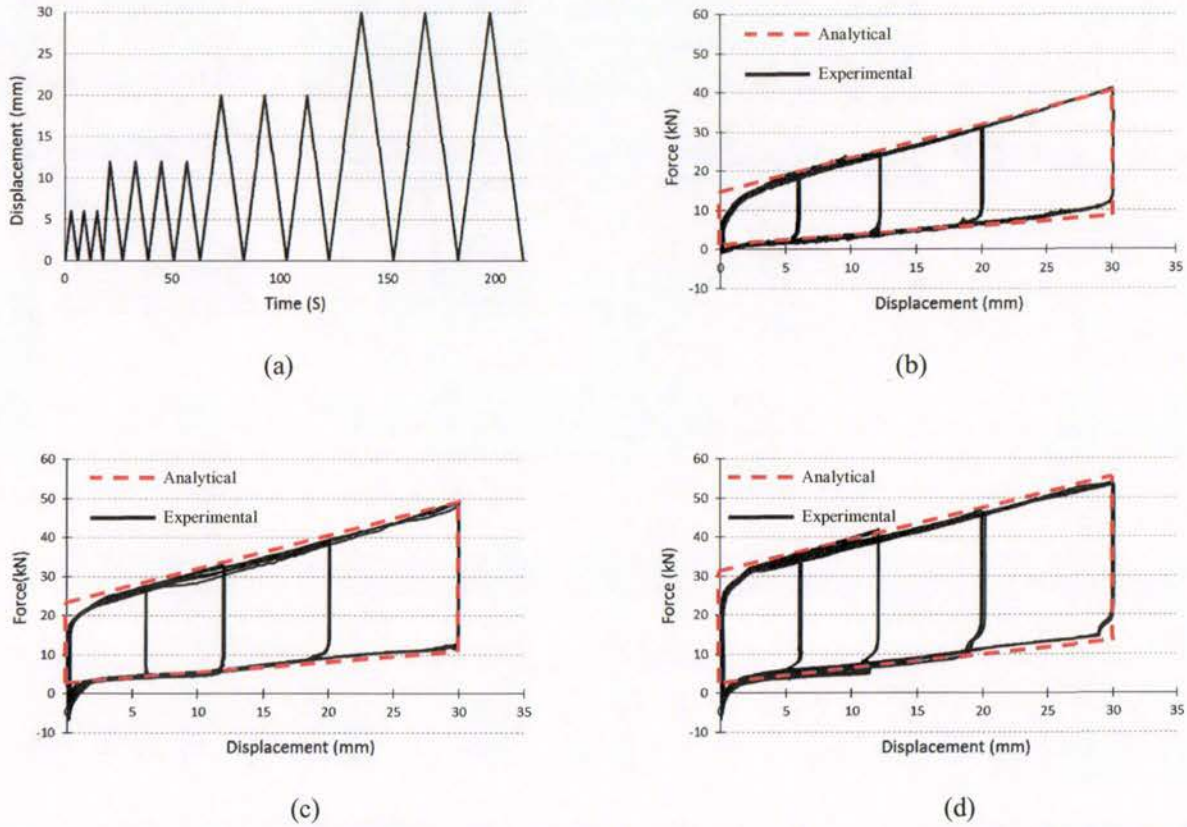

Fig. 5 – RSF joint experimental test: a) Displacement schedule b) hysteretic curves for F_{slip} = 15 kN c) hysteretic curves for F_{slip} = 24 kN d) hysteretic curves for F_{slip} = 31 kN

From Fig.5, it can be seen that the load-deformation behaviour of the RSF joint represents "flag-shaped" hysteretic curves which obviously imparts the self-centring behaviour as well as energy dissipation. Furthermore, the red dashed line in Fig.5(a), 5(b) and 5(c) shows the behaviour prediction of the joint determined by following the described analytical design procedure in the last section. It can be seen that the proposed equations can closely predict the behaviour of this innovative connection.

It should be noted that as the pre-stressing force in the bolts (consequently F_{slip}) increases, the maximum displacement capacity of the joint decreases. This is because of the pre-compression of the spring washers to provide the targeted slip force. Therefore, an optimized relationship between the slip force and the targeted

ultimate displacement should always be targeted in order the have an efficient connection. Another important observation from the test results is the stable behaviour of the connection. Symmetric flat slip-friction connections, in which the external mild steel plates slide directly against the hard steel slotted centre plates, have previously demonstrated performance in terms of maintaining strength, stiffness and hysteretic stability [17]. The mentioned characteristics which play a significant role when a low damage seismic solution is aimed for, are observed as well for the RSF joint in addition to the self-centring behaviour. From Fig.5, it can be noticed that the joint maintained its stiffness and strength through numerous cycles of loading and unloading.

Fig.6 shows the configuration of the tested RSF joint before and after slippage. The compaction of the Belleville washers allows the device to be expanded (see Fig.5(b)). Upon unloading, the preserved force in the springs brings back the centre plates to their original position.

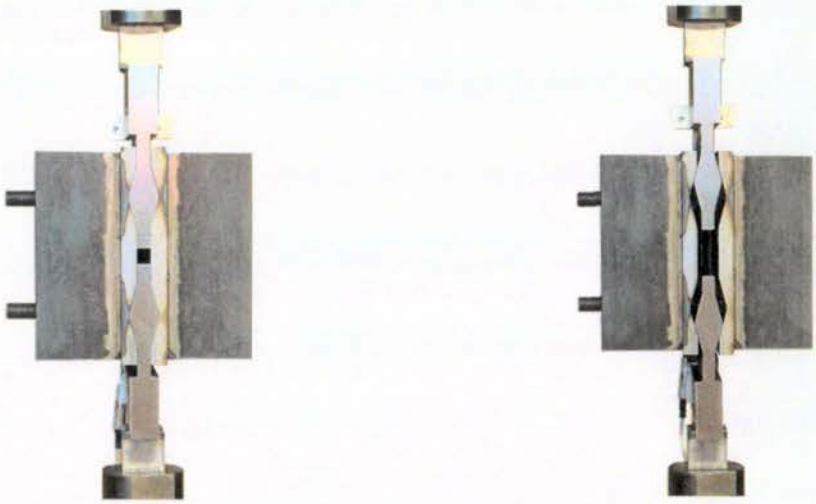

(a) (b)

Fig. 6 – RSF joint specimen: a) Before deformation b) After deformation (expansion of the plates)

4. Numerical Modelling of CLT buildings with RSF joints

4.1. The concept of CLT coupled walls with RSF connections

This section describes the numerical modelling of CLT coupled walls with RSF joints. The proposed system consists of coupled CLT walls joined together by two types of RSF joints that are hold-down connections and ductile links. The RSF hold-down device connects each wall to the foundation and the RSF ductile link connects the walls to any adjacent rocking CLT walls and/or the end columns. A schematic view of the proposed concept is displayed in Fig.7.

On the brink of rocking, the acting forces on each wall are RSF hold-down slip force (F_H), the sum of RSF ductile link slip forces ($\sum F_j$) and the vertical loads (W). It should be pointed out that this concept is mainly proposed for structural systems where the lateral load resisting system is separated from the gravity load resisting members. Therefore, the only considered vertical load in this paper is the self-weight of the CLT walls. Nevertheless, the introduced system is capable to mitigate all other types of gravity loads such as permanent and imposed loads.

Taking the moments about the rocking point of each wall, the total slip force for each wall ($F_H + \sum F_j$) can be determined by Eq. (7). If the walls have different geometry or material properties, the slip force for each one can be separately specified by following the same procedure with different h and b.

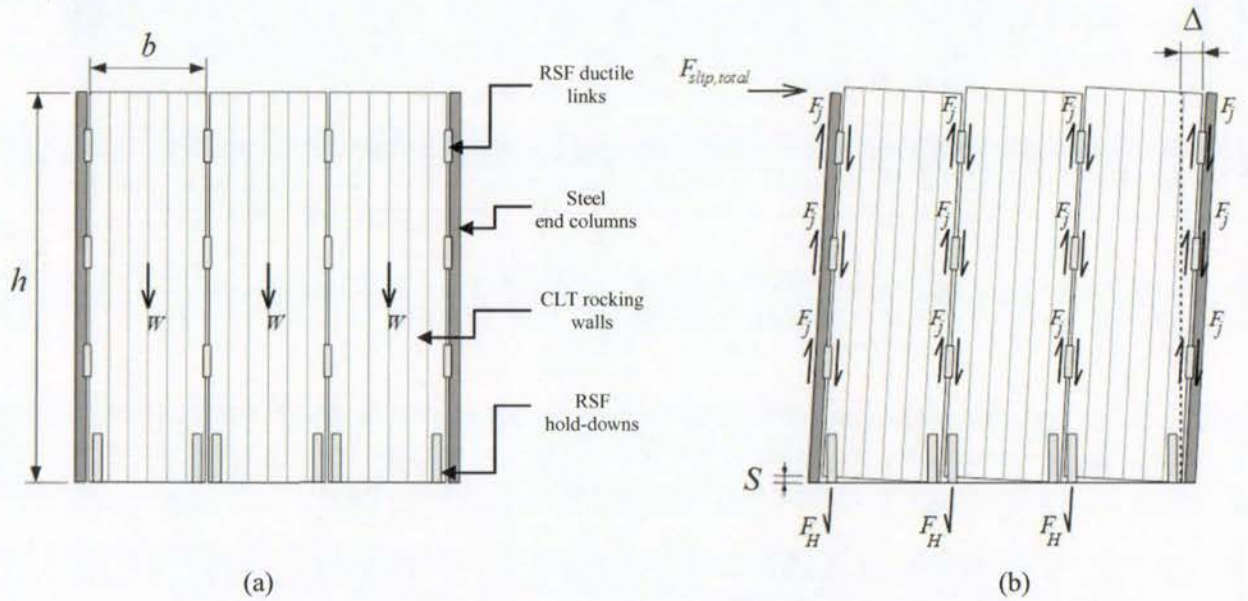

Fig. 7 – The concept of CLT coupled walls with RSF joints: a) Before rocking b) After rocking

$$F_H + \Sigma F_j = F_{slip,total} \frac{h}{b} - \frac{W}{2} \tag{7}$$

The RSF devices can be designed by Eq. (7) considering the fact that sum of the slip forces of the RSF ductile links has to be less than the RSF hold-down slip force. Otherwise, the sliding would first initiate in the hold-downs and the adjacent walls may be locked together. The slot length for RSF ductile links has to be twice that of the RSF hold-downs for the reason that they are designed to slide in both upward and downward directions while the hold-downs are intended to only move upward. Accordingly, the slot length for all hold-downs (S) and ductile links (2S) can be determined by Eq. (8) with respect to the required lateral displacement (Δ) (see Fig.7(b)). If the walls have different geometry, the slot lengths for the connections within each one of them should be calculated separately.

$$S = \Delta * \frac{b}{h} \tag{8}$$

4.2. Damper – Friction Spring Link Element

In order to model the RSF load-displacement behaviour, the Damper – Friction spring Link element in SAP2000 software package is adopted. This link element which is available in version 17 and above has many parameters. In order to model the RSF hysteretic behaviour, these parameters should be accurately calibrated in accordance with the design parameters of the RSF joint such as slip force, loading stiffness, maximum loading force, maximum unloading force and the residual force. To verify the accuracy of this link element in prediction of a RSF joint, a numerical model in SAP2000 is developed based on the experimental data of the tested RSF joint with a slip force of 15 kN (see Fig.(b)). The calibrated parameters for the friction spring link element are presented in Table 2. These parameters were determined according to the characteristics of the tested RSF specimen and the specifications of the associated Belleville springs.

Table 2 – Design parameters for the Damper – Friction Spring Link Element

Slipping stiffness (loading) (N/mm)	Slipping stiffness (unloading) (N/mm)	Pre-compression displacement (mm)	Stop displacement (mm)
828	156	-18.12	86.5

Fig. 8 compares the numerically obtained hysteretic loop with the experimental results. It can be seen that the Damper – Friction Spring Link element can accurately predict the load-displacement behaviour of a RSF joint. Because the RSF joint can represent a similar behaviour in tension and compression if it is designed for this purpose, the Spring Link element can accordingly be defined to respectively work in both directions.

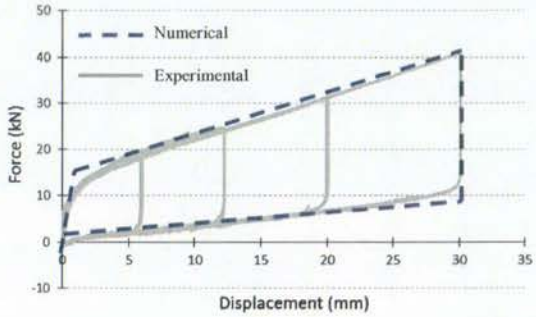

Fig. 8 – Comparison of the Friction Spring Link element and experimental data

4.3. Maximum Force in a Rocking CLT Walls with RSF joints

This study seeks to develop a low damage seismic solution comprised of rocking CLT walls with innovative RSF joints. In all low damage concepts in timber structures, the key point is that timber elements have to remain elastic including any connection between the timber and steel components and the ductile behaviour should be provided by the steel connections. These connections can be traditional mechanical fasteners such as nails, rivets and screws or can be more advanced connectors such as RSF joints. Accordingly, the first step in the design and modelling of CLT rocking walls with RSF joints is to determine the maximum tolerable lateral force at the top of a wall (F_E) which will allow the wall panel to remain elastic.

In order to evaluate the response of the CLT walls subjected to lateral loads, a 200 mm thick CLT wall (which will be used further in the numerical model) was modelled using the ABAQUS software package. The wall is 2 m wide and 8 m tall. All of the timber boards within the panel (longitudinal and transverse layers) were assumed to have a thickness of 45 mm, a width of 183 mm and an elastic modulus of 12000 MPa (MSG12 timber [22]) along the board's main axis (parallel to grain). The density of the timber was assumed as 540 kg/m^3. The timber boards were tied together at top and bottom to represent the glued surfaces. The only assumed value for the applied vertical loads was the self-weight of the panel. From the numerical analyses, it was found that the maximum horizontal force at the top of each wall that would result in the CLT boards reaching their characteristic strengths (f_t = 14 MPa and f_c = 25 MPa) is F_E = 87.6 kN (equals to overturning moment of 700.8 kNm). Fig.9 shows the general arrangement of the developed numerical model including the mesh and stress distribution. This numerical approach for modelling of CLT panels has previously been used by the authors and demonstrated promising results [18],[20],[23],[24],[25].

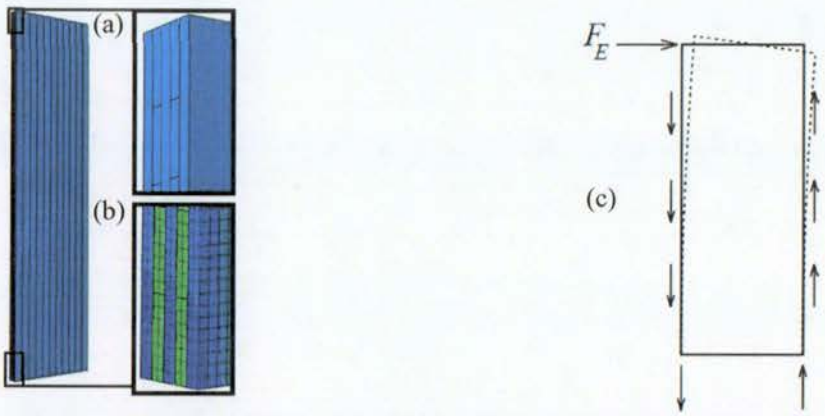

Fig. 9 – Numerical model of the CLT wall: a) Assembly b) Stress distribution c) Elastic deflection of the wall

4.4. Displacement-Control Quasi-Static Analyses of CLT Coupled Rocking Walls with RSF joints

The general arrangement of the proposed coupled wall system to be studied under displacement-control cyclic loading in SAP2000 is displayed in Fig.10. The system consists of three identical CLT walls with 8 m height and 2 m length. The walls have a thickness of 200 mm with the material properties similar to the wall model that was described in section 4.3. The investigated system includes two 400*400*10 mm steel box columns at the ends which are assumed to be pinned to the base. All three walls are attached to the foundation by RSF hold-downs. Furthermore, the walls are connected to the adjoining panels and/or the adjacent steel columns by RSF ductile links. The RSF joints are designed in accordance with the proposed design procedure in section 2 and also Eq. (7) and Eq. (8). Considering a self-weight of 17 kN for each one of the walls and based on the numerically obtained F_E = 87.6 kN from section 4.3, the maximum forces for the RSF joints attached to each wall are determined as 220 kN for the RSF hold-downs and 40 kN for the three assumed RSF ductile links along the edge of the walls (Eq. (7)). In this model, F_{slip} is considered as 40% of the maximum load in the joint ($F_{max,loading}$). However, for multi-story buildings, F_{slip} should be specified based on the Ultimate Limit State (ULS) earthquake loads and the total stiffness of the Belleville washers that are exploited. Also, the CLT panel is modelled using layers shell element.

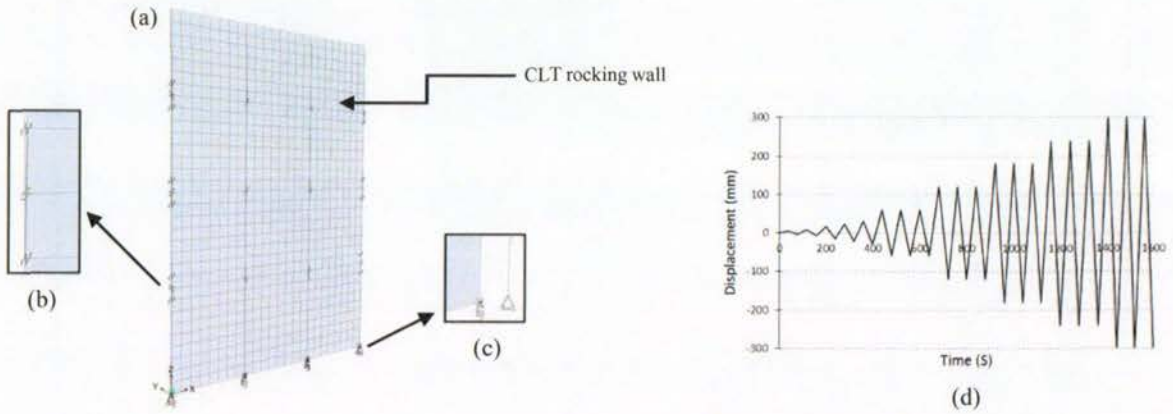

Fig. 10 – Numerical model of the CLT coupled walls with RSF joints: a) General arrangement b) RSF ductile link c) RSF hold-down d) Displacement-control load schedule

The RSF joints are modelled using the Damper – Friction Spring Link Element. The calculated design parameters are presented in Table 3. The displacement-control load schedule in Fig.10(d) is applied at the top of

the system to evaluate the total load-deformation behaviour. The maximum displacement in the load schedule is 300 mm representing 3.75 % of lateral drift.

Table 3 – Design parameters for the Damper – Friction Spring Link Elements representing the RSF joints

Value	Slipping stiffness (loading) (N/mm)	Slipping stiffness (unloading) (N/mm)	Pre-compression displacement (mm)	Stop displacement (mm)
RSF hold-down	1467	242	-75	75
RSF ductile link	267	44	-75	75

Fig.11 shows the numerical response of the system under the applied cyclic load regime. It is observable that the RSF hold-downs and the RSF ductile links have a flag-shaped hysteretic behaviour. Fig.11(c) illustrates the total lateral response of the coupled wall system. It can be seen that the system exhibits self-centring behaviour which can be attributed to the hysteretic behaviour of the exploited RSF joints. It should be emphasized that the only considered vertical load in this model is the self-weight of the wall. This means that the self-centring behaviour of the proposed structural system does not rely on the gravity loads neither on the use of post-tensioned cables. Moreover, Fig.11 evidently demonstrates the low damage characteristic of the proposed system as the hysteretic behaviour remained stable after numerous cycles of loading and unloading. Hence, the bounded area between the hysteretic loops increases over time. This clearly represents a significant rate of energy dissipation which furthers confirms the potential to have a resilient low damage seismic solution. Further experimental and analytical studies are being conducted by the authors to extend this innovative technology to different structural systems.

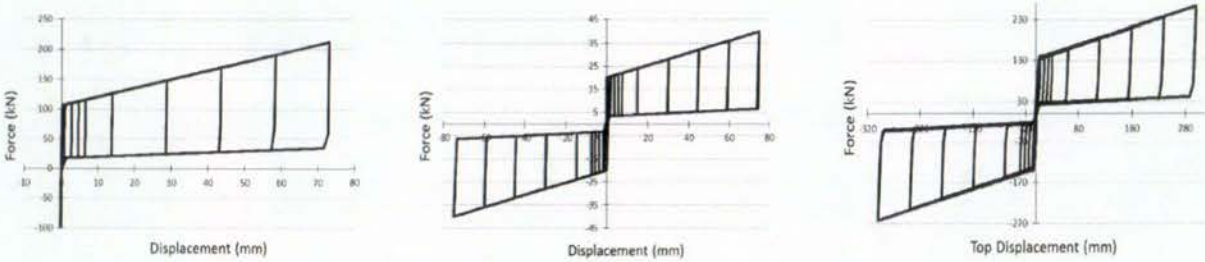

(a) (b) (c)

Fig. 11 – Numerical results of the CLT coupled walls with RSF joints: a) RSF hold-down hysteresis b) RSF ductile link hysteresis c) Total load-deformation behaviour of the system

5. Conclusions

From this study, it is evident that there is potential to significantly improve the seismic performance of timber structures by using the innovative Resilient Slip Friction (RSF) joints. Experimental joint component tests carried out on a RSF joint with three different levels of slip force exhibited stable flag-shaped hysteretic loops demonstrating the re-centring capacity as well as energy dissipation.

The Damper – Friction Spring link element in SAP2000 is introduced to represent the RSF joints in numerical modelling and the consequent numerically obtained hysteresis is validated by the component test results. A new structural system comprised of rocking CLT walls with RSF hold-downs at the foundation level and RSF ductile links along the edge of the panels is introduced. This system also includes steel end columns to de-couple the vertical movements of the perpendicular walls due to bi-directional rocking motion. The preliminary numerical results evidently confirms the potential to have a new resilient structural system for timber construction. The resilience of the system is attributed to the hysteretic behaviour of the RSF joints. Therefore, the proposed structural system can effectively be extended to steel and reinforced concrete structures.

6. Acknowledgment

The authors would like to thank the Earthquake Commission Research Foundation (EQC) for the financial support of the presented research.

7. References

[1] S. Gagnon, C. Pirvu, CLT handbook, cross laminated timber, FPInnovations, 2011.
[2] N. Priestley, S. Sritharan, J.R. Conley, S. Pampanin, Preliminary results and conclusions from the PRESSS five-story precast concrete test building, PCI J. 44 (1999) 42–67.
[3] A. Palermo, S. Pampanin, A. Buchanan, M. Newcombe, Seismic design of multi-storey buildings using laminated veneer lumber (LVL), New Zeland Society of Earthquake Engineering Conference (NZSEE), Taupo, New Zealand, 2005.
[4] A. Palermo, S. Pampanin, A.H. Buchanan, Experimental investigations on LVL seismic resistant wall and frame subassemblies, First European Conference on Earthquake Engineering and Seismology, Geneva, Switzerland, 2006.
[5] T. Smith, F. Ludwig, S. Pampanin, M. Fragiacomo, A. Buchanan, B. Deam, et al., Seismic response of hybrid-LVL coupled walls under quasi-static and pseudo-dynamic testing, New Zealand Society of Earthquake Engineering Conference (NZSEE), Palmerston North, New Zealand, 2007.
[6] A. Iqbal, S. Pampanin, A. Buchanan, A. Palermo, Improved seismic performance of LVL post-tensioned walls coupled with UFP devices, in: 8th Pacific Conference Earthquake Engineering, Singapore, 2007.
[7] A. Iqbal, S. Pampanin, A. Palermo, A.H. Buchanan, Performance and Design of LVL Walls Coupled with UFP Dissipaters, Journal of Earthquake Engineering, 19 (2015) 383–409.
[8] F. Sarti, A. Palermo, S. Pampanin, Development and Testing of an Alternative Dissipative Posttensioned Rocking Timber Wall with Boundary Columns, J. Struct. Eng. (2015) E4015011.
[9] A. Iqbal, T. Smith, S. Pampanin, M. Fragiacomo, A. Palermo, A.H. Buchanan, Experimental Performance and Structural Analysis of Plywood-Coupled LVL Walls, J. Struct. Eng. 142 (2015) 4015123.
[10] E.P. Popov, C.E. Grigorian, T.-S. Yang, Developments in seismic structural analysis and design, Eng. Struct. 17 (1995) 187–197.
[11] G.C. Clifton, G.A. MacRae, H. Mackinven, S. Pampanin, J. Butterworth, Sliding hinge joints and subassemblies for steel moment frames, in: Palmerst. North, New Zeal. Proc New Zeal. Soc. Earthq Eng Conf, 2007.
[12] H. Khoo, C. Clifton, G. MacRae, H. Zhou, S. Ramhormozian, Proposed design models for the asymmetric friction connection, Earthq. Eng. Struct. Dyn. 44 (2015) 1309–1324.
[13] A. Filiatrault, Analytical predictions of the seismic response of friction damped timber shear walls, Earthq. Eng. Struct. Dyn. 19 (1990) 259–273.
[14] W.Y. Loo, P. Quenneville, N. Chouw, A numerical study of the seismic behaviour of timber shear walls with slip-friction connectors, Eng. Struct. 34 (2012) 233–243.
[15] W.Y. Loo, C. Kun, P. Quenneville, N. Chouw, Experimental testing of a rocking timber shear wall with slip-friction connectors, Earthq. Eng. Struct. Dyn. 43 (2014) 1621–1639.
[16] Zarnani, P., Quenneville, P., A Resilient Slip Friction Joint, Provisional Patent no. 7083.
[17] W.Y. Loo, P. Quenneville, N. Chouw, A new type of symmetric slip-friction connector, J. Constr. Steel Res. 94 (2014) 11–22.
[18] Ashkan Hashemi, Reza Masoudnia, Pierre Quenneville, A Numerical Study of Coupled Timber Walls with Slip Friction Damping Devices, Construction and Building Materials, 2016 (In Press).
[19] F. Wanninger, A. Frangi, M. Fragiacomo, Long-term behavior of posttensioned timber connections, J. Struct. Eng. 141 (2014) 4014155.
[20] A. Hashemi, P. Zarnani, A. Valadbeigi, R. Masoudnia, P. Quenneville, Seismic resistant cross laminated timber structures using an innovative resilient friction damping system, New Zealand Society of Earthquake Engineering Conference (NZSEE), Christchurch, New Zealand, 2016.
[21] Pouyan Zarnani, Armin Valadbeigi, Pierre Quenneville, RESILIENT SLIP FRICTION (RSF) JOINT: A NOVEL CONNECTION SYSTEM FOR SEISMIC DAMAGE AVOIDANCE DESIGN OF TIMBER STRUCTURES, World Conference of Timber Engineering (WCTE), Vienna, Austria, 2016.
[22] A.H. Buchanan, N.Z.T.I. Federation, Timber design guide, New Zealand Timber Industry Federation, 1999.
[23] Ashkan Hashemi, Wei Y. Loo, Reza Masoudnia, Pouyan Zarnani, Pierre Quenneville, DUCTILE CROSS LAMINATED TIMBER (CLT) PLATFORM STRUCTURES WITH PASSIVE DAMPING, World Conference of Timber Engineering (WCTE), Vienna, Austria, 2016.
[24] Reza Masoudnia, Pouyan Zarnani, Ashkan Hashemi, Pierre Quenneville, INTRODUCING NEW BOARD LAMINATION TO CROSS LAMINATED TIMBER, World Conference of Timber Engineering (WCTE), Vienna, Austria, 2016.
[25] Reza Masoudnia, Pouyan Zarnani, Ashkan Hashemi, Pierre Quenneville, EVALUATION OF EFFECTIVE FLANGE WIDTH IN THE CLT COMPOSITE T-BEAMS, World Conference of Timber Engineering (WCTE), Vienna, Austria, 2016.

WCTE 2016
World Conference on Timber Engineering
August 22-25, 2016 | Vienna, Austria

DUCTILE CROSS LAMINATED TIMBER (CLT) PLATFORM STRUCTURES WITH PASSIVE DAMPING

Ashkan Hashemi[1], Wei Y. Loo[2], Reza Masoudnia[3], Pouyan Zarnani[4], Pierre Quenneville[5]

ABSTRACT: Multi-storey platform cross laminated timber (CLT) structures are becoming progressively desirable for engineers and owners. This is because they offer many significant advantages such as speed of fabrication, ease of construction, and excellent strength to weight ratio. With platform construction, stories are fixed together in a way that each floor bears into load bearing walls, therewith creating a platform for the next level. The latest research findings have shown that CLT platform buildings constructed with traditional fasteners can experience a high level of damage especially in those cases where the walls have adopted hold-down brackets and shear connectors with nails, rivets or screws. Thus, the current construction method for platform CLT structures is less than ideal in terms of damage avoidance. The main objective of this study is to develop a low damage platform timber panelised structural system using a new configuration of slip friction devices in lieu of traditional connectors. A numerical model of such a system is developed for a low rise CLT building and then is subjected to reversed cyclic load simulations in order to investigate its seismic performance. The result of these quasi-static simulations demonstrated that the system maintained the strength through numerous cycles of loading and unloading. In addition to this, the system is capable of absorbing significant amount of energy. The findings of this study demonstrate the proposed concept has the potential to be developed as a low damage seismic solution for CLT platform buildings.

KEYWORDS: Cross Laminated Timer, Low damage, Slip friction, Rocking walls, Platform construction.

1 INTRODUCTION

In recent years, Cross Laminated Timber (CLT) has been widely used for different types of buildings such as offices, commercial buildings, public buildings and multi-story residential complexes. In most cases, the platform method of construction is adopted. This method is perfectly suited for low rise to medium rise structures. The term "platform method" derives from the method of construction where the stories are like stacked shoe boxes joined together in a manner that each floor bears into load bearing walls, thereby creating a platform for the next level. The platform method is especially suited to structures which have a cellular plan. Internal wall panels can then be used to contribute to the cellular form and are used as load bearing components in addition to resisting the lateral loads. Typically, vertical loads from the walls and floors are supported by CLT wall panels which are connected to each other and to the floor panels by mechanical fasteners such as nailplates, rivets or screws. Since these panels are also the main lateral load resisting members, extensive research on the seismic behaviour of these structures are being conducted by many research groups around the world.

The most comprehensive experimental research about the seismic performance of CLT platform structures has been conducted within the SOFIE project [1] . That project included quasi-static tests on a single story building with different layouts, shake table tests on a three story CLT building and a series of full scale shake table tests on a seven story CLT building. The results showed that the CLT platform buildings with traditional connections are relatively stiff and can survive destructive seismic events with minimum damage. However, a number of connections (such as nailed hold-downs and nailed shear brackets) failed in bending and some withdrew from the timber elements. Additionally, high response accelerations particularly in the upper levels with a maximum acceleration of 3.8 g were recorded. Accelerations this high obviously have the potential to cause serious injury among the occupants, and it is desirable that a method to reduce them is considered.

Popovski et al. investigated the seismic response of the CLT wall panels of various arrangements and connection layouts [2,3]. It was concluded that these walls have adequate lateral resistance when nails or slender screws are used together with steel brackets. Moreover, the use of hold-downs with nails at the corners of the walls were

[1] Ashkan Hashemi, The University of Auckland, ahas439@aucklanduni.ac.nz
[2] Wei Y. Loo, Unitec Institute of Technology, wloo@unitec.ac.nz
[3] Reza Masoudnia, The University of Auckland, rmas551@aucklanduni.ac.nz
[4] Pouyan Zarnani, Auckland University of Technology, pouyan.zarnani@aut.ac.nz
[5] Pierre Quenneville, The University of Auckland, p.quenneville@auckland.ac.nz

proven to further improve the resistance to overturning from the lateral forces.

Garvic et al. experimentally investigated the cyclic behaviour of single and coupled CLT walls with different connections [4]. The test results confirmed that the layout and design of the connections govern the overall behaviour of the wall. While in-plane deformations of the panels were almost negligible, the observed plastification in the connection parts lead to local failure in the system.

Popovski et al. conducted a series of full scale quasi-static tests on a two story CLT house [5]. No global instability was observed even when the maximum force was reached. Regardless of the rigid connection between the floors and walls, rocking movement of the wall panels was not totally restricted by the floor above.

Yasumura et al. studied the mechanical performance of low-rise CLT structures with large and small panels subjected to reversed cyclic lateral loads [6]. They concluded that in the buildings with small panels, rotation of the panels was the major cause of the total deformation of the building. They also proposed a numerical model to predict the seismic behaviour of such structures.

Regardless of the adequate seismic resistance of the abovementioned CLT platform buildings, in almost all cases, the connections suffered from large inelastic deformation by the end of the earthquake or by the end of the cyclic test [7],[8]. This means that many of these connectors should be repaired or replaced after a major seismic event. This study introduces a new low damage seismic solution for CLT platform structures where traditional connectors are replaced with slip friction devices. This system is capable of dissipating large amount of seismic energy while avoiding inelastic damage to its elements through numerous cycles of loading and unloading. The performance of this system is investigated by quasi-static simulations with reversed cyclic load regimes.

2 ROCKING TIMBER WALLS WITH SLIP FRICTION CONNECTIONS

Passive sliding friction dampers were originally utilized for steel structures. Popov et al. introduced the symmetric slotted bolted connection which dissipates energy through friction while producing equilateral load-deformation loops in tension and compression [9].

Clifton et al. proposed the Asymmetric Sliding Hinge joint for steel moment resisting frames which had non-rectangular yet stable hysteretic behaviour [10]. For the first time in timber structures, Filiatrault utilized the sliding friction devices for timber sheathed shear walls [11]. His studies demonstrated a noticeable improvement in the hysteretic behaviour of the walls compared to traditional timber shear walls. Large amounts of dissipated energy was also observed at various lateral drifts up to a maximum of 1.5%.

Loo et al. investigated the application of slip friction connections as a replacement of traditional hold-downs for timber Laminated Veneer Lumber (LVL) walls [12,13]. Their experiments showed significantly improved seismic performance compared to traditional systems in terms of stability of hysteretic behaviour and residual deflections [16]. Additionally, and most importantly, the timber wall remained in the elastic region after several quasi static and dynamic numerical analyses.

Figure 1 shows a rocking CLT wall with slip friction hold-downs. F_H represents the applied lateral load at the top of the wall and W represents the applied vertical load to the wall including the self-weight of the wall and the gravity loads. Taking the moments about the rocking point of the wall, the slip force of the hold-down (F_{slip}) can be calculated by Equation 1.

$$F_{slip} = F_H \frac{h}{b} - \frac{W}{2} \quad (1)$$

When the applied horizontal load at the top reaches the threshold that the force in the hold-down exceeds F_H, the sliding is commenced in the device and the wall starts to rock. It should be pointed out that the in-plane elastic deflection of a CLT panel is negligible compared to the displacement due to rocking movement. Therefore, the elastic deflection of the wall panels are neglected in this study. In other words, the walls are assumed as rigid bodies during the rocking movement.

Note that since this study seeks to develop a low damage concept, all timber members (CLT panels) and their associated connections must remain in the elastic region. Therefore, the slip threshold for the friction devices (F_{slip}) should be specified in a way that the wall start to rock before any compression or tension failure occurs in the timber boards within the CLT panel.

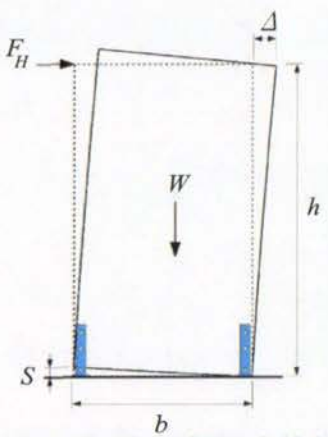

Figure 1: *Rocking wall with slip friction hold-downs*

As shown in Figure 2, slip friction hold-downs are comprised of several components. The centre plate (the wall embedded plate) is rigidly connected to the timber wall with mechanical fasteners. The outer plates clamp the centre slotted plate in a manner that the centre plate is sandwiched by them. When the imposed vertical force to the device overcomes the frictional resistance between the two surfaces, the centre plate starts to slide and energy will be dissipated through cycles of sliding. The slip threshold for a slip friction hold-down can be determined by Equation 2 where μ is the coefficient of friction between the two surfaces, n_b is the number of bolts and T_b is the tension force in each bolt [12].

$$F_{slip} = 2\mu n_b T_b \quad (2)$$

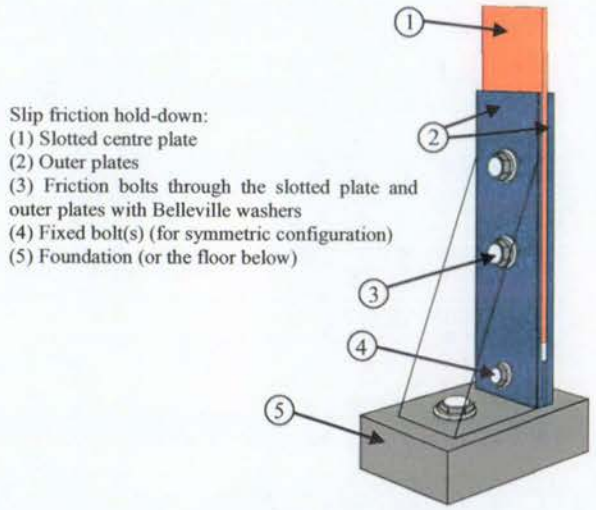

***Figure 2**: Slip friction hold-down connector*

3 PROPOSED SYSTEM FOR CLT PLATFORM CONSTRUCTION

Figure 3 schematically shows the introduced configuration for CLT platform structures. The wall panels are designed to resist both gravity and lateral loads. The proposed concept includes rocking CLT panels with relatively high height to weight ratio to ensure that the dominating deformation mechanism is the rotation of the walls.

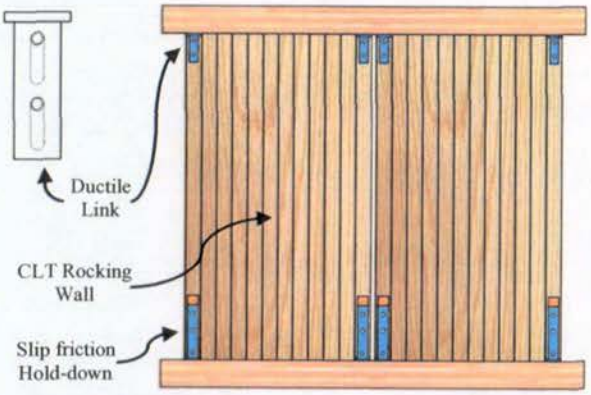

***Figure 3**: CLT panels with slip friction connections*

This configuration allows the individual walls to rock and provides a ductile response. Additionally, pre-defined gaps between the adjacent panels are considered to further increase the ductility of the system as the walls are free to rotate to a certain level before pounding on each other.
Each panel within the system is connected to the floor below (or the foundation in the base level) by slip friction hold-downs. These hold-downs are designed to slide when the induced lateral load at the top (upper floor diaphragm) reached a certain amount. Therefore, the walls are allowed to rock and energy will be dissipated at the joints.
Moreover, a slotted bolted connection is considered at the top of the walls that connects the wall to the upper floor. This connection, which is referred to as a "ductile link", is designed to accommodate the relative vertical displacement between the wall and the floor above while effectively transferring the lateral forces from the upper diaphragm to the wall. Figure 3 shows one possible solution for the ductile link.
During the full scale cyclic test of a two story CLT house with traditional metal connections, Popovski et al. reported that the sliding movement between the walls and floors has the highest contribution to the overall deformation of the structure [5]. This study focuses on the rocking movement of the walls (rather than sliding) and considers it as the dominating deformation mechanism. With this as the objective, a special low damage shear connector should be used between the walls and floors to efficiently transfer the shear forces while it is capable of accommodating the possible uplift caused by the rocking movement. Loo et al. proposed a solution for the shear key and verified its efficiency by experimental tests [13]. Nevertheless, the authors are currently working on different concepts for shear connectors which will be incorporated into the proposed structural system.
Figure 4 displays the deformed shape of the system. Out of plane bending of the floor diaphragm and the embedment of wall panels into the above and below floors allows the wall panels to rock about their corners. This is in agreement with the experimental findings of Popovski et al. [5] and Yasumura et al. [6].

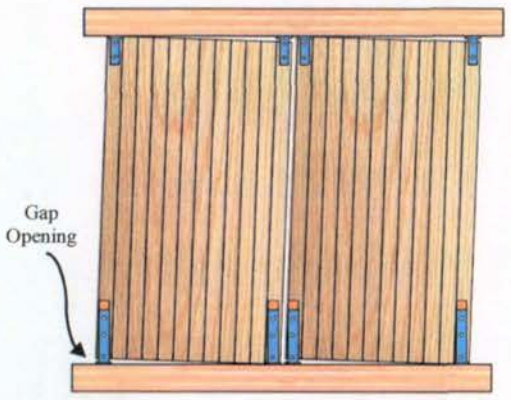

***Figure 4**: Deformed shape of the proposed concept for CLT platform structure with slip friction connections*

In the proposed concept, steel columns are considered at the corners and intersections to de-couple the relative movement of the perpendicular panels due to rocking. This is necessary to avoid the walls bearing on each other in bi-directional rocking (see Figure 5). The column are pin jointed at each floor level.

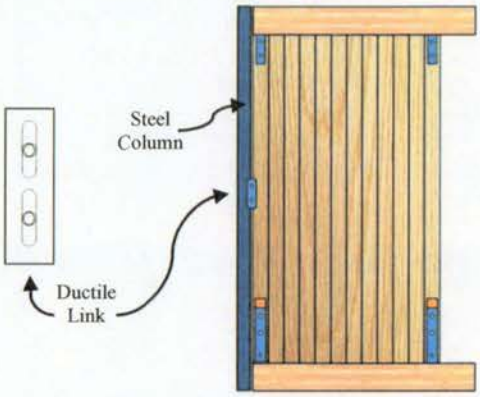

***Figure 5**: Steel columns at the corners to de-couple the relative movement of the perpendicular rocking walls*

The configuration of the connection between the CLT panel and the steel column are similar to the ductile link shown in Figure 3. However, in this case the slotted bolted connection is designed to be able to accommodate the upward and downward displacements caused by the relative rocking movement of the panels in both directions.

4 NUMERICAL MODELING OF A LOW RISE CLT BUILDING WITH SLIP FRICTION CONNECTIONS

4.1 DESCRIPTION OF THE MODEL

The work presented in this section targeted the overall performance of the CLT platform structures with slip friction connections under lateral loads. A numerical model of a two story CLT building similar to the one that has been tested by Popovski et al. [5] is developed in SAP2000 [14]. The model is subjected to quasi-static cyclic horizontal loads in both directions.

The prototype was 6.0 m long and 4.8 m tall with heights of 2.3 m for both stories. A five layer CLT section with 100 mm thickness (20 mm for each layer) is considered for both floors and walls. It should be pointed out that for real CLT structures, the thickness of the floor panels are normally greater than that of the walls to meet the serviceability criteria.

Along the East side of the first story, three rocking walls with 1.6, 1.5 and 0.9 meters width were considered while along the West side, three 1.3 m wide rocking walls were modelled. For the North and South sides of first story, four rocking walls with 2, 1.5, 1 and 1.5 m width were used (from West to East direction in Figure 6).

For the second story, three 2 m wide walls were considered on the North and South sides while three 1.6 m wide walls were modelled for the East and the West sides. In addition to the exterior walls, there were also two 1.6 m width partition walls in the North-South direction in both stories.

Four 0.8 m by 0.8 m window openings were modelled on both the North and South sides at both levels while two window openings with same dimensions were considered on the East and West sides of the second story. Furthermore, the first level had a 2.2 m wide door opening on the West side. Figure 6 shows the plan view of the modelled CLT building.

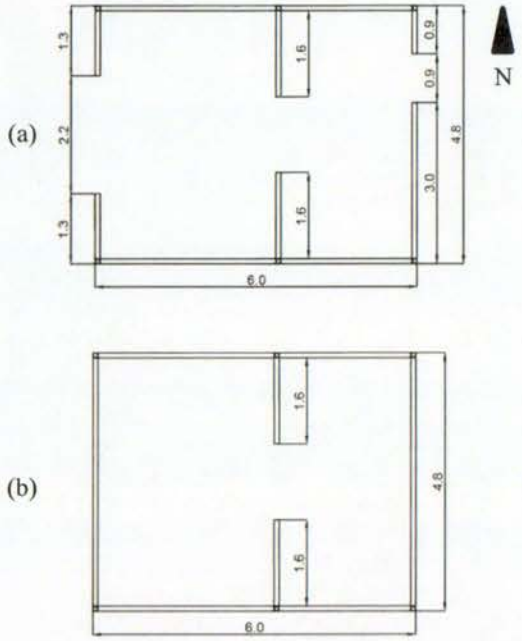

***Figure 6**: Plan view of the modelled CLT structure* [5]*: a) First story b) Second story*

4.2 SLIP THRESHOLD FOR THE SLIP FRICTION HOLD-DOWNS

In this paper, all of the mentioned rocking walls are assumed to be connected to the foundation or the floor below by slip friction hold-downs. Generally, in all low damage timber structural systems, the key point is that timber elements must remain in the "elastic" region and ductile behaviour of the of the system will be provided by the steel connections. These connections can be traditional connections with mechanical fasteners such as nails, rivets and screws or can be more advanced connectors such as slip friction devices (which are highly elasto-plastic). Accordingly, the first step in the design and modelling of CLT rocking walls with slip friction connections is to determine the maximum tolerable lateral force at the top (F_H) which will allow the wall panel to remain in the elastic region both before and after the friction device is activated and the wall starts to rock (see Figure 1).

While there are numerous analytical methods or numerical models for analysing LVL walls (and consequently specifying the lateral load carrying capacity F_H), there is lack of research studies about CLT walls under lateral forces with the focus on the timber boards. This can be mainly attributed to the highly non-uniform composition of CLT.

In this study, a series of finite element analyses were carried out using ABAQUS software package [15] to determine the maximum tolerable F_H for the seven different wall configurations in the CLT house prototype

(0.9 m to 2 m width and 2.3 m height). A five layer CLT panel with three 20 mm thick longitudinal layers and two 20 mm thick transverse layers with 183 mm width for all boards within the panel is assumed for all models. This arrangement of layers represents a conventional configuration for CLT in the New Zealand market. Table 1 shows the assigned mechanical properties to all timber borards within the models.

Table 1: *Material properties of a CLT board (MSG8*)*

E_L** (MPa)	E_R (MPa)	E_T (MPa)	f_c (MPa)	f_t (MPa)
8000	363	363	18	6

* Grade 8 machine stress graded sawn timber [16,17]
** Principal axes of a timber board [16]

A 3.5 kN/m^2 uniform load is assigned to both stories to represent the permanent loads, imposed loads and the self-weight of the CLT members. Owing to the reason that all walls within the CLT building have the same height and thickness, it is assumed that the applied vertical loads in each story is shared between the walls in accordance with their tributary area. Table 2 tabulates the calculated vertical loads for seven different widths for the walls.

Table 2: *Calculated vertical loads for rocking CLT walls*

Story	Wall	Height (m)	Width (m)	W (kN)
Second Story	W0.9	2.3	0.9	5.14
	W1.0	2.3	1.0	5.82
	W1.3	2.3	1.3	7.56
	W1.4	2.3	1.4	8.15
	W1.5	2.3	1.5	8.73
	W1.6	2.3	1.6	9.31
	W2.0	2.3	2.0	11.64
First Story	W0.9	2.3	0.9	11.37
	W1.0	2.3	1.0	11.63
	W1.3	2.3	1.3	15.12
	W1.4	2.3	1.4	16.29
	W1.5	2.3	1.5	17.45
	W1.6	2.3	1.6	18.61
	W2.0	2.3	2.0	23.27

To include the effect of axial loads on the elastic lateral strength of CLT panels, each wall model was analysed with zero axial load in addition to the two calculated axial load limits indicated in Table 1. In each model, the applied lateral force at the top is increased until the normal stress in one of the timber boards exceeds its permissible characteristic stress (f_c and f_t in Table 1).

To optimize the efficiency of CLT wall applications, wall panels have been placed with their outer layers parallel to the gravity loads [18]. Figure 7 illustrates the general arrangement of the developed numerical model for CLT walls. This numerical approach has previously been used by the authors and demonstrated promising results [19],[20]. Note that in Figure 7, the wall is flipped horizontally for better clarity.

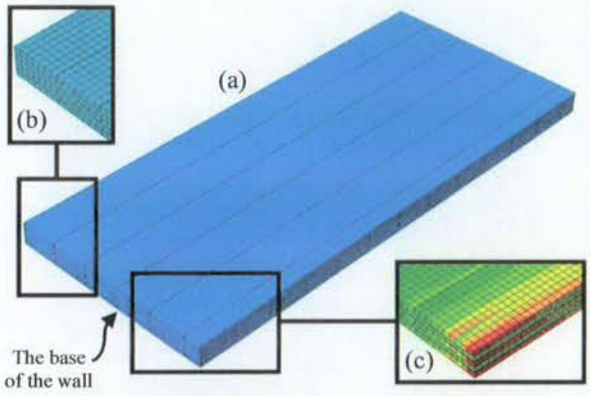

Figure 7: *Numerical model of a CLT wall panel: a) Assembly b) Mesh c) Stress distribution*

The details of the analysed models and the numerically obtained values for maximum tolerable F_H for each model are presented in Table 3.

Table 3: *F_H for CLT wall panels*

Model	Axial Load (kN)	F_H (kN)
W0.9-1	0.00	24.75
W0.9-2	5.14	24.95
W0.9-3	11.37	25.11
W1.0-1	0.00	27.51
W1.0-2	5.82	27.72
W1.0-3	11.63	27.90
W1.3-1	0.00	36.48
W1.3-2	7.56	36.82
W1.3-3	15.12	37.05
W1.4-1	0.00	39.76
W1.4-2	8.15	40.15
W1.4-3	16.29	40.42
W1.5-1	0.00	43.13
W1.5-2	8.73	43.46
W1.5-3	17.45	43.82
W1.6-1	0.00	46.34
W1.6-2	9.31	46.72
W1.6-3	18.61	47.08
W2.0-1	0.00	58.55
W2.0-2	11.64	59.03
W2.0-3	23.27	59.48

The relationship between the width to height ratio of the wall models with different levels of axial loads and F_H is displayed in Figure 8. It can be seen that the effect of the axial load is approximately 2 percent which can be conservatively neglected. Moreover, the results demonstrates a linear relationship between the aspect ratio and the lateral stiffness of the walls.

It should be pointed out that in many of the proposed low damage solutions for CLT construction, the gravity load resisting system is separated from the lateral load resisting system. The results of the presented study shows that the lateral strength of the CLT walls is not much affected by the applied axial loads at least in the investigated range of

the applied load. Furthermore, Figure 8 readily shows that a CLT panel can be replaced with an equivalent material providing that it stays in the elastic region.

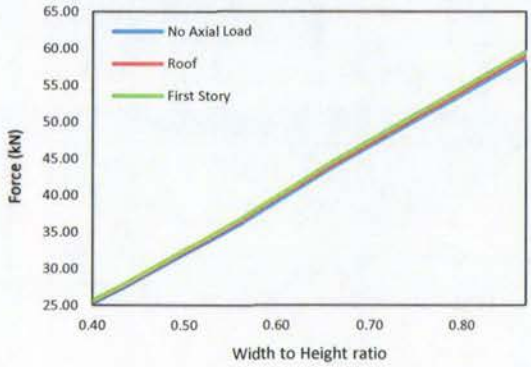

Figure 8: *Width to height ratio against F_H*

Based on the numerically obtained maximum F_H values for each wall (Table 3), the slip threshold for slip friction hold-downs (F_{slip}) is specified by Equation 1 (see Table 4). Note that the resultant forces are multiplied by 0.8 as the coefficient of safety.

Table 4: *Calculated slip thresholds (F_{slip})*

Story	Wall	F_{slip} (kN)
Second Story	W0.9	5.65
	W1.0	7.24
	W1.3	13.47
	W1.4	16.10
	W1.5	19.01
	W1.6	22.07
	W2.0	36.07
First Story	W0.9	3.56
	W1.0	4.91
	W1.3	10.45
	W1.4	12.85
	W1.5	15.52
	W1.6	18.35
	W2.0	31.42

4.3 NON-LINEAR ANALYSIS OF THE CLT BUILDING UNDER CYCLIC LATERAL LOADS

Figure 9 shows the developed numerical model in SAP2000 for the CLT building with slip friction devices. To model the hysteretic behaviour of the slip friction connections, three types of link elements are used. The multilinear plastic link with kinematic hysteretic behaviour is used to represent a bi-directional force-displacement loop without stiffness degradation through cycles of sliding. The gap element is used to restrict the negative vertical displacement in the hold-downs and the hook element is considered to specify the maximum displacement, or slot length, in the connector. The slot length was specified according to the geometry of the corresponding walls and the targeted lateral drift. For the walls with 0.9, 1.0, 1.3, 1.4, 1.5, 1.6 and 2.0 width, slot lengths of 34, 38, 49, 53, 57, 60 and 75 mm were respectively specified to make the walls capable of 3.75% rotation which is recommended by the New Zealand standard as the upper bound limit for a maximum credible earthquake (MCE) [21]. This numerical technique is experimentally validated by Loo et al. [13].

To model the ductile links that connect the rocking CLT wall to the upper floor, an elastic spring link element in addition to a gap element is used. The elastic spring element exhibits the characteristics of a rigid connection in both directions perpendicular to the element except for the vertical (or longitudinal) translational degree of freedom which allows the connections to freely accommodate the vertical movements. The gap element is considered to restrict the movement in the link to the upper floor level. Similar configuration is adopted for the ductile links that connect the CLT walls to the steel columns. The only difference is that the gap is set to the slot length because the link has to be able to accommodate both upward and downward vertical displacements (see Figure 5).

CLT panels are modelled by layered shell element with the indicated material properties in Table 1 that is assigned to each layer according to its angle.

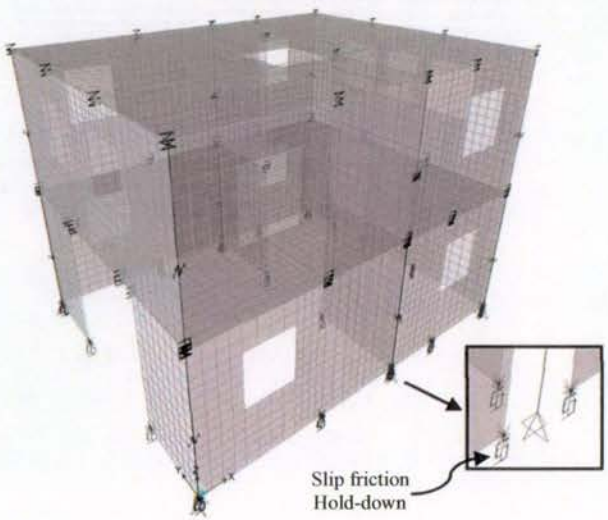

Figure 9*: Numerical model of the two story CLT house with slip friction connections*

It was decided to apply reversed cyclic lateral loads instead of displacements to ensure the inverted triangular distribution of earthquake loads were in conformance with the equivalent static method in NZS1170.5 [22]. From the non-linear pushover analysis, it is found that applying a 555 kN to the second story and half of it (277.5 kN) to the first story in the E-W direction, induces 115 mm deflection at the top of the building which corresponds to 2.5% of lateral drift. Therefore, the reversed cyclic load regime of Figure 9(a) is applied to the top floor in a manner that in each cycle, 50% of the force is applied to the first level. Note that the maximum force

was limited to 555 kN for the roof and 277.5 kN for the first floor.
Following a similar procedure, the load regime in Figure 9(b) is separately applied to the building in the N-S direction where the maximum load for the roof and the first level is 608 kN and 304 kN, respectively.

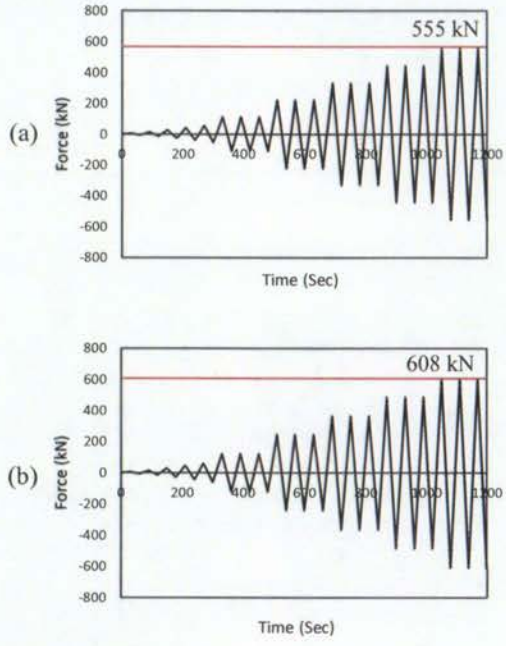

***Figure 9**: Load protocol for reversed cyclic loading: a) E-W direction b) N-S direction*

In Figure 11, the displacement at the top of the building is plotted against the base shear in both directions. It can be seen that the initial lateral stiffness of the structure remained almost intact through a large number of load cycles. This can be mainly attributed to the low damage nature imparted by the slip friction devices. The story drift of the roof level was larger than that of the first level which is in agreement with findings of Yasumura et al. during the full scale test of a low rise CLT platform building [6]. It should be emphasized that the system is designed in a way that the rocking movement of the walls is the main source of the horizontal movement of the floors and elastic deformation of the CLT panels is a secondary consideration. The slip between the wall panels and the floors is not considered in this model. However, in order to have a low damage design, a specifically designed type of shear connection should be used to transfer the shear forces from the walls to the floors which tolerates the gap opening due to the rocking motion.
Because of the low damage characteristic of the proposed system, the overall strength is maintained throughout the cyclic tests. This should be compared to the systems with traditional connectors where the total strength is drastically decreased after a few cycles and accordingly the rate of energy dissipation is correspondingly reduced [12].

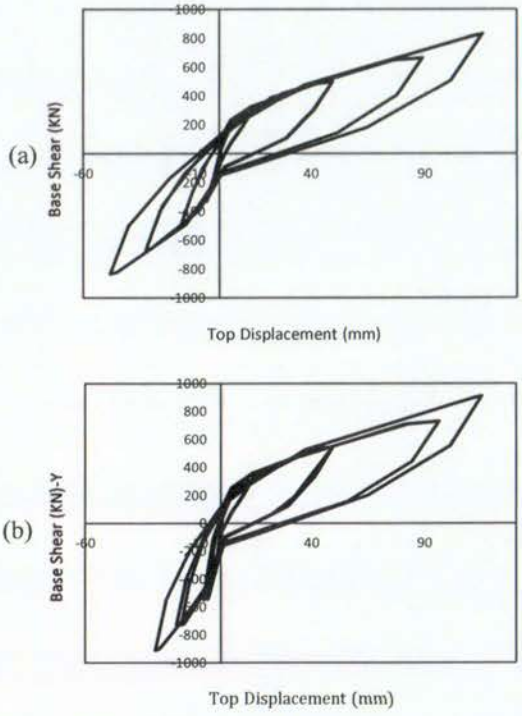

***Figure 11**: Cyclic behaviour of the structure: a) E-W direction b) N-S direction*

It can be seen that the force-deformation behaviour of the building is close to a flag-shape one. This means that the system inclines towards self-centring behaviour which is highly influenced by the vertical loads. In other words, to achieve a self-centring system, a balanced relationship between the slip force of the friction devices and the vertical loads is required. If the damper forces considerably exceed the gravity loads, self-centring is less likely to be achieved. On the contrary, much higher vertical loads will restrict the amplitude of sliding in the devices, therefore reducing the absorbed energy.
In this study, the slip forces are determined based on the maximum elastic lateral strength of the CLT panels in order to address the global behaviour of this new structural system. However, for real structures, the slip forces should be designed in a way that the slippage is triggered by Ultimate Limit State (ULS) earthquake loads. This means that the slip friction devices represent rigid connections against wind loads and Serviceability Limit State (SLS) earthquake loads. Consequently, when the building is subjected to ULS seismic forces, they start to slide and energy will be dissipated over the joints while the rocking movement of the panels provides the required ductility for the system.
Although the hysteretic loops in Figure 11 represent the potential for low damage behaviour, further experimental tests are required to confirm the global behaviour of the structure and to investigate the possible failure modes of the system. Despite the fact that the inelastic behaviour is localized in the slip friction devices, other failure modes especially in timber members should be accurately monitored.

5 CONCLUSIONS

Results of the quasi-static analyses on a numerical model of a two story CLT building with slip friction connections are presented in this paper. The objective was to investigate the cyclic behaviour of the model under lateral loads. To determine the slip threshold for the slip friction devices, series of rigorous finite element models were analysed in ABAQUS. The results showed that effect of axial loads on the lateral strength of the CLT panels is less than 2 percent for the investigated range of axial loads.

When a reversed cyclic lateral load regime is applied to the structure instead of displacements to ensure the inverted triangular distribution of earthquake loads in accordance with the New Zealand standard, the results showed that the system maintained its initial lateral strength well through numerous cycles of loading and unloading. Consequently, the system is capable of absorbing significant amount of seismic energy. Further experimental investigations are required to confirm the outcomes of this project.

Overall, the findings of this preliminary numerical study proved that the introduced system has the potential to be developed as a low damage seismic solution for CLT platform structures.

ACKNOWLEDGEMENT

The authors would like to greatly appreciate the Earthquake Commission Research Foundation (EQC) for the financial support of this research.

REFERENCES

[1] A. Ceccotti, C. Sandhaas, M. Okabe, M. Yasumura, C. Minowa, N. Kawai, SOFIE project–3D shaking table test on a seven-storey full-scale cross-laminated timber building, Earthq. Eng. Struct. Dyn. 42 (2013) 2003–2021.

[2] M. Popovski, E. Karacabeyli, Seismic behaviour of cross-laminated timber structures, in: Proc. World Conf. Timber Eng. Auckland, New Zeal., 2012.

[3] M. Popovski, J. Schneider, M. Schweinsteiger, Lateral load resistance of cross-laminated wood panels, in: World Conf. Timber Eng., 2010: pp. 20–24.

[4] I. Gavric, M. Fragiacomo, A. Ceccotti, Cyclic behavior of CLT wall systems: Experimental tests and analytical prediction models, J. Struct. Eng. 141 (2015) 4015034.

[5] M. Popovski, I. Gavric, Performance of a 2-Story CLT House Subjected to Lateral Loads, J. Struct. Eng. (2015) E4015006.

[6] M. Yasumura, K. Kobayashi, M. Okabe, T. Miyake, K. Matsumoto, Full-Scale Tests and Numerical Analysis of Low-Rise CLT Structures under Lateral Loading, J. Struct. Eng. (2015) E4015007.

[7] W.Y. Loo, P. Quenneville, N. Chouw, A numerical approach for simulating the behaviour of timber shear walls, Struct. Eng. Mech. 42 (2012) 383–407.

[8] E. Varoglu, E. Karacabeyli, S. Stiemer, C. Ni, Midply wood shear wall system: Concept and performance in static and cyclic testing, J. Struct. Eng. 132 (2006) 1417–1425.

[9] E.P. Popov, C.E. Grigorian, T.-S. Yang, Developments in seismic structural analysis and design, Eng. Struct. 17 (1995) 187–197.

[10] G.C. Clifton, G.A. MacRae, H. Mackinven, S. Pampanin, J. Butterworth, Sliding hinge joints and subassemblies for steel moment frames, in: Palmerst. North, New Zeal. Proc New Zeal. Soc. Earthq Eng Conf, 2007.

[11] A. Filiatrault, Analytical predictions of the seismic response of friction damped timber shear walls, Earthq. Eng. Struct. Dyn. 19 (1990) 259–273.

[12] W.Y. Loo, P. Quenneville, N. Chouw, A numerical study of the seismic behaviour of timber shear walls with slip-friction connectors, Eng. Struct. 34 (2012) 233–243.

[13] W.Y. Loo, C. Kun, P. Quenneville, N. Chouw, Experimental testing of a rocking timber shear wall with slip-friction connectors, Earthq. Eng. Struct. Dyn. 43 (2014) 1621–1639.

[14] Computers and Structures, SAP2000, (2011).

[15] Hibbitt, Karlsson, Sorensen, ABAQUS standard user's Manual, Hibbitt, Karlsson & Sorensen, 2014.

[16] A.H. Buchanan, N.Z.T.I. Federation, Timber design guide, New Zealand Timber Industry Federation, 1999.

[17] R. Masoudnia, P. Quenneville, STUB GIRDER FLOORING SYSTEM FOR TIMBER CONSTRUCTION, World Conference of Timber Engineering (WCTE), Qubec City, Canada, 2014.

[18] E. Karacabeyli, B. Douglas, B.S.L. Council, CLT Handbook, Cross laminated Timber, FPInnovations, 2013.

[19] A. Hashemi, P. Zarnani, A. Valadbeigi, R. Masoudnia, P. Quenneville, Seismic resistant cross laminated timber structures using an innovative resilient friction damping system, in: Proc. New Zeal. Soc. Earthq. Eng. Conf. (NZSEE), Christchurch, New Zeal., Christchurch, 2016.

[20] Ashkan Hashemi, Reza Masoudnia, Pierre Quenneville, A Numerical Study of Coupled Timber Walls with Slip Friction Damping Devices, Construction and Building Materials (In Press), 2016.

[21] N.Z. Standard, NZS1170. 5: 2004, Struct. Des. Actions-Part. 5 (2004).

[22] S.N.Z. technical Committee, Structural Design Actions (NZS 1170.5), Wellington, New Zeal. (2004).

Seismic Resistant Timber Walls with New Resilient Slip Friction Damping Devices

Ashkan Hashemi, The University of Auckland, New Zealand
Pouyan Zarnani, Auckland University of Technology, New Zealand
Armin Valadbeigi, The University of Auckland, New Zealand
Reza Masoudnia, The University of Auckland, New Zealand
Pierre Quenneville, The University of Auckland, New Zealand

Keywords: Cross Laminated Timber, Resilient Slip Friction joint, Self-centring, Seismic resilience, Energy dissipation

1 Introduction

Despite the fact that timber is intrinsically a non-ductile material, timber structures have performed well in terms of seismic performance. This is mainly because of the ductility of the mechanical steel connectors and their interaction with the timber elements. In modern design approaches, these connections are detailed to plastically deform while the timber members stay in the elastic region. Thus, the overall system achieves the required ductility. Latest research about the seismic performance of timber structures has shown that the hysteretic behaviour of the steel connections govern the total seismic performance of the structures. Traditional steel connections available for timber construction are typically comprised of mechanical fasteners such as nails, screws, rivets or bolts which are often subjected to non-recoverable damage in a design level earthquake. Therefore, the connections have to be replaced almost entirely after a severe seismic event.

Passive slip friction connectors including flat steel plates sliding over each other were originally employed in steel structures. Popov et al. (1995) introduced the *symmetric* slotted bolted connections which absorbs the seismic energy through friction during equilateral tension and compression cycles. Popov's comprehensive experiments demonstrated a nearly elastoplastic yet stable hysteretic behaviour. Clifton et al. (2007) proposed the *asymmetric* sliding hinge joint for steel moment resisting frames which had non-rectangular and stable force-deformation behaviour. Filiatrault (1990)

utilized the sliding friction devices for timber sheathed shear walls which resulted in a noticeable improvement in the hysteretic behaviour of the walls compared to the conventional timber shear walls. His studies showed that large amount of energy could be absorbed at different lateral drifts up to 1.5%. Loo et al. (2012, 2014, 2015) investigated the application of slip friction hold-downs as a replacement for traditional connectors in timber Laminated Veneer Lumber (LVL) walls. Their experiments showed a considerable improvement in the seismic performance compared to the traditional systems in terms of hysteretic behaviour and residual displacements. Hashemi et al. (2016) extended the application of slip friction connections to rocking Cross Laminated Timber (CLT) coupled wall systems. Their studies demonstrated that coupled walls with friction joints provide superior seismic performance in terms of ductility, energy dissipation and residual deflections compared to similar systems with traditional nailed connections.

This paper introduces a novel timber coupled wall system using innovative Resilient Slip Friction (RSF) joints and CLT panels as a low damage self-centring seismic solution for timber construction. The main objective of this work is to demonstrate how the adoption of the RSF joints in timber walls can improve the ductility of the wall systems while it offers a damage-free ductility zone. The outcomes of this work can be used to recommend more generous behaviour factor (q) compared to what has been proposed by Eurocode 8 (2013) when RSF technology is used.

The experiment carried out on a rocking CLT wall with RSF hold-downs is introduced. Moreover, a simple design procedure for predicting the hysteretic behaviour of the RSF joints in addition to design equations for the coupled wall system are presented. Based on the experimental results, implications to the way in which such a system could be designed in terms of the required ductility and the restoring force are discussed.

2 Resilient Slip Friction (RSF) joint

The energy absorption mechanism of the conventional slip friction connections comprised of sliding flat steel plates has already been proven as one of the most efficient structural damping systems. However, the lack of self-centring behaviour in these joints requires the use of a supplementary system to bring back the structure to its original position after an earthquake, which is always costly. One of the conventional solutions to provide self-centring is the use of post-tensioned tendons up the height of the walls. This solutions has two major disadvantages. Firstly, a significant rate of tendon force loss (30% or more) can take place during the service life of the building which substantially reduces the efficiency of the system and secondly, the post-tension force is highly dependent on the humidity of the environment which is very hard to control in most cases.

In this paper, a novel friction joint is introduced in which the components are arranged in such a way that the damping is achieved as well as self-centring, all in one device. Figure 1 displays the components and the assembly for the Resilient Slip Friction (RSF) joint (2015). The specific shape of the grooves combined with the use of Belleville washers (conical disc springs) and high strength bolts deliver the desirable self-centring behaviour. The angle of the grooves is designed in a way that at the time of unloading, the reversing force caused by the elastically compacted Belleville washers is larger than the resisting friction force between the surfaces. Thus, this force re-centres the slotted plates to their original position.

(a) (b) (c)

Figure 1. RSF joint: a) Cap plates and centre slotted plate b) Belleville spring washers c) Assembly

Based on the free body diagrams and the acting forces shown in Figure 2, a design procedure has been developed to predict the load-deformation behaviour of a symmetric double acting RSF joint (Zarnani et al. 2015). It should be noted that a double acting RSF joint is comprised of two centre slotted plates and two cap plates (see Figure 1(a)). Refer to (Loo et al. 2012) for more information about the differences between the symmetric and asymmetric configurations for slip friction connections. The slip force (F_{slip}) can be determined by Equation 1.

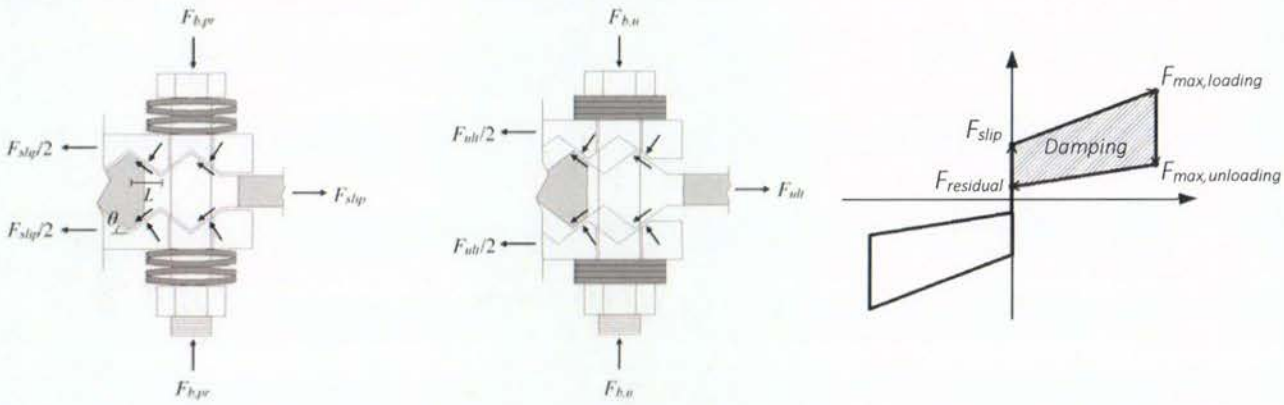

(a) (b) (c)

Figure 2. Schematic view of the symmetric RSF joint: a) Friction plates before slip b) Friction plates at ultimate deflection c) Schematic hysteretic loop

$$F_{slip} = 2n_b F_{b,pr}\left(\frac{\sin\theta + \mu_s \cos\theta}{\cos\theta - \mu_s \sin\theta}\right) \quad (1)$$

Where $F_{b,pr}$ is the clamping force in the bolts caused by the pre-stressing of the Belleville spring washers, n_b is the number of bolts, θ is the angle of the grooves and μ_s is the static coefficient of friction. Figure 2(c) shows the theoretical hysteretic loop for a RSF joint. The residual force in the joint at the end of the unloading can be determined by Equation 2 where μ_k is the kinetic coefficient of friction which can be assumed as $0.85\mu_s$.

$$F_{residual} = 2n_b F_{b,pr}\left(\frac{sin\theta - \mu_k cos\theta}{\cos\theta + \mu_k sin\theta}\right) \quad (2)$$

The ultimate force in loading ($F_{ult,loading}$) and unloading ($F_{ult,unloading}$) can be calculated by replacing μ_s and $F_{b,pr}$ in Equation 1 and Equation 2 with μ_k and $F_{b,u}$, respectively. The ultimate force in the bolts ($F_{b,u}$) can be determined by Equation 2 in which k_s and Δ_s are respectively the total stiffness of the of washers and their maximum deflection when they are fully compressed (the spring washers become flat).

$$F_{b,u} = F_{b,pr} + k_s \Delta_s \quad (3)$$

The maximum deflection in the joint can be calculated by Equation 4 where n_j is the number of joints acting in a series (e.g. n_j equals to 1 for a single acting joint and equals to 2 for a double acting one).

$$\delta_{max} = n_j \frac{\Delta_s}{\tan\theta} \quad (4)$$

The joint possesses a self-centring characteristic providing that Equation 5 and Equation 6 are satisfied. In Equation 6, L represents the horizontal distance between the top and bottom of a groove.

$$\mu_s < \tan\theta \quad (5)$$

$$L > \frac{\Delta_s}{\sin\theta} \quad (6)$$

3 Experimental testing of a Rocking CLT wall with RSF joints

Experimental tests were conducted on a CLT wall with RSF joints as the hold-down connectors to study the hysteretic behaviour of the wall which represents the performance of the proposed concept in terms of ductility, stability and self-centring capacity.

3.1 The assembly of the RSF hold-downs

The two identical RSF joints used in the test are shown in Figure 3. The RSF hold-downs are implemented in the notches at the bottom corner of the CLT wall. They consist of two centre slotted plate and two cap plates. The cap plates were manufactured using mild steel grade 350 and the centre plates were fabricated with high-strength Bisplate 80 steel. The angle of the grooves was 15 degrees in order to maximize the deformation capacity of the joint. Two 220 mm by 50 mm mild steel stiffener plates had later been welded to the cap plates to reinforce them against out of plane bending.

(a) (b) (c)

Figure 3. The tested RSF hold-down: a) Cap plates and centre slotted plates b) Belleville washers c) Assembly

The RSF joints were designed and built to be able to accommodate a maximum displacement of 65 mm in tension and 15 mm in compression. This was because of the relatively larger displacement demand in tension in comparison to the one in compression in a hold-down connector. These displacement thresholds were determined based on the analytical prediction of the RSF joint behaviour.

3.2 Materials and the test rig

The quasi-static cyclic tests were carried out on a five layer CLT wall with a height of 6000 mm and a width of 2020 mm. The hydraulic actuator was connected to the wall at 3350 mm of height. The CLT panel has five 40 mm thick layers made of MSG8 timber (1999) (200 mm thickness in total). Figure 4 shows the general arrangement of the test setup. The loading protocol displayed in Figure 5(a) was applied to the top of the wall with a loading rate of 1.25 mm/sec. To prove the efficiency of this novel low damage solution, a maximum drift amplitude of 3% was targeted to match the typical design yield limit recommended by the different building codes in the world. Moreover, because of the fact that the conventional beam-column connections with plastic hinges and also the hold-down connections of the shear walls are subjected to severe damage at lateral drifts more that 2%, it was decided to aim for a 3% lateral drift to demonstrate the functionality of the proposed concept. However, if more than 100

mm top displacement (equals to 3% of lateral drift) is demanded by the designer, the RSF joints can be redesigned to meet the required maximum lateral drift.

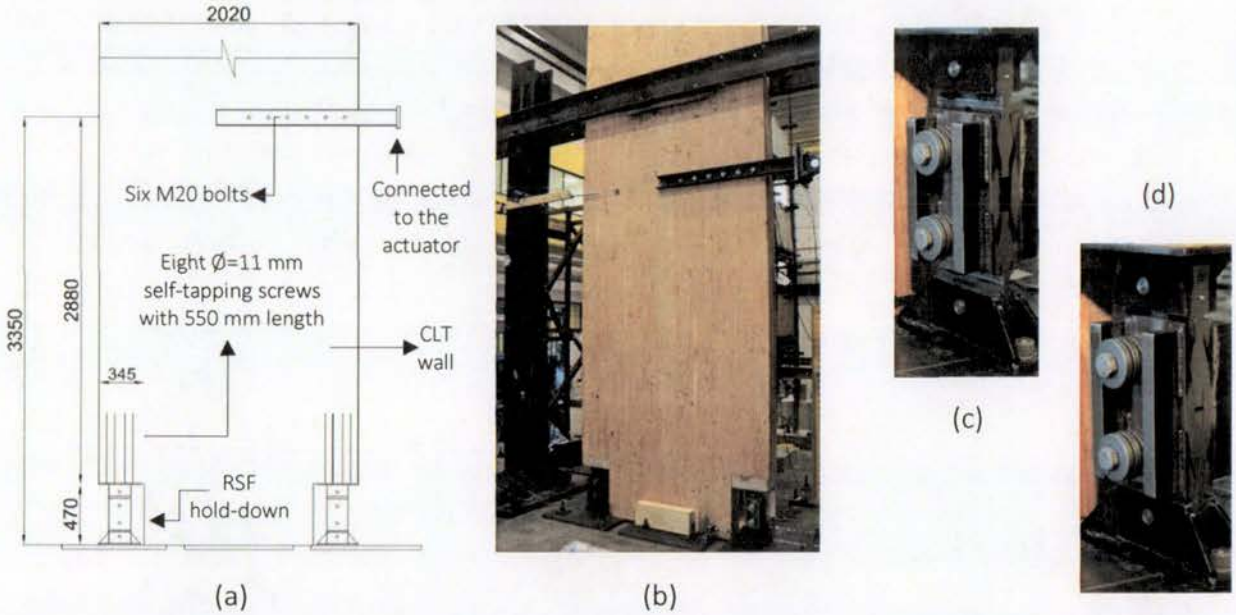

Figure 4. Experimental testing of rocking CLT wall with RSF joints: a) schematic test setup (dimentions are in mm) b) Test Specimen c) RSF joint deformation in tension d) RSF joint deformation in compression

The authors carried out eight tests in total on the wall. No damage was observed to the wall with no evidence of deterioration in strength or stiffness of the RSF joints. Figure 5(b) shows the typical hysteresis for the wall. For the displayed test, the pre-stressing force was approximately 50% of the maximum force. The flag-shaped hysteresis in Figure 5(b) clearly demonstrates the self-centring behaviour of the tested wall. It should be pointed out that despite the fact that the only applied vertical load was the self-weight of the wall, the wall exhibited a self-centring behaviour. This shows that the self-centring capacity within the proposed concept is independent of the applied gravity loads. Figure 4(b) and 4(c) display the deformed shape of the RSF hold-downs in tension and compression, respectively.

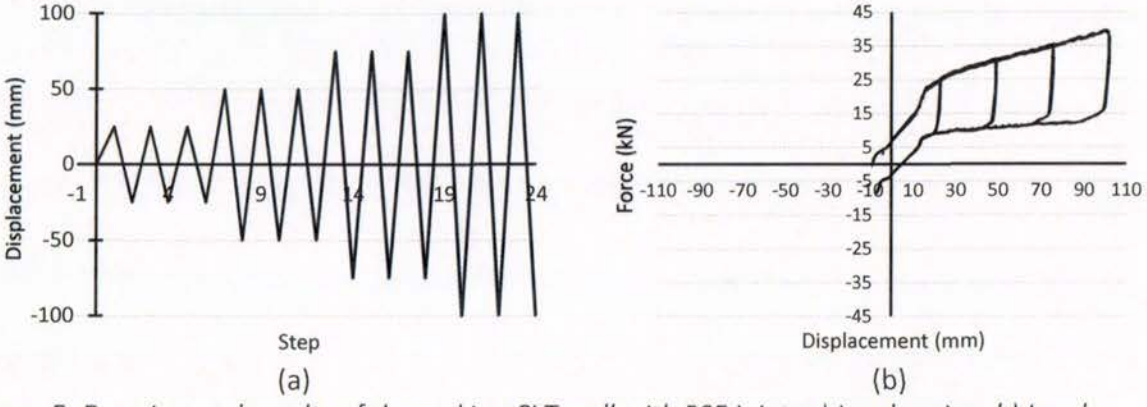

Figure 5. Experimental results of the rocking CLT wall with RSF joint: a) Load regime b) Load-deformation response

4 Ductility of the timber walls with RSF joints

RSF joints applied to massive rigid timber walls (such as CLT walls), provides a flag-shaped elasto-plastic behaviour. The provided ductility is basically limited by the maximum displacement of the RSF joint. The maximum displacement has to be determined to provide a damage-free ductility during a ULS earthquake or even MCE.

For timber structures in general, the overall ductility (μ) is found by dividing the failure displacement (δ_{max}) by the yield displacement (δ_y). These definitions are displayed in Figure 6(a). For the walls with RSF joints, a similar approach can be adopted to define the total ductility. Figure 5(b) shows that the wall systems with RSF joints offer a damage free ductility zone. This zone is associated with the RSF joints undergoing sliding thereby capping forces below the limit indicated by the designer. The ductility can be defined as $\mu_{rsf} = \delta_{rsf} / \delta_y$. The designer can decide on an appropriate value for μ_{rsf} corresponding to the relevant code recommendations for drift limits of ULS or MCE. It should be pointed out that the extra ductility (beyond the ductility that is provided by the RSF joints), depends on sufficient overstrength being provided by the other connections within the structures.

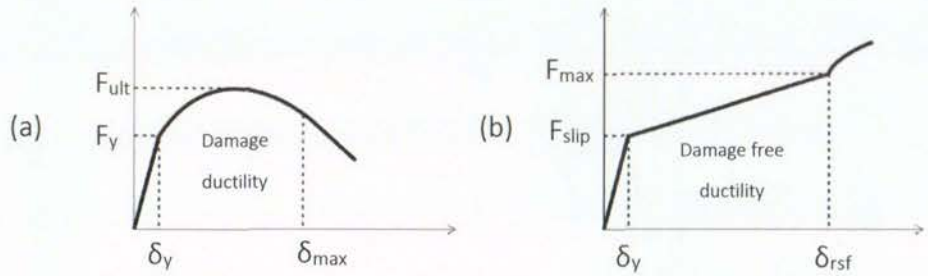

Figure 6. Defenisitons of the Wall strenght and ductility: a) Traditonal systems b) RSF joints

In view of a code application, higher q-factors compared to the recommended values by Eurocode 8 (2013) for seismic design of CLT buildings (q=2) should be allowed when RSF joints are used. This is because the adoption of RSF technology can improve the intrinsic ductility and also the cyclic behaviour of the jointed CLT buildings

5 Numerical modelling of the CLT coupled walls with RSF joints

5.1 The concept of the CLT coupled walls with RSF joints

The proposed system in this section is comprised of coupled CLT walls joined together by two types of RSF joints which are hold-down connections and ductile links. The RSF ductile links connects the CLT wall panels to adjacent walls and/or end steel columns. When two adjacent walls are connected together, the RSF hold-down con-

nects each wall to the foundation. The general arrangement of the proposed concept is displayed in Figure 7. On the brink of rocking, the acting forces on the walls connected to the adjacent CLT wall are the RSF hold-down force (F_H), the sum of RSF ductile link forces ($\sum F_j$) and the vertical loads (W). The acting forces for the walls connected to the end columns are the sum of RSF ductile link forces ($\sum F_j$) and the vertical loads (W). It should be noted that this concept is mainly proposed for structural systems where the lateral load resisting system is separated from the gravity load resisting members. Thus, the only considered vertical load in this study is the self-weight of the CLT walls. However, the proposed system can also be used for structures that include load bearing walls.

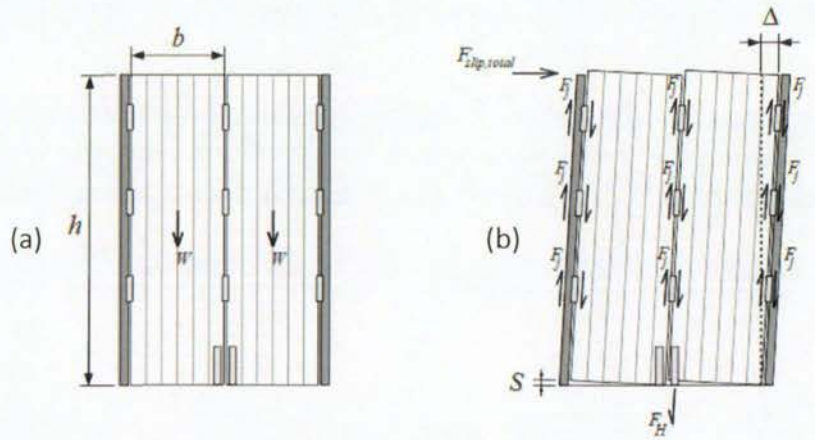

Figure 7. Coupled CLT walls with RSF joints: a) Before Rocking b) After Rocking (Note: Outside columns are restrained from any uplift)

Taking the moments about the rocking point of each wall, the total slip force ($F_H + \sum F_j$) can be determined by Equation 7.

$$F_H + \Sigma F_j = F_{slip}\frac{h}{b} - \frac{W}{2} \tag{7}$$

Where F_H is the slip force of the RSF hold-down, F_j is the slip force for the RSF ductile links, h is the height of the wall, b is the width of the wall, W is the self-weight of the wall and F_{slip} is the applied force at the top of the wall which triggers the slippage in the RSF joints. Note that $F_{slip,total}$ in Figure 7(b) is the applied horizontal slip force at the top of the coupled wall system. If the walls are identical, $F_{slip,total}$ is equally shared between them. However, if the walls within the system have different geometrical or material characteristics, $F_{slip,total}$ is proportional according to their lateral stiffness.

The RSF joints can be designed using Equation 7 considering the fact that for the adjacent walls with RSF hold-downs, the sum of the slip forces of the RSF ductile links has to be equal to the RSF hold-down slip force. Otherwise, the sliding would first initiate in the hold-downs and the walls might be locked together, cancelling the energy absorption potential in the inter-wall ductile links. The slot length for the RSF ductile links between the walls has to be twice that of the RSF hold-downs as they are designed to slide in both upward and downward directions while the hold-downs are in-

tended to only move upward. Accordingly, the slot length for all hold-downs (S) and ductile links ($2S$) can be determined by Equation 8 with respect to the required lateral displacement (Δ) (see Figure 7(b)). If the walls have different geometry, the slot lengths for the connections within each one of them should be calculated separately.

$$S = \Delta * \frac{b}{h} \tag{8}$$

It should be noted that the RSF hold-downs are rigid connections before slippage. Therefore, the applied horizontal force at the top of the wall (F_{slip}) has to be controlled to not exceed the amount that causes tension failure at the base of the wall.

5.2 Cyclic behaviour of CLT coupled walls with RSF joints

In order to model the RSF joint load-displacement behaviour, the Damper–Friction spring Link element in the SAP2000 software package is adopted. This type of element has proven to be able to accurately represent the cyclic behaviour of a RSF joint providing that its parameters are properly calibrated in accordance with the design parameters of the RSF joint such as the slip force, loading stiffness, maximum loading force, maximum unloading force and the residual force (Hashemi et al. 2016).

The general arrangement of the coupled wall system to be studied under displacement-control cyclic loading using the SAP2000 software package is displayed in Figure 8. The system consists of two identical CLT walls with 8 m height and 2 m length. All of the timber boards within the panel (longitudinal and transverse layers) were assumed to have a thickness of 40 mm, a width of 183 mm and an elastic modulus of 12000 MPa (MSG12 timber along the board's main axis). The density of the timber was assumed as 540 kg/m3. The walls have a thickness of 200 mm. This system includes two 200*200*10 mm steel box columns at the ends assumed to be pinned to the base. The walls are connected to the adjoining panels and/or the adjacent steel columns by RSF ductile links. Furthermore, the walls are attached to the foundation where the two CLT panels are positioned next to each other.

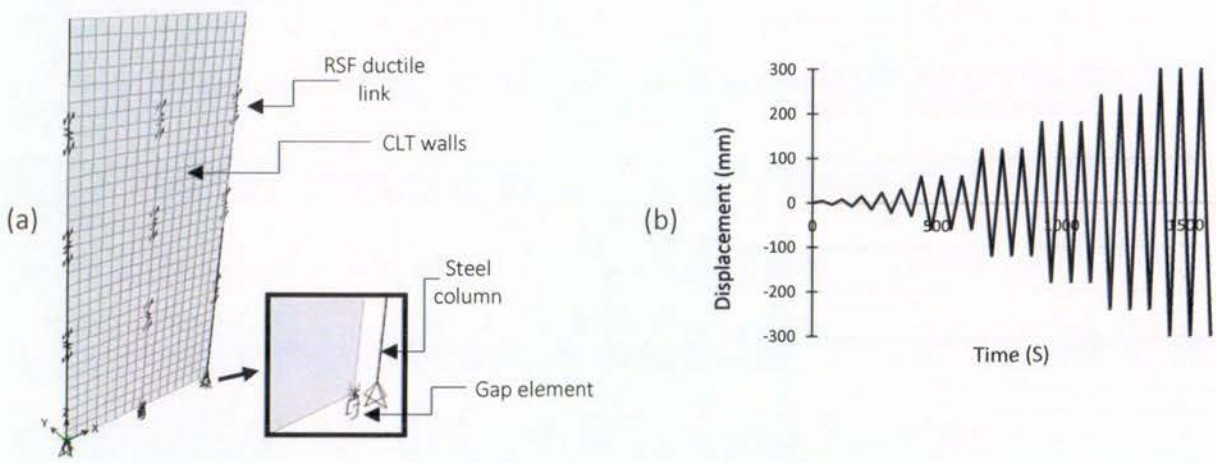

Figure 8. Numerical model of the CLT coupled walls with RSF joints: a) General arrangement b) Displacement-control load schedule

For this study, A 100 kN force applied at the top of the wall system is considered to represent the ULS earthquake force which the RSF joints are designed to resist to. The RSF joints are designed in accordance with the proposed design procedure in section 2 and also Equation 7. Considering a self-weight of 17 kN for each one of the walls, the maximum force for the RSF ductile links attached to the face of the steel columns is 130 kN, the maximum force for the RSF ductile links attached to the adjacent CLT wall is 65 kN and the maximum force for the RSF hold-downs is 195 kN. Note that three RSF ductile links are considered along the height of the walls. In this model, F_{slip} is considered as 50% of the maximum load in the joint ($F_{max,loading}$). Also, the CLT panel is modelled using layered shell element. The calculated design parameters are presented in Table 1. The displacement-control load schedule in Figure 8(a) is applied at the top of the system to evaluate the total load-deformation behaviour. The maximum displacement in the load schedule is 300 mm representing 3.75 % of lateral drift which is recommended by the New Zealand standard for MCE.

Table 1. Calibrated parameters for the numerical model of the RSF joints.

	Slipping stiffness (loading) (N/mm)	Slipping stiffness (Unloading) (N/mm)	Pre-compression displacement (mm)	Stop displacement (mm)
RSF hold-down	1300	281	-75	75
RSF ductile link attached the column	867	187	-75	75
RSF ductile link attached the wall	433	95	-75	75

Figure 9 shows the numerical response of the system under the applied cyclic load regime. It is observable that the RSF hold-downs and the RSF ductile links have a flag-shaped hysteretic behaviour. Figure 9(d) illustrates the total lateral response of the coupled wall system. It can be seen that the system exhibits a self-centring behaviour that can be attributed to the hysteretic behaviour of the RSF joints. It should be emphasized that the only considered vertical load in this model is the self-weight of the wall. This means that the self-centring behaviour of the proposed structural system does not rely on the gravity loads neither on the use of post-tensioned cables. Moreover, Figure 9 evidently demonstrates the low damage characteristic of the proposed system as the hysteretic behaviour remained stable after numerous cycles of loading and unloading. Hence, the bounded area between the hysteretic loops increases over time. This clearly represents a significant rate of energy dissipation which furthers confirms the potential to have a resilient low damage seismic solution. The damage free ductile zone is also observable in Figure 9 which can compared to Figure 6(b).

In this model, F_{slip} is considered as 50% of the maximum load in the joint ($F_{max,loading}$). However, for multi-story buildings, F_{slip} should be specified based on the Ultimate

Limit State (ULS) earthquake loads and the total stiffness of the Belleville washers that are exploited.

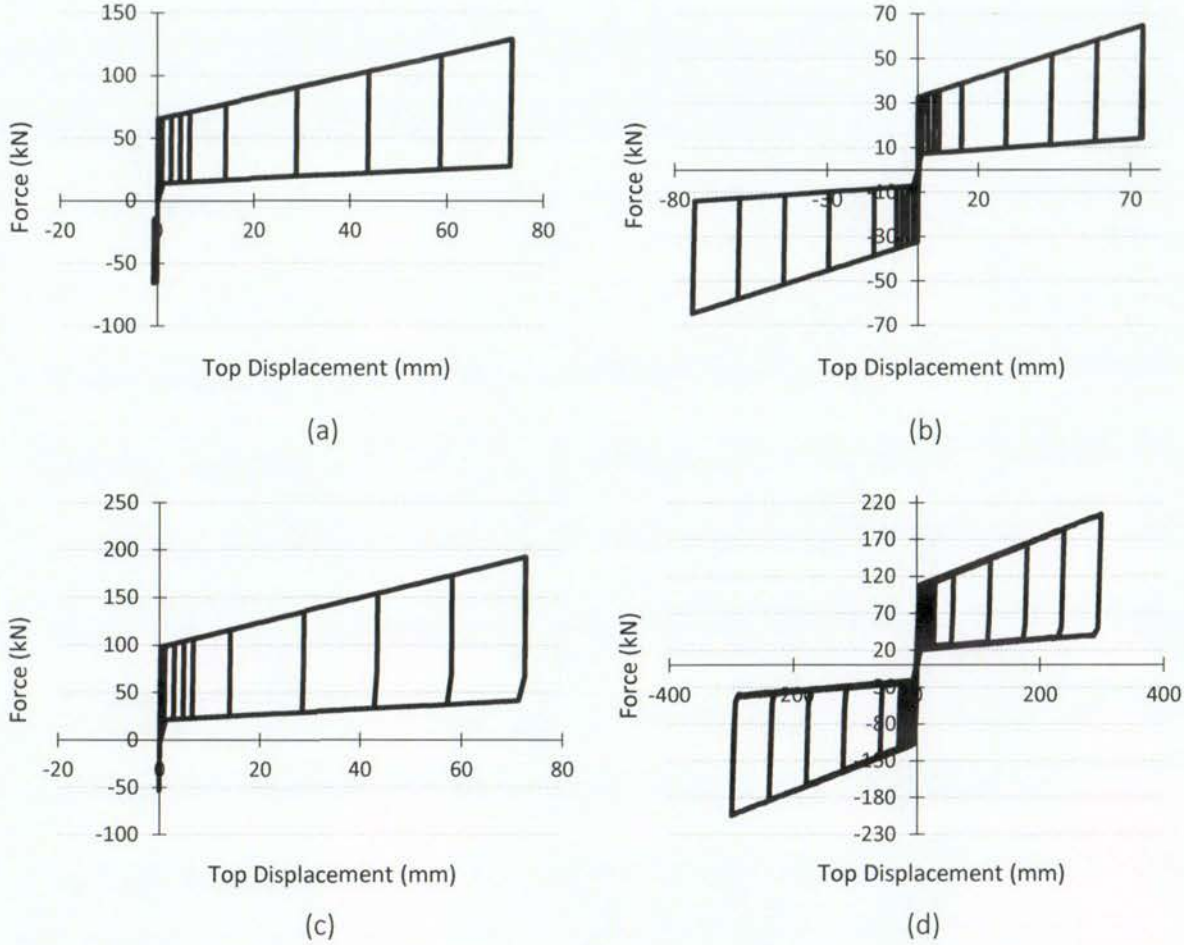

Figure 9. Numerically obtained hysteretic behaviour of the CLT coupled walls with RSF joints: a) RSF ductile link attached to the columns b) RSF ductile link attached to the CLT walls c) RSF hold-down d)Total system

5.3 Seismic performance of CLT coupled walls with RSF joints

In this section, the seismic response of the introduced coupled wall systems with RSF joints are presented. A seismic mass of 18000 kg are assigned to all of the walls in the model at two elevations up the height of the walls (top and middle). Four conventional time-history acceleration records were chosen for the earthquake loading. In accordance with NZS1170 (2002), each record was scaled to match the Christchurch 2500 year return period for MCE and 500 year return period for ULS. A type C soil (shallow soil site) was selected for ground motion scaling. Scale factors were determined with regards to a numerically obtained fundamental period of 0.47 seconds. The fundamental frequency was determined as 2.13 Hz. The scaled peak ground motions for both systems are presented in Table 2. The maximum horizontal displacements at the top of the system are shown in Figure 10. In accordance with

NZS1170.5, the maximum deformation limit of 2.5% (200 mm for this structure) is the reference upper bound applicable to the ULS (1/500 annual period of exceedance for ordinary structures) and a drift limit of 3.75% (300 mm for this structure) is recommended for MCE.

Table 2. Earthquake records and scaling.

Event	Year	PGA (g)	Scaled PGA (g) for ULS	Scaled PGA (g) for MCE
El-Centro	1940	0.31	0.25	0.46
Northridge	1994	0.23	0.28	0.48
Kobe	1995	0.82	0.27	0.55
Christchurch	2011	0.44	0.19	0.48

It is observable that the maximum displacements for all of the selected seismic events has not reached these limits. Moreover, no residual displacement was recorded in any of the time-history analyses demonstrating that the wall system is fully re-centred at the end of the earthquakes.

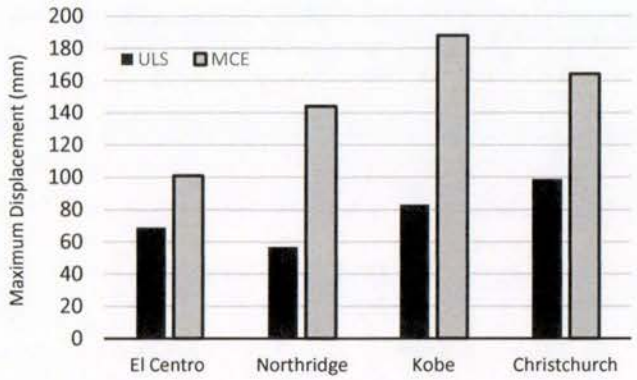

Figure 10. The maximum displacement at the top of the system subjecte to seismic loading

6 Conclusions

Experimental investigations on a rocking CLT wall with Resilient slip friction (RSF) joints as the hold-down connectors proved the feasibility of the concept and the wall demonstrated a stable flag-shaped hysteretic behaviour representing the self-centring characteristic. This is achieved considering the fact that the only applied gravity load was the self-weight of the CLT wall.

The adoption of the RSF joints as a substitute to the the traditional fasteners allows one to significantly improve the seismic response of the CLT rocking walls in terms of ductility and energy absorption capacity. RSF joints allow the available damage free ductility to be determined directly through the maximum displacements (slot lengths)

corresponding to a particular lateral drift limit. A design procedure to predict the load-deformation behaviour of the new RSF joints has been introduced in this paper which could serve as a reference as it is validated by large scale experimental tests.

A concept for CLT coupled walls with RSF joints as the hold-down connectors and also as the ductile links between the panels and between the panels and the end steel columns is introduced and numerically simulated. Results confirm that the proposed wall system can be considered as a high ductility class system with respect to the fact that the designer can determine the ductility by specifying the RSF joints design parameters. Moreover, compared to traditional systems, the strength degradation and pinching effect are eliminated.

In view of a code implementation, a more generous behaviour factor (q) can be allowed when dissipative connections such as RSF joints are adopted in CLT buildings. It should be emphasized that the use of RSF joints with predictable and limited behaviour makes the capacity design approach more realistically affordable for design of timber structures.

7 References

A. Hashemi, P. Zarnani, A. Valadbeigi, R. Masoudnia, P. Quenneville. (2016). "Seismic resistant cross laminated timber structures using an innovative resilient friction damping system." *Proceedings of New Zealand Society for Earthquake Engineering Conference (NZSEE), Christchurch, New Zealand*, Christchurch.

Buchanan, A. H., and Federation, N. Z. T. I. (1999). *Timber design guide*. New Zealand Timber Industry Federation.

Clifton, G. C., MacRae, G. A., Mackinven, H., Pampanin, S., and Butterworth, J. (2007). "Sliding hinge joints and subassemblies for steel moment frames." *Palmerston North, New Zealand: Proc of New Zealand Society for Earthq Eng Conf*.

Eurocode 8. (2013). "Design of structures for earthquake resistance-part 1: general rules, seismic actions and rules for buildings."

Filiatrault, A. (1990). "Analytical predictions of the seismic response of friction damped timber shear walls." *Earthquake engineering & structural dynamics*, Wiley Online Library, 19(2), 259–273.

A. Hashemi, R. Masoudnia, P. Quenneville. (2016). "A Numerical Study of Coupled Timber Walls with Slip Friction Damping Devices." *Construction and Building Materials*.

Loo, W. Y., Kun, C., Quenneville, P., and Chouw, N. (2014). "Experimental testing of a rocking timber shear wall with slip-friction connectors." *Earthquake Engineering & Structural Dynamics*, Wiley Online Library, 43(11), 1621–1639.

Loo, W. Y., Quenneville, P., and Chouw, N. (2012). "A numerical study of the seismic behaviour of timber shear walls with slip-friction connectors." *Engineering*

Structures, Elsevier, 34, 233–243.

Loo, W. Y., Quenneville, P., and Chouw, N. (2015). "Rocking Timber Structure with Slip-Friction Connectors Conceptualized As a Plastically Deformable Hinge within a Multistory Shear Wall." *Journal of Structural Engineering*, American Society of Civil Engineers, E4015010.

New Zealand Standard. (2002). "1170.1: 2002—structural design actions." *Wellington, New Zealand.*

P. Z arnani, P. Quenneville. (2015). "A Resilient Slip Friction Joint. " Provisional Patent no. 7083.

Popov, E. P., Grigorian, C. E., and Yang, T.-S. (1995). "Developments in seismic structural analysis and design." *Engineering structures*, Elsevier, 17(3), 187–197.